

**TRANSITION METAL-CATALYZED
FLUORINATION/¹⁸F FLUORINATION AND DECARBONYLATIVE
CARBON HETEROATOM BOND FORMATION**

by

Naoko Ichiishi

A dissertation submitted in partial fulfillment
of the requirements for the degree of
Doctor of Philosophy
(Chemistry)
in the University of Michigan
2016

Doctoral Committee:

Professor Melanie S. Sanford, Chair
Professor John P. Wolfe
Associate Professor Anne J. McNeil
Research Assistant Professor Peter J. Scott

© Naoko Ichiishi
2016

TO MY FAMILY
SUSAN JACOVELLI AND MIRA RACHWELL

ACKNOWLEDGEMENTS

Everything I have accomplished during my five years working on this thesis would not have been possible without an army of support. Melanie, you have been a wonderful mentor and role model. Your knowledge, creativity, and passion both amazed and intimidated me when I was a rotator in the lab, and still do so today. I admire your willingness to diversify and how you encourage your students to do the same. The focus of the group has expanded so much since I first joined, and I have learned so much because of the mobility. Thank you for letting me start PET collaboration and guide me throughout the time. You have encouraged and pushed me out of my comfort zone. I began my Ph. D. hating public speech and I lose my English when I was nervous. You have taught me how to be articulate and concise and make clear presentation throughout the Ph.D. It helped me gain my confidence. I appreciated that you have seen a great value in my work and helped me see it especially while I am applying for jobs. I greatly appreciate your honest feedbacks with me and ask me critical questions to address in order to improve science. And I cannot express enough of my appreciation. Your great mentorship molded me into who I am today. I have become a better chemist because of it. I admire your intelligence, courage and confidence and I hope that one day I can grow more like you. One of many things I love about your mentorship is that you ask us “what do you want to do?” in our careers and chemistry and you provide as tremendous support to our desire. I do respect that greatly.

To my committee members, Professors Wolfe, McNeil, and Scott, I thank you for your support and guidance over my time here. Prof. Wolfe, thank you for asking me the difficult questions about chemistry and not being too harsh if I didn't know the answers. Prof. McNeil, my summer rotation here I spend working in your lab. Since I have seen your talk at ACS, I admire your mechanistic works. Working on polymerization was

definitely was very new to me but my two months in the McNeil lab was so enjoyable and enlightening because of you, who were always willing to discuss chemistry when I knock your office door. Prof. Scott, you must have been very surprised when I first approached to you and ask about the possibility of our collaboration. It was one of the best decisions that I made in my life and I am so grateful that you said yes to it. I would not expect that when I first started that this PET collaboration expanded as much as today. Your knowledge, creativity, courageousness and enthusiasm to improve PET science are so admirable and I cannot appreciate enough for serving as my committee.

I was fortunate to be surrounded by wonderful collaborators. Alan, my first few papers in the graduate school did not come out if you were not willing to give a shot on computations of my Cu system. You were so warm and easy-going and really helpful when I ask you questions. Allen, it was a pleasure to work with you on PET collaborations. You were very patient and helpful throughout the project. Since you have joined our first PET project, we have got so much work done very fast as you volunteered helping us out making ^{18}F . I admire how passionate you are for everything ranging from basic organic chemistry to medicinal chemistry. We could talk hours just discuss on a fundamental chemistry topic. I will miss working with you. Andy and Missy, I am very grateful for you two working with me for PET projects.

Over my five years here at Michigan, I have been extremely fortunate to have such great mentors and peers to look up to. Yingda, your drive and energy towards your science is just stunning I was very lucky to have you as a bay-mate. You always ask a lot of questions and when I do not feel like running one more experiment, you encouraged me to try one more! Your perseverance and passion for science shaped my expectation and I hope I can live up to it. Joe, thank you so much for being a first team member of PET collaboration. Your knowledge in PET, synthesis and medicine were far beyond of me and I was so grateful when you joined our collaboration. It was not possible to keep on our collaboration without your knowledge and drive. There is no one who gets excited about good results as much as you did here and I miss your passion in science since you have left. Chelsea, I always considered you as my secret mentor when I was a first year. You are caring, funny and very driven to your goal. Every day you set a goal and aim to accomplish it like a game. I loved your work ethics and you

were also a great friend too. You were someone I could always go talk to you when I am down. When I need to think through some problems and I need to talk them out, you are always there for me and not only listened but thought them together. I felt so supported and I hope I would like to be a scientist like you. Sharon, even though it was really only about less than a year I spent with you, I was so glad that we were in touch with each other. Your emails always lit me up and I admire your deligence at work. You are also great at presentation and I always pursued to be like you when I give mine. At ACS San Francisco, when I heard your DFT talk and it was the clearest DFT talk I ever attended to. I am looking forward to our future friendship too. To Anna and Kate, you guys are everything I wanted to be when I first joined the group and I thank you for being great examples for me to follow. Ansis, thank you for your friendship and helpful discussions in chemistry. Christo, thank you for putting up with me for sharing my love for cats and for just being a great role model as a chemist in lab. I look up to you as a scientist and you are the most focused person I have ever met. I am so looking forward to seeing what you will acoomplish in your future career. Signe, Andy, Stefan and Alvaro, you guys are so smart and it was so muc fun to hang out even during your short stay. I would not think to go to ICIQ for summer without meeting you before. It was a pleasure to meet and get to know you all. Matt, Eugene and Megan, you are great post-docs that has so much knowledge that I can always go to if I have any question. Thank you for reading my thesis chapters and good suggestions about my chemistry last few months.

To Doug, Mónica and Amanda, you have helped me through my toughest times during grad school. Doug, you are such a wonderful person I met in Michigan and I can't be thankful enough for how lucky I am to get to know you. You are the example of what a post doc and good friend should be. You are always there for me whenever I am in my tough situations and I appreciate your support and perspective to see things clearly. You helped me regain a confidence in myself that I thought was stolen from me. Mónica, I would not have made it through my candidacy exam without your support. You are also a few of great friends that I can open up to. On days when I don't want to talk to anyone, you didn't let me keep being sad. You come to me and ask how everything with me or I can go to who can make everything better. I'm so grateful to you for simply being there when I need someone to talk to. Amanda, no one can replace your role in

my life. I am so grateful that I have you as a friend and thank you for your support. I look up to you as a scientist and I admired you for how brave you are. You always fight for yourself and even for others. We talk about everything and you laugh at my jokes and my accents and I miss that time so much. You are someone who goes out of your way to help someone that you care and that makes you so special. You are a great scientist I look up to and friend that I care. You have awed me for your accomplishments in last year while finding a balance to spend time with us. The time you, Monica and I spent was one of the few best times I had in graduate school. I really hope to have you three in my life even after graduate school.

As my time at Michigan has gone on, incredible younger scientists have joined the lab. I greatly thank the current members for making my time here so valuable. Nicole, you have been such a great friend and lab-mate during my time here. I love how we could talk about anything and laugh about it. I always wanted to have a sister and it felt like I have one when I talk to you. When I struggle in writing, you have helped me to make it crystal clear, and I appreciate your support throughout my thesis-writing period. It was great to you as a gym buddy and your dedication are so inspiring. Thank you for introducing me to the show "Friends." I am so proud of you for who you become today: a good scientist, writer and compassionate friend and I will miss you tremendously when I leave. Pablo, you are one of the most intelligent, hard-working, and dramatic people I know of. I admired how very focused and quick in learning you are and I believe you are the most diversified chemist in our group, given that you handled so many different projects. Nomaan, you have a fire and ambition in science and I appreciate your passion. You are always the one with whom I want to discuss science and everything. You are also always there for me when I need help. Melissa, I adore how you get excited to talk about chemistry, your family and nightmares. You have been growing to be a better scientist every day. Your perseverance in the difficult projects you have been working is simply admirable. Katarina, I am so impressed with how much you've grown as a chemist and I am so excited to see the great progress of the PET project. I hope your best luck. To Ian, Sydonie, James, BJ, Devin, and Liz, I am impressed with your enthusiasm to talk about chemistry and with how hard you work and I wish best luck of you all.

The true foundation of who I am as a scientist was laid by my family. It has been exactly 10 years since I left Japan but you all have given me great support. Mom, you sacrificed so much for your children, and I truly feel I am the luckiest person in the world that I have you in life. I am naturally serious and agonize over problems and you made me feel easy for them. I've learned to be independent and to have the confidence to pursue my goals because of you. To my brothers, Kenji and Tatsuya thank you for being the best brothers I could ask for and I admire you two hardly ever complain about anything but focus on having a good time with me when we hang out. You are the best brothers anyone could hope for. To dad, thank you for letting me study abroad and believing in me for pursuing Ph.D. Without your support and encouragement, I would have never even stepped foot in a college classroom. Susan Jacovelli, although we are not related, you are the first host mother I had in the U.S. and you taught me everything. I feel like I have a second mother in the U.S. Your encouragement and support really helped me get through my first two years of college. I would like to dedicate my thesis to my family and Susan Jacovelli and Mira Rachwell.

Finally, I would like to dedicate my thesis dissertation to Mrs. Mira Rachwell, who pushed me to go to graduate school when I wondered if I am smart enough to do so. You had told me that I deserve for a great thing. And no matter what happened, you never lost faith in me and it gave me a great strength. I hope you were happy to see who I have become from the heaven. I regret that I could not show you how your support took me this far. I am so thankful for your encouragement back in time and I hope you were proud of me to see who I am today.

TABLE OF CONTENTS

Dedication	ii
Acknowledgements	iii
List of Schemes	x
List of Figures	xiv
List of Tables	xvi
List of Abbreviation	xviii
Abstract	xxi
Chapter 1. Introduction	1
1.1 Significance of Fluorine	1
1.2 Key Considerations for Successful Fluorination Process	2
1.3 Classical Fluorination Process That Are Still In Use	3
1.4 Challenges with the Fluorination Process	5
1.5 Early Studies on Ar–F Bond Formation from Metal Complexes	5
1.6 Transitioning to Novel, More Cost-Effective Approach	10
1.7 References	15
Chapter 2. Cu-Catalyzed Fluorination of Diaryliodonium Salts with KF: Reaction Development and Mechanistic Investigations	17
2.1 Introduction	17
2.2 Results and Discussion	22
2.3 Conclusions	37
2.4 Perspective and Outlook	38
2.5 Experimental	39
2.6 Characterization	41
2.7 References	64
Chapter 3. Cu-Catalyzed [¹⁸F]Fluorination of (Mesityl)(Aryl)Iodonium	67

Salts and Synthetic Applications:

3.1 Introduction	67
3.2 Results and Discussion	73
3.3 Conclusions	87
3.4 Perspective and Outlook	88
3.5 Experimental	90
3.6 Characterization	94
3.7 References	112
Chapter 4. Development of Cu-Mediated [¹⁸F]Fluorination of Aryl Boronates and Synthesis of Ag[¹⁸F]F and Its Application	116
4.1 Introduction	116
4.2 Results and Discussion	118
4.3 Conclusions	144
4.4 Perspective and Outlook	144
4.5 Experimental	145
4.6 Characterization	149
4.7 References	153
Chapter 5. Pd-Catalyzed Decarbonylative Carbon–Heteroatom Bond Formation	155
5.1 Introduction	155
5.2 Results and Discussion	159
5.3 Conclusions	178
5.4 Perspective and Outlook	179
5.5 Experimental	180
5.6 Characterization	183
5.7 References	191

LIST OF SCHEMES

Chapter 1. Introduction	4
Scheme 1.1 Conventional Nucleophilic Fluorination Routes	4
Scheme 1.2 Representative Electrophilic Fluorination Method	4
Scheme 1.3 Hydrogen Bonding Energy of F----HF	5
Scheme 1.4 Simplified Proposed Catalytic Cycle for Metal-Catalyzed C–F Bond Formation	6
Scheme 1.5 Grushin’s First Isolated Pd(II)PhF Complex	6
Scheme 1.6 C _{sp2} –Halogen Bond Formation: Kinetics vs. Thermodynamics	7
Scheme 1.7 Thermal Reactivity of Pd-F Dimer	8
Scheme 1.8 Pd ^{0/II} -catalyzed Nucleophilic Aromatic Fluorination	8
Scheme 1.9 Transition Metal-Catalyzed Electrophilic Fluorination	9
Scheme 1.10 Transition Metal-Catalyzed Fluorination	10
Scheme 1.11 Moving Towards More Cost-Effective Approach: High-Valent Organometallic Copper Chemistry for Achieving C–F Bond Formation	11
Scheme 1.12 Riba’s Cu-catalyzed Halide Exchange	11
Scheme 1.13 Premise of My Thesis Objectives	12
Scheme 1.14 Doyle’s Asymmetric Epoxide Opening Fluorination	12
Scheme 1.15 Manabe’s Pd-Catalyzed Fluorocarbonylation	13
Chapter 2. Cu-Catalyzed Fluorination of Diaryliodonium Salts with KF: Reaction Development and Mechanistic Investigations	
Scheme 2.1 Fluorination of Diaryliodonium Salts with KF	18
Scheme 2.2 Electronically-Controlled Selectivity	19

Scheme 2.3 Sterically-Controlled Selectivity	20
Scheme 2.4 DiMagno's Stereoelectronically-Controlled Selectivity	20
Scheme 2.5. Reactivity of Mesityl Aryl Iodonium Salts with Transition Metals	21
Scheme 2.6. Cu-catalyzed Fluorination of Diaryliodonium Salts with F ⁻	21
Scheme 2.7 Copper-Mediated Fluorination of Iodoarenes (Hartwig)	22
Scheme 2.8 Proposed Mechanism	22
Scheme 2.9 Effect of Catalyst Source (Cu ^I vs. Cu ^{II})	28
Scheme 2.10 Co-Solvent (DMF/EtOAc) for the Cu-catalyzed Fluorination	29
Scheme 2.11 Key Equilibrium Between [(Mes)(Ar)I]F and [(Mes)(Ar)I] ⁺	32
Scheme 2.12 Slow addition of Bu ₄ NF•3H ₂ O	34
Scheme 2.13 One-Pot Approach to Fluoroarenes: <i>in situ</i> Iodonium Salts Formation	38
Chapter 3. Cu-Catalyzed [¹⁸ F]Fluorination of (Mesityl)(Aryl)Iodonium Salts and Synthetic Applications	
Scheme 3.1 Synthesis of [¹⁸ F]-FDG	69
Scheme 3.2 Nucleophilic Aromatic Radiofluorination	71
Scheme 3.3 Radiofluorination of (2-Thienyl)(Aryl)Iodonium Salts	72
Scheme 3.4 Ritter's Nucleophilic Radiofluorination using Pd- and Ni-Complexes	72
Scheme 3.5 Proposed Cu-mediated Radiofluorination of Diaryliodonium Reagents	73
Scheme 3.6 Rapid Cu-Catalyzed Fluorination of (Mesityl)Aryl Iodonium Salt	74
Scheme 3.7 Cu-Catalyzed Fluorination of (Mesityl)phenyl Iodonium Salts with KF as the Limiting Reagent	74
Scheme 3.8 Cu-catalyzed [¹⁸ F]Fluorination and Quantification of Radiochemical Conversion	76
Scheme 3.9 Does Isotopic Dilution Occur Under the Optimized Condition?	80
Scheme 3.10 Current Synthesis of 4-[¹⁸ F]F-MHPG	83
Scheme 3.11 Attempted Radiofluorination of 17	84
Scheme 3.12 Automated Synthesis of [¹⁸ F]MHPG 16	86
Scheme 3.13 Acid-Promoted S _N Ar Reaction and Loss of ¹⁸ F-label from the CABS13	87
Scheme 3.14 Radiofluorination of (Mesityl)(2-chloro-3-iodopyridine)Iodonium Salt	87

Scheme 3.15 Possible Future Direction for the Radiofluorination of Pyridyl-Containing Heterocycles	88
Scheme 3.16 Direct Fluorination of Iodonium Salt Precursors by a Cu-Mediated Pathway	89
Chapter 4. Development of Cu-Mediated [¹⁸ F]Fluorination of Aryl Boronates and Synthesis of Ag[¹⁸ F]F and Its Application	
Scheme 4.1 Cu-Mediated Fluorination of Precursors for (Mesityl)(Aryl)iodonium Salts	117
Scheme 4.2 Cu-Mediated Fluorination of Aryl Trifluoroborates with KF	119
Scheme 4.3 Preliminary Results of Cu-mediated Fluorination	119
Scheme 4.4 Proposed Mechanism of the Cu-Mediated Fluorination of Ar–BF ₃ K	120
Scheme 4.5 Acceleration of Transmetalation in Miyaura Borylation and Possible Application to Cu-Mediated Fluorination of Aryl Trifluoroborates	121
Scheme 4.6 Doyle's and Grove's Elution [¹⁸ F]fluoride with Metal Complexes	123
Scheme 4.7 Cu– ¹⁸ F Formation Through Elution Method	125
Scheme 4.8 Gouverneur's Cu-catalyzed Radiofluorination of Boron Pinacol Esters	126
Scheme 4.9 Radiofluorination of Boron Pinacol Ester	127
Scheme 4.10 Utilization of Less Expensive Cu(OTf) ₂	128
Scheme 4.11 Cu-mediated Radiofluorination of Aryl Boronic Acids	130
Scheme 4.12 Possible Roles of Pyridine in the Cu-mediated Radiofluorination	132
Scheme 4.13 Cu-Mediated Fluorination of Aryl Trifluoroborates	134
Scheme 4.14 Fluorination Protocols with AgF	136
Scheme 4.15 Cu-Mediated [¹⁸ F]Fluorination of (Mesityl)(Aryl)iodonium Tetrafluoroborates with Ag ¹⁸ F	139
Scheme 4.16 Hartwig's Cu-mediated Fluorination of Aryl Iodides	139
Scheme 4.17 Direct Access by Cu-mediated [¹⁸ F]Fluorination with Ag ¹⁸ F	140
Scheme 4.18 Fluorination of 15 with Ag ¹⁸ F	141
Scheme 4.19 Proposed Mechanism of Cu-mediated Fluorination of Aryl Iodide	141

Chapter 5. Pd-Catalyzed Decarbonylative Carbon Heteroatom Bond Formations

Scheme 5.1 CO-insertion vs. CO-deinsertion	155
Scheme 5.2 Decarbonylation of Aldehydes (eq. 1) and Acid Chlorides (eq.2)	156
Scheme 5.3 Decarboxylative and Decarbonylative Cross Coupling Reactions	157
Scheme 5.4 Sanford's Decarbonylation at Pd ^{II} (Ruphos)(R _f COO)	157
Scheme 5.5 Our Ultimate Aim: Decarbonylative Fluorination	158
Scheme 5.6 Rh-mediated Decarbonylative Halogenation	160
Scheme 5.7 Pd-catalyzed Decarbonylative Chlorination	160
Scheme 5.8 Hunsdiecker Type Halogenation (eq 1) and Halogenation via a High-Valent Pd ^{IV} (eq 2) and Representative "Oxidant-X" for the Oxidation of Pd ^{II}	161
Scheme 5.9 C _{sp2} -Halogen Bond Formation	161
Scheme 5.10 Translating Pd-Catalyzed Decarbonylative Chlorination to Fluorination	167
Scheme 5.11 Buchwald's Pd-catalyzed Fluorination of Aryl Bromide	168
Scheme 5.12 Attempts at Pd-catalyzed Decarbonylative Fluorination	168
Scheme 5.13 Formation of Cross-Coupled Product	169
Scheme 5.14 Stoichiometric Reaction of Benzoyl Fluoride 18 to Pd(P(<i>t</i> -Bu) ₃) ₂	169
Scheme 5.15 Grushin's Stoichiometric Study	169
Scheme 5.16 Yamamoto's Decarbonylative Thioetherification	171
Scheme 5.17 Current Limitations: C-S bond Cleavage	174
Scheme 5.18 Decarbonylation of Vinyl and Benzylic Substrates	174
Scheme 5.19 Outcome of Decarbonylative C-S Coupling with S-phenyl 3-Phenylpropane Thiolate	175
Scheme 5.20 Resonance Stabilization of Amide Functionality	175
Scheme 5.21 Attempted Decarbonylative Amination Reactions	176
Scheme 5.22 Attempted Decarbonylative C-O Coupling Reactions	176
Scheme 5.23 Ni Insertion into C _{acyl} -O Bond Cleavage and Decarbonylation	177
Scheme 5.24 Amination, Etherification and Suzuki Coupling from Acid Chlorides	178

LIST OF FIGURES

Chapter 1. Introduction

Figure 1.1 Prevalence of Aryl Fluorides in Various Fields and Representative Examples	2
Figure 1.2 Comparisons of Fluorination Methods in Industry	3
Figure 1.3 Cost Analysis of Fluorinating Reagent (Aldrich accessed 2013)	4
Figure 1.4 Conventional Pd ^{0/II} vs. High-Valent Pd ^{II/IV} Catalytic Cycles	9
Figure 1.5 Proposed Catalytic Cycle for Pd-Catalyzed Decarbonylative Fluorination	13

Chapter 2. Cu-Catalyzed Fluorination of Diaryliodonium Salts with KF: Reaction Development and Mechanistic Investigations

Figure 2.1 Symmetrical vs. Unsymmetrical Ar ₂ I ⁺	18
Figure 2.2 Selectivity in Metal-free Arylation Reactions with Diaryliodonium Salts	19
Figure 2.3 Substrate Scope of Cu-catalyzed Fluorination	25
Figure 2.4. Proposed Cu ^{I/III} Catalytic Cycle	27
Figure 2.5 PhF Formation as a Function of Time in the Reaction of [Mes(Ph)I] ⁺ with KF Catalyzed by Cu(OTf) ₂ (◆, red) and Cu(OTf)(CH ₃ CN) ₄ (•, orange) in DMF at 60 °C	28
Figure 2.6 Three Possible Active Cu ^I Complexes Generated <i>in Situ</i>	34
Figure 2.7 Energy Profile for the Reaction of [(Mes)(Ph)I] ⁺ with CuF(DMF) at 60 °C. Energies ΔG(ΔH) in kcal/mol	35

Chapter 3. Cu-Catalyzed [¹⁸F]Fluorination of (Mesityl)(Aryl)Iodonium Salts and Synthetic Applications:

Figure 3.1 Positron Emission Tomography (PET)	67
Figure 3.2 Chemical Structures of [¹⁸ F]FDDNP, [¹⁸ F]T807 and [¹⁸ F]THK5117	68
Figure 3.3 Personalized Medicine	69
Figure 3.4 Brain Image of Patient with Brain Tumor with Low Grade Astrocytoma	70
Figure 3.5 Chemical Structure of [¹⁸ F]MHPG and [¹³¹ I]MIBG	82
Figure 3.6 Representative Radiotracers Containing 2-[¹⁸ F]fluoropyridine	86
Chapter 4. Development of Cu-Mediated [¹⁸ F]Fluorination of Aryl Boronates and Synthesis of Ag[¹⁸ F]F and Its Application	
Figure 4.1 Dry-Down Procedure for Synthesis of KF-Cryptand Complex	118
Figure 4.2 TLC Scan Image of the Reaction with TBAOAc	122
Figure 4.3 Cu-mediated Radiofluorination of Other Boron Reagents	131
Figure 4.4 Available Automated Nucleophilic [¹⁸ F]fluoride	135
Figure 4.5 Diagram of QMA and Standard Operating Procedure	138
Figure 4.6 Radiofluorination of 4-iodobiphenyl	142
Figure 4.7 Radiofluorination of 15 in <i>t</i> BuCN/CH ₃ CN	143
Chapter 5. Pd-Catalyzed Decarbonylative Carbon Heteroatom Bond Formations	
Figure 5.1 Comparison of (a) Cross-Coupling Reactions and (b) Proposed Mechanism of Decarbonylative Fluorination	159
Figure 5.2 Chlorinated Pharmaceuticals and Agrochemicals	160
Figure 5.3 Tuning Reaction Apparatus for CO Extrusion	166
Figure 5.4 Substrate Scope of Pd-catalyzed Decarbonylative Chlorination (Set-up B)	167
Figure 5.5 Representative Organic Molecules Containing Diaryl Sulfides	170
Figure 5.6 Substrate Scope of Ar-S-Ph	173

LIST OF TABLES

Chapter 1. Introduction

Table 1.1 Ph–X Bond Strengths for X = F, Cl, Br, I 6

Table 1.2 Comparison of Thermodynamics and Kinetics Involving C_{sp2}–Halogen Bond Formation 7

Chapter 2. Cu-Catalyzed Fluorination of Diaryliodonium Salts with KF: Reaction Development and Mechanistic Investigations

Table 2.1 Evaluation of Copper Salts 23

Table 2.2. Cu-catalyzed Fluorination of [Mes(Ph)I]⁺ as a Function of Cu Precatalyst and Solvent 29

Table 2.3. Cu^{III} Trapping Experiment 31

Table 2.4. Evaluation of Different Fluoride Sources 31

Table 2.5 Computation for Reactions of Cu^I and [Mes(Ph)I]⁺ with Donor Ligands Present During Cu-Catalyzed Reactions 32

Table 2.6. KF Loading Study 33

Chapter 3. Cu-Catalyzed [¹⁸F]Fluorination of (Mesityl)(Aryl)Iodonium Salts and Synthetic Applications:

Table 3.1 Evaluation of Cu Salts with Iodonium Salt **1** to Yield 4-[¹⁸F]anisole 77

Table 3.2 Scope of Cu-Mediated [¹⁸F]fluorination of (Mesityl)(Aryl)Iodonium Salts 78

Table 3.3. Studies on Counteranion Effects 80

Table 3.4 Influence of Temperature 81

Table 3.5 Specific Activity Calculation 82

Table 3.6 Cu-Mediated Radiofluorination of 19	85
---	----

Chapter 4. Development of Cu-Mediated [¹⁸F]Fluorination of Aryl Boronates and Synthesis of Ag[¹⁸F]F and Its Application

Table 4.1 Examination on Air and Water Tolerance of the Protocol	119
Table 4.2 Acetate Salt Additives for Cu-mediated Reactions	121
Table 4.3 Elution Studies with Cu Catalysts	124
Table 4.4 Carrier-Added Cu-Mediated Fluorination	126
Table 4.5 Evaluation of Weak Ionic bases/acids for ¹⁸ F-Fluoride Elution	128
Table 4.6 Radiofluorination of Aryl Boroxines	133
Table 4.7 Cu-Mediated Fluorination of Aryl Boroxines	133
Table 4.8 Synthesis of Ag ¹⁸ F	137
Table 4.9 Preconditions of QMA Cartridge for Ag ¹⁸ F Synthesis	138

Chapter 5. Pd-Catalyzed Decarbonylative Carbon Heteroatom Bond Formations

Table 5.1 Ligand Screen with Different Denticity	162
Table 5.2 Buchwald's Biarylmonophosphine Ligand Screen (in a sealed 4 mL vial)	163
Table 5.3 Palladium Precatalyst Screening (in a sealed 4 mL vial)	164
Table 5.4 Temperature Study (in a sealed 4 mL vial)	165
Table 5.5 Control Studies (Set-Up B)	166
Table 5.6 Preliminary Investigation of Decarbonylative C–S Cross-Coupling Reactions for the Synthesis of Diaryl Sulfide (Set-Up B or E)	172
Table 5.7 Ligand Screen for Thioetherification	172

LIST OF ABBREVIATIONS

Å	Angstrom
A	amplifier
Ac	Acetyl
AD	Alzheimer's disease
Ar	Aryl
Boc	<i>tert</i> -Butyloxycarbonyl
Bu	butyl
Ci	Curie (unit)
cGMP	Current Good Manufacturing Practice regulations
COD	1,5-Cyclooctadiene
CTE	Chronic traumatic encephalopathy
C°	Celsius
DBN	1,5-Diazabicyclo[4.3.0]non-5-ene
DFT	Density Functional Theory
DG	Directing group
DMF	<i>N,N</i> -Dimethylformamide
EtOAc	Ethyl acetate
Et ₂ O	Diethyl ether
18-crown-6	1,4,7,10,13,16-hexaoxacyclooctadecane
FDDNP	2-(1-(6-[(2-[¹⁸ F]fluoroethyl)(methyl)amino]2-naphthyl)ethylidene)malononitrile
FDG	fluorodeoxyglucose
FEP	Fluorinated ethylene propylene
g	gram

GC	Gas chromatography
GC-MS	Gas chromatography mass spectrometry
DMSO	Dimethyl sulfoxide
HPLC	High performance liquid chromatography
HRMS	High-resolution mass spectrometry
Hz	Hertz
Kryptofix	4,7,13,16,21,24-Hexaoxa-1,10-diazabicyclo[8.8.8]hexacosane
L-DOPA	L-3,4-dihydroxyphenylalanine
M	Molarity
m-CPBA	<i>meta</i> -chloroperoxybenzoic acid
Me	Methyl
Mes	Mesityl
MesF	fluoromesitylene
MesI(OAc) ₂	Iodomesitylene diacetate
MHPG	4-[¹⁸ F]Fluoro- <i>m</i> -hydroxyphenethylguanidine
MIBG	<i>meta</i> -Iodobenzylguanidine
mL	mililiter
MPPF	2'-methoxyphenyl-(<i>N</i> -2'-pyridinyl)- <i>p</i> -fluoro-benzamidoethylpiperazine
NHC	<i>N</i> -heterocyclic carbene
NMP	<i>N</i> -methyl-2-pyrrolidone
NMR	Nuclear Magnetic Resonance
OAc	Acetate
OTf	Trifluoromethane sulfonate
OTs	tosylate
PEB	[¹⁸ F]3-fluoro-5-[(pyridine-3-yl)ethynyl]benzonitrile
PET	Positron Emission Tomography
Ph	phenyl
PhF	fluorobenzene
ppm	parts per million

PTFE	Polytetrafluoroethylene
PVDF	Polyvinylidene fluoride
Py	pyridine
QMA	quaternary ammonium
RAD	Radiation absorbed dose
RCC	Radiochemical conversion
RCY	Radiochemical yield
Rf	retardation factor
Salen	2,2'-Ethylenebis(nitrilomethylidene)diphenol, N,N'-Ethylenebis(salicylimine)
SA	Specific activity
SAR	Structural activity relationship
S _N Ar	Nucleophilic aromatic substitution
t _{1/2}	Half-life
TBA	<i>tetrabutylammonium</i>
<i>t</i> BuCN	Trimethylacetonitrile
TFA	Trifluoroacetic acid
TLC	Thin-layer chromatography
UV-vis	Ultraviolet-visible spectroscopy

ABSTRACT

The development of novel methods to incorporate fluorine and fluoroalkyl groups into organic molecules is highly desirable, as these substituents can impart unique stability, reactivity and biological properties. Over the past decade, tremendous efforts have been expended to develop transition metal-catalyzed aromatic fluorination methodologies. Nevertheless, carbon–fluorine bond formation remains challenging, especially in the context of general, functional group-tolerant late-stage fluorinations of arenes. Ultimately, gaining direct accessibility to highly functionalized and complex fluorinated pharmaceutical and radiopharmaceutical precursors is a central objective of this field.

Chapter 1 describes the key challenges in the field C–F bond formation key considerations in industry, as well as the relevant history and precedent for the work detailed herein.

Chapter 2 begins with our initial development of the copper-catalyzed fluorination of unsymmetrical diaryliodonium salts with KF. This transformation proceeds with high chemoselectivity and yields. Detailed computational and experimental mechanistic analyses established the key role of the solvent in catalysis and rationalized the chemoselectivity in Cu-catalyzed reactions of unsymmetrical iodonium salts.

Chapter 3 describes detailed efforts into the translation of the Cu-catalyzed fluorination of diaryliodonium salts to radiofluorination. The fluorine-18 radionuclide is the most widely utilized for *in vivo* imaging by positron emission tomography. However, the lack of rapid, practical radiofluorination methods hinders newly developed radiotracers entering into clinic. We have identified conditions that rapidly incorporate fluorine-18 into electron-rich arenes in 20 minutes under mild conditions. Importantly this chemistry can be further applied to synthesize clinically important radiotracers.

Chapter 4 details the exploration of the Cu-mediated radiofluorination of aryl boronates and aryl halides. Extensive studies on developing a new elution method allowed operationally simple, highly reproducible means to make anhydrous $^{18}\text{F}^-$ effective for Cu catalysis.

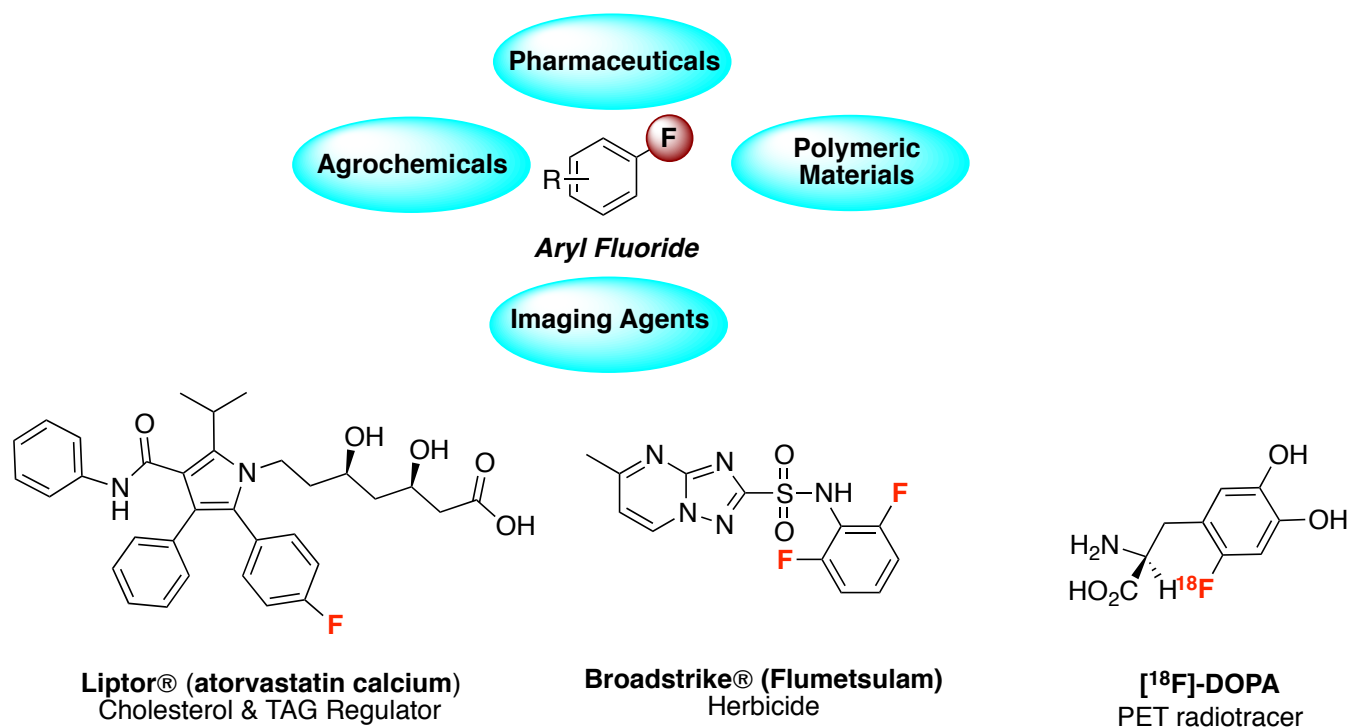
Chapter 5 investigates a novel Pa-catalyzed decarbonylative fluorination method to incorporate a carbon-fluorine bond. The protocol aims to utilize aryl fluorides as both the fluorine and arene source that oxidatively adds to metals in a single step, thereby minimizing the complexity and waste in this step of the synthesis. This work was further extended to form various carbon-heteroatom bonds, starting from acid chlorides in one pot.

CHAPTER 1. INTRODUCTION

1.1 SIGNIFICANCE OF FLUORINE

Fluorinated organic compounds, particularly aryl fluorides, have found numerous applications in pharmaceuticals, agrochemicals, radiopharmaceuticals and polymeric materials.¹ The replacement of C–H bonds with C–F bonds can lead to improvement of the stability, reactivity, and/or biological properties of organic molecules (Figure 1.1). Approximately 40% of agrochemicals and 20% of pharmaceuticals contain at least one fluorine atom, often located on aromatic rings. In addition, fluorocarbon based polymers (PTFE, PVDF, FEP and fluoroelastomers) are widely used in automotives, electronics, chemical processing, and industrial equipment. By 2019, the global fluoropolymer market is projected to reach approximately 8 billion dollars in revenue.² Additionally, fluorine-18 (¹⁸F) tagged radiotracers are abundant in radiopharmaceuticals. Positron Emission Tomography (PET) is a minimally invasive imaging technique that provides physiochemical information. Greater than 90% of PET scans are performed annually using ¹⁸F-labeled molecules. Due to the ideal half-life of ¹⁸F (110 minutes), ¹⁸F radiotracers are broadly useful for monitoring *in vivo* metabolic processes that are critical for drug discovery and disease diagnosis. For these reasons, chemists have long sought to develop methods for constructing medicinally relevant carbon-fluorine bonds.¹

Figure 1.1. Prevalence of Aryl Fluorides in Various Fields and Representative Examples

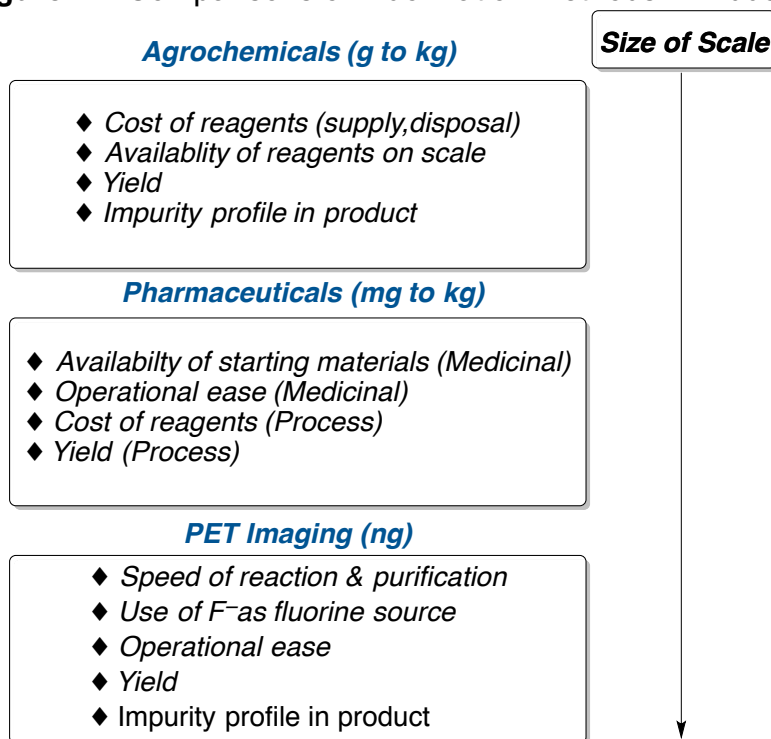


1.2 KEY CONSIDERATIONS FOR SUCCESSFUL FLUORINATION PROCESS

For the successful development of new fluorination methods, it is important to consider differences in scale between pharmaceuticals, agrochemicals and PET imaging techniques and incorporate these considerations into the design of a new transformation (Figure 1.2). In agrochemicals and pharmaceuticals (especially for applications in process chemistry), the total cost, the availability of reagents, and the yield of the fluorinated products are the key factors sought in a fluorination method. In contrast, medicinal chemistry or PET imaging has other priorities for choosing an appropriate fluorination method. Generally radiopharmaceuticals and lead drug molecules are only synthesized in milligram to nanogram quantities. Therefore, speed, operational ease, and late-stage derivatization are often the key considerations for these transformations. When using the short-lived [¹⁸F]fluoride radionuclide, the speed and operational ease of the radiofluorination are particularly critical for radiopharmaceutical synthesis. Due to the limited lifetime of [¹⁸F]fluoride, it is ideal to incorporate [¹⁸F]fluoride at a late stage of synthesis. Similarly, late-stage fluorination is

especially important in medicinal chemistry (even in agrosience) to evaluate fluorinated molecules in structure activity relationship (SAR) studies.³ The SAR studies are to determine the relationship between chemical structures and their biological activities that evokes target biological effects. Therefore, enabling late-stage derivatization of substituents in architecturally complex molecules will provide ease of such testings.

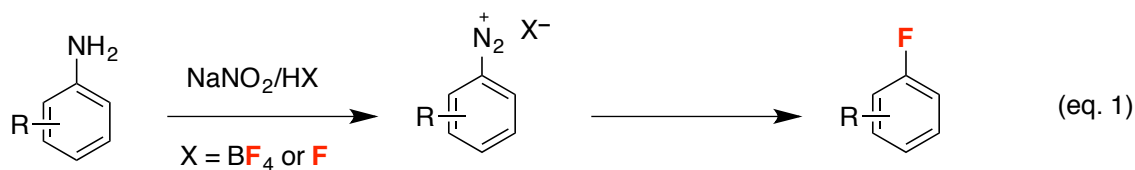
Figure 1.2 Comparisons of Fluorination Methods in Industry⁴



1.3 CLASSIC FLUORINATION PROCESSES THAT ARE STILL IN USE

The most common nucleophilic aromatic fluorination methods today were developed in the late 19th to 20th centuries and are still widely utilized in industrial chemistry.⁵ The two conventional fluorination processes are the Balz-Schiemann reaction (eq. 1, Scheme 1.1)⁶ and halox fluorination reactions⁷ (eq. 2, Scheme 1.1). The Balz-Schiemann reaction involves the thermal decomposition of diazonium tetrafluoroborates/fluorides, synthesized by the diazotization of the corresponding aromatic amine.⁵ The halox fluorination method converts activated chloroarenes into the corresponding fluoroarenes in the presence of alkali-metal fluorides (eq. 2).

Scheme 1.1 Conventional Nucleophilic Fluorination Routes³⁻⁵



A number of electrophilic aromatic fluorination methods are also well-known (Scheme 1.2).^{1,5} However, the use of toxic fluorine gas,⁸ poor regioselectivity, and/or the requirement for expensive electrophilic fluorinating reagents (i.e. Selectfluor) make these methods less economical for industrial scale synthesis (Figure 1.3).⁹

Scheme 1.2 Representative Electrophilic Fluorination Method^{6,7}

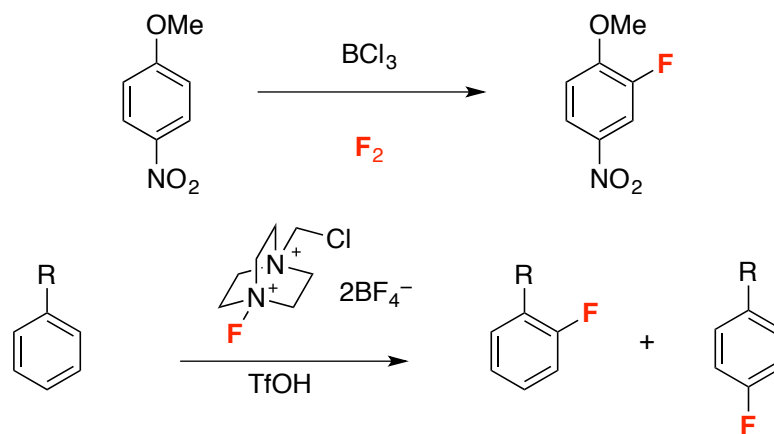


Figure 1.3 Cost analysis of Fluorinating Reagent (Aldrich accessed 2013)

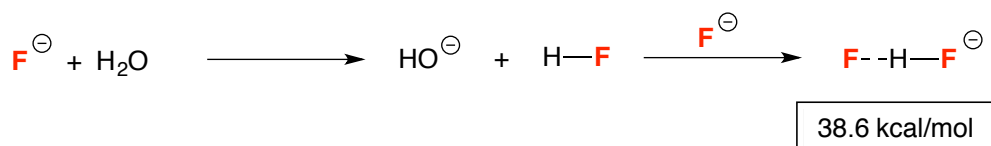
"F ⁺ "	 \$9,633/mol	 \$29,504/mol	 Selectfluor® \$1162/mol	 \$88,295/mol
"F ⁻ "	AgF \$1264/mol	CsF \$181/mol	KF \$35.6/mol	

Importantly, both the nucleophilic and electrophilic methods described in this section do not meet key considerations for methods suitable for pharmaceutical or radiopharmaceutical synthesis. These conventional methods require forcing conditions and possess poor functional group tolerance. As a result, one typically has to resort to *de novo* syntheses in order to evaluate fluorinated molecules in SAR studies in pharmaceuticals or agrochemicals.

1.4 CHALLENGES WITH THE FLUORINATION PROCESS

Despite the wide utility of fluorinated compounds, there are a limited number of practical synthetic methods for aromatic fluorination. One of the challenges associated with C-F bond formation is the low nucleophilicity of the fluoride (F^-).¹⁰ Common, inexpensive fluoride salts (e.g. KF and CsF) are poorly soluble in organic solvents and even traces of water can attenuate the nucleophilicity of fluoride by strong hydrogen bonding interactions (38.6 kcal mol⁻¹ for bifluoride, HF_2^-). Thus these methods require rigorously anhydrous conditions to achieve high yields, which can be a drawback in terms of practical synthesis (Scheme 1.3).¹¹

Scheme 1.3 Hydrogen Bonding Energy of $F\cdots HF$ ¹¹



1.5 EARLY STUDIES ON $AR-F$ BOND FORMATION FROM METAL FLUORIDE COMPLEXES

Over the past decade, there has been tremendous progress in the development of transition metal-catalyzed cross-coupling reactions to form C-F bonds.¹² Such reactions are believed to proceed via the simplified catalytic cycle shown in Scheme 1.5. Stoichiometric studies were carried out to gain insight into the C-F bond formation event. In theory, the carbon-fluorine bond is a thermodynamically favorable process as a $C_{Ar}-F$ bond possesses the highest bond dissociation energy ($F > Cl > Br > I$) (Table 1.1).¹³ Being thermodynamically allowed, transition-metal catalyzed fluorination of aryl halides would initially seem a suitable target for catalysis. However, early attempts at examining

the fluorination of aryl halides/pseudohalides catalyzed by low-valent transition metals (i.e. Ni, Pd, Pt, Ru, Co and Rh) were unsuccessful (Scheme 1.4).¹⁴

Scheme 1.4 Simplified Proposed Catalytic Cycle for Metal-Catalyzed C–F Bond

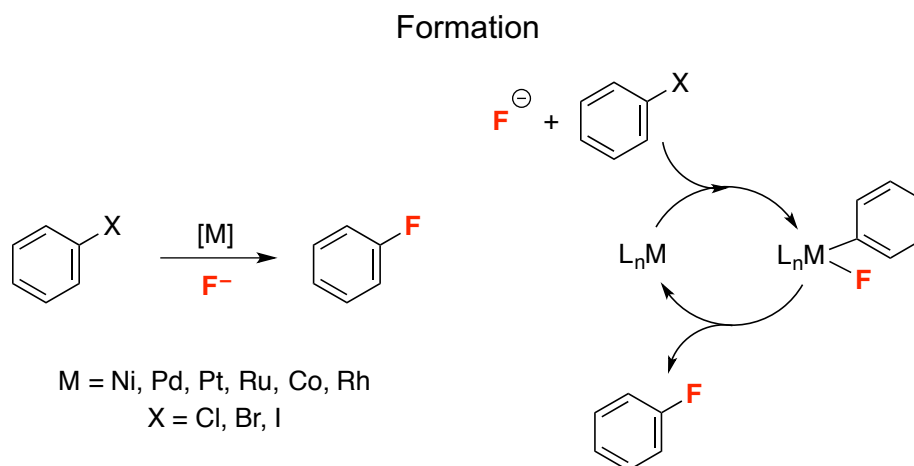
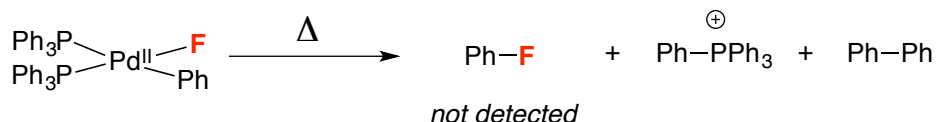


Table 1.1 Ph–X Bond Strengths for X = F, Cl, Br, I¹³

X	Ph–X Bond Strengths (kcal/mol)
F	126
Cl	96
Br	81
I	65

For example, in 2002, Grushin reported the synthesis and characterization of the first palladium fluoride complex (PPh₃)₂PdPhF.¹⁵ However, this Pd^{II} complex did not undergo reductive elimination to form the desired Ph–F upon heating (Scheme 1.5). This study identified reductive elimination of aryl fluoride from Pd^{II} as the challenging step of this transformation.

Scheme 1.5 Grushin's First Isolated Pd(II)PhF Complex



Mechanistic studies by Hartwig and coworkers revealed the relationship between electronegativity of halogens and activation energy in the context of C_{Ar}–X bond formation from {Pd[P(o-tol)₃](Ar)(μ–X)}₂ (X = Cl, Br and I) (Scheme 1.6).¹⁶ First, increasing electronegativity of the reacting halide increases the thermodynamic driving force but decreases the rate (i.e. increases the activation energy) for reductive elimination. Their calculated equilibrium constants K_{eq} correlated with the bond strength

of the resultant product Ph–X, while the rates of reductive elimination of aryl halides showed the opposite trend. Faster rate of reductive elimination for bromoarene and iodoarenes were attributed to the higher polarizability and greater electron-donating ability of these halogens. This explains why the reductive elimination to form a *thermodynamically* feasible C_{Ar}–F bond is *kinetically* challenging. Second, in their study, the reductive elimination of haloarene occurs via a three-coordinated arylpalladium^{II} halide monomer by cleaving the starting dimer, accompanied by the ligation of P(*t*-Bu)₃. Therefore, since the starting dimers were shown thermally stable unless the addition of ligand to facilitate the cleavage of M–F bridge, it suggested the fluoride-bridged dimer can be similarly a resting state of Pd^{II}ArF complex before reductive elimination to occur.

Scheme 1.6 C_{sp2}–Halogen Bond Formation: Kinetics vs. Thermodynamics

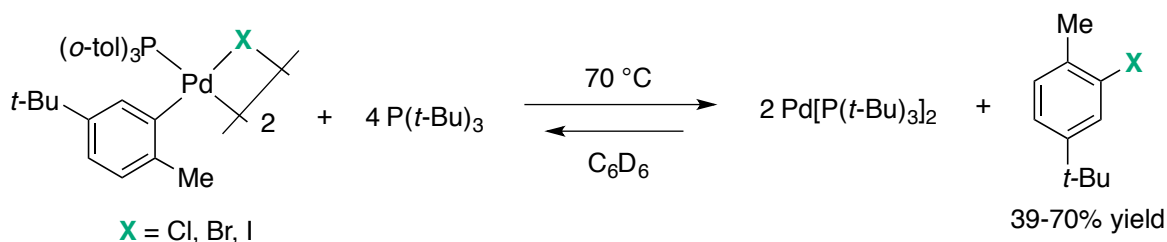
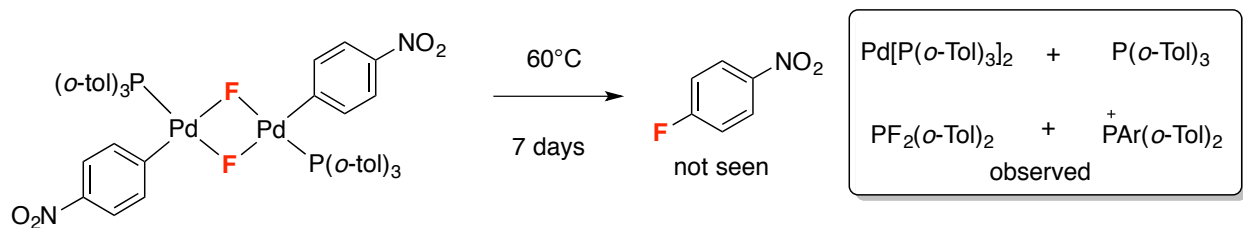


Table 1.2 Comparison of Thermodynamics and Kinetics Involving C_{sp2}–Halogen Bond Formation

X	K _{eq}	Ph–X (kcal/mol)	k _{obs} (s ⁻¹)
Cl	9.0 x 10 ⁻²	96	1.28 x 10 ⁻⁴
Br	2.3 x 10 ⁻³	81	1.42 x 10 ⁻⁴
I	3.7 x 10 ⁻⁵	65	--

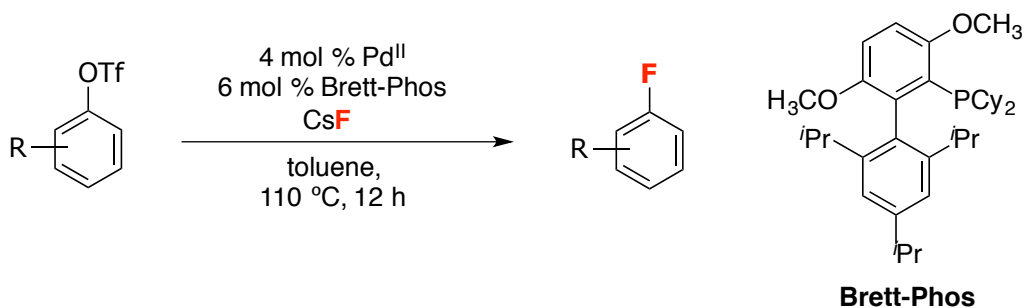
In 2007, Yandulov computationally and experimentally studied aryl fluoride reductive elimination from Pd^{II}.¹⁷ His computational studies revealed that the monomer LPd^{II}(Ar)(F) forms a fluoride-bridged dimer that is stable to reductive elimination. Experimentally, it was shown no reductive elimination of 4-fluoronitrobenzene was observed from {Pd[P(*o*-tol)₃](*p*-NO₂Ph)(μ-F)}₂ after stirring at 60 °C for a week (Scheme 1.7). Thus, the stable Pd^{II} dimer formation was identified as the key remaining obstacle to Ar-F reductive elimination in this system.

Scheme 1.7 Thermal Reactivity of Pd-F Dimer



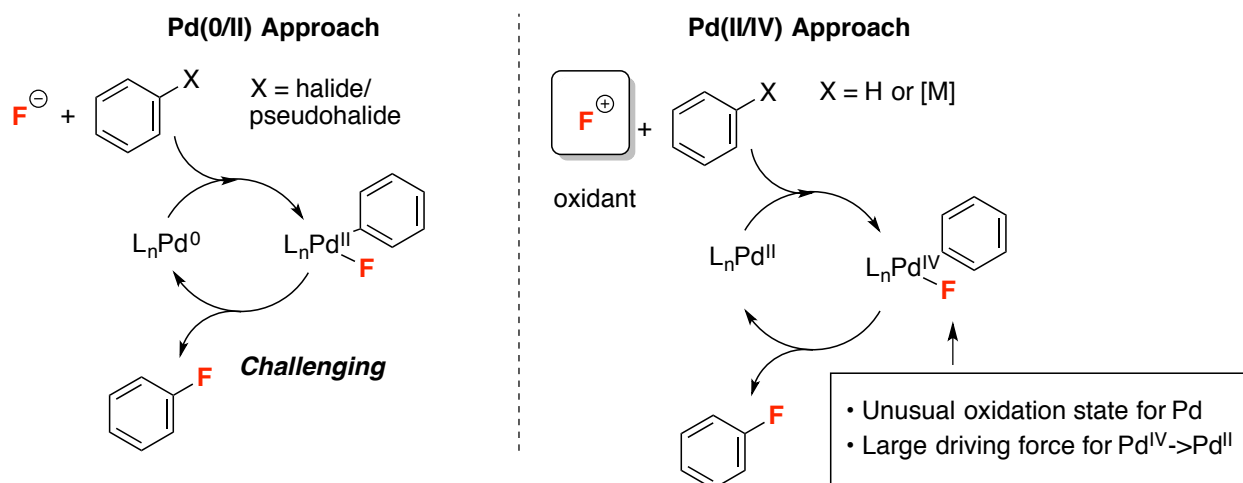
Shortly after, Buchwald and coworkers disclosed the Pd-catalyzed nucleophilic aromatic fluorination of aryl triflates using CsF as a fluorinating reagent. A bulky monodentate biarylphosphine ligand, BrettPhos, was found to stabilize a three coordinate intermediate that subsequently underwent reductive elimination. This was the first example of nucleophilic fluorination achieved through a $\text{Pd}^{0/\text{II}}$ catalytic cycle.¹⁸ Despite this advancement, this fluorination method still has a limited substrate scope, results in the formation of undesirable regioisomers,¹⁹ and requires long reaction times. More recent efforts have demonstrated Pd-catalyzed fluorination of aryl triflates and aryl bromides under milder conditions.²⁰

Scheme 1.8 $\text{Pd}^{0/\text{II}}$ -catalyzed Nucleophilic Aromatic Fluorination¹⁸⁻²⁰



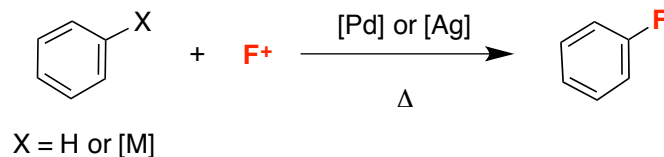
Collectively, these examples demonstrate that reductive elimination of haloarenes from Pd^{II} center is a challenging transformation. As an alternative approach for $\text{C}_{\text{Ar}}\text{-F}$ bond formation, the Sanford lab has employed electrophilic fluorinating reagents (F^+) to access high-valent $\text{Pd}^{\text{IV}}(\text{Ar})\text{F}$ complexes.^{21,20} This high-energy intermediate can then undergo facile reductive elimination to form the desired $\text{C}_{\text{Ar}}\text{-F}$ product (Figure 1.4).²² The thermodynamic instability of Pd^{IV} is believed to be a driving force for this difficult $\text{C}_{\text{Ar}}\text{-F}$ bond formation.

Figure 1.4 Conventional Pd^{0/II} vs. High-Valent Pd^{II/IV} Catalytic Cycles



In 2006, the Sanford lab disclosed the first Pd^{II/IV} catalyzed aryl fluorination of C–H bonds using *N*-fluoropyridinium oxidants as the electrophilic fluorinating oxidant.²³ More recently, the Yu lab further extended our initial work in C_{Ar}–F bond formation.²⁴ Another closely related example is Ritter's Ag-catalyzed electrophilic fluorination of aryl stannanes,^{25,26} aryl boronic acids²⁷ and aryl silanes²⁸ using Ag catalyst and Selectfluor. In all cases, the current limitations are the use of electrophilic fluorinating reagent as an oxidant in conjunction with use of noble metals (Scheme 1.9). Although our group has demonstrated reductive elimination of aryl fluorides from putative Pd^{IV} intermediates, these above oxidative C–F bond forming processes are unfortunately not readily amenable to integration into alkali MF-based catalytic fluorination cycles. This transformation requires the use of expensive F⁺ reagents in stoichiometric amounts. Hence, for a scale-up synthesis, it remains cost-prohibitive and it is unsuitable for PET chemistry,²⁹ as nucleophilic fluoride is preferred for this application.

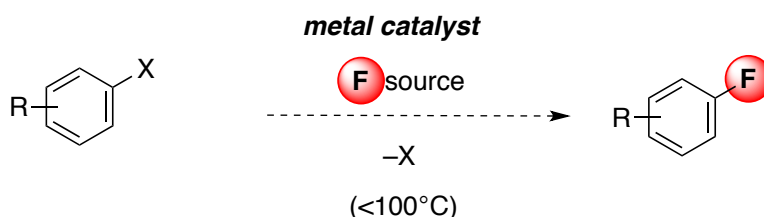
Scheme 1.9 Transition Metal-Catalyzed Electrophilic Fluorination



1.6 TRANSITIONING TO NOVEL, MORE COST-EFFECTIVE APPROACH

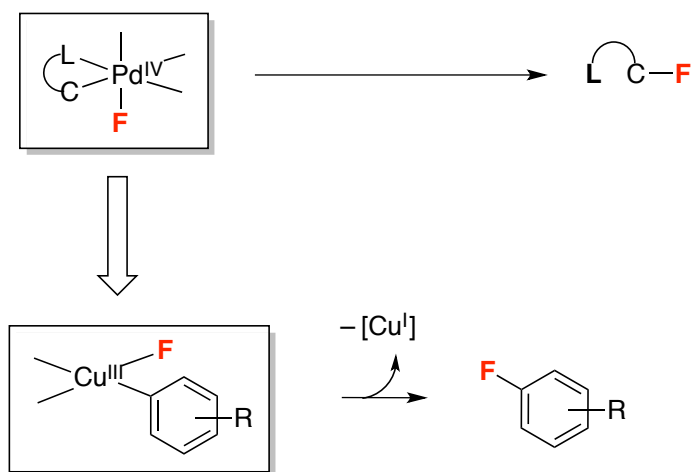
The goal of my thesis is to develop novel nucleophilic fluorination methods that are practical and efficient. A key unmet need in the field is a mild and general aryl fluorination protocol, allowing $C_{Ar}-F$ bond formation at a late stage of syntheses of complex molecules, using nucleophilic fluoride (Scheme 1.10). In order to solve this long-standing challenge, we have considered two approaches towards nucleophilic fluorination: Cu-catalyzed fluorination and Pd-catalyzed decarbonylative fluorination.

Scheme 1.10 Transition Metal-Catalyzed Fluorination



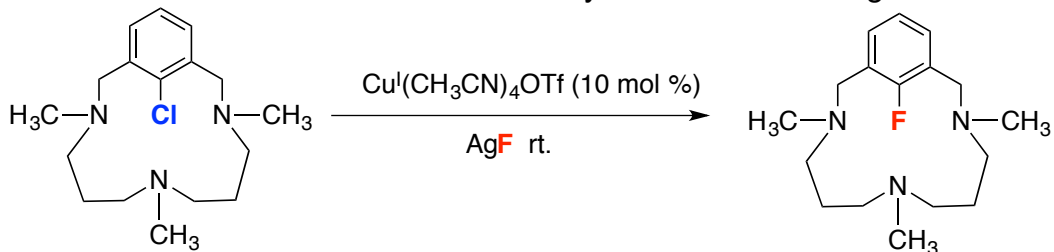
Cu-catalyzed Nucleophilic Fluorination. In order to target a milder reaction that is more functional group compatible and inexpensive, one strategy is to find a means to oxidize a metal center to access high-valent intermediates in the presence of oxidant and nucleophilic fluoride. We hypothesized that such an approach might be feasible with Cu catalysis.³⁰ The use of ‘high-valent’ organometallic copper intermediates has recently been used to achieve difficult bond formations (Scheme 1.11). The development of copper and palladium catalysis has been closely related as both metals have been used extensively in the construction of similar types of carbon–carbon and carbon–heteroatom bonds.³⁰ Therefore, one of my thesis goals is aimed towards developing a novel, more cost-effective fluorination approach utilizing nucleophilic fluoride sources (F^-) and copper, an inexpensive and earth-abundant first row transition metal (Scheme 1.14). High-valent Cu^{III} , like Pd^{IV} , should facilitate the formation of challenging bonds such as aryl-fluorides, sharing the nature of high reactivity in catalysis.^{30,31}

Scheme 1.11 Moving Towards More Cost-Effective Approach: High-Valent Organometallic Copper Chemistry for Achieving C–F Bond Formation



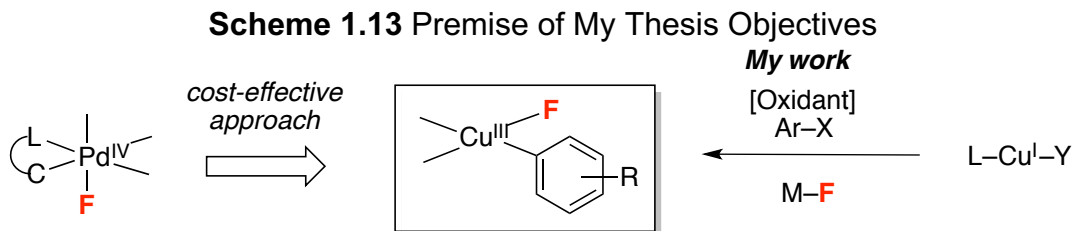
This investigation was further inspired by work from the Ribas lab in which C–F bond formation at Cu^{III} was demonstrated utilizing a macrocyclic ligand (Scheme 1.12). Although Riba’s report only shows a single substrate for such transformation, computational studies revealed low activation barriers for the reductive elimination step. Their excellent work fueled our interest in the use of Cu for developing more general fluorination methods. The low cost of Cu compared to other noble metals renders it a particularly attractive alternative. Hence, copper mediated fluorination has become a rapidly developing field of research. However, when my investigation first started, there was no general Cu fluorination method that used substoichiometric/catalytic amounts of Cu.

Scheme 1.12 Riba’s Cu-catalyzed Halide Exchange



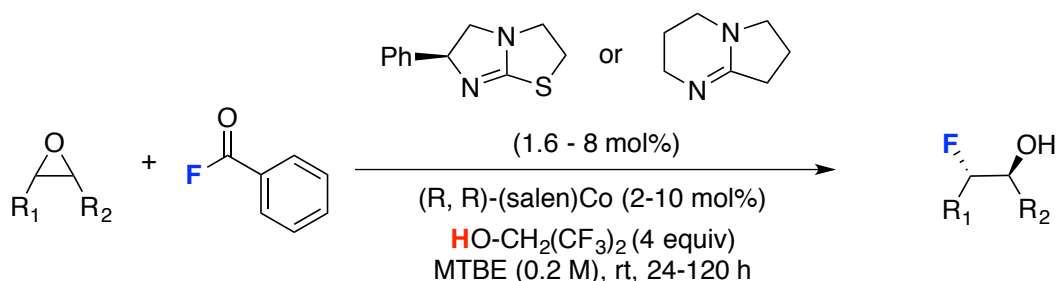
The first objective of my thesis was to develop a general Cu-catalyzed/mediated-fluorination method that proceeded via high-valent Cu^{III} intermediates. This transformation would be highly cost effective and could extend the current scope of nucleophilic fluorination, given the facile reductive elimination expected from a high-

valent Cu intermediate (Scheme 1.13). While we are investigating our Cu-mediated fluorination, many including Hartwig and Ritter, have contributed to the field.³²



Pd-Catalyzed Decarbonylative Fluorination. The second aim of my thesis was to develop a transition metal catalyzed nucleophilic fluorination utilizing non-alkali metal fluoride sources. One drawback of the fluorination is the poor solubility of alkali metal fluorides. The ideal fluoride reagent is KF because of its abundant availability and low cost, but the rate of reaction can be hindered by the low solubility of fluoride in organic solvents such as DMSO, DMF or CH₃CN. This often leads to a necessity of phase transfer catalysts (tetraalkylammonium salts, phosphonium salts or cryptands).³³ One of the underexplored fluorinating reagents is benzoyl fluoride. Doyle first demonstrated the use of benzoyl fluoride as a fluorinating reagent for asymmetric epoxide opening reactions (Scheme 1.14).³⁴ (-)-Tetraamisolet and DBN were utilized as Lewis bases that could attack the carbonyl to expel a nucleophilic fluoride. This well-solvated nucleophilic fluoride was then reacted with external electrophiles.

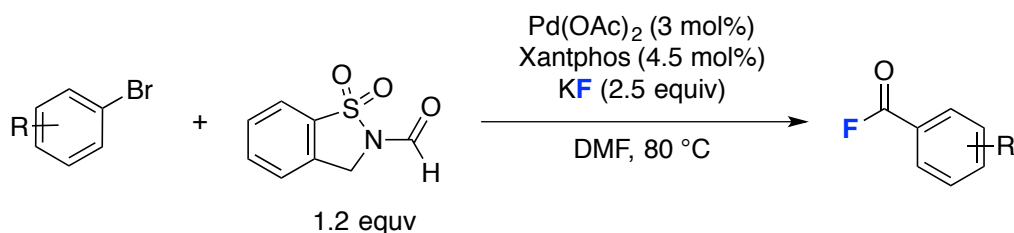
Scheme 1.14 Doyle's Asymmetric Epoxide Opening Fluorination



One can envision that electron-rich transition metals could insert into the C_{acyl}-F bond at the oxidative addition step, followed by decarbonylation and reductive elimination of aryl fluorides to complete the catalytic cycle (Figure 1.4). As an added advantage, acyl fluorides are known to be stable to column chromatography and easily accessible from corresponding carboxylic acids. A closely related example of the reverse reaction was

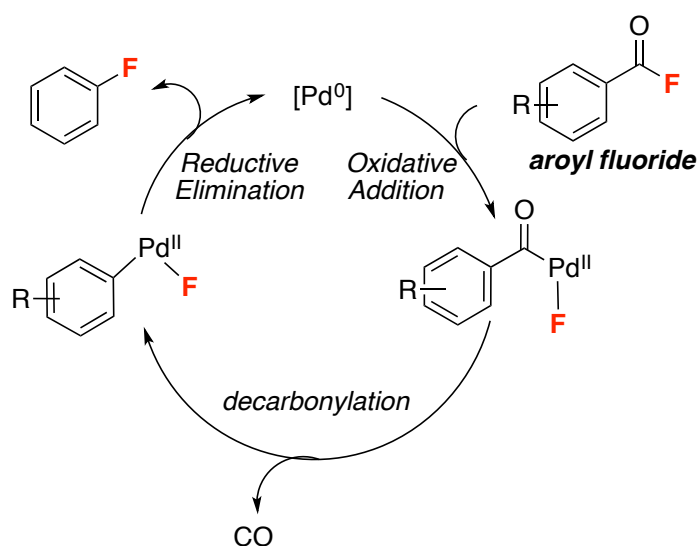
demonstrated by Manabe and his colleagues.³⁵ They recently have shown that Pd-catalyzed carbonylative fluorination to produce acid fluoride products is possible using *N*-formyl saccharin as a CO source (Scheme 1.15).

Scheme 1.15 Manabe's Pd-Catalyzed Fluorocarbonylation



Though there is no mechanistic proposal in the article, this protocol suggests the accessibility of a putative Pd^{II}(Acyl)F complex. Furthermore, Grushin and coworkers previously observed the formation of (PPh₃)₂Pd(COPh)F by ¹H NMR below 10 °C.³⁶ Given that Ar–F reductive elimination at Pd^{II} has been demonstrated under specific reaction conditions,^{20g} we reasoned that the proposed Pd-decarbonylative fluorination should also be feasible based on microscope reversibility. In addition, a number of decarbonylation reactions have been reported at a Pd⁰ center, thereby supporting the feasibility of our proposed method.³⁷ Such a protocol would be efficient and atom economical, as the benzoyl fluoride would serve as both the fluoride and aryl source, and CO would be the byproduct in the overall transformation (Figure 1.5).

Figure 1.5 Proposed Catalytic Cycle for Pd-Catalyzed Decarbonylative Fluorination



In summary, this dissertation describes our work in the development of Cu-catalyzed fluorination of diaryliodonium salts and its mechanistic elucidation (Chapter 2), translation of the Cu method to [^{18}F] fluorination (Chapter 3), and development of Ag^{18}F elution and translation of known ^{19}F -methods with Ag^{18}F (Chapter 4). These chapters are followed by preliminary studies of the development of decarbonylative functionalizations of arenes (Chapter 5).

1.7 REFERENCES

- (1) (a) Furuya, T.; Kamlet, A. S.; Tobias, R. *Nature* **2011**, 473, 470. (b) Purser, S.; Moore, P. R.; Swallow, S.; Gouverneur, V. *Chem. Soc. Rev.* **2008**, 37, 320. (c) Campbell, M. G.; Tobias, R. *Chem. Rev.* **2014**, 115, 612. (d) Wang, J.; Sánchez-Roselló, M.; Aceña, J. L.; del Pozo, C.; Sorochinsky, A. E.; Fustero, S.; Soloshonok, V. A.; Liu, H. *Chem. Rev.* **2014**, 114, 2432.
- (2) Markets and Markets. Fluoropolymers Market Worth \$8,816.4 Million by 2019. <http://www.marketsandmarkets.com/PressReleases/fluoropolymers.asp> (accessed January 26, 2016).
- (3) Purser, S.; Moore, P. R.; Swallow, S.; Gouverneur, V. *Chem. Soc. Rev.* **2008**, 37, 320.
- (4) Sanford, M.S. *Development of Fluorination Reactions: Fundamental Research to Industrial Applications*. In CENTC Summer School, Seattle, Washington, July 2015.
- (5) Siegemund, G.; Schwertfeger, W.; Feiring, A.; Smart, B.; Behr, F.; Vogel, H.; McKusick, B.; Kirsch, P. *Fluorine Compounds, Organic*; Wiley-VCH Verlag GmbH & Co. KGaA.
- (6) (a) Balz, G.; Schiemann, G. *Ber. Deutsch. Chem. Ges.* **1927**, 60, 1186. (b) Swain, C. G.; Rogers, R. J. *J. Am. Chem. Soc.* **1975**, 97, 799.
- (7) (a) Gottlieb, H. B. *J. Am. Chem. Soc.* **1936**, 58, 532. (b) Adams, D. J.; Clark, J. H. *Chem. Soc. Rev.* **1999**, 28, 225.
- (8) Chambers, R. D.; Hutchinson, J.; Sandford, G. *J. Fluorine. Chem.* **1999**, 100, 63.
- (9) Zupan, M.; Iskra, J.; Stavber, S. *Bull. Chem. Soc. Jpn.* **1995**, 68, 1655.
- (10) Pearson, R. G.; Sobel, H. R.; Songstad, J. *J. Am. Chem. Soc.* **1968**, 90, 319.
- (11) Larson, J. W.; McMahon, T.B. *Inorg. Chem.* **1984**, 23, 2029.
- (12) (a) Liang, T.; Neumann, C. N.; Tobias, R. *Angew. Chem. Int. Ed.* **2013**, 52, 8214. (b) Champagne, P. A.; Desroches, J.; Hamel, J.-D.; Vandamme, M.; Paquin, J.-F. *Chem. Rev.* **2015**, 115, 9073.
- (13) Grushin, V. V.; Alper, H. *Chem. Rev.* **1994**, 94, 1047.
- (14) Grushin, V. V. *Acc. Chem. Res.* **2010**, 43, 160.
- (15) Grushin, V. V. *Chem. Eur. J.* **2002**, 8, 1006.
- (16) Roy, A. H.; Hartwig, J. F. *Organometallics* **2004**, 23, 1533.
- (17) Yandulov, D. V.; Tran, N. T. *J. Am. Chem. Soc.* **2007**, 129, 1342.
- (18) Watson, D. A.; Su, M.; Teverovskiy, G.; Zhang, Y.; García-Fortanet, J.; Kinzel, T.; Buchwald, S. L. *Science* **2009**, 325, 1661.
- (19) Milner, P. J.; Kinzel, T.; Zhang, Y.; Buchwald, S. L. *J. Am. Chem. Soc.* **2014**, 136, 15757.
- (20) (a) Sather, A. C.; Lee, H. G.; La Rosa, De, V. Y.; Yang, Y.; Müller, P.; Buchwald, S. L. *J. Am. Chem. Soc.* **2015**, 137, 13433. (b) Milner, P. J.; Yang, Y.; Buchwald, S. L. *Organometallics* **2015**, 34, 4775. (c) Sather, A. C.; Lee, H. G.; Colombe, J. R.; Zhang, A.; Buchwald, S. L. *Nature* **2015**, 524, 208. (d) Lee, H. G.; Milner, P. J.; Buchwald, S. L. *J. Am. Chem. Soc.* **2014**, 136, 3792. (e) Lee, H. G.; Milner, P. J.; Buchwald, S. L. *Org Lett* **2013**, 15, 5602. (f) Milner, P. J.; Maimone, T. J.; Su, M.; Chen, J.; Müller, P.; Buchwald, S. L. *J. Am. Chem. Soc.* **2012**, 134, 19922. (g) Maimone, T. J.; Milner, P. J.; Kinzel, T.; Zhang, Y.; Takase, M. K.; Buchwald, S. L. *J. Am. Chem. Soc.* **2011**, 133,

-
18106. (h) Noël, T.; Maimone, T. J.; Buchwald, S. L. *Angew. Chem. Int. Ed.* **2011**, *50*, 8900.
- (21) (a) Camasso, N. M.; Pérez-Temprano, M. H.; Sanford, M. S. *J. Am. Chem. Soc.* **2014**, *136*, 12771. (b) Pérez-Temprano, M. H.; Racowski, J. M.; Kampf, J. W.; Sanford, M. S. *J. Am. Chem. Soc.* **2014**, *136*, 4097. (c) Racowski, J. M.; Gary, J. B.; Sanford, M. S. *Angew. Chem. Int. Ed.* **2012**, *51*, 3414. (d) Ball, N. D.; Kampf, J. W.; Sanford, M. S. *J. Am. Chem. Soc.* **2010**, *132*, 2878.
- (22) The Ritter lab is the other significant contributors to disclose Pd^{IV}(Ar)(F) complexes see: (a) Furuya, T.; Kaiser, H. M.; Tobias, R. *Angew. Chem. Int. Ed.* **2008**, *47*, 5993. (b) Furuya, T.; Tobias, R. *J. Am. Chem. Soc.* **2008**, *130*, 10060. (c) Furuya, T.; Benitez, D.; Tkatchouk, E.; Strom, A. E.; Tang, P.; Goddard, W. A., III; Tobias, R. *J. Am. Chem. Soc.* **2010**, *132*, 3793.
- (23) Hull K. L.; Anani, W. Q.; Sanford, M. S. *J. Am. Chem. Soc.*, **2006**, *128*, 7134.
- (24) Yu, J.-Q.; Wang, X.; Mei, T.-S. *J. Am. Chem. Soc.* **2009**, *131*, 7520-7521.
- (25) Tang, P.; Furuya, T.; Ritter, T. *J. Am. Chem. Soc.* **2010**, *132*, 12150.
- (26) Furuya, T.; Strom, A. E.; Ritter, T. *J. Am. Chem. Soc.* **2009**, *131*, 1662.
- (27) Furuya, T.; Ritter, T. *Org. Lett.* **2009**, *11*, 2860.
- (28) Tang, P.; Ritter, T. *Tetrahedron*, **2011**, *67*, 4449.
- (29) Lee, E.; Kamlet, A. S.; Powers, D. C.; Neumann, C. N.; Boursalian, G. B.; Furuya, T.; Choi, D. C.; Hooker, J. M.; Tobias, R. *Science* **2011**, *334*, 639.
- (30) Hickman, A. J.; Sanford, M. S. *Nature* **2012**, *484*, 177.
- (31) Casitas, A.; Ribas, X. *Chem. Sci.* **2013**, *4*, 2301.
- (32) Neumann, C. N.; Tobias, R. *Angew. Chem. Int. Ed.* **2015**, *54*, 3216.
- (33) Allen, L. J.; Lee, S. H.; Cheng, Y.; Hanley, P. S.; Muhuhi, J. M.; Kane, E.; Powers, S. L.; Anderson, J. E.; Bell, B. M.; Roth, G. A.; Sanford, M. S.; Bland, D. C. *Org. Process Res. Dev.* **2014**, *18*, 1045.
- (34) Kalow, J. A.; Doyle, A. G. *J. Am. Chem. Soc.* **2010**, *132*, 3268.
- (35) Ueda, T.; Konishi, H.; Manabe, K. *Org. Lett.* **2013**, *15*, 5370.
- (36) Fraser, S. L.; Antipin, M. Y.; Khroustalyov, A. V. N.; Grushin, V. V. *J. Am. Chem. Soc.* **1997**, *119*, 4769.
- (37) (a) Maleckis, A.; Sanford, M. S. *Organometallics* **2014**, *33*, 3831. (b) Maleckis, A.; Sanford, M. S. *Organometallics* **2014**, *33*, 2653.

CHAPTER 2. CU-CATALYZED FLUORINATION OF DIARYLIODONIUM SALTS WITH KF: REACTION DEVELOPMENT AND MECHANISTIC INVESTIGATIONS

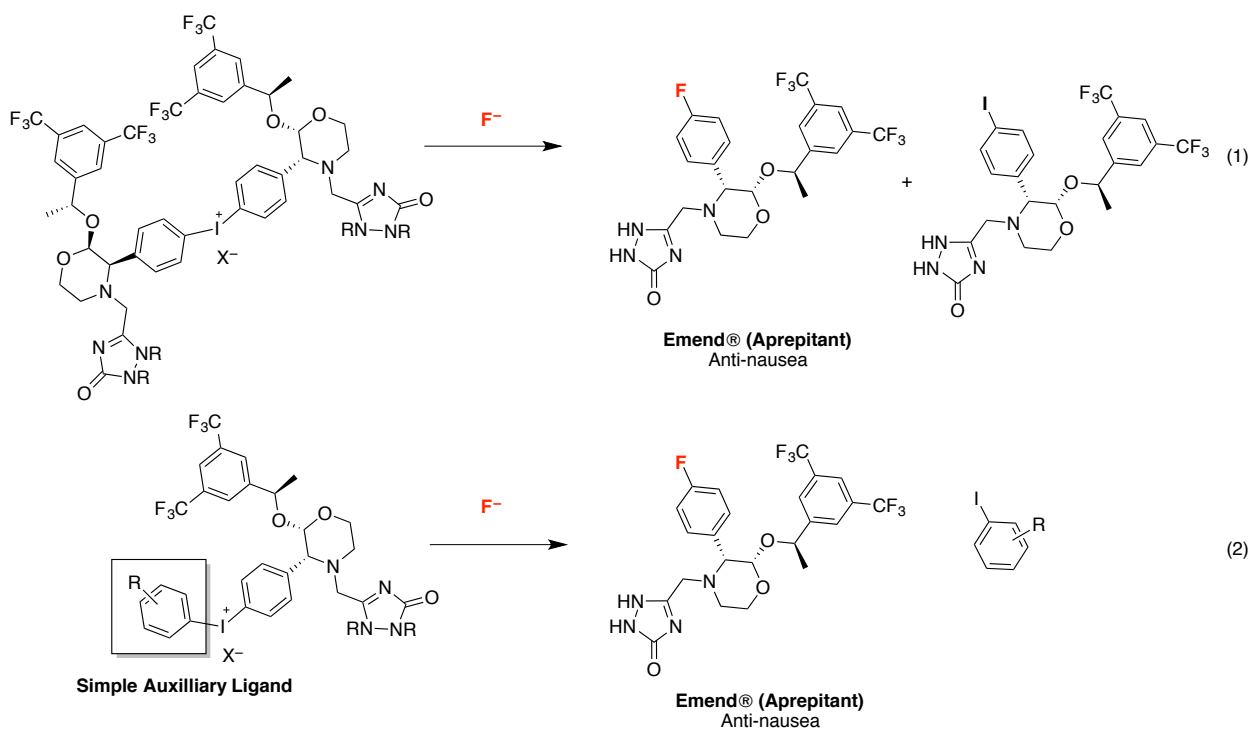
2.1 INTRODUCTION

Over the past decade, tremendous effort has been expended to develop transition metal-catalyzed fluorination reactions to address limitations in classical methods.¹ Nevertheless, carbon–fluorine bond formation remains a challenging chemical transformation, especially in the context of general, functional group-tolerant, late-stage fluorination of arenes. Ultimately, the direct fluorination of highly functionalized and complex small molecules is a critical goal for fluorine chemistry. In addition to the Balz-Schiemann reaction and halox fluorination (Chapter 1 Scheme 1.1 eq 2), the fluorination of diaryliodonium salts is a known method of forming C(aryl)-F bonds and it has been known since the first report by Van Der Puy in 1982 (Scheme 2.1).² This protocol typically affords high yield with symmetrical iodonium salts (Ar_2I^+). In contrast, with unsymmetrical iodonium salts ($\text{Aryl}(\text{auxillary})\text{I}^+$), both the yield and selectivity are often significantly diminished.

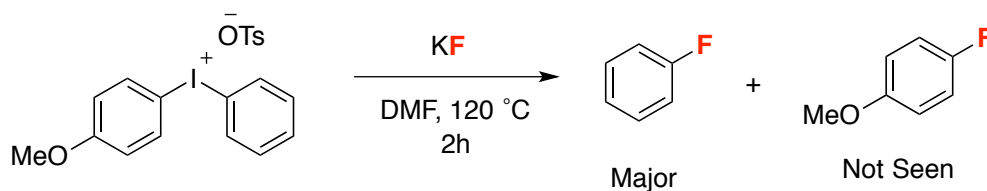
However, unsymmetrical aryl(auxiliary)iodonium salts are especially attractive precursors because they are inherently less wasteful than their symmetrical counterparts, especially in the context of the late-stage fluorination of complex organic molecules (Figure 2.1). For example, Emend (Arepitant) is a fluorine-containing anti-nausea drug for patients undergoing chemotherapy, and the current state-of-art of synthesis involves 10 steps. If symmetrical iodonium salts are used for fluorination, Emend is accessible regardless of which Ar-I(III) bond is cleaved (Scheme 2.1, eq 1). However, the synthesis of the corresponding aryl counterpart (Emend-I) can be time-consuming and not economical. In addition, the oxidation of Iodine center with highly functionalized molecules can be cumbersome. As such, it would be highly

advantageous to have a method in which a simple sacrificial aryl counterpart could be incorporated in iodine(III) that could direct the incoming fluoride nucleophile to functionalize the desired aryl group (Figure 2.1, eq 2).

Figure 2.1 Symmetrical vs. Unsymmetrical Ar_2I^+



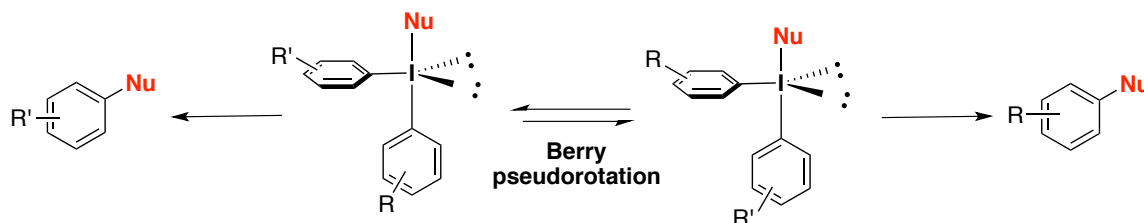
Scheme 2.1 Fluorination of Diaryliodonium Salts with KF^2



A key challenge associated with fluorination of unsymmetrical diaryliodonium salts is controlling selectivity. It is generally accepted that diaryliodonium salts react with nucleophiles under metal-free conditions via a T-shaped Ar_2I-Nu intermediate, with the nucleophile and one of the aryl groups in the hypervalent bond. The reaction proceeds by thermally-induced reductive elimination: ligand coupling between the nucleophile and the equatorial aryl group. When the two aryl ligands at the I(III) center are different, the two T-shaped intermediates undergo rapid equilibrium through Berry pseudorotation.³ Previous studies have revealed that at the I(III) center, nucleophiles preferentially react with the more electron-deficient aryl ring and/or sterically congested *ipso* carbon atom

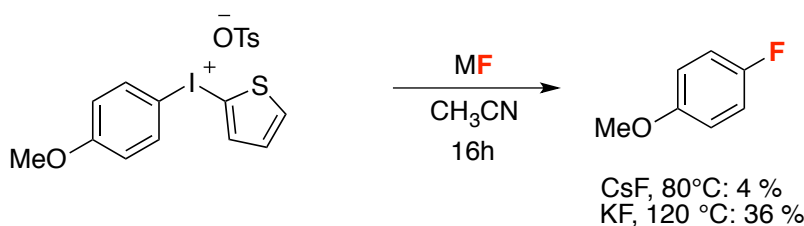
(i.e. the so-called “*ortho* effect”)⁴ (Figure 2.2). Thus, the selectivity of Ar₂I⁺ fluorinations can be increased by appropriate selection of auxiliary ligands on I^{III} center.

Figure 2.2 Selectivity in Metal-free Arylation Reactions with Diaryliodonium Salts



Electronic Effects. The selectivity of the reaction is influenced by electronic effects, resulting in the functionalization of the less electron rich aryl group via reductive elimination. However, it is generally challenging to achieve high selectivity with diaryliodonium salts of two electronically similar aryl groups as ligands. In 2008, Coenen demonstrated the radiofluorination of electron-rich arenes using the highly electron rich 2-thienyl group as a directing ligand.⁵ A positive Hammett value was measured for the reaction, which suggests that electron-withdrawing substituents accelerate the reaction rate, and, in principle, this should translate to the non-radiofluorination chemistry as well. However, using cold fluoride ¹⁹F⁻, low yields were observed with either CsF or KF (Scheme 2.2).⁶ Furthermore, the 2-thienyl iodonium salts are generally challenging to synthesize and unstable to long term storage. Hence, this electronic effect is not commonly used for achieving the control of regioselectivity and development of a more robust approach is still required.

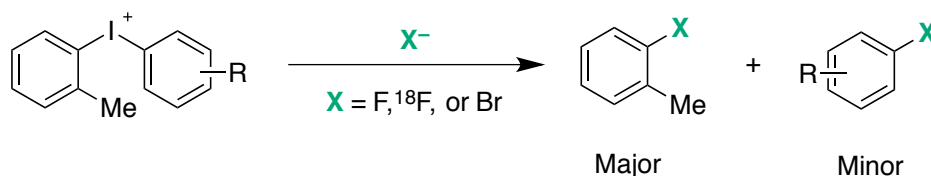
Scheme 2.2 Electronically-Controlled Selectivity



Steric effects. Steric influences are another means to control the chemoselectivity of nucleophilic functionalizations of diaryliodonium salts.⁷ An intriguing feature of the reaction of diaryliodonium salts with nucleophiles is the influence of substituents, which have been reported to direct an incoming nucleophile to attack the *ortho*-substituted aryl ring (Scheme 2.3).⁸ These are commonly called *ortho* effects. *Ortho* effects likely

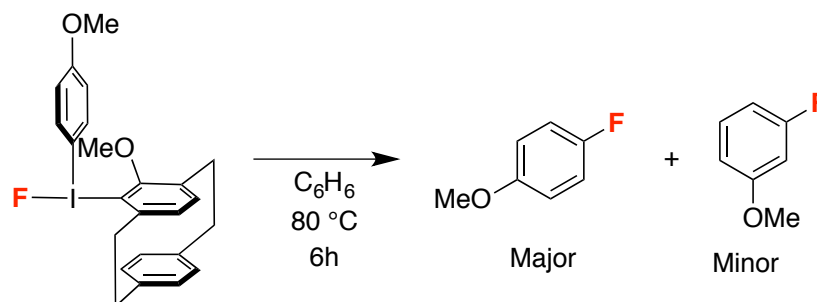
originate from two factors: (1) bulkier aryl rings prefer a more spacious equatorial site *syn* to the nucleophile and (2) *ortho*-substituted aryl rings prefer conformations in which the pi-system is aligned with the incoming nucleophile.^{7,9} However, only a small number of electronically similar aryl rings have been investigated and highly electron-rich derivatives (for example, 2-Me-4-OMePh) have not been successfully employed.¹⁰

Scheme 2.3 Sterically-Controlled Selectivity



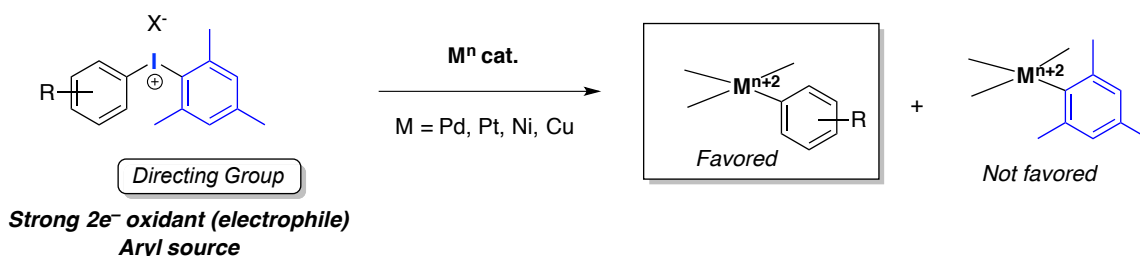
In addition to *ortho* effects, in 2010 DiMagno and co-workers introduced a concept called Stereoelectronic Control of Unidirectional Reductive Elimination (SECURE)¹¹ where they demonstrated that sterically bulky cyclophane-derived directing groups can forcibly lock the geometry of diaryliodonium salts. Severe out-of-plane, but little in-plane steric congestion from the cyclophane group leads to a highly strained transition state for reductive elimination (Scheme 2.3). However, this process still involves high reaction temperatures and often leads to the formation of regioisomeric products (minor product in Scheme 2.3) via aryne intermediates. Furthermore, the cyclophane starting material requires a multi-step synthesis.

Scheme 2.4 DiMagno's Stereoelectronically-Controlled Selectivity



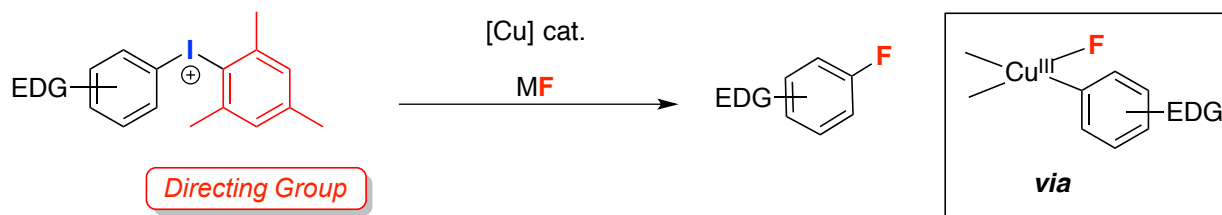
One possible solution to this challenge is the introduction of catalysis into the transformation. Hypervalent iodine(III) oxidants are widely known in transition metal catalysis as powerful oxidants, providing access to high-valent Pd(IV),¹² Pt(IV),¹³ Ni(IV)¹⁴ and Cu(III)¹⁵ intermediates. Not only can I(III) reagents serve as $2e^-$ oxidants, but they can also serve as an aryl source for coupling with a nucleophilic ligand (Scheme 2.5).

Scheme 2.5 Reactivity of Mesityl Aryl Iodonium Salts with Transition Metals



In particular, seminal reports were disclosed by MacMillan, Gaunt, and Suna in which Cu-catalyzed C–H arylation was achieved using diaryliodonium salts as an aryl source.¹⁶ With a mesityl group as a sacrificial aryl ligand on I(III), exclusive transfer of the smaller aryl group was observed. We hypothesized that the addition of nucleophilic fluoride to such reactions would enable C–F bond formation via reductive elimination from a high-valent Cu(III) complex (Scheme 2.6).

Scheme 2.6 Cu-Catalyzed Fluorination of Diaryliodonium Salts with F⁻



To develop the proposed transformation, we sought to identify a suitable system that enables the selective fluorination of diaryliodonium salts using nucleophilic fluoride (F⁻), with the goal of accessing electron-rich fluoroarenes. The nucleophilic fluorination of electron-rich arenes is a long-standing challenge in the field of C–F bond formation, since such compounds can not be accessed using traditional S_NAr fluorination reactions.

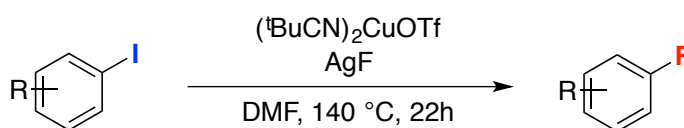
This chapter describes our work towards the development of the Cu-catalyzed fluorination of diaryliodonium salts with potassium fluoride. This work represents the first example of a general method for nucleophilic fluorination using *catalytic* Cu.¹⁷ Included in this chapter are: (1) methodology development and (2) experimental and computational mechanistic investigations of this new Cu-catalyzed fluorination reaction.¹⁸

2.2 RESULTS AND DISCUSSION

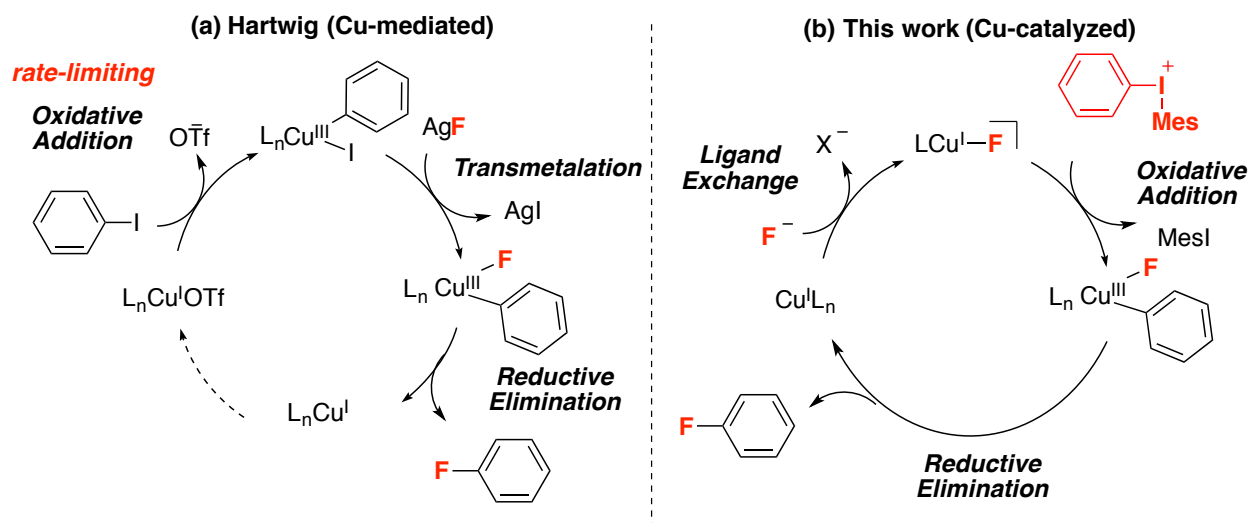
Development of Cu-catalyzed fluorination of diaryliodonium salts with KF.

Our initial studies focused on developing a Cu-catalyzed method for arene fluorination that proceeds under mild conditions. In 2012, Fier and Hartwig reported the first Cu^{I/III}-mediated nucleophilic fluorination of aryl iodides (ArI) using silver fluoride (Scheme 2.7).¹⁹ However, the use of a superstoichiometric non-commercial copper catalyst, a high reaction temperature (140 °C) and long reaction times (22 h) were required. These conditions are necessary because of the high energy barrier for oxidative addition of iodoarenes to the Cu^I center, which is the proposed rate-limiting step of the reaction (Scheme 2.8a). Furthermore, this methodology does not provide access to electron rich fluoroarenes such as 4-fluoroanisole. We envisioned that the use of highly electrophilic diaryliodonium salts (Ar₂I⁺), which undergo fast oxidative addition, would enable much milder nucleophilic fluorination and potentially address these limitations (Scheme 2.8b).

Scheme 2.7 Copper-Mediated Fluorination of Iodoarenes (Hartwig)



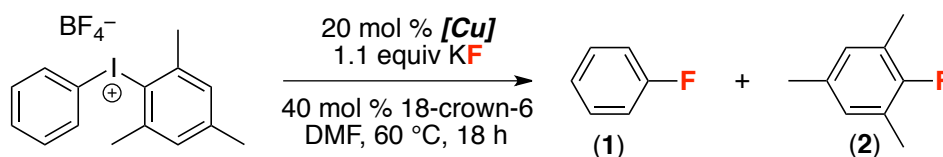
Scheme 2.8. Proposed Mechanisms



Evaluation of Copper Catalysts: Our initial experiments were directed toward

assessing the feasibility of Cu-catalysis through evaluation of a series of different copper salts. In the absence of copper salts, only fluoromesitylene **2** was detected by ^{19}F NMR spectroscopy under our reaction conditions. This selectivity was expected based on the previous literature (for example, see Scheme 2.3, above).¹⁶ A series of Cu(I) and Cu(II) salts were tested in conjunction with KF and 18-crown-6 to solubilize the KF. Copper (II) trifluoromethanesulfonate $[\text{Cu}(\text{OTf})_2]$ gave the best yield of 85% with an excellent selectivity of 98:2 (Table 2.1, entry 9). Subsequent studies showed that the 18-crown-6 is unnecessary, but it speeds up the reaction. Overall, this transformation reached completion in 3 h, giving 81% yield of **1** and a 97:3 product ratio compared to 44% yield without 18-crown-6 under otherwise analogous conditions (Table 2.1, entry 10).

Table 2.1 Evaluation of Copper Salts



Entry	[Cu]	Yield	Selectivity (1:2)
1	none	28	1:>99
2	$(t\text{BuCN})_2\text{CuOTf}$	44	>99:1
3	CuBr	51	92:8
4	$(\text{CH}_3\text{CN})_4\text{CuOTf}$	73	96:4
5	$\text{Cu}(\text{OAc})_2$	41	>99:1
6	CuBr_2	26	>99:1
7	CuF_2	29	24:76
8	$\text{Cu}(\text{TFA})_2 \cdot \text{H}_2\text{O}$	22	82:18
9	$\text{Cu}(\text{OTf})_2$	85	98:2
10 ^a	$\text{Cu}(\text{OTf})_2$	81	97:3
11 ^b	$\text{Cu}(\text{OTf})_2$	44	97:3

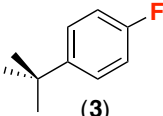
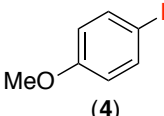
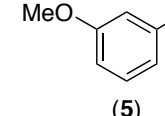
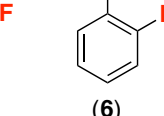
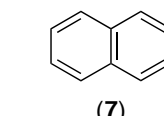
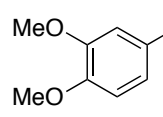
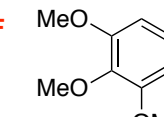
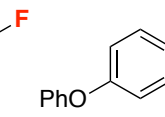
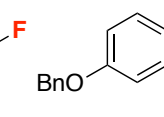
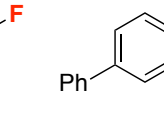
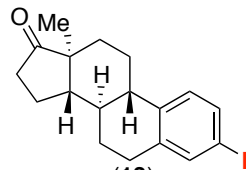
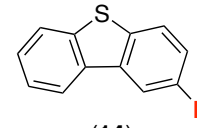
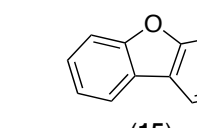
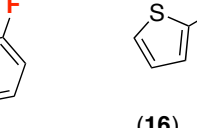
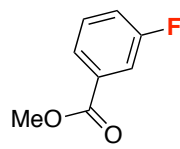
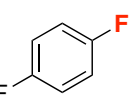
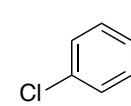
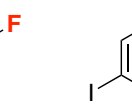
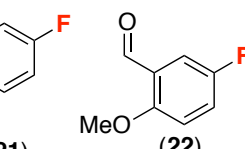
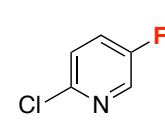
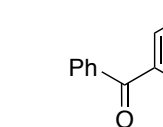
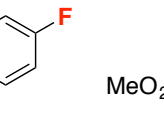
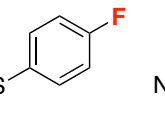
^a 0.4 equiv 18-crown-6; reaction time = 3 h. ^b 0 equiv 18-crown-6; reaction time = 3 h

Substrate Scope: Having confirmed that the mesityl group is a good directing group, we next investigated the scope of this transformation with substrates of the general structure $[\text{Mes-I-Ar}]\text{BF}_4$, where Ar = electron rich (hetero)aromatic ring. These substrates were the focus of our study because they are typically the most challenging substrates for traditional nucleophilic fluorination reactions.^{20,21} As summarized in Figure 2.3, fluorinated products **3-26** were all obtained in good yield and high selectivity from this reaction. All products with boiling points over 180 °C were isolated, and the purity of

the isolated products was >98% unless otherwise noted. Gratifyingly, electron-rich arenes underwent fluorination smoothly under mild conditions with the use of nucleophilic fluoride. As discussed above, many of these products were previously difficult to access unless electrophilic fluoride (F^+) was used.²² Remarkably, even 2-fluorothiophene **16** could be formed, albeit under more forcing conditions (130 °C for 2 h). This highly electron-rich heterocycle was previously used as a sacrificial directing group in uncatalyzed diaryliodonium fluorination reactions (Scheme 2.3). With these electron rich substrates, the analogous Cu-free reactions proceeded in modest yields and provided Mes-F **2** as the major product.

Substrates bearing electron-withdrawing substituents on the Ar ring were also investigated. When the substituents were moderately electron-withdrawing, Cu catalysis resulted in significant enhancements in yield and selectivity (e.g., **18-22**) relative to the uncatalyzed nucleophilic fluorination reaction. Aryl halides (**19-21**) and aldehyde (**22**) substituents were tolerated under the reaction conditions. Substrates bearing strongly electron withdrawing groups (e.g., **24-26**) reacted in good yield and selectivity in both the presence and absence of Cu. This trend is consistent with prior reports of uncatalyzed fluorination of diaryliodonium reagents. One particularly noteworthy substrate in this series is chloropyridine **23**. Cu-catalyzed fluorination generated **23** in a modest 33% yield but with high selectivity for fluorination at the 5-position. This substitution pattern is often challenging to access in nucleophilic fluorination reactions due to the high propensity of 2-chloropyridines to participate in S_NAr .

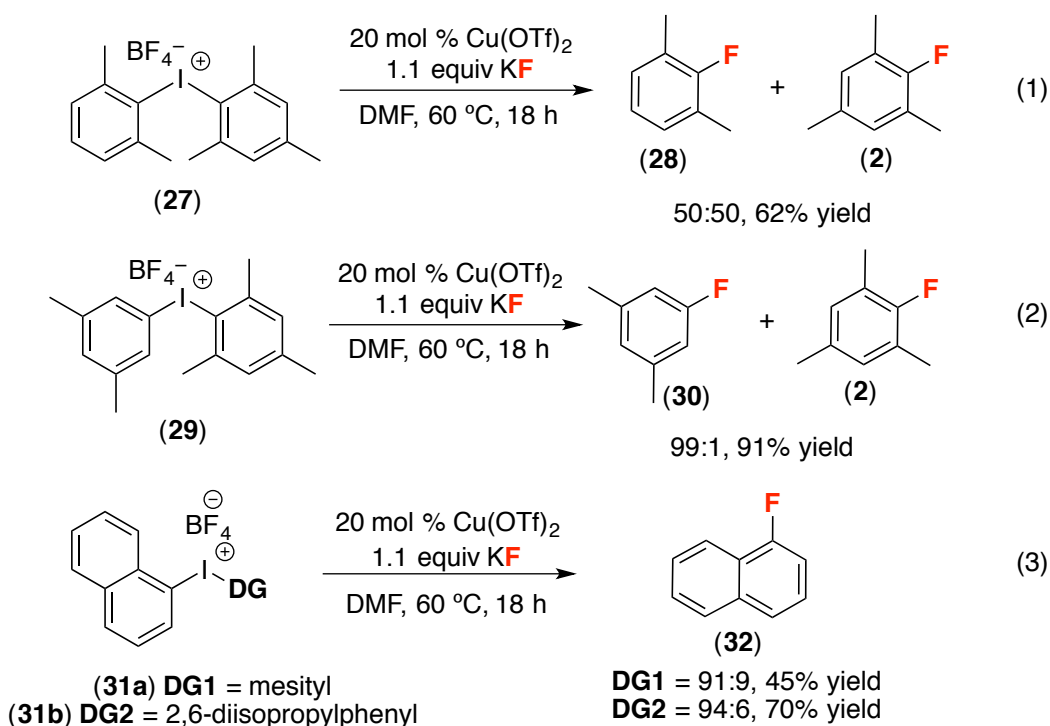
Figure 2.3 Substrate Scope of Cu-catalyzed Fluorination^a

					
with [Cu]^b	73% (99:1)	85% (99:1)	54% (96:4)	50% (96:4)	87% (98:2)
without [Cu]^b	42% (5:95)	51% (2:98)	29% (31:69)	42% (98:2)	72% (50:50)
Isolated yield^c	nd	nd	nd	nd	78%
					
with [Cu]^b	99% (96:4)	62% (98:2) ^c	98% (98:2) ^d	83% (96:4) ^d	86% (95:5)
without [Cu]^b	27% (4:96)	28% (4:96)	87% (5:95)	77% (<1:99)	56% (21:79)
Isolated yield^c	74%	53%	81%	81%	85%
					
with [Cu]^b	86% (96:4) ^d	58% (98:2) ^d	73% (83:17) ^d	42% (>99:1) ^e	
without [Cu]^b	50% (10:90)	47% (10:90)	77% (10:90)	49% (2:98) ^e	
Isolated yield^c	72%	56%	50%	nd	
					
with [Cu]^b	73% (96:4)	92% (86:14) ^d	74% (94:6) ^d	77% (95:5)	66% (97:3)
without [Cu]^b	64% (50:50)	55% (10:90)	61% (28:72)	72% (42:58)	1% (>99:1)
Isolated yield^c	70% ^g	nd	nd	54% ^g	67%
					
with [Cu]^b	33% (97:3) ^{f,h}	76% (95:5)	67% (94:6)	54% (93:7)	
without [Cu]^b	54% (67:33) ^h	83% (92:8)	82% (95:5)	51% (93:7)	
Isolated yield^c	nd	63%	nd	nd	

^aConditions: [Mes-I-aryl]BF₄ (1 equiv), Cu(OTf)₂ (0 or 0.2 equiv), KF (1.1 equiv), 18-crown-6 (0.4 equiv), DMF (0.1 M), 60 °C, 18 h. ^bYields (combined of Ar-F + 2) determined by ¹⁹F NMR. ^cnd = not determined (non-isolable)

product). ^dWith 0.5 equiv Cu(OTf)₂. ^e5 equiv of CsF, 130 °C, 2 h. ^fWith 1 equiv of Cu(OTf)₂. ^g95% purity. ^hWith 1.1 equiv CsF at 25 °C.

As expected, a large erosion in selectivity was observed with electron rich substrates bearing ortho-substituents (eq 1). For instance, **27** underwent unselective fluorination to provide a 62% yield of a 50 : 50 mixture of **28** and **2**. In contrast, the electronically similar, but less sterically hindered substrate **29** afforded 91% yield of **30** with high selectivity (**30** : **2** = 99 : 1). The chemoselectivity and yield of 1-fluoronaphthalene could be enhanced with an even more sterically congested directing group 2,6-diisopropylphenyl (**31b**) to afford 70% yield with high selectivity (**32**:**2** = 94:6) (eq 3).

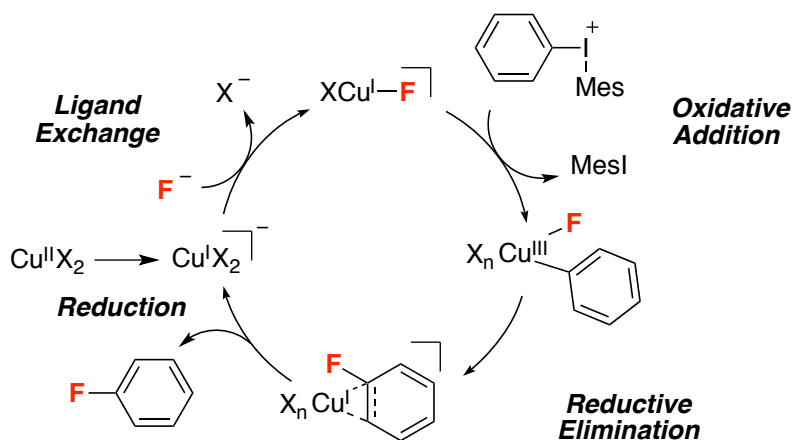


In summary, a Cu-catalyzed fluorination of diaryliodonium salts with KF was developed. This is the first general fluorination process that uses *catalytic* Cu to achieve high yields and selectivities with electron-rich arenes. The iodonium substrates are readily available in a single step from commercial MesI(OAc)₂ and diverse boronic acid derivatives, and the less-sterically hindered aryl ligand on iodine is fluorinated with high selectivity.

Mechanistic investigations into Cu^{III}-Catalyzed Fluorination of Diaryliodonium Salts. We next sought to elucidate the mechanism of this highly

practical fluorination reaction. Over the past several years, there have been numerous studies on the development of Cu-catalyzed cross-couplings of diaryliodonium salts with diverse coupling partners.^{23,24,25,26} Although a number of literature reports have probed the mechanisms of metal-free reactions of diaryliodonium salts with nucleophiles,²⁷ there is still little known about the detailed mechanism of aryl transfer from diaryliodonium salts to transition metals like Cu.²⁸ For example, the nature of the active Cu catalyst that reacts with the diaryliodonium salt has not been elucidated in most systems. Furthermore, the mechanistic origin of the selectivity of aryl transfer from unsymmetrical I(III) reagents to transition metal centers is poorly understood.²⁷ We propose that the Cu-catalyzed fluorination of diaryliodonium salts proceeds via a Cu^{I/III}-catalytic cycle (Figure 2.4). In this part of chapter, our computational and experimental mechanistic investigation of the Cu-catalyzed fluorination protocol is detailed. To gain further mechanistic insights, Prof. Allan Canty conducted density functional theory (DFT) calculations on the Cu(OTf)₂-catalyzed fluorination of [Ph-I-Mes]BF₄ with KF.

Figure 2.3 Proposed Cu^{I/III} Catalytic Cycle



Time studies: Our initial mechanistic proposal involves Cu(I) as the active catalyst (Scheme 2.7a). As such, we were intrigued that a copper(II) precatalyst gives a better overall yield. When an analogous Cu(I) salt $[(\text{CH}_3\text{CN})_4\text{Cu}^{\text{I}}\text{OTf}]$ was used, it led to a lower yield of 73% (Table 2.1, entry 4). In order to probe the reactivity of these Cu salts in more detail, we selected $(\text{CH}_3\text{CN})_4\text{CuOTf}$ and $\text{Cu}(\text{OTf})_2$ as pre-catalysts and performed time studies. A faster rate was observed with $(\text{CH}_3\text{CN})_4\text{CuOTf}$ for the first

120 minutes of the reaction, suggesting that the Cu^{I} salt may form an active catalyst more rapidly under the reaction conditions (Figure 2.5). However, the $\text{Cu}(\text{OTf})_2$ catalyst provided a higher yield of 85% yield at 18 hours (Scheme 2.8, eq 1). GC-MS analysis and isolation of the side product confirmed the formation of biphenyl as a by-product in 10% yield (along with traces of benzene, mesitylene and diphenyl ether) (Scheme 2.9, eq 2); thus, we concluded that for promoting the desired fluorination reaction, $\text{Cu}(\text{II})$ is a more ideal pre-catalyst since there are less of side products formed under the conditions.

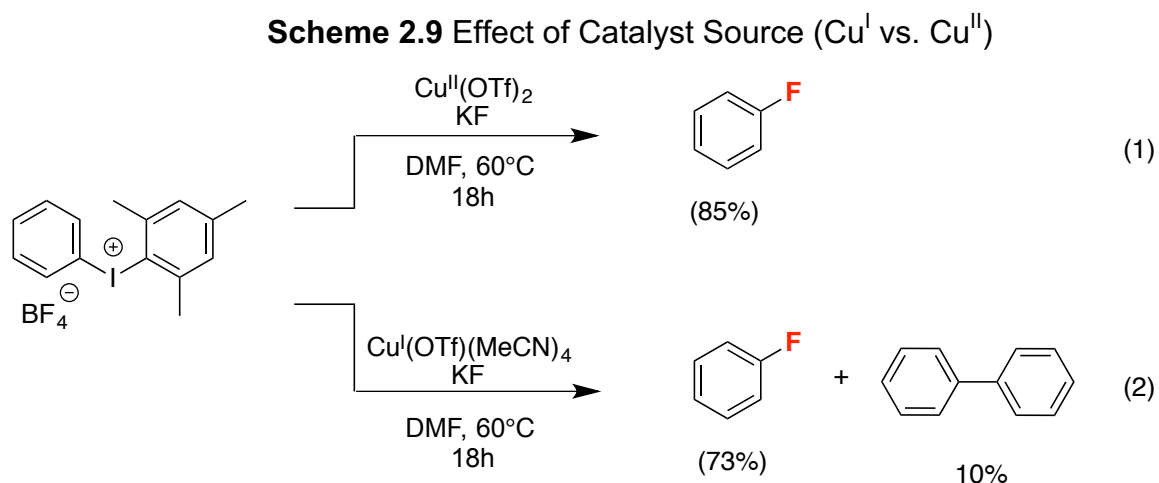
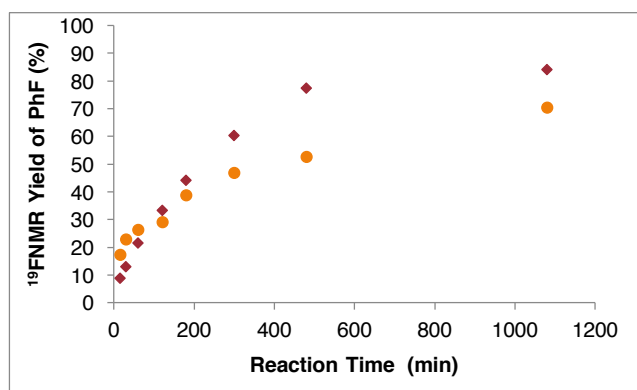


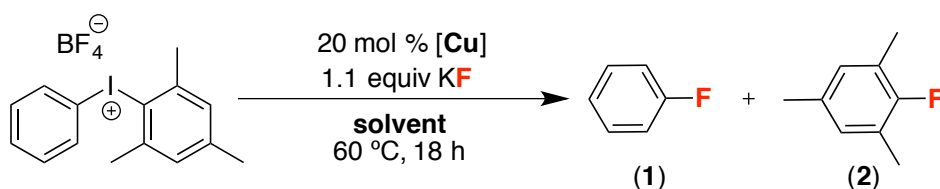
Figure 2.5 PhF Formation as a Function of Time in the Reaction of $[\text{Mes}(\text{Ph})\text{I}]^+$ with KF Catalyzed by $\text{Cu}(\text{OTf})_2$ (◆, red) and $\text{Cu}(\text{OTf})(\text{CH}_3\text{CN})_4$ (●, orange) in DMF at 60°C



Oxidation state of the Copper catalyst: Literature reports of Cu-catalyzed transformations often propose $\text{Cu}(\text{I})/\text{Cu}(\text{III})$ catalytic cycles; however, few mechanistic studies have been conducted to probe the oxidation state of the active catalyst that participates in oxidative addition. To gain further insights, both $(\text{MeCN})_4\text{Cu}^{\text{I}}\text{OTf}$ and

$\text{Cu}^{\text{II}}(\text{OTf})_2$ were subjected to the standard reaction conditions with various solvents. A strong solvent dependence was observed for reactions catalyzed by both copper complexes. Dipolar aprotic solvents such as DMF and NMP showed high selectivity and good yields whereas ethyl acetate and toluene afforded low yields. Interestingly, in EtOAc and toluene, the Cu catalyzed reactions switched the selectivity and favored fluoromesitylene **2** as a major product. Moreover, reactions catalyzed by Cu^{I} salts resulted in lower yields than those catalyzed by Cu^{II} salts (all but NMP solvent, Table 2.2).

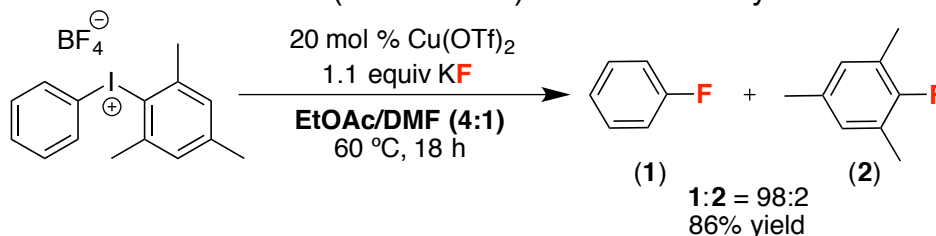
Table 2.2. Cu-catalyzed Fluorination of $[\text{Mes}(\text{Ph})\text{I}]^+$ as a Function of Cu Precatalyst and Solvent



Solvent	[Cu]	Yield (PhF:MesF)
DMF	$\text{Cu}(\text{OTf})_2$	85% (98:2)
DMF	$\text{Cu}(\text{OTf})(\text{CH}_3\text{CN})_4$	73% (99:1)
NMP	$\text{Cu}(\text{OTf})_2$	38% (95:5)
NMP	$\text{Cu}(\text{OTf})(\text{CH}_3\text{CN})_4$	55% (>99:1)
EtOAc	$\text{Cu}(\text{OTf})_2$	39% (13:87)
EtOAc	$\text{Cu}(\text{OTf})(\text{CH}_3\text{CN})_4$	39% (13:87)
toluene	$\text{Cu}(\text{OTf})_2$	35% (14:86)
toluene	$\text{Cu}(\text{OTf})(\text{CH}_3\text{CN})_4$	34% (13:87)

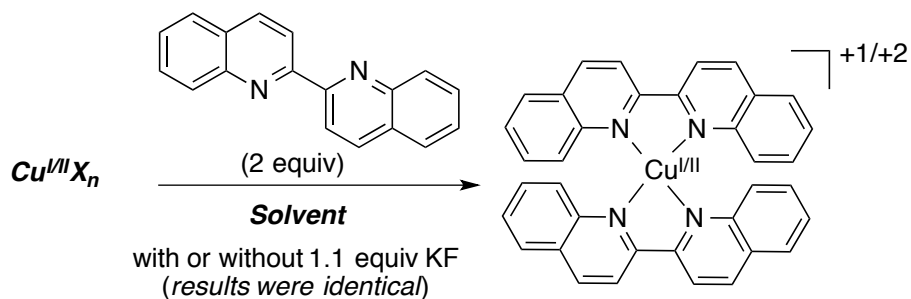
It is worth noting that the fluorination process was also tested using a 4 : 1 mixture of EtOAc/DMF as solvent (0.1 M in PhIMes). Gratifyingly, this solvent system afforded 86% overall yield (98 : 2 selectivity) while using only EtOAc as solvent could not result in the desired selectivity (Scheme 2.10).

Scheme 2.10 Co-Solvent (DMF/EtOAc) for the Cu-catalyzed Fluorination



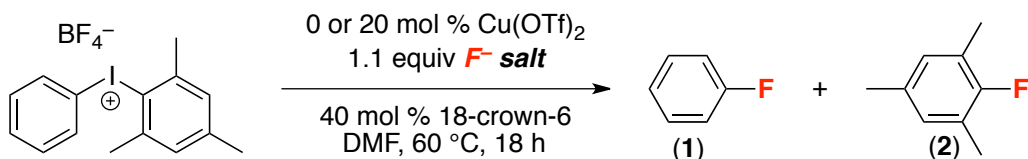
This set of results led us to hypothesize that the two precatalysts might be operating via an analogous Cu^{I} active species. In the case of $\text{Cu}(\text{OTf})_2$, the copper

catalyst is presumably reduced to Cu^{I} *in situ*, accounting for the slower initial rate with this precatalyst (Figure 2.1). Notably, DMF is known to reduce transition metals.²⁹ To test for this possibility, we aimed for colorimetric detection of Cu^{I} by means of Cu^{I} trapping experiments. Lockhart has demonstrated that 2,2'-biquinoline (biq) has a strong binding affinity for Cu^{I} , and the resulting complexes exhibit a characteristic intense purple color ($\lambda_{\text{max}} = 540 \text{ nm}$).³⁰ Thus, we used this ligand to interrogate the oxidation state of Cu formed when $\text{Cu}(\text{OTf})_2$ is dissolved in a variety of solvents (Table 2.3). An intense purple color was observed in DMF and NMP within 5 min at room temperature in both the presence and absence of 1.1 equiv of KF, indicating the formation of Cu^{I} in these solvents. UV-vis spectroscopic analysis of these purple solutions showed a λ_{max} between 540 and 550 nm, further consistent with the formation of Cu^{I} under these conditions. In sharp contrast, when $\text{Cu}(\text{OTf})_2$ and biq were stirred in EtOAc or toluene, an orange precipitate formed, which is indicative of the formation of $[\text{Cu}^{\text{II}}(\text{biq})_2]$.³¹ This orange precipitate was then treated with DMF, and it immediately turned to intense purple solution at room temperature. Overall, this experiment supported the hypothesis that DMF is necessary for reduction of Cu^{II} to Cu^{I} to occur at 60 °C. Different selectivity was observed depending on solvents, and DMF is proven necessary for an active Cu^{I} species based on observation of the selectivity analogous to metal-free reactions in EtOAc and toluene. Thus, we concluded that Cu^{I} species are available with both the $\text{Cu}(\text{OTf})_2$ and $\text{Cu}(\text{OTf})(\text{CH}_3\text{CN})_4$ precatalysts, and that Cu^{I} is likely to be the active catalyst in both systems.

Table 2.3. Cu^{III} Trapping Experiment

[Cu]	Solvent	λ_{max}	Color
Cu(OTf) ₂	DMF	540	dark purple solution
Cu(OTf)(MeCN) ₄	DMF	540	dark purple solution
Cu(OTf) ₂	NMP	550	light purple solution
Cu(OTf) ₂	EtOAc	n/a	orange precipitate
Cu(OTf) ₂	toluene	n/a	orange precipitate

Evaluation of Fluoride Salts: We next sought to evaluate a series of fluoride salts to test if we can further enhance both yield and selectivity in these systems. In sharp contrast to KF, which is not readily soluble in DMF at room temperature, reactions conducted with more soluble salts such as CsF or Me₄NF led to a switch in the ratio of **1:2** (Table 2.4 entry 2, 4 respectively). This result was intriguing as it suggests that a high initial concentration of fluoride in the reaction mixture readily generates the undesired product **2**, and that was counterintuitive, as low solubility of KF and CsF is always discussed as a challenge associated with nucleophilic fluorination reactions.

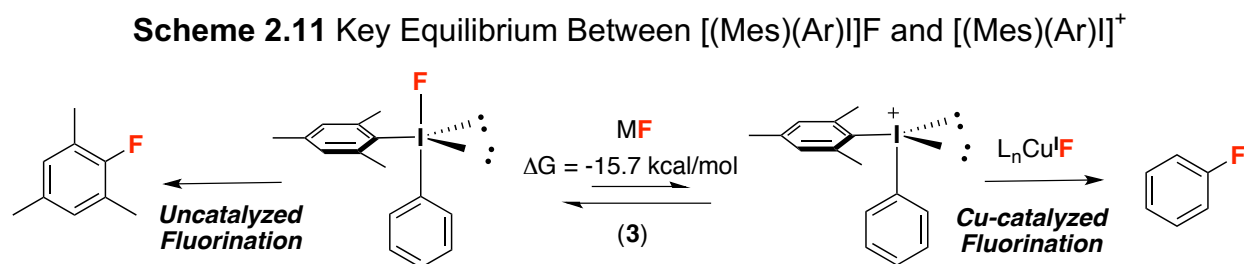
Table 2.4. Evaluation of Different Fluoride Sources

Entry	Fluoride	% Yield w/o Cu	Selectivity (1:2) w/o Cu	% Yield with Cu	Selectivity (1:2) with Cu
1	KF	39	18:82	85	98:2
2	CsF	93	22:78	72	21:79
3	AgF	9	22:78	13	85:15
4	Me ₄ NF	78	28:72	40	25:75
5	Bu ₄ NF	57	28:72	69	26:74

Computational Studies on Ligand Exchange at I(III) center and Cu: The results in Table 2.4 suggest that a low initial concentration of fluoride is key for a selective transformation. In order to better understand this observation, we turned to DFT calculations in collaboration with Prof. Allan Canty from University of Tasmania, Australia.³² His DFT calculations show that both Cu and [(Mes)(Ph)I]⁺ are thermodynamically favored to bind to F⁻ (entries 3, 6-9). In DMF, the cationic form of the iodonium salt ([Mes(Ph)I]⁺ **3**) undergoes facile oxidative addition to the Cu^I catalyst. However, when there is a high concentration of fluoride in solution, **3** is readily converted to Mes(Ph)IF (**4**). Compound **4** is not reactive with Cu^I, and instead undergoes uncatalyzed reductive elimination to selectively form the undesired product MesF (**2**) (Scheme 2.10). Hence, we hypothesized that the dramatic change in selectivity with more soluble fluoride sources is due to a change in the resting state of the diaryliodonium salt from the cation [Mes(Ph)I]⁺ to the neutral species Mes(Ph)IF (Scheme 2.10).

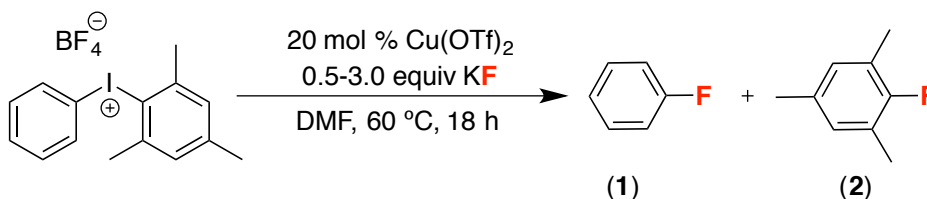
Table 2.5 Computation for Reactions of Cu^I and [Mes(Ph)I]⁺ with Donor Ligands Present During Cu-Catalyzed Reactions

Entry	Ligand Exchange at I ^{III} and Cu ^I centers	ΔG (kcal/mol)
1	[Mes(Ph)I] ⁺ + DMF → [Mes(Ph)I(DMF)] ⁺	2.7
2	[Mes(Ph)I] ⁺ + OTf ⁻ → Mes(Ph)I(OTf)	1.6
3	[Mes(Ph)I] ⁺ + F ⁻ → Mes(Ph)IF	-15.7
4	[Cu(DMF) ₂] ⁺ + OTf ⁻ → Cu(OTf)(DMF) + DMF	0.7
5	Cu(OTf)(DMF) + OTf ⁻ → [Cu(OTf) ₂] ⁻ + DMF	2.0
6	[Cu(DMF) ₂] ⁺ + F ⁻ → CuF(DMF) + DMF	-20.7
7	CuF(DMF) + F ⁻ → [CuF ₂] ⁻ + DMF	-16.4
8	[Cu(OTf) ₂] ⁺ + F ⁻ → [CuF(OTf)] ⁻ + OTf ⁻	-20.8
9	[CuF(OTf)] ⁻ + F ⁻ → [CuF ₂] ⁻ + OTf ⁻	-19.1



Impact of KF Stoichiometry: To test this proposal experimentally, we examined the impact of the ratio of KF to $(\text{Cu}(\text{OTf})_2 + \mathbf{3})$ on catalysis. These studies were conducted using 20 mol % of $\text{Cu}(\text{OTf})_2$ and 1 equiv of $[\text{Mes}(\text{Ph})\text{I}]^+$, and the amount of KF was varied from 0.5 equiv to 3.0 equiv relative to the iodonium reagent. At 1.4 equiv of KF, the iodonium reagent should be saturated with F^- , assuming that all of the KF is soluble. The extent of Cu-catalysis versus the uncatalyzed, background reaction can be estimated based on the ratio of products PhF: MesF. Under Cu-catalyzed conditions, PhF is favored by $\geq 97: 3$, while the uncatalyzed reaction affords an approximately 20 : 80 ratio of PhF : MesF. As shown in Table 2.6, an outcome consistent with Cu catalysis was observed up to 1.25 equiv of KF. However, significant erosion of selectivity was observed at 1.5 equiv suggesting that presence of excess fluoride is detrimental. Furthermore, with 2.0 or more equiv of KF, the observed selectivity was identical to that of the uncatalyzed reaction, suggesting that the iodine(III) reagent has been completely converted to **4** and no Cu catalysis is occurring under these conditions

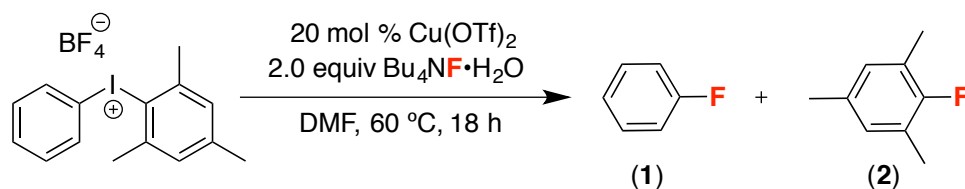
Table 2.6 KF Loading Study



entry	KF (equiv)	Yield PhF ^a	Yield MesF ^a	Ratio (PhF:MesF)
1	0.5	37%	<1%	>99 : 1
2	1.1	83%	1%	99 : 1
3	1.25	74%	2%	98 : 2
4	1.5	25%	22%	53 : 47
5	2.0	10%	40%	20 : 80
6	3.0	9%	34%	21 : 79

To further probe the hypothesis, slow addition of $\text{Bu}_4\text{NF}\cdot 3\text{H}_2\text{O}$ was performed. By adding 2.0 equiv of $\text{Bu}_4\text{NF}\cdot 3\text{H}_2\text{O}$ in DMF dropwise over 7 hours, the exclusive formation of **1** was observed, which is complementary to the result of the addition of 2 equiv of $\text{Bu}_4\text{NF}\cdot 3\text{H}_2\text{O}$ in one portion (Scheme 2.12). This further indicates that Cu catalysis is slower with high KF concentration in the reaction.

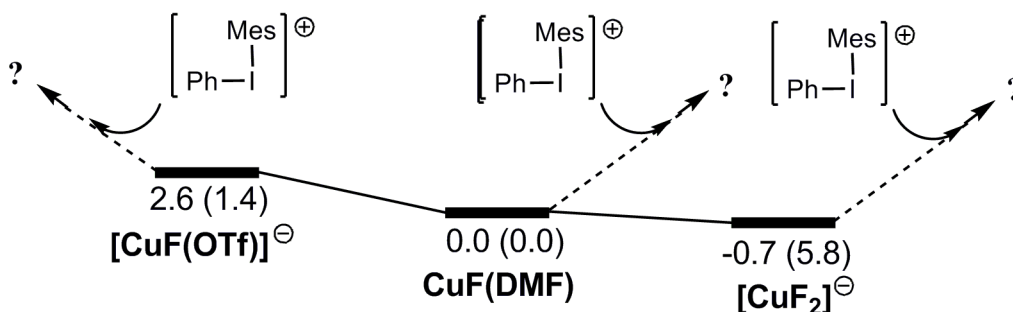
Scheme 2.12 Slow addition of $\text{Bu}_4\text{NF}\cdot 3\text{H}_2\text{O}$



Bu_4NF added slowly over 7 h: 29% yield of ArF; PhF : MesF = >99 : 1
 Bu_4NF added in one portion: 29% yield of ArF; PhF : Mes F = 18 : 78

Potential Fluorocopper(I) Reactants: The computations in Table 2.5 also illustrate the competitive nature of DMF and triflate as ligands for Cu^{I} (entries 4 and 5). We therefore computationally examined the possibility of three different active Cu^{I} complexes as reactants in the oxidative addition step: $[\text{Cu}(\text{OTf})\text{F}]^-$, $\text{Cu}(\text{DMF})\text{F}$ and $[\text{CuF}_2]^-$. Their thermodynamic profile was successfully computed and found to be very similar to each other, differing by less than $3.3 \text{ kcal mol}^{-1}$ (Figure 2.6). Under the standard fluorination conditions, the formation of all three Cu^{I} species is possible; consequently, we next computed reasonable energy pathways for the formation of fluorinated product **1**. DFT calculations show four low energy pathways for oxidative transfer of Ph^+ from $[\text{Mes}(\text{Ph})\text{I}]^+$ to Cu^{I} . These pathways proceed from $[\text{CuF}(\text{OTf})]^-$ (2 pathways), $[\text{CuF}(\text{DMF})]$ (1 pathway) and $[\text{CuF}_2]^-$ (1 pathway). These are all likely feasible under the standard reaction conditions (Figure 2.6).

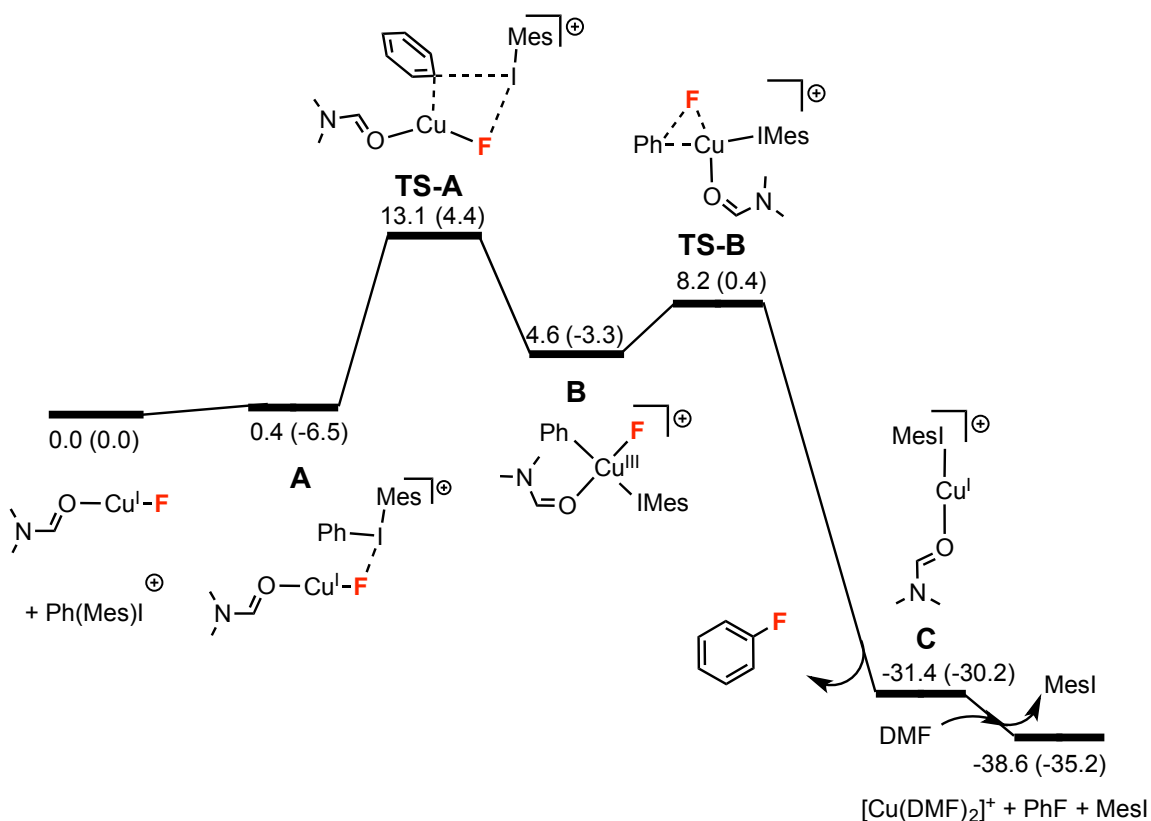
Figure 2.6 Three Possible Active Cu^{I} Complexes Generated *in Situ*



The concentration of DMF relative to $\text{Cu}(\text{OTf})_2$ under the standard reaction conditions is 12.9 M; thus, the formation of $\text{CuF}(\text{DMF})$ seems very likely. For $\text{CuF}(\text{DMF})$, the energy profile of the pathway to product formation is shown in Figure 2.6, and all barriers are reasonable. However, the activation energies for all transfer reactions are higher than the lowest energy pathways for $[\text{Cu}(\text{OTf})\text{F}]^-$ and $[\text{CuF}_2]^-$, noting the uncertainties in comparing energy barriers between the three systems. Furthermore, the

energy pathway from CuF(DMF) does not lead to a viable transition structure for mesityl group transfer. Notably, reductive elimination of PhF from (DMF)Cu^{III}FPh is a very facile process (from **B** to **C** via **TS-B**), only requiring a ΔG^\ddagger of 3.6 kcal/mol, which is substantially lower than for the oxidation processes. Ribas and co-workers previously computed C–F bond-forming reductive elimination at a five-coordinated Cu^{III} center containing a tetradentate macrocyclic ligand, [Cu^{III}F(L-C,N,N',N'')] ⁺ (see Scheme 1.12 in Chapter 1).³³ For this macrocycle, a ΔG^\ddagger of 16.2 kcal/mol was calculated, which is notably higher than in the current system. This may be due to either (1) the extra stability provided by their polydentate ligand and/or (2) the differences between reductive elimination from four- versus five-coordinate Cu^{III} centers. Further studies will be required to delineate this difference.

Figure 2.7 Energy profile for the reaction of [Mes(Ph)I]⁺ with CuF(DMF) at 60°C. Energies $\Delta G(\Delta H)$ in kcal/mol.



Two other possible active Cu^I species ([CuF(OTf)]⁻ and [CuF₂]⁻) were computed and predicted to catalyze the reaction with reasonable energy barriers. However, these

data do not definitely rule out one species over the other as the active species for the catalytic fluorination reaction. We attempted to experimentally probe the $[\text{CuF}_2]^-$ pathway by using CuF_2 as a precatalyst; however, this Cu salt only works when an equimolar amount is present relative to $[\text{ArMesI}]^+$. When substoichiometric amounts of CuF_2 are present, the selectivity is switched to fluoromesitylene **2**. This might be due to the low concentration of fluoride in the reaction.

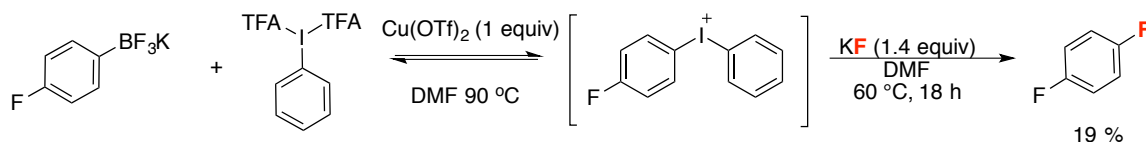
2.3 CONCLUSIONS

In summary, this chapter has described a mild Cu-catalyzed nucleophilic fluorination of unsymmetrical diaryliodonium salts with KF. Using the mesityl group as auxiliary directing ligand at the I(III) center, this protocol preferentially fluorinates the less sterically hindered aromatic group. The reaction exhibits a broad substrate scope (particularly with electron rich arene substrates) and proceeds with high chemoselectivity and functional group tolerance. A combination of experimental and density functional theory (DFT) investigations provide evidence for a Cu^I/Cu^{III} catalytic cycle. The key to selective Cu-catalyzed fluorination is to keep the fluoride concentration low relative to the iodonium reagent. This allows the cationic [Mes(Ar)I⁺] to be available for oxidative “Ar⁺” transfer to the Cu^I center with one or two fluoride ligands: Cu(DMF)F, [CuF(OTf)]⁻ and [CuF₂]⁻. Energy profiles of these possible Cu catalysts were computationally evaluated, and it was found that all show low-energy pathways to fluorinated products. In all cases, oxidative addition is computed as the rate-limiting step. Reductive elimination to form the Ar–F bond is computed to be very facile, which is in contrast to Pd⁰/Pd^{II} catalytic cycles.

2.4 PERSPECTIVE AND OUTLOOK

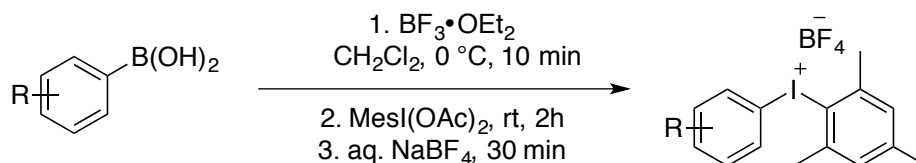
Although Cu-catalyzed fluorination of (Mesityl)(Aryl)iodonium salts with KF demonstrates superior reactivity to other precursors such as aryl halides/pseudohalides, direct access from readily available reagents would be very desirable. Along these lines, forming diaryliodonium salts *in situ* would offer an even more practical method. This *in situ* generation would avoid the cumbersome step of isolation of the iodonium species. As a preliminary result, 19% of 1,4-difluorobenzene was obtained when potassium 4-fluorophenyl trifluoroborate and bis(trifluoroacetoxy)iodobenzene were heated with 1 equivalent of $\text{Cu}(\text{OTf})_2$ at 90°C , followed by addition of 1.4 equivalents of KF at 60°C (Scheme 2.13). Further optimization is required, but this result suggests that the possibility of a one-pot approach to fluoroarenes from aryl trifluoroborate salts and commercially available I(III) reagents. It would be a highly practical method toward making a wide variety of clinically relevant molecules, especially in drug discovery as well as PET radiotracers.

Scheme 2.13 One-Pot Approach to Fluoroarenes: *in Situ* Iodonium Salts Formation³⁴

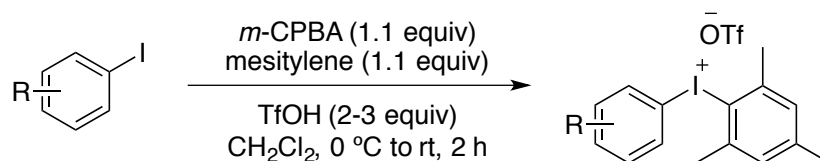


2.5 EXPERIMENTAL

Synthesis of Diaryliodonium Salts:

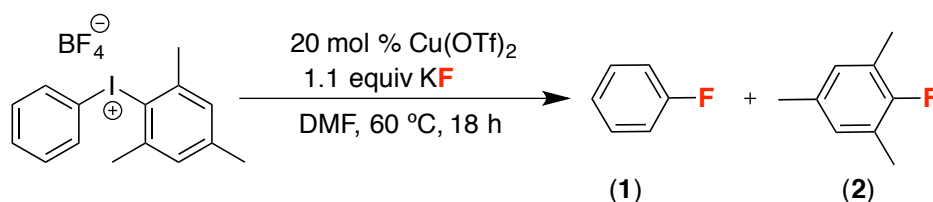


General Procedure A: Tetrafluoroborate Salts. $[\text{Ar}-\text{I}-\text{Mes}]\text{BF}_4$ substrates were prepared by the following procedure adapted from the literature:³⁵ the indicated arylboronic acid (1.0 equiv) and CH_2Cl_2 (0.075 M) were combined in an oven-dried round-bottom flask equipped with a stir bar. The mixture was cooled to 0 °C, $\text{BF}_3 \cdot \text{OEt}_2$ (1.10 equiv) was added, and the mixture was stirred for 10 min. 2-(Diacetoxyiodo)mesitylene (1.05 equiv) was then added as a solution in CH_2Cl_2 (0.33 M), and the mixture was warmed to room temperature and stirred for 2 h. The reaction was quenched by the addition of sat. aqueous NaBF_4 . After 30 minutes of vigorous stirring, the aqueous layer was extracted with CH_2Cl_2 (2x). The combined organic layers were dried over MgSO_4 , filtered, and concentrated under vacuum. Et_2O was added to the residual solid and the diaryliodonium tetrafluoroborate was collected via filtration, washed with Et_2O , dried under vacuum overnight, and stored in a drybox under N_2 until use.



General Procedure B: Triflate Salts. $[\text{Ar}-\text{I}-\text{Mes}]\text{OTf}$ substrates were prepared by the following procedure adapted from the literature:³⁶ to an oven-dried round-bottom flask equipped with a stir bar was added *m*-CPBA (1.10 equiv), CH_2Cl_2 (0.20 M), the indicated iodoarene (1.00 equiv), and mesitylene (1.10 equiv). The mixture was cooled to 0 °C and TfOH (2-3 equiv) was added dropwise while stirring. The reaction was then warmed to room temperature and stirred for 2 h. The solvent was removed under vacuum and Et_2O was added to provide a heterogeneous mixture, which was cooled to -20 °C for at least 30 min. The diaryliodonium triflate was collected on a fritted glass

funnel, washed with Et₂O, dried under vacuum overnight, and stored in a glovebox under N₂ until use.



General Procedure for the Fluorination of Diaryliodonium Salts with KF.

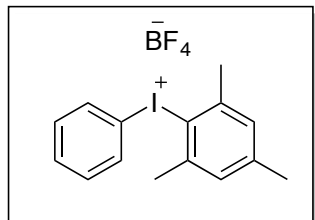
General Procedure a Cu-Catalyzed Reaction on Small Scale. In a glovebox, substrate (0.05 mmol, 1 equiv), Cu(OTf)₂ (3.6 mg, 0.01 mmol, 0.2 equiv unless otherwise noted), KF (3.2 mg, 0.055 mmol, 1.1 equiv unless otherwise noted), and 18-crown-6 (5.3 mg, 0.02 mmol, 0.4 equiv) were combined with DMF (0.5 mL) in a 4 ml vial. The vial was sealed with a Teflon-lined cap, and the reaction mixture was stirred at 60 °C for 18 h unless otherwise noted. After cooling to room temperature, the reaction was quenched with sat. aqueous NaHCO₃ (0.5 mL), and 1-fluoro-3-nitrobenzene (5.3 μL, 0.05 mmol, 1 equiv) was added as an internal standard. The reaction mixture was diluted with CH₂Cl₂ (2 mL), and was analyzed by ¹⁹F NMR spectroscopy and GC-MS.

General Procedure b: Non-Catalyzed (Cu-Free) Reaction on Small Scale. Reactions were conducted analogously to General Procedure A, but in the absence of Cu.

General Procedure c: Cu-Catalyzed Reaction on Larger Scale for Isolation. Reactions were conducted analogously to General Procedure A, but on a 0.1–0.5 mmol scale as indicated. After quenching with NaHCO₃, the mixture was extracted with pentane (3 x 10 mL) and the combined organic layers were dried over MgSO₄, filtered, and concentrated by rotovap at 0 °C. The resulting crude residue was purified by flash column chromatography.

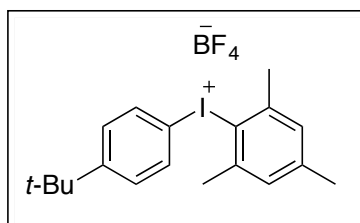
2.6 CHARACTERIZATION

a. Mesityl(Aryl)iodonium Salts:



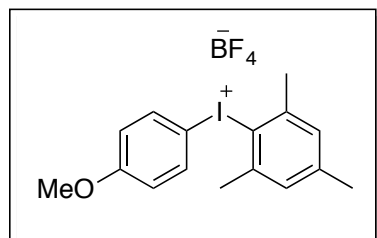
Diaryliodonium Salt 1. General procedure A was followed using phenylboronic acid (1.22 g, 10 mmol), providing **1** as an off-white solid (2.79 g, 68% yield). The ^1H , ^{13}C , and ^{19}F NMR spectroscopic data were identical to that reported previously in the literature.³⁷ HRMS $[\text{M-BF}_4]^+$ Calcd for $\text{C}_{15}\text{H}_{16}\text{I}^+$: 323.0291;

Found: 323.0301.



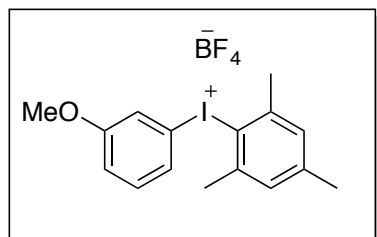
Diaryliodonium Salt 2. General procedure A was followed using 4-(*tert*-butyl)phenylboronic acid (267 mg, 1.5 mmol), providing **2** as a white solid (510 mg, 73% yield). ^1H NMR (700 MHz, $\text{DMSO-}d_6$): δ 7.86 (d, J = 8.4 Hz, 2H), 7.50 (d, J = 8.4 Hz, 2H), 7.21 (s, 2H), 2.60 (s, 6H), 2.29 (s, 3H), 1.24

(s, 9H). ^{13}C NMR (176 MHz, $\text{DMSO-}d_6$): δ 154.7, 142.9, 141.4, 134.1, 129.7, 128.9, 123.2, 111.8, 34.8, 30.7, 26.3, 20.5. ^{19}F NMR (376 MHz, $\text{DMSO-}d_6$): δ -148.2, -148.3. HRMS $[\text{M-BF}_4]^+$ Calcd for $\text{C}_{19}\text{H}_{24}\text{I}^+$: 379.0917; Found: 379.0924.



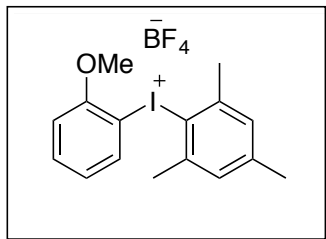
Diaryliodonium Salt 3. General procedure A was followed using 4-methoxyphenylboronic acid (454 mg, 3.0 mmol), providing **3** as an off-white solid (1.01 g, 76% yield). The ^1H , ^{13}C , and ^{19}F NMR spectroscopic data were identical to that reported previously in the literature.³⁸ HRMS $[\text{M-BF}_4]^+$ Calcd for $\text{C}_{16}\text{H}_{18}\text{IO}^+$: 353.0397; Found: 353.0404.

Diaryliodonium Salt 4. General procedure A was followed using 3-



methoxyphenylboronic acid (454 mg, 3.0 mmol), providing **4** as a mustard-yellow solid (240 mg, 30% yield). ^1H NMR (700 MHz, $\text{DMSO-}d_6$): δ 7.56 (s, 1H), 7.43-7.40 (multiple peaks, 2H), 7.23 (s, 2H), 7.20 (d, J = 7.7 Hz, 1H), 3.78 (s, 3H), 2.60 (s, 6H), 2.30 (s, 3H). ^{13}C NMR (176 MHz,

$\text{DMSO-}d_6$): δ 160.5, 143.2, 141.7, 132.6, 129.8, 126.0, 123.5, 120.0, 117.2, 114.4, 54.8, 26.3, 20.5. ^{19}F NMR (376 MHz, $\text{DMSO-}d_6$): δ -148.2, -148.3. HRMS $[\text{M-BF}_4]^+$ Calcd for



$C_{16}H_{18}IO^+$: 353.0397; Found: 353.0405.

Diaryliodonium Salt 5. General procedure A was followed using 2-methoxyphenylboronic acid (456 mg, 3.0 mmol), providing **5** as a white solid (1.05 g, 100% yield). 1H NMR (700 MHz, DMSO- d_6): δ 8.15 (d, $J = 7.0$ Hz, 1H), 7.64 (t, $J =$

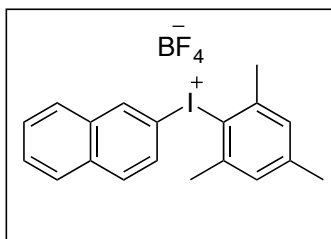
7.0 Hz, 1H), 7.29 (d, $J = 7.0$ Hz, 1H), 7.17 (s, 2H), 7.08 (t, $J = 7.0$ Hz, 1H), 3.87 (s, 3H), 2.60 (s, 6H), 2.27 (s, 3H). ^{13}C NMR (176 MHz, DMSO- d_6): δ 156.6, 142.7, 141.8, 137.6, 134.6, 129.6, 123.3, 121.5, 113.3, 103.9, 56.8, 25.9, 20.5. ^{19}F NMR (376 MHz, DMSO- d_6):

δ

-14

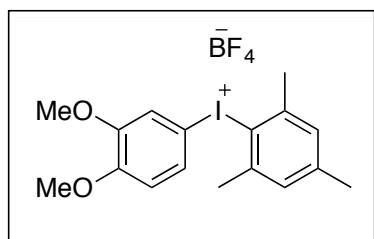
8.2, -148.3. HRMS $[M-BF_4]^+$ Calcd for $C_{16}H_{18}IO^+$: 353.0397; Found: 353.0406.

Diaryliodonium Salt 6. General procedure A was followed using naphthalene-2-



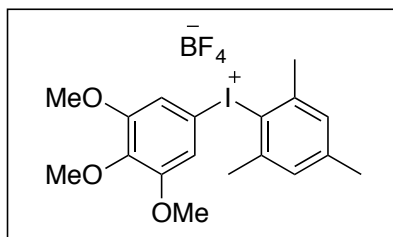
boronic acid (516 mg, 3.0 mmol), providing **6** as an off-white solid (805 mg, 73% yield). The 1H , ^{13}C , and ^{19}F NMR spectroscopic data were identical to that reported previously in the literature.³⁸ HRMS $[M-BF_4]^+$ Calcd for $C_{19}H_{18}I^+$: 373.0448; Found: 373.0456.

Diaryliodonium Salt 7 General procedure A was followed using 3,4-



dimethoxyphenylboronic acid (546 mg, 3.0 mmol), providing **7** as a light brown solid after 3x recrystallization from DCM/hexane (1.02 g, 72% yield). 1H NMR (700 MHz, DMSO- d_6): δ 7.58 (s, 1H), 7.48 (d, $J = 7.0$ Hz), 7.20 (s, 2H), 7.02 (d, $J = 7.0$ Hz, 1H), 3.78 (s, 3H), 3.77 (s, 3H), 2.62 (s,

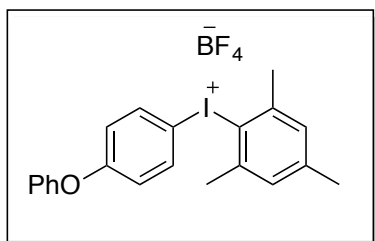
6H), 2.29 (s, 3H). ^{13}C NMR (176 MHz, DMSO- d_6): δ 151.7, 150.1, 142.9, 141.5, 129.7, 128.2, 123.0, 117.7, 114.2, 102.8, 56.2, 55.8, 26.3, 20.5. ^{19}F NMR (376 MHz, DMSO- d_6): δ -148.2, -148.3. HRMS $[M-BF_4]^+$ Calcd for $C_{17}H_{20}IO_2^+$: 383.0502; Found: 383.0508.



Diaryliodonium Salt 8. General procedure A was followed using 3,4,5-trimethoxyphenylboronic acid (318 mg, 1.5 mmol), providing **8** as a brown solid (266 mg, 35% yield). The material was recrystallized 3x from $CHCl_3$ /pentane prior to use. 1H NMR (700 MHz, DMSO-

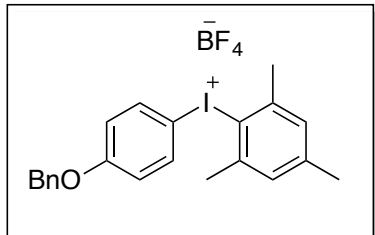
d_6): δ 7.28 (s, 2H), 7.22 (s, 2H), 3.77 (s, 6H), 3.67 (s, 3H), 2.65 (s, 6H), 2.30 (s, 3H). ^{13}C NMR (176 MHz, $\text{DMSO-}d_6$): δ 154.4, 143.1, 141.7, 140.5, 129.7, 122.8, 112.6, 106.8, 60.4, 56.7, 26.5, 20.5. ^{19}F NMR (376 MHz, $\text{DMSO-}d_6$): δ -148.2, -148.3. HRMS $[\text{M-BF}_4]^+$ Calcd for $\text{C}_{18}\text{H}_{22}\text{IO}_3^+$: 413.0608; Found: 413.0613.

Diaryliodonium Salt 9. General procedure A was followed using 4-(phenoxy)phenylboronic acid (642 mg, 3.0 mmol), providing **9** as a white solid (1.14 g, 76% yield). ^1H NMR (700 MHz, $\text{DMSO-}d_6$): δ 7.97 (d, $J = 8.4$ Hz, 2H), 7.45 (t, $J = 8.4$ Hz, 2H), 7.25 (t, $J = 8.4$ Hz, 1H), 7.21 (s, 2H), 7.09 (d, $J = 8.4$ Hz, 2H), 7.03 (d, $J = 8.4$ Hz, 2H), 2.61 (s, 6H), 2.29 (s, 3H). ^{13}C NMR (176 MHz, $\text{DMSO-}d_6$): δ 160.1,

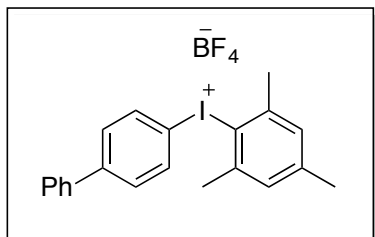


154.6, 143.0, 141.5, 136.9, 130.5, 129.7, 125.1, 123.0, 120.5, 120.1, 106.0, 26.3, 20.5. ^{19}F NMR (376 MHz, $\text{DMSO-}d_6$): δ -148.2, -148.3. HRMS $[\text{M-BF}_4]^+$ Calcd for $\text{C}_{21}\text{H}_{20}\text{IO}^+$: 415.0553; Found: 415.0549.

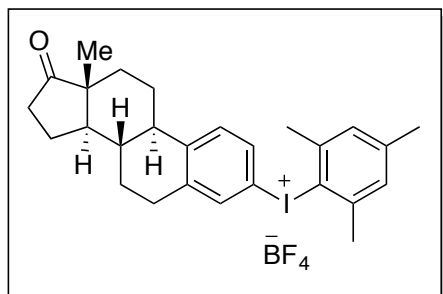
Diaryliodonium Salt 10. General procedure A was followed using 4-(benzyloxy)phenylboronic acid (684 mg, 3.0 mmol), providing **10** as a white solid (867 mg, 56% yield). ^1H NMR (700 MHz, $\text{DMSO-}d_6$): δ 7.92 (d, $J = 9.1$ Hz, 2H), 7.42 (d, $J = 8.4$ Hz, 2H), 7.38 (t, $J = 8.4$ Hz, 2H), 7.33 (t, $J = 8.4$ Hz, 1H), 7.19 (s, 2H), 7.11 (d, $J = 9.1$ Hz, 2H), 5.14 (s, 2H), 2.60 (s, 6H), 2.28 (s, 3H). ^{13}C NMR (176 MHz, $\text{DMSO-}d_6$): δ 160.8, 142.9, 141.3, 136.6,



136.1, 129.7, 128.5, 128.2, 127.9, 123.1, 118.3, 103.6, 69.7, 26.2, 20.5. ^{19}F NMR (376 MHz, $\text{DMSO-}d_6$): δ -148.2, -148.3. HRMS $[\text{M-BF}_4]^+$ Calcd for $\text{C}_{22}\text{H}_{22}\text{IO}^+$: 429.0710; Found: 429.0706.

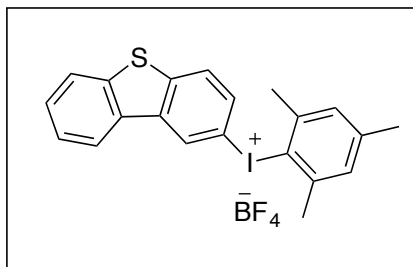


Diaryliodonium Salt 11. General procedure A was followed using 4-biphenylboronic acid (594 mg, 3.0 mmol), providing **11** as a white solid (1.05 g, 72% yield). The ^1H , ^{13}C , and ^{19}F NMR spectroscopic data were identical to that reported previously in the literature.³⁹ HRMS $[\text{M-BF}_4]^+$ Calcd for $\text{C}_{21}\text{H}_{20}\text{I}^+$: 399.0604; Found: 399.0615.



Diaryliodonium Salt 12. General procedure A was followed using the corresponding estrone-derived boronic acid (prepared by a literature procedure^{40,41} (253 mg, 0.8 mmol), providing **12** as an off-white solid (342 mg, 73% yield). ¹H NMR (700 MHz, DMSO-*d*₆): δ 7.74 (s, 1H), 7.70 (d, *J* = 8.4 Hz, 1H), 7.39 (d, *J* = 8.4

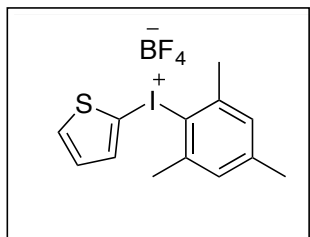
Hz, 1H), 7.21 (s, 2H), 2.86 (m, 2H), 2.61 (s, 6H), 2.42 (dd, *J* = 10.5, 8.4 Hz, 1H), 2.30-2.29 (multiple peaks, 5H), 2.07 (m, 1H), 1.94 (m, 2H), 1.74 (d, *J* = 9.1 Hz, 1H), 1.56-1.46 (multiple peaks, 3H), 1.38-1.37 (multiple peaks, 3H), 0.80 (s, 3H). ¹³C NMR (176 MHz, DMSO-*d*₆): δ 219.4, 144.1, 142.9, 141.5, 140.9, 134.4, 131.7, 129.7, 128.9, 2.5, 111.2, 49.5, 47.2, 43.7, 36.8, 35.3, 31.2, 28.7, 26.4, 25.4, 24.9, 21.1, 20.5, 13.4. ¹⁹F NMR (376 MHz, DMSO-*d*₆): δ -148.2, -148.3. HRMS [M-BF₄]⁺ Calcd for C₂₇H₃₂I O⁺: 499.1492; Found: 499.1500.



Diaryliodonium Salt 13 General procedure A was followed using dibenzo[*b,d*]thien-2-ylboronic acid (315 mg, 1.4 mmol), providing **13** as a brown solid (464 mg, 77% yield). ¹H NMR (700 MHz, DMSO-*d*₆): δ 9.15 (s, 1H), 8.52 (d, *J* = 7.7 Hz, 1H), 8.19 (d, *J* = 7.0 Hz, 1H), 8.12 (d, *J* = 8.4 Hz, 1H), 8.05 (dd, *J* = 7.0, 1.4 Hz, 1H), 7.61-7.55

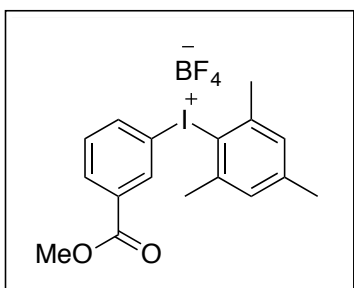
(multiple peaks, 2H), 7.20 (s, 2H), 2.69 (s, 6H), 2.27 (s, 3H). ¹³C NMR (176 MHz, DMSO-*d*₆): δ 142.9, 142.1, 141.6, 139.1, 137.3, 133.6, 132.0, 129.7, 128.9, 128.4, 126.5, 125.4, 123.3, 123.2, 122.8, 110.4, 26.4, 20.5. ¹⁹F NMR (376 MHz, DMSO-*d*₆): δ -148.2, -148.3. HRMS [M-BF₄]⁺ Calcd for C₂₁H₁₈IS⁺: 429.0168; Found: 429.0174.

Diaryliodonium Salt 14. General procedure A was followed using dibenzofuran-4-boronic acid (636 mg, 3.0 mmol), providing **14** as a white solid (1.02 g, 68% yield).

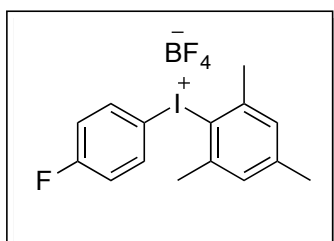


^1H NMR (700 MHz, DMSO- d_6): δ 8.46 (d, J = 7.0 Hz, 1H), 8.32 (d, J = 7.0 Hz, 1H), 8.22 (d, J = 7.0 Hz, 1H), 7.85 (d, J = 7.0 Hz, 1H), 7.65 (t, J = 7.0 Hz, 1H), 7.53-7.49 (multiple peaks, 2H), 7.17 (s, 2H), 2.75 (s, 6H), 2.22 (s, 3H). ^{13}C NMR (176 MHz, DMSO- d_6): δ 155.4, 153.8, 143.5, 142.1,

134.6, 130.1, 129.6, 126.2, 126.1, 125.9, 124.9, 123.6, 123.4, 122.7, 112.4, 95.4, 26.3, 20.4. ^{19}F NMR (376 MHz, DMSO- d_6): δ -148.2, -148.3. HRMS $[\text{M}-\text{BF}_4]^+$ Calcd for $\text{C}_{21}\text{H}_{18}\text{IO}^+$: 413.0397; Found: 413.0398.

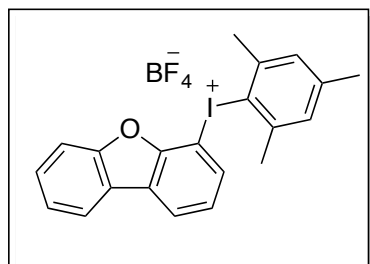


Diaryliodonium Salt 15. Substrate **15** was prepared according to a literature procedure.⁴² The ^1H , ^{13}C , and ^{19}F NMR were identical to that reported previously. HRMS $[\text{M}-\text{BF}_4]^+$ Calcd for $\text{C}_{13}\text{H}_{14}\text{IS}^+$: 328.9855; Found: 328.9858.



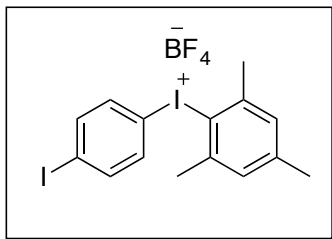
Diaryliodonium Salt 16. General procedure A was followed using 3-(methoxycarbonyl)phenylboronic acid (360 mg, 2.0 mmol), providing **16** as a white powder (325 mg, 35% yield). ^1H NMR (700 MHz, DMSO- d_6): δ 8.49 (s, 1H), 8.13 (d, J = 7.0 Hz, 1H), 8.07 (d, J = 7.0 Hz, 1H), 7.63 (t, J = 7.0 Hz, 1H), 7.25 (s, 2H), 3.89 (s, 3H), 2.59 (s, 6H), 2.29 (s, 3H).

^{13}C NMR (176 MHz, DMSO- d_6): δ 164.5, 143.4, 141.7, 138.3, 134.5, 132.3, 132.2, 132.0, 129.9, 122.5, 114.5, 52.9, 26.3, 20.6. ^{19}F NMR (376 MHz, DMSO- d_6): δ -148.2, -148.3. HRMS $[\text{M}-\text{BF}_4]^+$ Calcd for $\text{C}_{17}\text{H}_{18}\text{IO}_2^+$, 381.0346; Found: 381.0353.



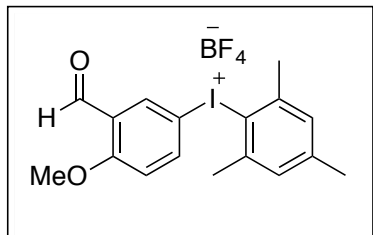
Diaryliodonium Salt 17. General procedure A was followed using 4-fluorophenylboronic acid (419 mg, 1.1 mmol), providing **17** as a white powder (363 mg, 85% yield). The ^1H and ^{13}C NMR spectroscopic data were identical to that reported previously in the literature.³⁷ ^{19}F NMR (376 MHz, DMSO- d_6): δ -107.3 (app tt, J = 9.8, 7.7 Hz), -148.2,

-148.3. HRMS $[\text{M}-\text{BF}_4]^+$ Calcd for $\text{C}_{15}\text{H}_{15}\text{FI}^+$: 341.0197; Found: 341.0196.



Diaryliodonium Salt 18. General procedure A was followed using 4-chlorophenylboronic acid (235 mg, 1.5 mmol), providing **18** as a white powder (310 mg, 45% yield). The ^1H and ^{13}C NMR spectroscopic data were identical to that reported previously in the literature.³⁷ ^{19}F NMR (376 MHz,

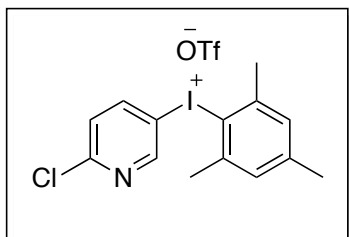
DMSO- d_6): δ -148.2, -148.3. HRMS $[\text{M}-\text{BF}_4]^+$ Calcd for $\text{C}_{15}\text{H}_{15}\text{ClI}^+$: 356.9901; Found: 356.9903.



Diaryliodonium Salt 19. General procedure A was followed using 4-iodophenylboronic acid (372 mg, 1.5 mmol), providing **19** as a white powder (500 mg, 63% yield). The ^1H and ^{13}C NMR spectroscopic data were identical to that reported previously in the literature.³⁴ ^{19}F

NMR (376 MHz, DMSO- d_6): δ -148.2, -148.3. HRMS $[\text{M}-\text{BF}_4]^+$ Calcd for $\text{C}_{15}\text{H}_{15}\text{I}_2^+$: 448.9258; Found: 448.9256.

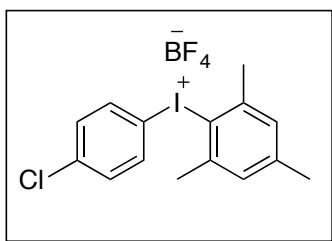
Diaryliodonium Salt 20. General procedure A was followed using 3-formyl-4-methoxyboronic acid (540 mg, 3.0 mmol), providing **20** as a white solid (323 mg, 23%



yield). ^1H NMR (700 MHz, DMSO- d_6): δ 10.3 (s, 1H), 8.18 (s, 1H), 8.13 (d, J = 9.1 Hz, 1H), 7.34 (d, J = 9.1 Hz, 1H), 7.21 (s, 2H), 3.95 (s, 3H), 2.59 (s, 6H), 2.30 (s, 3H). ^{13}C NMR (176 MHz, DMSO- d_6): δ 177.8, 153.2, 133.2, 131.6, 131.5, 124.0, 119.8, 116.2, 112.9, 106.8, 94.1, 46.7, 16.3, 10.5. ^{19}F

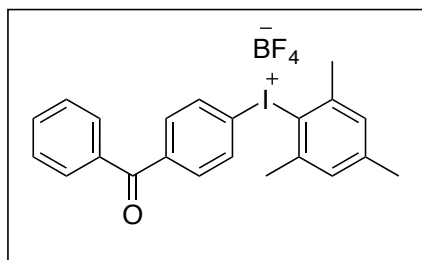
NMR (376 MHz, DMSO- d_6): δ -148.2, -148.3. HRMS $[\text{M}-\text{BF}_4]^+$ Calcd for $\text{C}_{17}\text{H}_{18}\text{IO}_2^+$: 381.0346; Found 381.0349.

Diaryliodonium Salt 21. General procedure B was followed using 2-chloro-5-iodopyridine (700 mg, 3.0 mmol), providing **21** as a brown

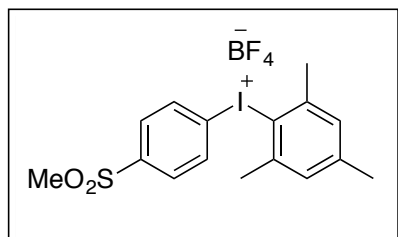


solid (300 mg, 22% yield). ^1H NMR (700 MHz, DMSO- d_6): δ 8.93 (s, 1H), 8.42 (d, J = 8.4 Hz, 1H), 7.69 (d, J = 8.4 Hz, 1H), 7.23 (s, 2H), 2.61 (s, 6H), 2.30 (s, 3H). ^{13}C NMR (176 MHz, DMSO- d_6): δ 153.7, 153.1, 145.1, 143.4, 141.7, 129.9, 127.7, 122.8, 112.2, 26.3, 20.5. ^{19}F NMR (376 MHz, DMSO- d_6): δ -

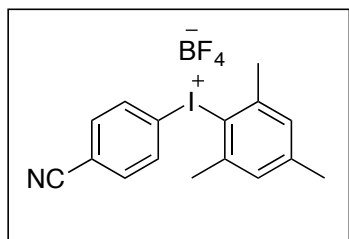
61.7. HRMS $[\text{M}-\text{OTf}]^+$ Calcd for $\text{C}_{11}\text{H}_8\text{ClIN}^+$: 357.9854; Found 357.9857.



Diaryliodonium Salt 22. General procedure A was followed using 4-benzoylphenylboronic acid (678 mg, 3.0 mmol). The product mixture was further purified by flash column chromatography using 0-20% MeOH/DCM as the eluent to afford a white solid (532 mg, 34% yield). ^1H NMR (700 MHz, $\text{DMSO-}d_6$): δ 8.10 (d, $J = 7.0$ Hz, 2H), 7.78 (d, $J = 8.4$ Hz, 2H), 7.68 (multiple peaks, 3H), 7.54 (t, $J = 7.0$ Hz, 2H), 7.26 (s, 2H), 2.63 (s, 6H), 2.32 (s, 3H). ^{13}C NMR (176 MHz, $\text{DMSO-}d_6$): δ 195.0, 143.1, 141.6, 139.5, 135.9, 134.2, 133.4, 132.1, 129.8, 129.7, 128.7, 123.3, 119.4, 26.8, 21.0. ^{19}F NMR (376 MHz, $\text{DMSO-}d_6$): δ -148.2, -148.3. HRMS $[\text{M-BF}_4]^+$ Calcd for $\text{C}_{22}\text{H}_{20}\text{IO}^+$: 427.0553; Found: 427.0553.

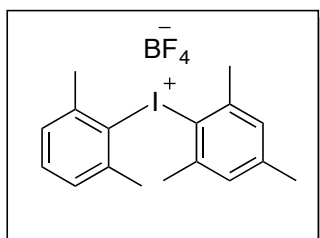


Diaryliodonium Salt 23. General procedure A was followed using 4-(methylsulfonyl)phenylboronic acid (600 mg, 3.0 mmol), providing **23** as a white solid (169 mg, 35% yield). ^1H NMR (700 MHz, $\text{DMSO-}d_6$): δ 8.20 (d, $J = 7.0$ Hz, 2H), 8.00 (d, $J = 7.0$ Hz, 2H), 7.26 (s, 2H), 3.28 (s, 3H), 2.61 (s, 6H), 2.31 (s, 3H). ^{13}C NMR (176 MHz, $\text{DMSO-}d_6$): δ 143.6, 143.5, 141.8, 135.2, 129.9, 129.8, 122.7, 119.7, 43.0, 26.3, 20.5. ^{19}F NMR (376 MHz, $\text{DMSO-}d_6$): δ -148.2, -148.3. HRMS $[\text{M-BF}_4]^+$ Calcd for $\text{C}_{16}\text{H}_{18}\text{IO}_2\text{S}^+$: 401.0067; Found: 401.0068.



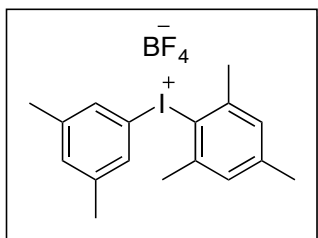
Diaryliodonium Salt 24. General procedure A was followed using 4-cyanophenylboronic acid (438 mg, 1.0 mmol), providing **24** as an off-white solid (209 mg, 16% yield). ^1H NMR (700 MHz, $\text{DMSO-}d_6$): δ 8.11 (d, $J = 8.4$ Hz, 2H), 7.95 (d, $J = 8.4$ Hz, 2H), 7.25 (s, 2H), 2.58 (s, 6H), 2.31 (s, 3H).

^{13}C NMR (176 MHz, $\text{DMSO-}d_6$): δ 143.5, 141.8, 135.0, 134.9, 129.9, 122.8, 119.6, 117.5, 114.4, 26.3, 20.5. ^{19}F NMR (376 MHz, $\text{DMSO-}d_6$): δ -148.2, -148.3. HRMS $[\text{M-BF}_4]^+$ Calcd for $\text{C}_{16}\text{H}_{15}\text{IN}^+$: 348.0244; Found: 328.0240.



Diaryliodonium Salt 25 (Compound 27). General procedure A was followed using 2,6-dimethylphenylboronic acid (157 mg, 1.05 mmol), providing **25** as a white solid (331 mg, 72% yield). ^1H NMR (700 MHz, $\text{DMSO-}d_6$): δ 7.51 (t, $J = 7.0$ Hz, 1H), 7.40

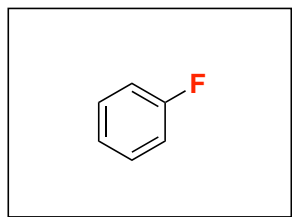
(d, $J = 7.0$ Hz, 2H), 7.24 (s, 2H), 2.54 (s, 6H) 2.51 (s, 6H), 2.32 (s, 3H). ^{13}C NMR (176 MHz, DMSO- d_6): δ 142.8, 142.2, 142.0, 132.5, 130.3, 129.6, 122.6, 118.8, 25.5, 25.3, 20.4. ^{19}F NMR (376 MHz, DMSO- d_6): δ -148.2, -148.3. HRMS $[\text{M-BF}_4]^+$ Calcd for $\text{C}_{17}\text{H}_{20}\text{I}^+$: 351.0604; Found: 351.0613.



Diaryliodonium Salt 26 (Compound 29). General procedure A was followed using 3,5-dimethylphenylboronic acid (224 mg, 1.5 mmol), providing **26** as a white solid (479 mg, 73% yield). ^1H NMR (700 MHz, DMSO- d_6): δ 7.64 (s, 2H), 7.27 (s, 1H), 7.21 (s, 2H), 2.60 (s, 6H), 2.30 (s, 3H), 2.28 (s, 6H). ^{13}C NMR (176 MHz, DMSO- d_6): δ 142.9, 141.6, 141.5, 133.4, 131.9, 129.7, 122.2, 114.1, 26.3, 20.6, 20.5. ^{19}F NMR (376 MHz, DMSO- d_6): δ -148.2, -148.3. HRMS $[\text{M-BF}_4]^+$ Calcd for $\text{C}_{17}\text{H}_{20}\text{I}^+$: 351.0604; Found: 351.0603.

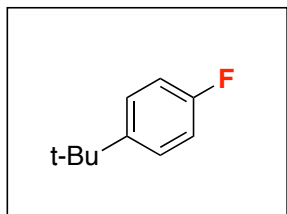
Diaryliodonium Salt 27 (Compound 31b). General procedure A was followed using naphthalene-1-boronic acid (258 mg, 1.5 mmol) and 2,6-(diisopropyl)iodobenzene diacetate,⁴³ providing **27** as a beige solid (364 mg, 72% yield). ^1H NMR (700 MHz, DMSO- d_6): δ 8.23-8.20 (multiple peaks, 3H), 8.09 (d, $J = 8.4$ Hz, 1H), 7.88 (t, $J = 7.0$ Hz, 1H), 7.75 (t, $J = 7.0$ Hz, 1H), 7.57 (m, 2H), 7.42 (d, $J = 7.0$ Hz, 2H), 3.49 (septet, $J = 7.0$ Hz, 2H), 1.12 (d, $J = 7.0$ Hz, 12H). ^{13}C NMR (176 MHz, DMSO- d_6): δ 151.2, 136.2, 134.3, 133.3, 133.1, 131.0, 129.5, 129.4, 128.5, 128.0, 127.8, 127.7, 126.9, 118.0, 24.1. ^{19}F NMR (376 MHz, DMSO- d_6): δ -148.2, -148.3. HRMS $[\text{M-BF}_4]^+$ Calcd for $\text{C}_{22}\text{H}_{24}\text{I}^+$: 415.0917; Found: 415.0920.

b. Fluorinated Product:

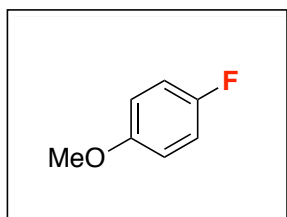


Fluorinated Product 1, Small Scale. General procedure A was followed using diaryliodonium salts **1** (20.5 mg, 0.05 mmol, 1.0 equiv). The fluorinated product **1** was

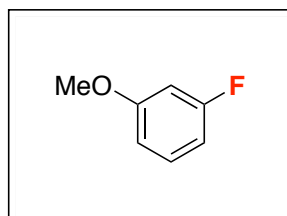
formed in 85% yield as a 98:2 mixture of **1:2** as determined by ^{19}F NMR spectroscopic analysis of the crude reaction mixture. The ^{19}F NMR spectral data for **1** matched that of an authentic sample (Matrix Scientific, m, -113.02 ppm in DMF). The identity of the product was further confirmed by GCMS analysis, where the product peak was observed at 3.56 min.



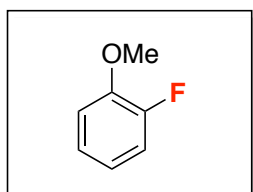
Fluorinated Product 3, Small Scale. General procedure A was followed using diaryliodonium salts **2** (23.3 mg, 0.05 mmol, 1.0 equiv). The fluorinated product **3** was formed in 73% yield as a 99:1 mixture of **3:2** as determined by ^{19}F NMR spectroscopic analysis of the crude reaction mixture. ^{19}F NMR (376 MHz, CDCl_3): δ -119.61 ppm (lit. -119.0 ppm).⁴⁴ The identity of the product was further confirmed by GCMS analysis, where the product peak was observed at 10.6 min.



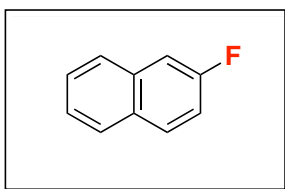
Fluorinated Product 4, Small Scale. General procedure A was followed using diaryliodonium salts **3** (22.0 mg, 0.05 mmol, 1.0 equiv). The fluorinated product **4** was formed in 85% yield as a 99:1 mixture of **4:2** as determined by ^{19}F NMR spectroscopic analysis of the crude reaction mixture. The ^{19}F NMR spectral data for **4** matched that of an authentic sample (Oakwood Products, -124.27 ppm in DMF). The identity of the product was further confirmed by GCMS analysis, where the product peak was observed at 9.50 min.



Fluorinated Product 5, Small Scale. General procedure A was followed using diaryliodonium salts **4** (22.0 mg, 0.05 mmol, 1.0 equiv). The fluorinated product **5** was formed in 54% yield as a 96:4 mixture of **5:2** as determined by ^{19}F NMR spectroscopic analysis of the crude reaction mixture. The ^{19}F NMR spectral data for **5** matched that of an authentic sample (Aldrich, m, -111.07 ppm in DMF). The identity of the product was further confirmed by GCMS analysis, where the product peak was observed at 9.37 min.



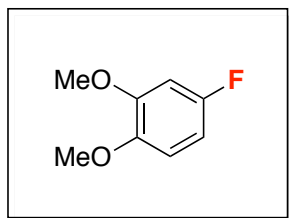
Fluorinated Product 6, Small Scale. General procedure A was followed using diaryliodonium salts **5** (22.0 mg, 0.05 mmol, 1.0 equiv). The fluorinated product **6** was formed in 48% yield as a 96:4 mixture of **6:2** as determined by ^{19}F NMR spectroscopic analysis of the crude reaction mixture. The ^{19}F spectral data for **6** matched that of authentic sample (Matrix Scientific, m, -135.47 ppm in DMF). The identity of the product was further confirmed by GCMS analysis, where the product peak was observed at 9.74 min.



Fluorinated Product 7, Small Scale. General procedure A was followed using diaryliodonium salts **6** (23.0 mg, 0.05 mmol, 1.0 equiv). The fluorinated product **7** was formed in 86% yield as a 98:2 mixture of **6:2** as determined by ^{19}F NMR spectroscopic analysis of the crude reaction mixture. ^{19}F NMR (376 MHz, DMF): $\delta -123.40$ ppm. The identity of the product was further confirmed by GCMS analysis, where the product peak was observed at 12.7 min.

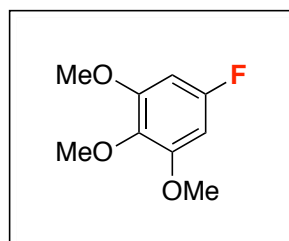
Fluorinated Product 7, Scale-Up for Isolation. General procedure C was followed using diaryliodonium salts **6** (230 mg, 0.5 mmol, 1.0 equiv), $\text{Cu}(\text{OTf})_2$ (36.0 mg, 0.1 mmol, 0.2 equiv), KF (32.0 mg, 0.55 mmol, 1.1 equiv), 18-crown-6 (53.0 mg, 0.2 mmol, 0.4 equiv), and DMF (5.0 mL). The crude reaction mixture was purified by flash column

chromatography using 100% pentane as the eluent, affording product **7** as a white solid (56.9 mg, 78% yield, $R_f = 0.48$ in 100% pentane, mp = 54-55 °C). The ^1H , ^{13}C , and ^{19}F NMR spectroscopic data were identical to that reported previously in the literature.⁴⁵ HRMS EI $[\text{M}]^+$ Calcd for $\text{C}_{10}\text{H}_7\text{F}$: 146.0532; Found 146.0532.



Fluorinated Product 8, Small Scale. General procedure A was followed using diaryliodonium salts **7** (23.5 mg, 0.05 mmol, 1.0 equiv). The fluorinated product **8** was formed in 99% yield as a 96:4 mixture of **8:2** as determined by ^{19}F NMR spectroscopic analysis of the crude reaction mixture. ^{19}F NMR (376 MHz, DMF): $\delta -123.11$ ppm. The identity of the product was further confirmed by GCMS analysis, where the product peak was observed at 12.3 min.

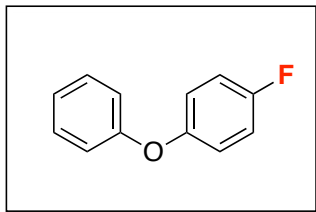
Fluorinated Product 8, Scale-Up for Isolation. General procedure C was followed using diaryliodonium salts **7** (235 mg, 0.5 mmol, 1.0 equiv), $\text{Cu}(\text{OTf})_2$ (36.0 mg, 0.1 mmol, 0.2 equiv), KF (32.0 mg, 0.55 mmol, 1.1 equiv), 18-crown-6 (53.0 mg, 0.2 mmol, 0.4 equiv), and DMF (5.0 mL). The crude reaction mixture was purified by flash column chromatography using 0–50% Et_2O in pentane as the eluent, affording product **8** as a colorless oil (12.3 mg, 74% yield, $R_f = 0.57$ in 90% pentane/10% Et_2O). The ^1H , ^{13}C , and ^{19}F NMR spectroscopic data were identical to that reported previously in the literature.⁴⁶ HRMS EI $[\text{M}]^+$ Calcd for $\text{C}_8\text{H}_9\text{FO}_2$: 156.0587; Found 156.0586.



Fluorinated Product 9, Small Scale. General procedure A was followed using diaryliodonium salts **8** (25.0 mg, 0.05 mmol, 1.0 equiv). The fluorinated product **9** was formed in 62% yield as a 98:2 mixture of **9:2** as determined by ^{19}F NMR spectroscopic

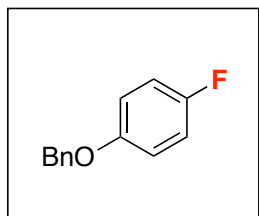
analysis of the crude reaction mixture. ^{19}F NMR (376 MHz, DMF): δ -125.32 ppm. The identity of the product was further confirmed by GCMS analysis, where the product peak was observed at 13.9 min.

Fluorinated Product 9, Scale-Up for Isolation. General procedure C was followed using diaryliodonium salts **8** (75.0 mg, 0.15 mmol, 1.0 equiv), $\text{Cu}(\text{OTf})_2$ (27.1 mg, 0.075 mmol, 0.5 equiv), KF (9.6 mg, 0.165 mmol, 1.1 equiv), 18-crown-6 (15.9 mg, 0.06 mmol, 0.4 equiv), and DMF (1.5 mL). The crude reaction mixture was purified by flash column chromatography using 0–10% Et_2O in pentane as the eluent, affording product **9** as a colorless crystalline solid (14.3 mg, 51% yield, R_f = 0.71 in 90% pentane/10% Et_2O , mp = 54-55 °C) containing 2% 3,4,5-trimethoxyiodobenzene as an impurity. ^1H NMR (700 MHz, CDCl_3): δ 6.31 (d, J = 9.8 Hz, 2H), 3.83 (s, 6H), 3.79 (s, 3H). ^{13}C NMR (176 MHz, CDCl_3): δ 159.4 (d, J = 240 Hz), 153.9 (d, J = 12.3 Hz), 134.4 (d, J = 4.6 Hz), 93.0 (d, J = 26.6 Hz), 61.1, 56.3. ^{19}F NMR (376 MHz, CDCl_3): δ -113.63 (t, J = 10.1 Hz). HRMS EI $[\text{M}]^+$ Calcd for $\text{C}_9\text{H}_{11}\text{FO}_3$: 187.0765; Found: 187.0763.



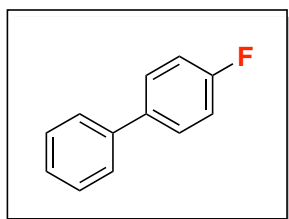
Fluorinated Product 10, Small Scale. General procedure A was followed using diaryliodonium salts **9** (25.1 mg, 0.05 mmol, 1.0 equiv) and $\text{Cu}(\text{OTf})_2$ (9.0 mg, 0.025 mmol, 0.5 equiv). The fluorinated product **9** was formed in 95% yield as a 98:2 mixture of **10:2** as determined by ^{19}F NMR spectroscopic analysis of the crude reaction mixture. ^{19}F NMR (376 MHz, DMF): δ -120.22 ppm. The identity of the product was further confirmed by GCMS analysis, where the product peak was observed at 14.8 min.

Fluorinated Product 10, Scale-Up for Isolation. General procedure C was followed using diaryliodonium salts **9** (251 mg, 0.5 mmol, 1.0 equiv), $\text{Cu}(\text{OTf})_2$ (90.0 mg, 0.25 mmol, 0.5 equiv), KF (32.0 mg, 0.55 mmol, 1.1 equiv), 18-crown-6 (53.0 mg, 0.2 mmol, 0.4 equiv), and DMF (5.0 mL). The crude reaction mixture was purified by flash column chromatography using 100% pentane as the eluent, affording product **10** as a colorless oil (76.1 mg, 81% yield, $R_f = 0.53$ in 100% pentane) containing 2% phenoxybenzene as an impurity. The ^1H , ^{13}C , and ^{19}F NMR spectroscopic data were identical to that reported previously in the literature.⁴⁷ HRMS EI $[\text{M}]^+$ Calcd for $\text{C}_{12}\text{H}_9\text{FO}$: 188.0637; Found 188.0640.



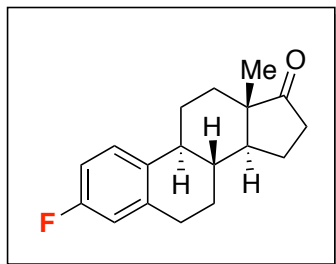
Fluorinated Product 11, Small Scale. General procedure A was followed using diaryliodonium salts **10** (25.8 mg, 0.05 mmol, 1.0 equiv) and $\text{Cu}(\text{OTf})_2$ (9.0 mg, 0.025 mmol, 0.5 equiv). The fluorinated product **11** was formed in 83% yield as a 96:4 mixture of **11:2** as determined by ^{19}F NMR spectroscopic analysis of the crude reaction mixture. ^{19}F NMR (376 MHz, DMF): δ -124.00 ppm. The identity of the product was further confirmed by GCMS analysis, where the product peak was observed at 6.43 min.

Fluorinated Product 11, Scale-Up for Isolation. General procedure C was followed using diaryliodonium salts **10** (258 mg, 0.5 mmol, 1.0 equiv), Cu(OTf)₂ (90.0 mg, 0.25 mmol, 0.5 equiv), KF (32.0 mg, 0.55 mmol, 1.1 equiv), 18-crown-6 (53.0 mg, 0.2 mmol, 0.4 equiv), and DMF (5.0 mL). The crude reaction mixture was purified by flash column chromatography using 0–5% Et₂O in pentane as the eluent, affording product **11** as a white solid (81.8 mg, 81% yield, R_f = 0.63 in 90% pentane/10% Et₂O, mp = 49-50 °C) containing 2% 4-benzyloxyiodobenzene as an impurity. The ¹H, ¹³C, and ¹⁹F NMR spectroscopic data were identical to that reported previously in the literature.⁴⁸ HRMS EI [M]⁺ Calcd for C₁₃H₁₁FO: 202.0794; Found 202.0794.



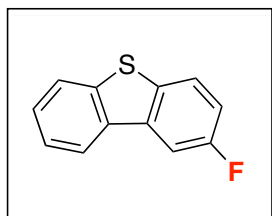
Fluorinated Product 12, Small Scale. General procedure A was followed using diaryliodonium salts **11** (24.3 mg, 0.05 mmol, 1.0 equiv). The fluorinated product **12** was formed in 86% yield as a 95:5 mixture of **12:2** as determined by ¹⁹F NMR spectroscopic analysis of the crude reaction mixture. ¹⁹F NMR (376 MHz, DMF): δ –115.92 ppm. The identity of the product was further confirmed by GCMS analysis, where the product peak was observed at 14.6 min.

Fluorinated Product 12, Scale-Up for Isolation. General procedure C was followed using diaryliodonium salts **11** (243 mg, 0.5 mmol, 1.0 equiv), Cu(OTf)₂ (90.0 mg, 0.25 mmol, 0.5 equiv), KF (32.0 mg, 0.55 mmol, 1.1 equiv), 18-crown-6 (53.0 mg, 0.2 mmol, 0.4 equiv), and DMF (5.0 mL). The crude reaction mixture was purified by flash column chromatography using 100% pentane as the eluent, affording product **12** as a white solid (69.7 mg, 81% yield, R_f = 0.48 in 100% pentane, mp = 69-70 °C). The ¹H, ¹³C, and ¹⁹F NMR spectroscopic data were identical to that reported previously in the literature.⁴⁵ HRMS EI [M]⁺ Calcd for C₁₂H₉F: 172.0688; Found 172.0693.



Fluorinated Product 13, Small Scale. General procedure A was followed using diaryliodonium salts **12** (29.3 mg, 0.05 mmol, 1.0 equiv) and $\text{Cu}(\text{OTf})_2$ (9.0 mg, 0.025 mmol, 0.5 equiv). The fluorinated product **13** was formed in 86% yield as a 96:4 mixture of **13:2** as determined by ^{19}F NMR spectroscopic analysis of the crude reaction mixture. ^{19}F NMR (376 MHz, DMF): δ -118.18 ppm. The identity of the product was further confirmed by GCMS analysis, where the product peak was observed at 9.10 min using the following GC oven temperature program: start at 100 °C, ramp 15 °C/min to 240 °C, and hold for 1 min.

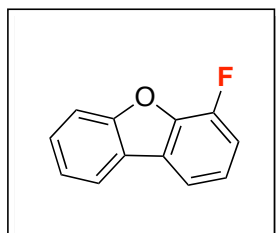
Fluorinated Product 13, Scale-Up for Isolation. General procedure C was followed using diaryliodonium salts **12** (58.6 mg, 0.1 mmol, 1.0 equiv), $\text{Cu}(\text{OTf})_2$ (18.1 mg, 0.05 mmol, 0.5 equiv), KF (6.4 mg, 0.11 mmol, 1.1 equiv), 18-crown-6 (10.6 mg, 0.04 mmol, 0.4 equiv), and DMF (1.0 mL). The crude reaction mixture was purified by flash column chromatography using 90% hexanes/10% EtOAc as the eluent, affording product **13** as a colorless crystalline solid (19.6 mg, 72% yield, R_f = 0.20 in 90% hexanes/10% EtOAc, mp = 175-176 °C). The ^1H , ^{13}C , and ^{19}F NMR spectroscopic data were identical to that reported previously in the literature.⁴¹ HRMS EI $[\text{M}]^+$ Calcd for $\text{C}_{18}\text{H}_{21}\text{FO}$: 272.1576; Found 272.1581.



Fluorinated Product 14, Small Scale. General procedure A was followed using diaryliodonium salts **13** (25.8 mg, 0.05 mmol, 1.0 equiv) and $\text{Cu}(\text{OTf})_2$ (9.0 mg, 0.025 mmol, 0.5 equiv). The fluorinated product **14** was formed in 58% yield as a 98:2 mixture of **14:2** as determined by ^{19}F NMR spectroscopic analysis of the crude reaction mixture.

^{19}F NMR (376 MHz, DMF): δ -117.3 ppm. The identity of the product was further confirmed by GCMS analysis, where the product peak was observed at 7.84 min.

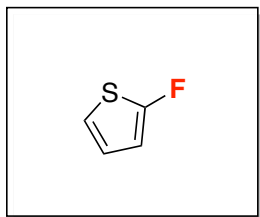
Fluorinated Product 14, Scale-Up for Isolation. General procedure C was followed using diaryliodonium salts **13** (51.6 mg, 0.1 mmol, 1.0 equiv), $\text{Cu}(\text{OTf})_2$ (18.1 mg, 0.05 mmol, 0.5 equiv), KF (6.4 mg, 0.11 mmol, 1.1 equiv), 18-crown-6 (10.6 mg, 0.04 mmol, 0.4 equiv), and DMF (1.0 mL). The solvent was evaporated at room temperature, and the crude reaction mixture was purified by flash column chromatography using 100% pentane as the eluent, affording product **14** as a white solid (11.3 mg, 56% yield, R_f = 0.67 in 100% pentane, mp = 83-84 °C). The ^1H , ^{13}C , and ^{19}F NMR spectroscopic data were identical to that reported previously in the literature.⁴⁹ HRMS EI $[\text{M}]^+$ Calcd for $\text{C}_{12}\text{H}_7\text{FS}$: 202.0252; Found 202.0253.



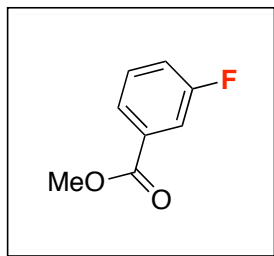
Fluorinated Product 15, Small Scale. General procedure A was followed using diaryliodonium salts **14** (25.0 mg, 0.05 mmol, 1.0 equiv) and $\text{Cu}(\text{OTf})_2$ (9.0 mg, 0.025 mmol, 0.5 equiv). The fluorinated product **15** was formed in 73% yield as a 83:17 mixture of **15:2** as determined by ^{19}F NMR spectroscopic analysis of the crude reaction mixture. ^{19}F NMR (376 MHz, DMF): δ -134.90 ppm. The identity of the product was further confirmed by GCMS analysis, where the product peak was observed at 6.20 min.

Fluorinated Product 15, Scale-Up for Isolation. General procedure C was followed using diaryliodonium salts **14** (250 mg, 0.5 mmol, 1.0 equiv), $\text{Cu}(\text{OTf})_2$ (90.4 mg, 0.25 mmol, 0.5 equiv), KF (32.0 mg, 0.55 mmol, 1.1 equiv), 18-crown-6 (52.8 mg, 0.20 mmol, 0.4 equiv), and DMF (5.0 mL). Product **15** proved difficult to separate from the impurity 2-iododibenzofuran. Thus, the crude reaction mixture was subjected to the following conditions adapted from the literature⁵⁰ in order to convert 2-iododibenzofuran into dibenzofuranol, thereby facilitating purification of **15**: CuI (47.6 mg, 0.25 mmol, 0.5 equiv), 8-hydroxyquinoline (50.8 mg, 0.35 mmol, 0.7 equiv), and DMSO (2.0 mL) were combined in a 4 mL vial. In a separate 20 mL vial equipped with a stir bar, the crude

reaction mixture (containing **15** + the aryl iodide impurity), aqueous tetrabutylammonium hydroxide [1.0 mL of a ~1.5 M solution (Fluka), 1.5 mmol, 3.0 equiv], and H₂O (2.9 mL) were combined. To the resultant cloudy suspension, the CuI/8-hydroxyquinoline solution was added via syringe and the reaction was stirred at 100 °C for 16 h. After cooling to room temperature, the reaction mixture was diluted with sat. aqueous NaHCO₃ (1 mL) and H₂O (10 mL). The mixture was extracted with pentane (3 x 10 mL) and the combined organic layers were washed with 1 M NaOH, dried over MgSO₄, filtered, and concentrated by rotovap at 0 °C. The resulting crude residue was purified by flash column chromatography using 100% pentane as the eluent, affording product **S29** as a white solid (46.4 mg, 50% yield, R_f = 0.56 in 100% pentane, mp = 50-51 °C). ¹H NMR (400 MHz, CDCl₃): δ 7.95 (d, *J* = 7.0 Hz, 1H), 7.72 (dd, *J* = 6.4, 1.2 Hz, 1H), 7.63 (d, *J* = 8.4 Hz, 1H), 7.51 (td, *J* = 8.4, 1.2 Hz, 1H), 7.38 (td, *J* = 8.4, 1.2 Hz, 1H), 7.30-7.21 (multiple peaks, 2H). ¹³C NMR (156 MHz, CDCl₃): δ 156.8, 149.3, 147.9, 143.1, 128.2, 124.2, 123.6, 123.5, 121.3, 116.5, 113.9 (d, *J* = 17.5 Hz), 112.4. ¹⁹F NMR (376 MHz, CDCl₃): δ -136.7 (q, *J* = 5.6 Hz). HRMS EI [M]⁺ Calcd for C₁₂H₇FO: 186.0481; Found 186.0483.

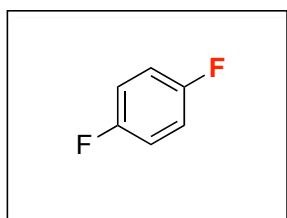


Fluorinated Product 16, Small Scale. General procedure A was followed using diaryliodonium salts **15** (20.8 mg, 0.05 mmol, 1.0 equiv), Cu(OTf)₂ (18.1 mg, 0.05 mmol, 1.0 equiv), and CsF (30.4 mg, 0.2 mmol, 4.0 equiv) at 130 °C for 2 h. The fluorinated product **16** was formed in 42% yield as a >99:1 mixture of **16:2** as determined by ¹⁹F NMR spectroscopic analysis of the crude reaction mixture. ¹⁹F NMR (376 MHz, DMF): δ -134.10 ppm (lit. -134.44 ppm in CDCl₃).⁵¹ The identity of the product was further confirmed by GCMS analysis, where the product peak was observed at 3.28 min.



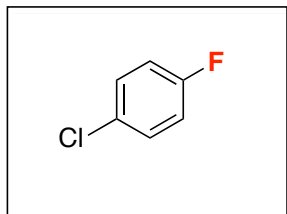
Fluorinated Product 17, Small Scale. General procedure A was followed using diaryliodonium salts **16** (23.4 mg, 0.05 mmol, 1.0 equiv). The fluorinated product **17** was formed in 73% yield as a 96:4 mixture of **17:2** as determined by ^{19}F NMR spectroscopic analysis of the crude reaction mixture. ^{19}F NMR (376 MHz, DMF): δ -112.61 ppm. The identity of the product was further confirmed by GCMS analysis, where the product peak was observed at 11.5 min.

Fluorinated Product 17, Scale-Up for Isolation. General procedure C was followed using diaryliodonium salts **16** (187 mg, 0.4 mmol, 1.0 equiv), $\text{Cu}(\text{OTf})_2$ (28.9 mg, 0.08 mmol, 0.2 equiv), KF (25.6 mg, 0.44 mmol, 1.1 equiv), 18-crown-6 (42.3 mg, 0.16 mmol, 0.4 equiv), and DMF (4.0 mL). The crude reaction mixture was purified by flash column chromatography using 0–5% Et_2O in pentane as the eluent, affording product **17** as a colorless oil (43.1 mg, 70% yield, R_f = 0.44 in 100% pentane) containing 5% 3-(methoxycarbonyl)iodobenzene as an impurity. The ^1H , ^{13}C , and ^{19}F NMR spectroscopic data were identical to that reported previously in the literature.⁵² HRMS EI $[\text{M}]^+$ Calcd for $\text{C}_8\text{H}_7\text{FO}_2$: 154.0430; Found 154.0432.

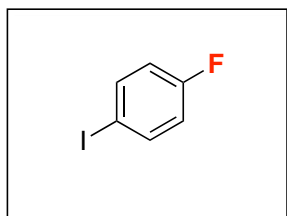


Fluorinated Product 18, Small Scale. General procedure A was followed using diaryliodonium salts **17** (21.4 mg, 0.05 mmol, 1.0 equiv) and $\text{Cu}(\text{OTf})_2$ (9.0 mg, 0.025 mmol, 0.5 equiv). The fluorinated product **18** was formed in 92% yield as a 86:14 mixture of **18:2** as determined by ^{19}F NMR spectroscopic analysis of the crude reaction mixture. The ^{19}F spectral data for **18** matched that of an authentic sample (Alfa Aesar,

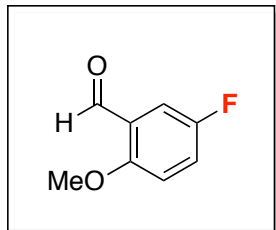
m, -120.01 ppm in DMF). The identity of the product was further confirmed by GCMS analysis, where the product peak was observed at 3.71 min.



Fluorinated Product 19, Small Scale. General procedure A was followed using diaryliodonium salts **18** (22.2 mg, 0.05 mmol, 1.0 equiv) and $\text{Cu}(\text{OTf})_2$ (9.0 mg, 0.025 mmol, 0.5 equiv). The fluorinated product **19** was formed in 74% yield as a 94:6 mixture of **19:2** as determined by ^{19}F NMR spectroscopic analysis of the crude reaction mixture. The ^{19}F spectral data for **19** matched that of an authentic sample (Oakwood Products, m, -117.38 ppm in DMF). The identity of the product was further confirmed by GCMS analysis, where the product peak was observed at 7.97 min.

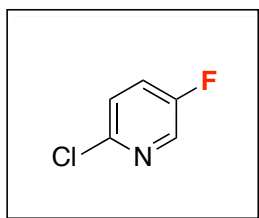


Fluorinated Product 20, Small Scale. General procedure A was followed using diaryliodonium salts **19** (26.8 mg, 0.05 mmol, 1.0 equiv) and $\text{Cu}(\text{OTf})_2$ (9.0 mg, 0.025 mmol, 0.5 equiv). The fluorinated product **20** was formed in 77% yield as a 95:5 mixture of **20:2** as determined by ^{19}F NMR spectroscopic analysis of the crude reaction mixture. The ^{19}F spectral data for **20** matched that of an authentic sample (Aldrich, m, -114.40 ppm in DMF). The identity of the product was further confirmed by GCMS analysis, where the product peak was observed at 11.0 min.



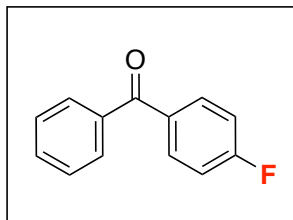
Fluorinated Product 21, Small Scale. General procedure A was followed using diaryliodonium salts **20** (23.4 mg, 0.05 mmol, 1.0 equiv). The fluorinated product **21** was formed in 66% yield as a 97:3 mixture of **21:2** as determined by ¹⁹F NMR spectroscopic analysis of the crude reaction mixture. ¹⁹F NMR (376 MHz, DMF): δ -120.75 ppm. The identity of the product was further confirmed by GCMS analysis, where the product peak was observed at 13.2 min.

Fluorinated Product 21, Scale-Up for Isolation. General procedure C was followed using diaryliodonium salts **20** (140 mg, 0.3 mmol, 1.0 equiv), Cu(OTf)₂ (21.6 mg, 0.06 mmol, 0.2 equiv), KF (19.2 mg, 0.33 mmol, 1.1 equiv), 18-crown-6 (31.8 mg, 0.12 mmol, 0.4 equiv), and DMF (3.0 mL). The crude reaction mixture was purified by flash column chromatography using 10–60% Et₂O in pentane as the eluent, affording product **2** as a colorless crystalline solid (mg, 67% yield, R_f = 0.37 in 90% pentane/10% Et₂O, mp = 40–41 °C), containing 2% 2-methoxybenzaldehyde as an impurity. The ¹H, ¹³C, and ¹⁹F NMR spectroscopic data were identical to that reported previously in the literature.⁵³ HRMS EI [M]⁺ Calcd for C₈H₇FO₂: 154.0424; Found 154.0430.



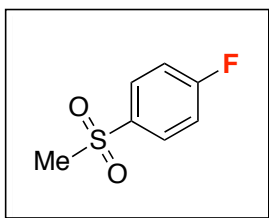
Fluorinated Product 22, Small Scale. General procedure A was followed using diaryliodonium salts **21** (25.4 mg, 0.05 mmol, 1.0 equiv), Cu(OTf)₂ (18.1 mg, 0.05 mmol, 1.0 equiv), and CsF (8.35 mg, 0.055 mmol, 1.1 equiv) at room temperature. The fluorinated product **22** was formed in 33% yield as a 97:3 mixture of **22:2** as determined by ¹⁹F NMR spectroscopic analysis of the crude reaction mixture. The ¹⁹F spectral data for **22** matched that of an authentic sample (Aldrich, m, -128.94 ppm in DMF). The

identity of the product was further confirmed by GCMS analysis, where the product peak was observed at 8.88 min.



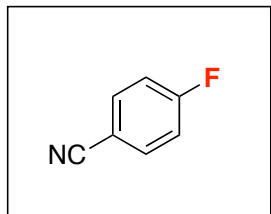
Fluorinated Product 23, Small Scale. General procedure A was followed using diaryliodonium salts **22** (23.4 mg, 0.05 mmol, 1.0 equiv) and $\text{Cu}(\text{OTf})_2$ (9.0 mg, 0.025 mmol, 0.5 equiv). The fluorinated product **23** was formed in 76% yield as a 95:5 mixture of **23:2** as determined by ^{19}F NMR spectroscopic analysis of the crude reaction mixture. ^{19}F NMR (376 MHz, DMF): δ -105.72 ppm. The identity of the product was further confirmed by GCMS analysis, where the product peak was observed at 6.75 min.

Fluorinated Product 23, Scale-Up for Isolation. General procedure C was followed using diaryliodonium salts **22** (128 mg, 0.3 mmol, 1.0 equiv), $\text{Cu}(\text{OTf})_2$ (54.2 mg, 0.15 mmol, 0.5 equiv), KF (19.2 mg, 0.33 mmol, 1.1 equiv), 18-crown-6 (31.8 mg, 0.12 mmol, 0.4 equiv), and DMF (3.0 mL). The crude reaction mixture was purified by flash column chromatography using 10–60% Et_2O in pentane as the eluent, affording product **23** as a white solid (37.8 mg, 63% yield, R_f = 0.60 in 95% pentane/5% Et_2O , mp = 42–43 °C). The ^1H , ^{13}C , and ^{19}F NMR spectroscopic data were identical to that reported previously in the literature.⁵⁴ HRMS EI $[\text{M}]^+$ Calcd for $\text{C}_{13}\text{H}_9\text{FO}$: 200.0637; Found 200.0637.

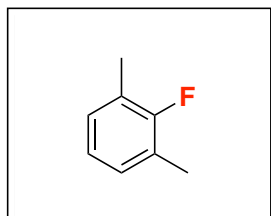


Fluorinated Product 24, Small Scale. General procedure A was followed using diaryliodonium salts **23** (24.4 mg, 0.05 mmol, 1.0 equiv). The fluorinated product **24** was formed in 62% yield as a 94:6 mixture of **24:2** as determined by ^{19}F NMR spectroscopic analysis of the crude reaction mixture. The ^{19}F NMR spectral data for **24** matched that of an authentic sample (Oakwood, m, -104.46 ppm in DMF). The identity of the product

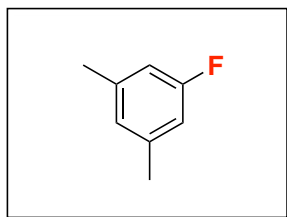
was further confirmed by GCMS analysis, where the product peak was observed at 14.4 min.



Fluorinated Product 25, Small Scale. General procedure A was followed using diaryliodonium salts **24** (26.1 mg, 0.05 mmol, 1.0 equiv). The fluorinated product **25** was formed in 52% yield as a 93:7 mixture of **25:2** as determined by ^{19}F NMR spectroscopic analysis of the crude reaction mixture. The ^{19}F NMR spectral data for **25** matched that of an authentic sample (Oakwood, m, -102.54 ppm in DMF). The identity of the product was further confirmed by GCMS analysis, where the product peak was observed at 10.2 min.



Fluorinated Product 26, Small Scale. General procedure A was followed using diaryliodonium salts **25** (21.9 mg, 0.05 mmol, 1.0 equiv). The fluorinated product **26** was formed in 31% yield as a 50:50 mixture of **26:2** as determined by ^{19}F NMR spectroscopic analysis of the crude reaction mixture. The ^{19}F NMR spectral data for **26** matched that of an authentic sample (Apollo Scientific, m, -121.53 ppm in DMF). The identity of the product was further confirmed by GCMS analysis, where the product peak was observed at 8.78 min.

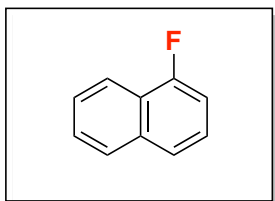


Fluorinated Product 27, Small Scale. General procedure A was followed using diaryliodonium salts **26** (21.9 mg, 0.05 mmol, 1.0 equiv). The fluorinated product **27** was

formed in 91% yield as a 99:1 mixture of **27**:**2** as determined by ^{19}F NMR spectroscopic analysis of the crude reaction mixture. The ^{19}F NMR spectral data for **27** matched that of an authentic sample (Oakwood, m, -114.66 ppm). The identity of the product was further confirmed by GCMS analysis, where the product peak was observed at 8.74 min.

Fluorinated Product 32, Small Scale. General procedure A was followed using diaryliodonium salts **27** (23.0 mg, 0.05 mmol, 1.0 equiv) and $\text{Cu}(\text{OTf})_2$ (9.0 mg, 0.025 mmol, 0.5 equiv). The fluorinated product **32** was formed in 70% yield as a 94:6 mixture of **32**:**2** as determined by ^{19}F NMR spectroscopic analysis of the crude reaction mixture. ^{19}F NMR (376 MHz, DMF): $\delta -123.39$ ppm. The identity of the product was further confirmed by GCMS analysis, where the product peak was observed at 12.8 min.

Fluorinated Product 27, Scale-Up for Isolation. General procedure C was followed using diaryliodonium salts **27** (138 mg, 0.3 mmol, 1.0 equiv), $\text{Cu}(\text{OTf})_2$ (54.2 mg, 0.15 mmol, 0.5 equiv), KF (19.2 mg, 0.33 mmol, 1.1 equiv), 18-crown-6 (31.8 mg, 0.12 mmol, 0.4 equiv), and DMF (3.0 mL). The crude reaction mixture was



purified by flash column chromatography using 100% pentane as the eluent, affording product **32** as a colorless oil (23.6 mg, 54% yield, $R_f = 0.66$ in 100% pentane) containing 3% 2-iodo-1,3-diisopropylbenzene as an impurity. The ^1H , ^{13}C , and ^{19}F

NMR spectroscopic data were identical to that reported previously in the literature.⁴⁵

HRMS EI $[\text{M}]^+$ Calcd for $\text{C}_{13}\text{H}_9\text{F}_3$: 146.0532; Found 146.0532.

2.7 REFERENCES

- (1) (a) Watson, D. A.; Su, M.; Teverovskiy, G.; Zhang, Y.; Garcia-Fortanet, J.; Kinzel, T.; Buchwald, S. L. *Science*. **2009**, 325, 1661. (b) Lee, E.; Hooker, J. M.; Ritter, T. *J. Am. Chem. Soc.* **2012**, 134, 17456. (c) Truong, T.; Klimovica, K.; Daugulis, O. *J. Am. Chem. Soc.* **2013**, 135, 9342.
- (2) (a) Van Der Puy, M. *J. Fluorine Chem.* **1982**, 21, 385. (b) Grushin, V. V.; Kantor, M. M.; Tolstaya, T. P.; Shcherbina, T. M. *Izv. Akad. Nauk SSSR Ser. Khim.* **1984**, 2332.
- (3) (a) Ochiai, M. *Top. Curr. Chem.* **2003**, 224, 5. (b) Malgren, J.; Santoro, S.; Jalalian, N.; Himo, F.; Olofsson, B. *Chem. Eur. J.* **2013**, 19, 10334.
- (4) Pinto de Magalhães, H.; Lüthi, H. P.; Togni, A. *Org. Lett.* **2012**, 14, 3830.
- (5) Ross, T. L.; Ermert, J.; Hocke, C.; Coenen, H. H. *J. Am. Chem. Soc.* **2007**, 129, 8018.
- (6) Unpublished results
- (7) Grushin, V. R. *Acc. Chem. Res.* **1992**, 25, 529.
- (8) (a) Yamada, Y.; Kashima, K.; Okawara, M. *Bull. Chem. Soc. Jpn.* **1974**, 47, 3179. (b) Chun, J.-H.; Lu, S.; Lee, Y.-S.; Pike, V. W. *J. Org. Chem.* **2010**, 75, 3332. (c) Yamada, Y.; Okawara, M. *Bull. Chem. Soc. Jpn.* **1972**, 45, 1860. (d) Larcer, K. M.; Wiegand, G. H. *J. Org. Chem.* **1976**, 41, 3360.
- (9) (a) Grushin, V. V.; Demkina, I. I.; Tolstaya, T. P. *J. Chem. Soc., Perkin Trans. 2* **1992**, No. 4, 505. (b) Carroll, M. A.; Martín-Santamaría, S.; Pike, V. W.; Rzepa, H. S.; Widdowson, D. A. *J. Chem. Soc., Perkin Trans. 2* **1999**, 12, 2707.
- (10) Ochiai, M.; Kitagawa, Y.; Takayama, N.; Takaoka, Y.; Shiro, M. *J. Am. Chem. Soc.* **1999**, 121, 9233.
- (11) Wang, B.; Graskemper, J. W.; Qin, L.; DiMagno, S. G. *Angew. Chem. Int. Ed.* **2010**, 49, 4079.
- (12) Pd(IV): Neufeldt, S. R.; Sanford, M. S. *Acc. Chem. Res.*, **2012**, 45, 936.
- (13) Pt(IV): Wagner, A. M.; Hickman, A. J.; Sanford, M. S. *J. Am. Chem. Soc.* **2013**, 135, 15710.
- (14) Ni(IV): Bour, J. R.; Camasso, N. M.; Sanford, M. S. *J. Am. Chem. Soc.* **2015**, 137, 8034.
- (15) Casitas, A.; Ribas, X. *Chem. Sci.* **2013**, 4, 2301.
- (16) For Cu-catalyzed reactions with Ar₂I⁺, see: (a) Sokolovs, I.; Lubriks, D.; Suna, E. *J. Am. Chem. Soc.* **2014**, 136, 6920. (b) Zhu, S.; MacMillan, D. W. C. *J. Am. Chem. Soc.* **2012**, 134, 10815. (c) Fañanas-Mastral, M.; Feringa, B. L. *J. Am. Chem. Soc.* **2014**, 136, 9894. (d) Lv, T.; Wang, Z.; You, J.; Lan, J.; Gao, G. *J. Org. Chem.* **2013**, 78, 5723. (e) Cullen, S. C.; Shekhar, S.; Nere, N. K. *J. Org. Chem.* **2013**, 78, 12194. (f) Xu, J.; Zhang, P.; Gao, Y.; Chen, Y.; Tang, G.; Zhao, Y. *J. Org. Chem.* **2013**, 78, 8176. (g) Vaddula, B.; Leazer, J.; Varma, R. S. *Adv. Syn. Catal.* **2012**, 354, 986. (h) Baralle, A.; Fensterbank, L.; Goddard, J.-P.; Ollivier, C. *Chem. Eur. J.* **2013**, 19, 10809. (i) Kieffer, M. E.; Chuang, K. V.; Reisman, S. E. *J. Am. Chem. Soc.* **2013**, 135, 5557. (c) Collins, B. S. L.; Suero, M. G.; Gaunt, M. J. *Angew. Chem., Int. Ed.* **2013**, 52, 5799. (j) Phipps, R. J.; McMurray, L.; Ritter, S.; Duong, H. A.; Gaunt, M. J. *J. Am. Chem. Soc.* **2012**, 134, 10773. (e) Zhu, S.; MacMillan, D. W. C. *J. Am. Chem. Soc.* **2012**, 134, 10815. (k)

- Duong, H. A.; Gilligan, R. E.; Cooke, M. L.; Phipps, R. J.; Gaunt, M. J. *Angew. Chem., Int. Ed.* **2011**, *50*, 463. (g) Phipps, R. J.; Gaunt, M. J. *Science* **2009**, *323*, 1593.
- (17) Ichiishi, N.; Canty, A. J.; Yates, B. F.; Sanford, M. S. *Org. Lett.* **2013**, *15*, 5134.
- 18 Ichiishi, N.; Canty, A. J.; Yates, B. F.; Sanford, M. S. *Organometallics* **2014**, *33*, 5525.
- (19) Fier, P. S.; Hartwig, J. F. *J. Am. Chem. Soc.* **2012**, *134*, 10795.
- (20) (a) Furuya, T.; Kamler, A. S.; Ritter, T. *Nature* **2011**, *471*, 470. (b) Purser, S.; Moore, P. R.; Swallow, S.; Gouverneur, V. *Chem. Soc. Rev.* **2008**, *37*, 320.
- (21) Furuya, T.; Kuttruff, C.; Ritter, T. *Curr. Opin. Drug Discovery Dev.* **2008**, *11*, 803.
- (22) (a) Ye, Y.; Sanford, M. S. **2013**, *135*, 4648. (b) Fier, P. S.; Luo, J.; Hartwig, J. F. *J. Am. Chem. Soc.* **2013**, *135*, 2552.
- (23) For examples of metal-free nucleophilic reactions with diaryliodonium salts, see ref 1 and: (a) Wagner, A. M.; Sanford, M. S. *J. Org. Chem.* **2014**, *79*, 2263. (b) Umierski, N.; Manolikakes, G. *Org. Lett.* **2013**, *15*, 188. (c) Jalalian, N.; Ishikawa, E. E.; Silva, L. F.; Olofsson, B. *Org. Lett.* **2011**, *13*, 1552. (d) Laudge, K. P.; Jang, K. S.; Lee, S. Y.; Chi, D. Y. *J. Org. Chem.* **2012**, *77*, 5705. (e) Grushin, V. V.; Kantor, M. M.; Tolstaya, T. P.; Scherbina, T. M. *Izv. Akad. Nauk SSSR, Ser. Khim.* **1984**, 2338.
- (24) For reviews on diaryliodonium salts, see: (a) Yusubov, M. S.; MaskaeV, A. V.; Zhdankin, V. V. *Arkivov* **2011**, *2011*, 370. (b) Merritt, E. A.; Olofsson, B. *Angew. Chem. Int. Ed.* **2009**, *48*, 9052. (c) Canty, A. J.; Rodemann, T.; Ryan, J. H. *Adv. Organomet. Chem.* **2008**, *55*, 279. (d) Zhdankin, V. V.; Stang, P. J. *Chem. Rev.* **2008**, *108*, 5299. (e) Deprez, N. R.; Sanford, M. S. *Inorg. Chem.* **2007**, *46*, 1924. (f) Zhdankin, V. V. *Chem. Rev.* **2002**, *102*, 2523.
- (25) For Cu-catalyzed C-heteroatom coupling reactions with Ar₂I⁺, see: (a) Sokolovs, I.; Lubriks, D.; Suna, E. *J. Am. Chem. Soc.* **2014**, *136*, 6920. (b) Fañanás-Mastral, M.; Feringa, B. L. *J. Am. Chem. Soc.* **2014**, *136*, 9894. (c) Lv, T.; Wang, Z.; You, J.; Lan, J.; Gao, G. *J. Org. Chem.* **2013**, *78*, 5723. (d) Cullen, S. C.; Shekhar, S.; Nere, N. K. *J. Org. Chem.* **2013**, *78*, 12194. (e) Xu, J.; Zhang, P.; Gao, Y.; Chen, Y.; Tang, G.; Zhao, Y. *J. Org. Chem.* **2013**, *78*, 8176. (f) Vaddula, B.; Leazer, J.; Varma, R. S. *Adv. Syn. Catal.* **2012**, *354*, 986.
- (26) Other selected examples on transition metal catalyzed coupling reaction with Ar₂I⁺: (a) Wagner, A. M.; Sanford, M. S. *Org. Lett.* **2011**, *13*, 288. (b) Wagner, A. M.; Hickman, A. J.; Sanford, M. S. *J. Am. Chem. Soc.* **2013**, *135*, 15710. (c) Becht, J.-M.; Drian, C. L. *Org. Lett.* **2008**, *10*, 3161. (d) Beletskaya, I. P.; Davydov, D. V.; Gorovoy, M. S. *Tetrahedron Lett.* **2002**, *43*, 6221.
- (27) (a) Malmgren, J.; Santoro, S.; Jalalian, N.; Himo, F.; Olofsson, B. *Chem. Eur. J.* **2013**, *19*, 10334. (b) Grushin, V. V. *Acc. Chem. Res.* **1992**, *25*, 529. (c) Grushin, V. V.; Demkina, I. I.; Tolstaya, T. P. *J. Chem. Soc. Perkin Trans. 2* **1992**, 505. (d) Chun, J. H.; Lu, S.; Lee, Y. S.; Pike, V. W. *J. Org. Chem.* **2010**, *75*, 3332.
- (28) DFT calculations on Cu-catalyzed reactions with diaryliodonium salts: (a) Chen, B.; Hou, X.-L.; Li, Y.-X.; Wu, Y.-D. *J. Am. Chem. Soc.* **2011**, *133*, 7668. DFT calculations on Pd-catalyzed reactions with diaryliodonium salts (b) Canty, A. J.; Ariafard, A.; Sanford, M. S.; Yates, B. F. *Organometallics* **2013**, *32*, 544.

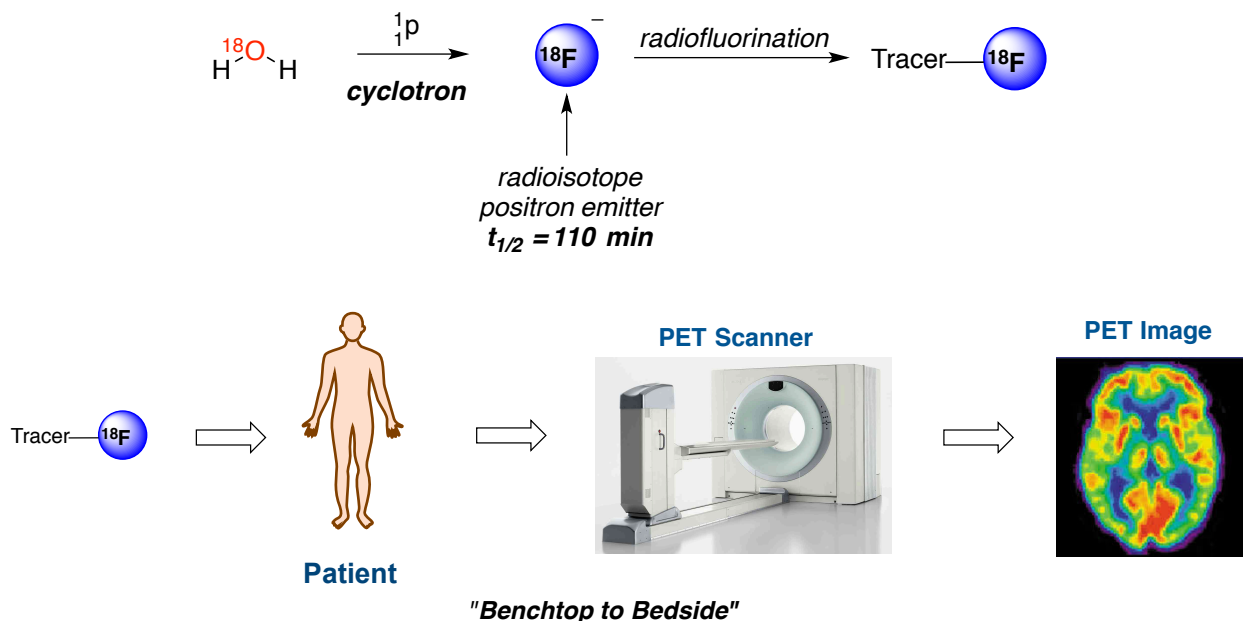
- (29) (a) Muzart, J. *Tetrahedron*, **2009**, *65*, 8313. (b) Malkhasian, A. Y. S.; Finch, M. E.; Nikolovski, B.; Menon, A.; Kucera, B. E.; Chavez, F. A. *Inorg. Chem.* **2007**, *46*, 2950. (c) Teo, J. J.; Chang, Y.; Zeng, H. C. *Langmuir* **2006**, *22*, 7369.
- (30) Lockhart, T. P. *J. Am. Chem. Soc.* **1983**, *105*, 1940.
- (31) Ali, B. F.; Al-Sou'od, K.; Al-Jaar, N.; Nassar, A.; Zaghal, M. H.; Judeh, Z.; Al-Far, R.; Al-Refai, M.; Ibrahim, M.; Mansi, K.; Al-Obaidi, K. H. *J. Coord. Chem.* **2006**, *59*, 229.
- (32) Gaussian 09 was used at the BP86 level for calculations with *N,N*-dimethylformamide as solvent and utilizing the quadruple- ξ valence polarized def2-QZVP basis set on Cu and iodine along with the corresponding ECP and the 6-311pG(2d,p) basis set on other atoms.
- (33) Casitas, A.; Canta, M.; Solà, M.; Costas, M.; Ribas, X. *J. Am. Chem. Soc.* **2011**, *133*, 19386.
- (34) Unpublished results
- (35) Chen, D.-W.; Ochiai, M. *J. Org. Chem.* **1999**, *64*, 6804.
- (36) Bielawski, M.; Zhu, M.; Olofsson, B. *Adv. Synth. Catal.* **2007**, *349*, 2610.
- (37) Kieffer, M. E.; Chuang, K. V.; Reisman, S. E. *Chem. Sci.* **2012**, *3*, 3170.
- (38) Bigot, A.; Williamson, A. E.; Gaunt, M. J. *J. Am. Chem. Soc.* **2011**, *133*, 13778.
- (39) Allen, A. E.; Macmillan, D. W. C. *J. Am. Chem. Soc.* **2011**, *133*, 4260.
- (40) Ahmed, V.; Liu, Y.; Silvestro, C.; Taylor, S. D. *Bioorg. Med. Chem.* **2006**, *14*, 8564.
- (41) Furuya, T.; Strom, A. E.; Ritter, T. *J. Am. Chem. Soc.* **2009**, *131*, 1662.
- (42) Deprez, N. R. *Development of and mechanistic insights into palladium catalyzed C-H arylation reactions*. Ph.D. Thesis, University of Michigan, Ann Arbor, MI, 2010, pp 60-61.
- (43) McKillop, A.; Kemp, D. *Tetrahedron* **1989**, *45*, 3299.
- (44) Lothian, A. P.; Ramsden, C. A.; Shaw, M. M.; Smith, R. G. *Tetrahedron*, **2011**, *67*, 2788.
- (45) Ye, Y.; Sanford, M. S. *J. Am. Chem. Soc.*, **2013**, *135*, 4648.
- (46) Stegmann, H. B.; Deuschle, G.; Schuler, P. *J. Chem. Soc., Perkin Trans. 2* **1994**, 547.
- (47) Kim, H. J.; Kim, M.; Chang, S. *Org. Lett.* **2011**, *13*, 2368.
- (48) Kim, A.; Powers, J. D.; Toczko, J. F. *J. Org. Chem.* **2006**, *71*, 2170.
- (49) Jepsen, T. H.; Larsen, M.; Jørgensen, M.; Solanko, K. A.; Bond, A. D.; Kadziola, A.; Nielson, M. B. *Eur. J. Org. Chem.* **2011**, 53.
- (50) Paul, R.; Ali, M. A.; Punniyamurthy, T. *Synthesis*, **2010**, *24*, 4268.
- (51) Onys'ko, P. P.; Kim, T. V.; Kiseleva, O. I.; Rassukana, Y. V.; Gakh, A. A. *J. Fluorine Chem.* **2009**, *130*, 501.
- (52) Li, L.-C.; Ren, J.; Liao, T.-G.; Jiang, J.-X.; Zhu, H.-J. *Eur. J. Org. Chem.* **2007**, *2007*, 1026.
- (53) Vallgård, J.; Appelberg, U.; Csöreg, I.; Hacksell, U. *J. Chem. Soc., Perkin Trans. 1* **1994**, 461.
- (54) Tang, P.; Ritter, T. *Tetrahedron* **2011**, *67*, 4449.

CHAPTER 3. CU-CATALYZED [¹⁸F]FLUORINATION OF (MESITYL)(ARYL)IODONIUM SALTS AND SYNTHETIC APPLICATIONS

3.1 INTRODUCTION

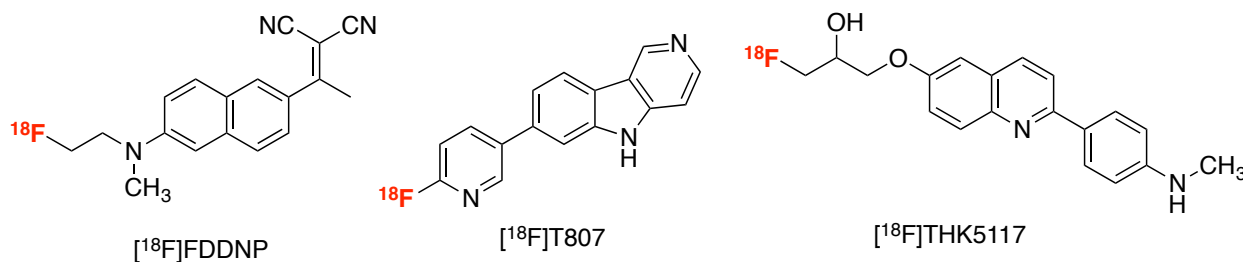
Positron emission tomography (PET) is a powerful and minimally invasive medical imaging technique that provides kinetic physiochemical information.¹ The most commonly used radioisotope for PET is fluorine-18, which offers the advantages of high resolution imaging (ca. 2.5 mm in tissue), a relatively long half-life ($t_{1/2} = 109.7$ min), compared to that of ¹¹C ($t_{1/2} = 20.3$ minutes) and minimal perturbation of radioligand binding. Furthermore, ¹⁸F⁻ can be easily prepared from [¹⁸O]water via the ¹⁸O(p,n)¹⁸F nuclear reaction, making ¹⁸F radiotracers ideal for monitoring *in vivo* metabolic processes.²

Figure 3.1 Positron Emission Tomography (PET)



In the clinical setting, PET imaging is used to assist in the early diagnosis and treatment of brain diseases, including nascent Alzheimer's disease (AD) and Chronic Traumatic Encephalopathy (CTE).³ Currently, definitive clinical diagnosis of AD^{3a} or CTE^{3b} relies on the detection of plaques and neurofibrillary tangles by post-mortem analysis. In contrast, by using PET, CTE and AD can be diagnosed *in vivo* by measuring the concentration and damage of tau protein (CTE) and β -amyloid (AD) respectively. The early development of ^{18}F -radiotracers for CTE diagnosis was limited to mainly C_{sp^3} -labeled ^{18}F -tracers such as [^{18}F]FDDNP⁴ to image the desired pathologies in living humans. However, these molecules were prone to undesired metabolic processes leading to loss of [^{18}F]fluoride as a leaving group. These shortcomings spurred efforts to develop other radiopharmaceuticals such as [^{18}F]T807⁵ and [^{18}F]THK5117,⁶ which can identify tau-protein deposits in living human brains years before symptoms appear (Figure 3.2).^{7,8}

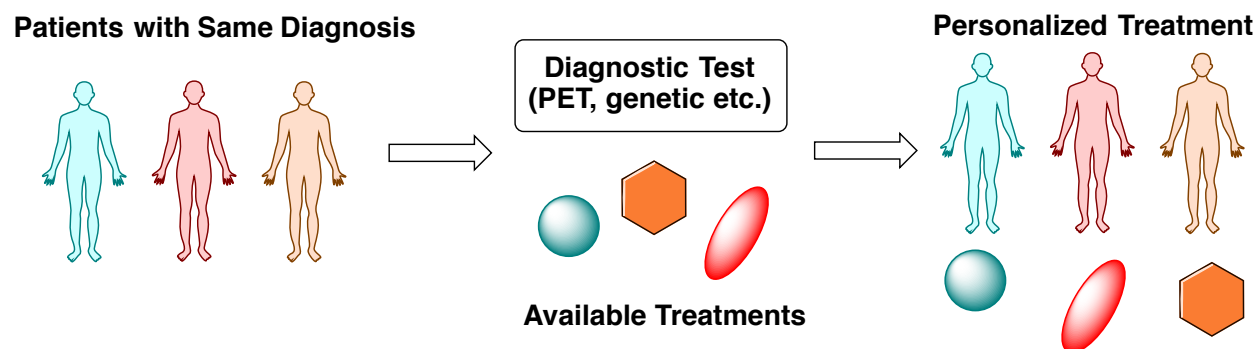
Figure 3.2 Chemical Structures of [^{18}F]FDDNP, [^{18}F]T807 and [^{18}F]THK5117



The discovery and development of novel therapeutics in the pharmaceutical industry demands enormous time and expenditure. The entire process from target identification, to clinical evaluation and ultimately to approval can take nearly a decade. As such, drug development costs for a typical pharmaceutical can be higher than \$10 billion.⁹ Therefore, the pharmaceutical industry strongly desires to utilize any technique that has the ability to ensure that the experimental agent is interacting with the sought-after target and producing a consistent biological response. In this context, PET imaging techniques can make a significant contribution to the pharmaceutical discovery process by aiding in the selection of the most encouraging lead agents in early clinical development and reducing the aforementioned risks. PET imaging is also a valuable tool for establishing *in vivo* target engagement and dose-dependent target occupancy.¹⁰

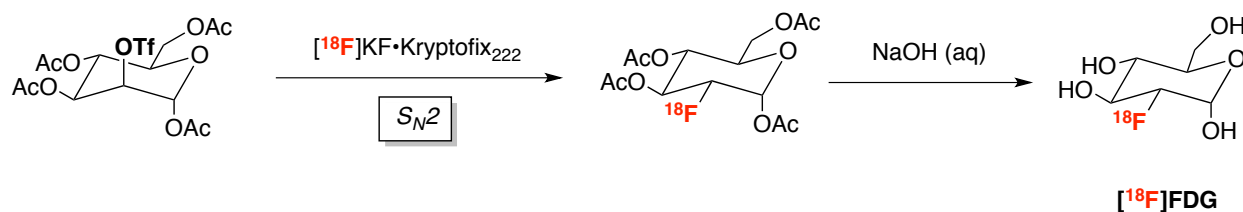
PET can also be used for diagnostic imaging, which monitors the metabolic processes of administered medicines/drug candidates in a patient. This can enable selection of suitable medical treatment for individuals (“personalized therapies”). Such advancements will be highly useful and practical for human healthcare in the future (Figure 3.3).¹¹ More specifically, PET imaging technique is used for predicting response to therapy¹² and monitoring response to therapy.¹³ Furthermore, it can provide clinical trial enrichment. Currently, there are problems with diagnostic accuracy in dementia of only 60 – 85% when using clinical symptoms. It is attributed to problems with expensive clinical trials and also figuring out if a patient is improving is very subjective in dementia patients. Therefore, PET and a pharmacological biomarker of disease is used to get the right patients in clinical trials and monitor response to therapy.¹⁴

Figure 3.3 Personalized Medicine



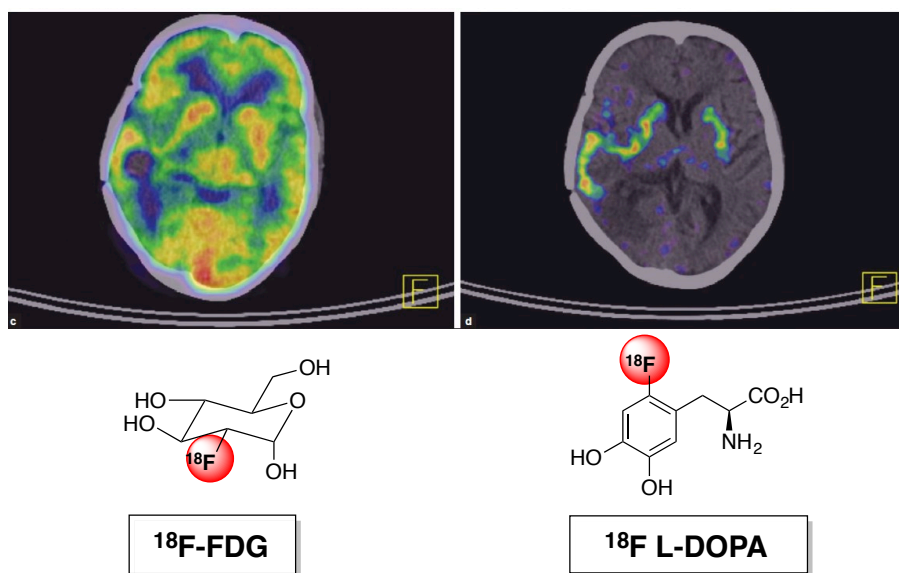
Despite the advantages of PET imaging techniques, the development of novel ^{18}F radiotracers is currently impeded by a scarcity of general and effective radiofluorination methods. At present, the most successful radiopharmaceutical is [^{18}F]fludeoxyglucose (FDG), which contains a $\text{C}_{\text{sp}^3}\text{-}^{18}\text{F}$ bond. As the result of its FDA-approved status and simple, well-established synthetic protocol, [^{18}F]FDG is used in greater than 90% of PET scans conducted in the United States annually (Scheme 3.1).¹⁵

Scheme 3.1 Synthesis of [^{18}F]FDG



The major shortcoming of [^{18}F]FDG as a radiotracer is its lack of *in vivo* site-specificity. Jacob and colleagues have compared different radiotracer probes (^{18}F -FDG, ^{18}F -L-DOPA and ^{13}N -Ammonia) for patients with low-grade brain tumors¹⁶ and demonstrated that although ^{18}F -FDG is known as an excellent tracer for oncological studies,¹⁷ the high background use of glucose (and therefore background uptake of [^{18}F]FDG) in the healthy brain complicates identification and staging of brain tumors with this tracer. An alternative radiotracer with no (or minimal) normal background activity, such as ^{18}F -L-DOPA, would offer advantages, as it is selectively taken up into tumor cells with large amino acid pools, thus allowing invaluable imaging brain tumor imaging (Figure 3.4). Despite the attractive attributes of this tracer, [^{18}F]-L-DOPA is still a mostly investigational radiopharmaceutical that has not advanced to routine clinical use because the current-state-of-the-art synthetic methodologies are not capable of sufficiently producing [^{18}F]-L-DOPA for routine clinical use.¹⁸

Figure 3.4 Brain Image of Patient with Brain Tumor with Low Grade Astrocytoma¹⁶

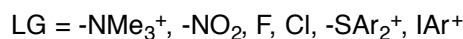


There are currently few robust synthetic procedures for the incorporation of ^{18}F into organic molecules with sufficient speed, selectivity, yield, radiochemical purity, and reproducibility to provide imaging materials for clinical application. Methodologies for the late stage nucleophilic [^{18}F]fluorination of electron-rich aromatic substrates remain an especially long-standing challenge in the PET community.¹⁹ The majority of radiofluorination methods for electron-rich aromatics utilize electrophilic fluorinating

reagents derived from $[^{18}\text{F}]\text{F}_2$.¹ However, $[^{18}\text{F}]\text{F}_2$ production typically requires $^{19}\text{F}_2$ as a carrier gas, which leads to low specific activity (SA; a ratio of ^{18}F -tracer/ ^{19}F -tracer) radiotracers (typically <1.0 Ci/mmol) and requires specialized facilities for handling this highly toxic gas.

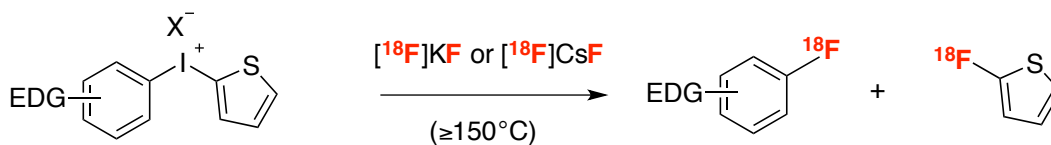
The development of $[^{18}\text{F}]\text{KF}$ production from $[^{18}\text{O}]\text{water}$ has provided the means to synthesize high SA radiotracers ($>1,000$ Ci/mmol) through nucleophilic substitution (typically $\text{S}_{\text{N}}2$ or $\text{S}_{\text{N}}\text{Ar}$).¹ However, the use of $[^{18}\text{F}]\text{KF}$ is generally limited to the formation of primary $\text{sp}^3\text{-C-F}$ bonds or $\text{sp}^2\text{-C-F}$ bonds contained in activated electron-deficient aromatic groups (Scheme 3.2).

Scheme 3.2 Nucleophilic Aromatic Radiofluorination



Two major strategies have been used to address these limitations. The first involves radiofluorination of powerful electrophiles, such as diaryliodonium salts.²⁰ Diaryliodonium salts bearing 2-thienyl functional groups have been shown to react with $[^{18}\text{F}]\text{KF}$ at elevated temperatures (≥ 150 °C) to afford $[^{18}\text{F}]\text{fluoroarenes}$ (Scheme 3.3).²¹ In these systems, the 2-thienyl group is used as a directing group that enables selective radiofluorination of the less electron-rich aromatic ligand on iodine, with moderate to good selectivity.²¹ However, the $[(\text{thienyl})(\text{aryl})\text{I}]^+$ starting materials are often challenging to prepare, suffer from low stability, and have a limited shelf-life.²² Furthermore, substrates bearing electron neutral or donating aromatic substituents often require high temperatures, react with modest regioselectivity, demonstrate limited functional group tolerance, and provide low radiochemical yields.²¹ As such, this strategy has proven inadequate to access important radiotracers, most notably 6- $[^{18}\text{F}]\text{fluoro-L-DOPA}$ derivatives.²³ It was noted after our publication, DiMugno demonstrated a successful radiofluorination of 6- $[^{18}\text{F}]\text{fluoro-L-DOPA}$.²⁴

Scheme 3.3 Radiofluorination of (2-thienyl)(aryl)iodonium Salts

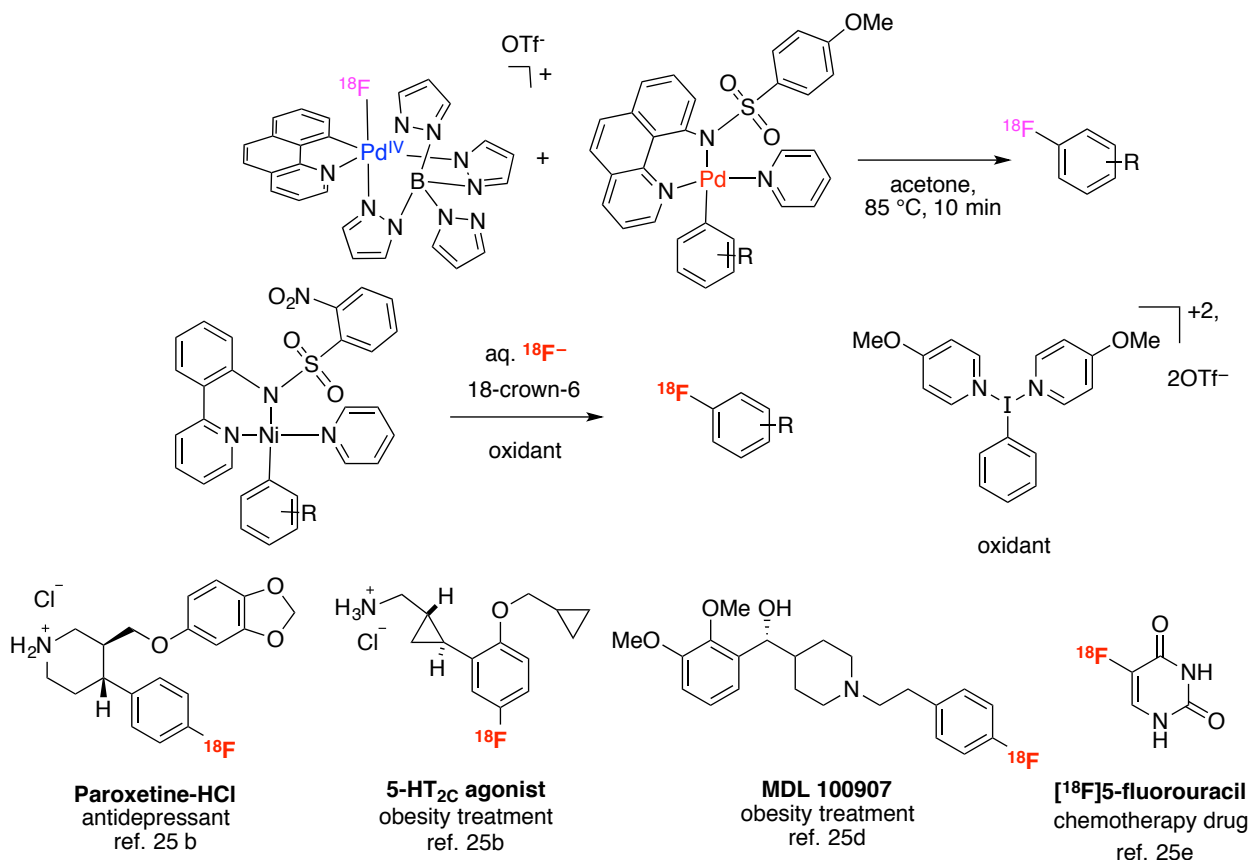


Challenging Synthesis
Moderate stability, shelf life

Modest yields
Regioisomers

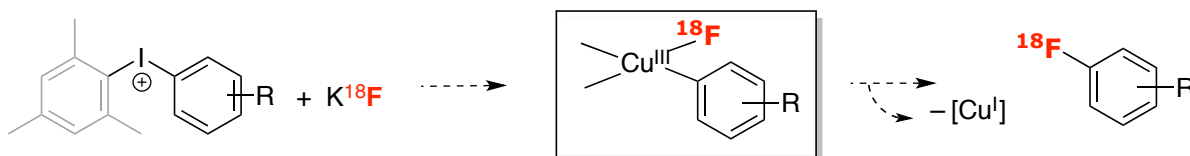
A second strategy applies transition metal catalysts and/or reagents to achieve nucleophilic radiofluorination.^{25, 26} Transition metal catalysis offers opportunities for accelerating radiofluorination reaction rates as well as enhancing selectivity and reactivity. For instance, Hooker and Ritter pioneered nucleophilic radiofluorination methods utilizing Pd^{25a-b} and Ni^{25c} complexes (Scheme 3.4). These systems were successfully applied to synthesize various radiotracers, including paroxetine,^{25b} a 5-HT_{2c} agonist,^{25b} MDL 100907,^{25d} and 5-fluorouracil.^{25e} However, the requirement for the multistep synthesis of organometallic reagents under inert atmospheres has thus far limited adoption of these chemistries by non-experts.²⁷

Scheme 3.4 Ritter's Nucleophilic Radiofluorination using Pd- and Ni-complexes



In Chapter 2, the development of Cu-catalyzed fluorination of (mesityl)(aryl)iodonium salts with KF was detailed. We sought to translate this methodology to radiofluorination for the synthesis of diverse ^{18}F -labeled aromatic substrates that previously were difficult to access using conventional methods. We hypothesized that, through the merging of transition metal catalysis with fluorination of diaryliodonium reagents, our goal to develop a practical and selective procedure for routine PET tracer syntheses would be achieved (Scheme 3.5).²⁸

Scheme 3.5 Proposed Cu-mediated Radiofluorination of Diaryliodonium Reagents



This chapter describes our investigation into translating the Cu-catalyzed fluorination of (mesityl)(aryl)iodonium salts with KF into a radiofluorination method. This work was conducted in collaboration with Professor Peter Scott, and his colleagues in the UM Department of Radiology.^{29,30} As detailed below, we successfully developed a practical, rapid and highly selective Cu-catalyzed radiofluorination of (mesityl)(aryl)iodonium salts using $[\text{}^{18}\text{F}]\text{KF}$ to access ^{18}F -labeled electron-rich, neutral, and deficient aryl fluorides under a single set of reaction conditions. This methodology was applied to the synthesis of analogues of radiotracer molecules with potential clinical applications, including a protected version of $[\text{}^{18}\text{F}]\text{F-DOPA}$.

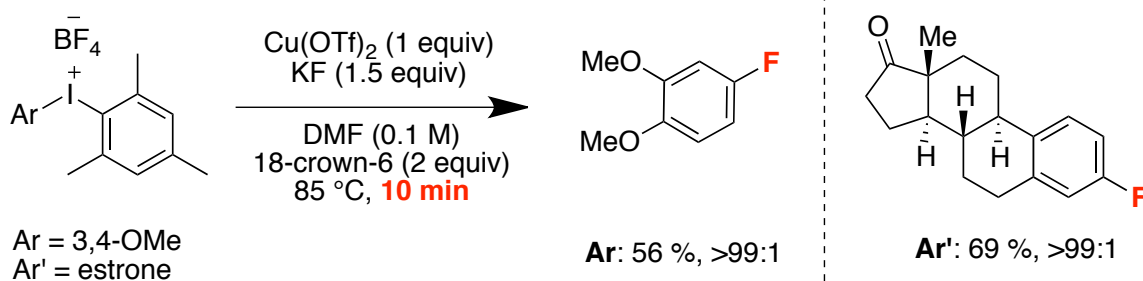
3.2 RESULTS AND DISCUSSION

The translation of our previously reported Cu-catalyzed fluorination method,³¹ first required us to consider key challenges for $[\text{}^{18}\text{F}]\text{fluorination}$: (1) reaction stoichiometry has to be compatible with nanomolar concentrations of the radionuclide; (2) radiochemical reaction times must be short (typically 3 to 30 min) due to the limited half-lives of PET radionuclides (^{11}C $t_{1/2} = 20.38$ min, ^{18}F $t_{1/2} = 109.7$ min); (3) radiochemical yields (RCY) of the radiopharmaceutical must be high enough, such that after completion of quality control testing (20 min to 1 h) and transport of the dose(s) to the PET imaging center (minutes to hours) there is a sufficient dose remaining to administer to the patient(s); (4) methods should generate radiopharmaceuticals in high specific

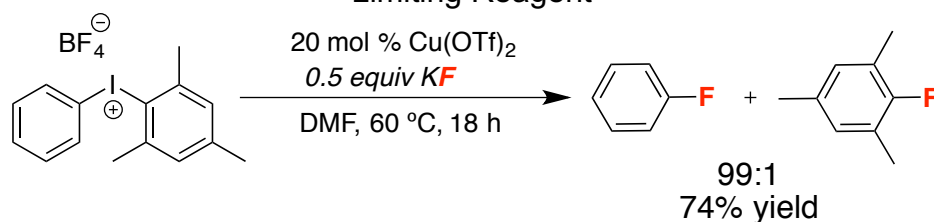
activity ($>1 \text{ Ci mmol}^{-1}$). Specific activity is the activity of a given radioisotope per unit mass. Synthesis of ^{18}F -radiopharmaceuticals with high specific activity provides quantitative information that is important for assessing radioactivity in certain environments. This is readily achievable using high specific activity nucleophilic fluoride, but cannot be achieved using electrophilic ^{18}F - ^{19}F gas as the fluoride source. (5) For a novel PET radiochemistry methodology to find the greatest applicability it must be operationally simple and readily translatable to PET Centers all over the world for use by non-experts. Many imaging centers do not have the luxury of trained organic chemists on staff.

As a demonstration of the potential for Cu-catalyzed ^{18}F -fluorination of (mesityl)aryl iodonium salts, we first optimized reaction conditions to increase the rate of the transformation. We found that the use of a stoichiometric amount of $\text{Cu}(\text{OTf})_2$ and of 18-crown-6 enabled the formation of 3,4-dimethoxyfluorobenzene (**Ar**, Scheme 3.6) and fluoroestrone (**Ar'**) in good yield and excellent selectivity within 10 minutes. We also found during the course of mechanistic investigation studies (details are discussed in chapter 2) that fluoride can be the limiting reagent and still afford product in 74% yield with 99:1 selectivity (Scheme 3.7).

Scheme 3.6 Rapid Cu-Catalyzed Fluorination of (Mesityl)Aryl iodonium Salts



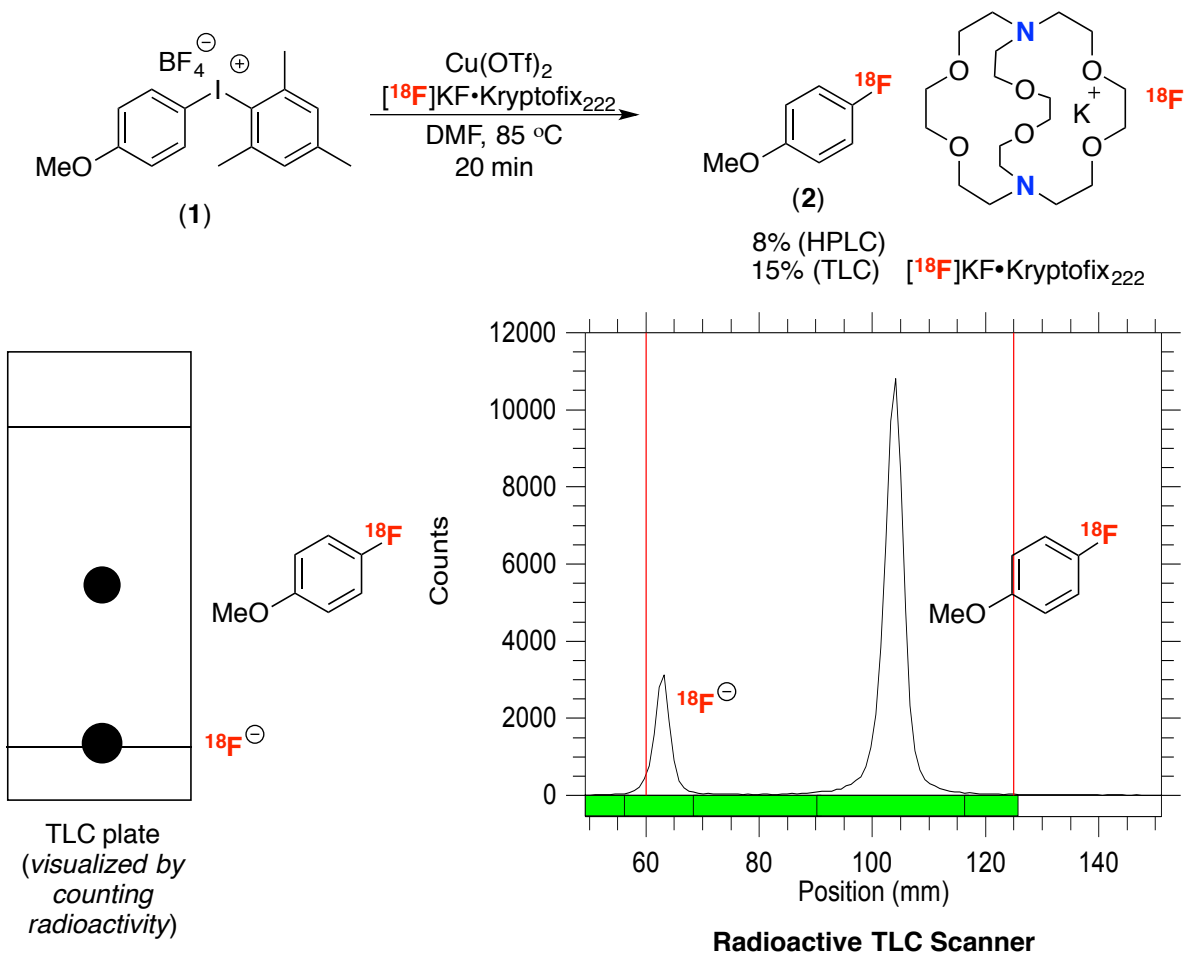
Scheme 3.7 Cu-Catalyzed Fluorination of (Mesityl)phenyl Iodonium Salts with KF as the Limiting Reagent^a



^aYield calculated based on the amount of KF.

Preliminary Results and Key Considerations. Having identified conditions to achieve the rapid fluorination of highly electron-rich substrates, we next tested our Cu-catalyzed protocol under ^{18}F -fluorination conditions. The iodonium salt $[\text{Mes-I-}p\text{OMePh}]^+$ was selected as a model compound, as previous literature reports have demonstrated that 4-methoxyphenyl groups are difficult to ^{18}F -label, typically affording low yields (0-4% radiochemical yield (RCY)).³² To isolate ^{18}F fluoride, we utilized Kryptofix ($\text{K}_{2,2,2}$) as a phase transfer catalyst to form KF-Kryptofix complex (shown in Scheme 3.8). Our first trial using ^{18}F KF-Kryptofix afforded product **1** in 8% yield in 20 min (as determined by radio-HPLC). High selectivity was observed for 4- ^{18}F fluoroanisole, and <1% of ^{18}F fluoromesitylene was detected by radio-TLC or radio-HPLC. To put this initial result into context, if 10% RCC of a desired ^{18}F -labeled product is obtained, the yield is good enough to be considered for automated synthesis. We quickly identified that radio-HPLC had some discrepancy in quantifying product yields, and was therefore not suitable for quantitative reaction analysis. A radioactivity detecting TLC scanner allowed for more accurate quantification of the radioactivity on TLC-plates, because the mass was 100% conserved, whereas loss of ^{18}F fluoride can occur on the HPLC, likely due to the hydrogen bonding to free silanol during inefficient reverse phase column capping process.³³ As such, RCCs computed from HPLC traces tend to be higher than the actual value.³⁴ Using this TLC method, 15% RCC was obtained for the model compound. Furthermore, HPLC was primarily used for qualitative analysis to determine the radiochemical purity of the reaction mixture and identify the radioactive compounds observed by TLC. This was done by co-injecting authentic samples of unlabeled ^{19}F reference standards with the reaction mixture (see the experimental section for further information).

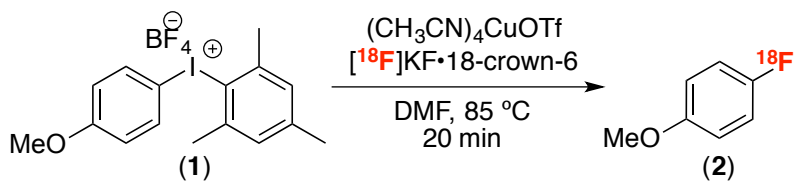
Scheme 3.8 Cu-catalyzed [^{18}F]fluorination and Quantification of Radiochemical Conversion



Evaluation of Cu-precatalyst: Kryptofix contains two nitrogen atoms (highlighted in blue, Scheme 3.8) that could potentially coordinate to Cu *in situ*.³⁵ Hence, 18-crown-6 was next explored as the phase transfer catalyst, resulting in an improved $36 \pm 19\%$ RCC (entry 1, Table 3.1). To further address the irreproducibility issue, we sought an alternate Cu precursor to catalyze the radiofluorination. A variety of Cu^I and Cu^{II} complexes were examined (see entries 2-4). Commercially available and bench stable $(\text{CH}_3\text{CN})_4\text{CuOTf}$ proved optimal, providing high radiochemical conversion and improved reproducibility ($70 \pm 11\%$ RCC over $n = 11$, entry 4). A control experiment in the absence of Cu provided no detectable 4- $[\text{}^{18}\text{F}]$ fluoroanisole and only 6% RCC of $[\text{}^{18}\text{F}]$ fluoromesitylene (entry 5). The highest yields and reproducibility were achieved under the following condition: 6 μmol loading of **1**, 1:1 molar ratio of CuOTf to **1**, 85 °C,

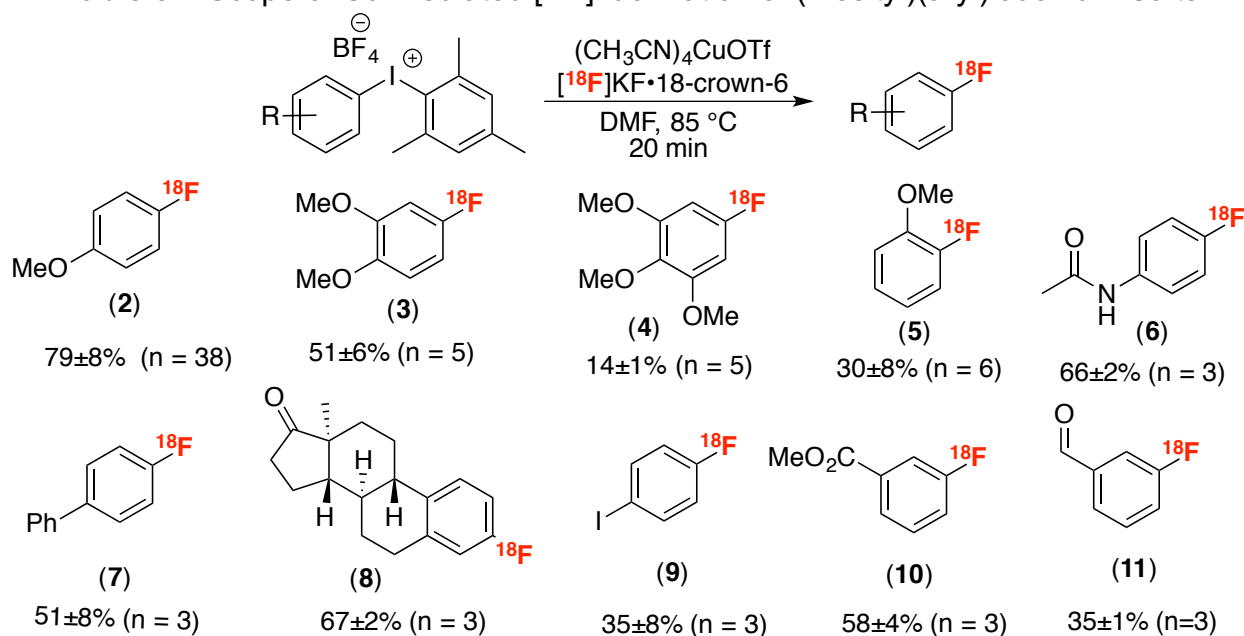
20 min, in a total volume of 750 μ L DMF. Using these conditions, **2** was obtained in 79 \pm 8% (n = 38).

Table 3.1 Evaluation of Cu Salts with Iodonium Salt **1** to yield 4- 18 F]-anisole



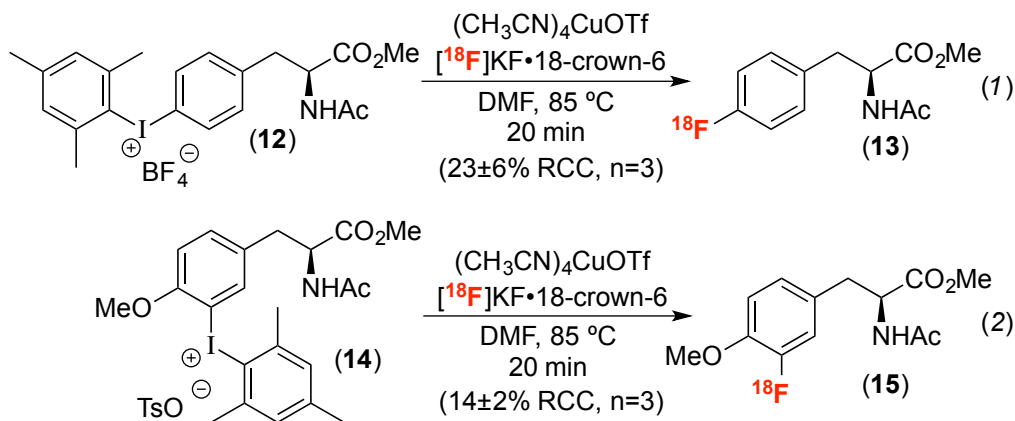
Entry	[Cu]	[Cu]:(1)	RCC 2
1	Cu(OTf) ₂	1:2	36 \pm 19% (n = 15)
2	CuCO ₃ ·Cu(OH) ₂	1:2	10 \pm 6% (n = 3)
3	CuOTf·toluene	1:2	43 \pm 15% (n = 3)
4	(CH ₃ CN) ₄ CuOTf	1:2	70 \pm 11% (n = 11)
5	none	n/a	<1%
6	(CH ₃ CN) ₄ CuOTf	1:1	79 \pm 8% (n = 38)

As described above, we obtained better results with Cu(I) precatalysts versus Cu(II) precatalysts for PET chemistry. Previously, in the course of mechanistic studies using KF, (CH₃CN)₄CuOTf was shown to have faster initial reaction rates relative to Cu(OTf)₂ (Chapter 2, Figure 2.3). We hypothesize that this is why (CH₃CN)₄CuOTf is a better choice of precatalyst for these 20 min radiofluorination reactions. This catalyst is stable in DMF and the stock solution can stand on benchtop after approximately 3 hours and still show the same reactivity. In PET chemistry, poor reproducibility is frequently observed, and an initial concern was that merging Cu-catalysis to radiofluorination under ambient conditions would lead to challenges. However, despite the ambient atmosphere, this chemistry proved highly tolerant of air and moisture and was highly reproducible. This Cu protocol obviates the need for extensive drying of reagents.³⁶ As a demonstration of the high practicality of this methodology, multiple scientists have performed radiofluorinations using these conditions and the outcomes were quite reproducible with radiochemical yields within a range of \pm 10%.

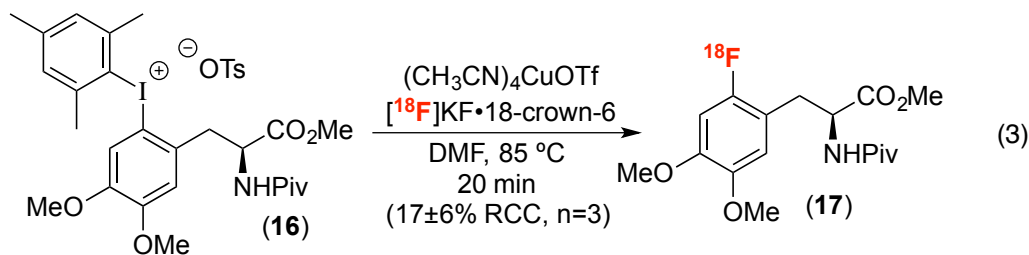
Table 3.2 Scope of Cu-Mediated [¹⁸F]fluorination of (Mesityl)(aryl)iodonium Salts

Substrate Scope. We next examined the substrate scope of this radiofluorination. As shown in Table 3.2, this protocol affords modest to good RCCs with a series of highly electron-rich substrates within 20 minutes (**2–5**, **7** and **8**). This chemistry is also tolerant of a wide variety of important functional groups, including amides **6**, esters **10**, iodo **9** substituents, and aldehydes.

Three (mesityl)(aryl)iodonium salts derived from aromatic amino acids (**12**, **14**, and **16**) were prepared and subjected to the radiofluorination protocol in collaboration with Dr. Joseph Topczewski. Without any additional optimization, the radiolabeled products **13**, **15**, and **17** were obtained in 17-23% RCC (eq 1-3). Importantly, **13** represents the protected analog of 4-[¹⁸F]fluoro-L-phenylalanine (F-PHE), a radiotracer originally developed in the 1970s as a probe of pancreatic cancer and cerebral protein synthesis.³⁷ However, clinical applications of F-PHE to tumor imaging have not been realized partially due to a deficiency of acceptable radiosynthesis procedures. The original doses of F-PHE were prepared in low specific activity (<0.01 Ci/mmol) and required a dose “approaching toxic levels in order to obtain adequate sample count rates.”^{21b,38} The current protocol affords protected F-PHE (**13**) in 23% RCC (eq 1) as well as the more electron-rich 3-[¹⁸F]fluorotyrosine derivative **15** in 14% RCC (eq 2).



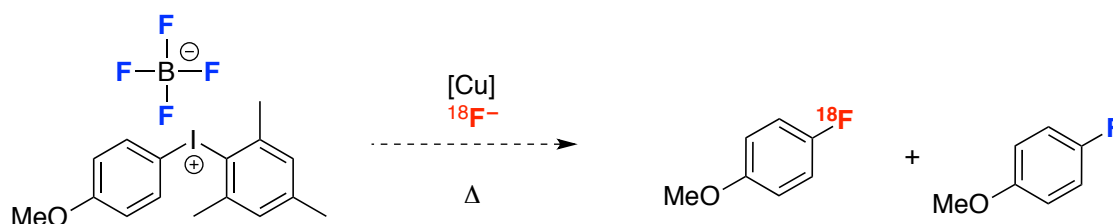
Finally, protected 6- $[\text{}^{18}\text{F}]$ fluoro-L-DOPA **17** was prepared in $17\pm 6\%$ RCC (eq 3). As discussed above, this molecule has been of great interest to the PET community since the 1970's due to its numerous clinical applications.^{39,40} Traditionally, 6- $[\text{}^{18}\text{F}]$ fluoro-L-DOPA was employed in studies of the dopaminergic system and post-treatment monitoring of Parkinson's disease.^{9a} More recently, applications of 6- $[\text{}^{18}\text{F}]$ fluoro-L-DOPA have expanded into oncology, such as the study of neuroendocrine tumors, as well as congenital hyperinsulinism.^{9b} The most significant limitation to the use of 6- $[\text{}^{18}\text{F}]$ fluoro-L-DOPA is the most common method to prepare this radiotracer uses toxic and low specific activity $[\text{}^{18}\text{F}]\text{F}_2$ gas. However, despite decades of research, there is no routine automated synthesis of ^{18}F -DOPA in clinical use. To further demonstrate the utility of this method, we have performed an automated synthesis of **17** from the shelf stable salt **16**. This afforded a $17\pm 6\%$ RCC of **17** (ca. 60 mCi) with a SA of 4000 ± 2000 Ci/mmol (n = 2), thus offering a practical F-DOPA synthesis for further clinical development.



Isotopic Exchange. One concern in the radiofluorination of tetrafluoroborate salts such as **1** is the possibility for isotopic dilution, via $^{18}\text{F}/^{19}\text{F}$ exchange between the $[\text{}^{19}\text{F}]\text{BF}_4^-$ counter ion and $[\text{}^{18}\text{F}]\text{KF}$.⁴¹ Although it is often expressed as a concern, isotopic exchange of $^{18}\text{F}/^{19}\text{F}$ under the temperature of thermal decomposition of

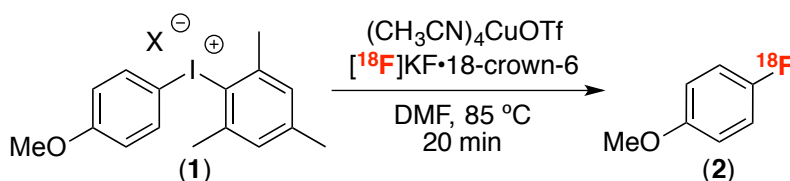
diaryliodonium salts has not been thoroughly investigated to date (Scheme 3.9). Previously, Berridge observed isotopic exchange of $^{18}\text{F}/^{19}\text{F}$ from tetrafluoroborate anion in the context of the Balz-Schiemann reaction.⁴² In addition, Knochel replaced tetrafluoroborate derivatives with tetrachloroborate anions and $[\text{}^{18}\text{F}]\text{Bu}_4\text{NF}$ to radiofluorinate p-toluidine diazonium tetrachlorate in good radiochemical yield. A side product, $[\text{}^{18}\text{F}]\text{BFCl}_3^-$, was also formed in the transformation.⁴³

Scheme 3.9 Does Isotopic Dilution Occur Under the Optimized Condition?



In principle, this issue could be addressed by changing the counter ion;⁴⁴ however, an evaluation of different $[\text{4-OMePh-I-Mes}]\text{X}$ salts showed that the highest radiochemical yields were obtained with BF_4 (entry 1, Table 3.3), potentially due to the enhanced solubility of the tetrafluoroborate salt towards undesired side reactions. On the contrary, fluoride-free counter ions, such as tosylate (entry 2) or bromide (entry 5), led to a steep erosion in yield.

Table 3.3. Studies on Counteranion Effects

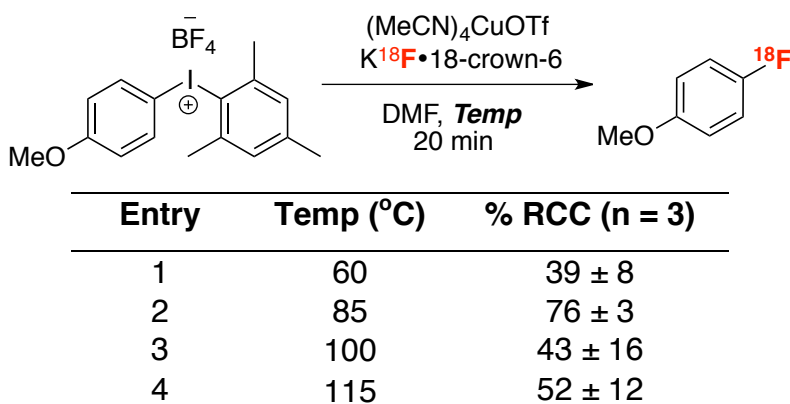


Entry	X	RCC
1	BF_4	$79\pm 8\%$ (n = 38)
2	TsO	$45\pm 26\%$ (n = 3)
3	PF_6	$53\pm 7\%$ (n = 3)
4	TfO	<1%
5	Br	<1%

Furthermore, we examined the influence of temperature, identifying $85\text{ }^\circ\text{C}$ as the optimal. Interestingly, as we evaluated elevated temperatures not only did the RCC of **2** decrease, but the UV trace of the HPLC analysis became increasingly more complex

This suggests that side reactions occur at high temperatures with faster relative rates (Table 3.4). These observations led us to consider whether isotopic exchange may occur at higher temperature.

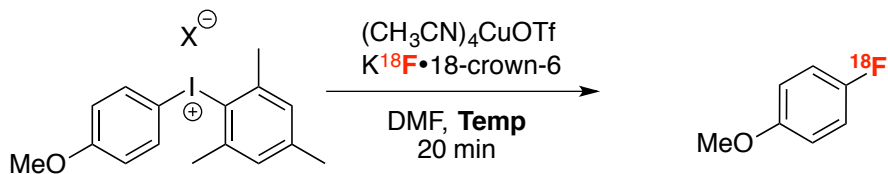
Table 3.4 Influence of Temperature^a



Specific Activity Study. Specific activity is the ratio of $^{18}\text{F}/^{19}\text{F}$ (Ci/mmol), which measures isotopic dilution under the reaction conditions. In our studies, automated syntheses were conducted in a standard automated synthesis module with 1500 mCi initial activity of ^{18}F . To test whether isotopic dilution from the BF_4 counter ion occurs under our optimized conditions, we compared the specific activity (SA) of the 4- ^{18}F fluoroanisole product obtained from [4-OMePh-I-Mes] BF_4 to that from [4-OMePh-I-Mes]OTs. Under automated conditions, [4-OMePh-I-Mes] BF_4 afforded a RCY of $40 \pm 10\%$ and a SA of 1800 ± 800 Ci/mmol ($n=3$), while [4-OMePh-I-Mes]OTs afforded $10 \pm 2\%$ RCY with a comparable SA of 3000 ± 1000 Ci/mmol ($n=3$). Within the error of the measurement, these values are approximately the same. These results indicate that, while there might be a slight decrease in SA between the BF_4 and OTs analogs, isotopic dilution is not a significant problem under these reaction conditions as it was predicted that the specific activity would be below 1000 Ci/mmol if significant isotopic exchange occurs under the reaction condition.⁴⁵ For a proof-of-concept, this reaction was repeated with [4-OMePh-I-Mes] BF_4 at 150°C and found that not only the RCC decreased to $6 \pm 1\%$, but specific activity of the reaction mixture was significantly reduced to 300 ± 170 Ci/mmol (entry 3). This suggested that isotopic exchange is very rapid under the thermally forcing conditions. The addition of the copper mediator allows both a decrease

to the reaction temperature and the use of readily soluble iodonium salts which overall accelerate the desired radiofluorination.

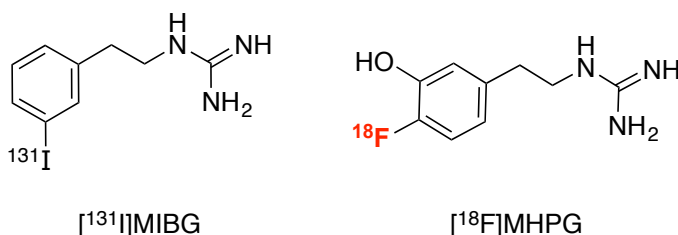
Table 3.5 Specific Activity Calculation



Entry	X	Temp (°C)	RCC	Specific Activity (SA) (Ci/mmol)
1	BF ₄	85	40±10% (n = 3)	1800±800
2	OTs	85	10±2% (n = 3)	3000±1000
3	BF ₄	150	6±1% (n = 3)	300±170

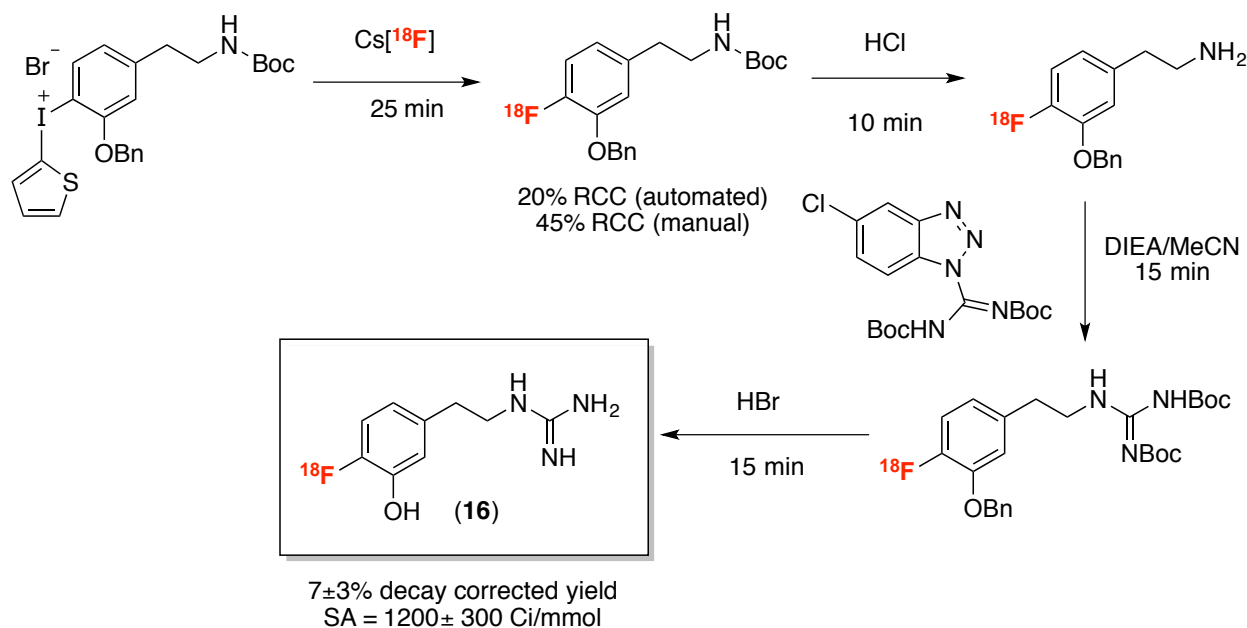
Synthesis of ¹⁸F-MHPG. We next sought to apply our Cu-mediated nucleophilic radiofluorination of (mesityl)(aryl)iodonium salts to the development of a high yielding, automated, and clinically useful synthesis of the radiotracer 4-[¹⁸F]fluoro-*m*-hydroxyphenethylguanidine (4-[¹⁸F]MHPG). Developed by Professor David Raffel and his colleagues at University of Michigan, [¹⁸F]MHPG is a promising radiotracer for quantifying regional cardiac sympathetic nerve density in the human heart.⁴⁶ There are only a few radiotracers reported that are selective for the cardiac nerve system *in vivo*. [¹³¹I]*meta*-iodobenzylguanidine ([¹³¹I]MIBG)⁴⁷ is one of the first radiopharmaceuticals developed for scintigraphic imaging of presynaptic sympathetic nerve fibers. These radiotracers can visualize changes in the regional distribution of cardiac sympathetic nerves in many heart diseases, such as congestive heart failure, diabetic autonomic neuropathy, myocardial infarction, cardiac arrhythmia and Parkinson's disease.⁴⁸ Preliminary results from the Raffel group suggest that **16** could out-perform MIBG, which is the current standard of care (Figure 3.5).

Figure 3.5 Chemical Structure of [¹⁸F]MHPG and [¹³¹I]MIBG

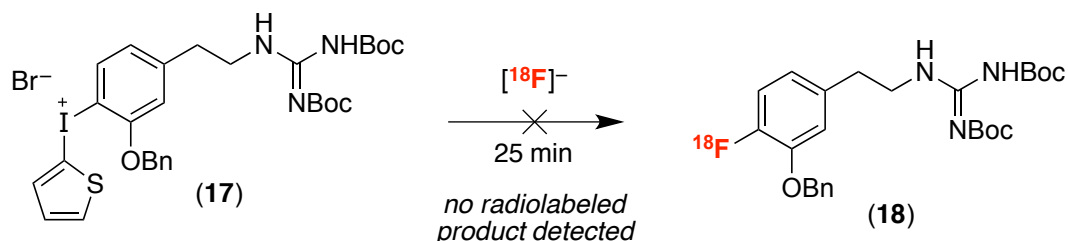


Despite great promise for [^{18}F]MHPG as a radiotracer, there is not a viable synthesis in place to meet clinical demand. The current state-of-art method for the synthesis of 4- ^{18}F]MHPG involves three linear steps that take place following the ^{18}F -labeling of (2-thienyl)(m-benzoylphenethyl(*N*-Boc)amine)iodonium bromide. A severe ^{18}F -decay occurred during the following steps. In total this route affords a $7\pm 3\%$ radiochemical yield of 4- ^{18}F]MHPG, which is equal to less than 100 mCi of activity (~ 10 -20 mCi) at the end of the synthesis (Scheme 3.10). Overall the time from the end of bombardment (i.e. the complete production of nucleophilic [^{18}F]fluoride from the cyclotron) for this method exceeds 1 hour, and therefore results in a significant loss of radioactivity. The authors hypothesized that late-stage radiofluorination of an intermediate such as **17**, could circumvent the aforementioned problems, but their attempts to achieve late-stage radiofluorination was unfortunately unsuccessful (Scheme 3.11). This part of chapter 3 describes our efforts toward applying our Cu-mediated [^{18}F]fluorination protocol to the synthesis of 4- ^{18}F]F-MHPG.

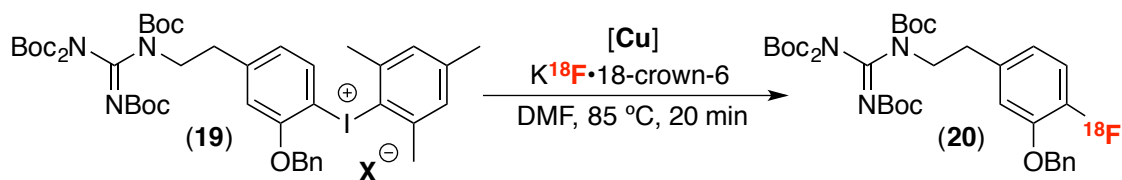
Scheme 3.10 Current Synthesis of 4- ^{18}F]F-MHPG



Scheme 3.11 Attempted Radiofluorination of **17**



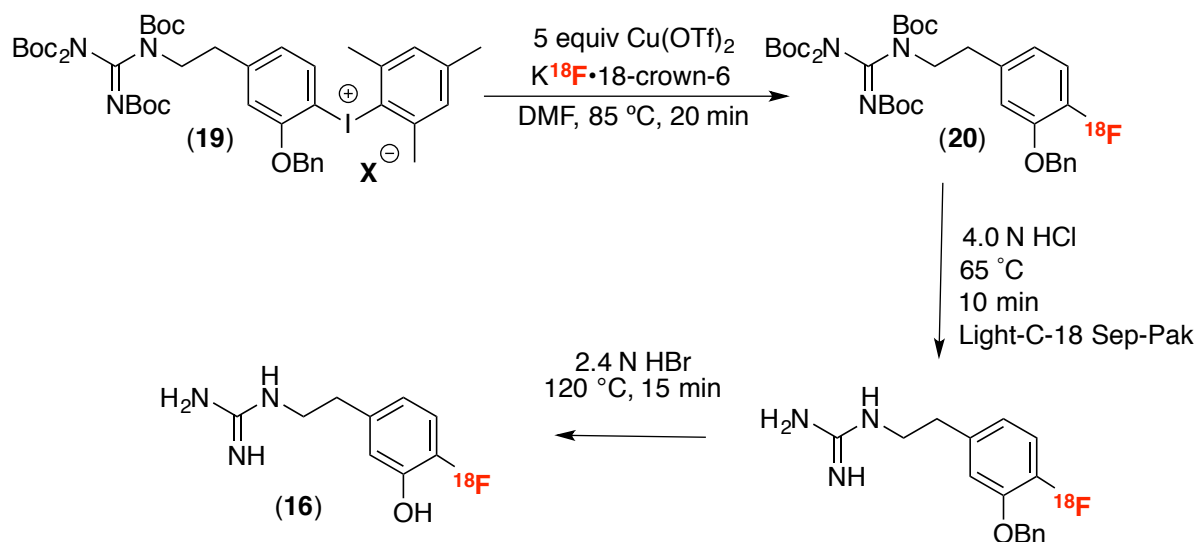
Our preliminary investigation began by first synthesizing an iodonium tosylate salt **19-OTs** and subjecting it to our optimized Cu-mediated $[^{18}\text{F}]$ fluorination reaction conditions. Protecting groups were required to obviate hydrogen bonding with $[^{18}\text{F}]$ fluoride, and we aimed to deprotect after the radiofluorination step. Unfortunately, under our standard conditions the desired product **20** was not observed (Table 3.6, entry 1-3). We noted that **19-OTs** is only sparingly soluble in DMF at room temperature; therefore we also evaluated the PF_6 derivative as a means to enhance solubility and potentially improve RCC. Indeed, the hexafluorophosphate salt is fully soluble under the reaction conditions, and it afforded a 7% RCC (entry 5). With $(\text{CH}_3\text{CN})_4\text{CuOTf}$, the yield remained unchanged when using 1 or 5 equiv of Cu relative to **19-PF₆** (entry 4 and 5). However, the use of 1 equiv of $\text{Cu}(\text{OTf})_2$ afforded a significant enhancement in yield (entry 6); furthermore, using 5 equiv $\text{Cu}(\text{OTf})_2$ provided a 44% RCC, our best result to date (entry 8). The results in Table 3.10 demonstrate that the Cu-mediated ^{18}F -fluorination of the late-stage intermediate **19** is feasible and that this substrate is highly sensitive to reaction conditions (e.g., counterion, Cu source, and Cu loading). Given these observations, we anticipate that the RCC for radiofluorination of the MHPG derivative **19** can be further improved.

Table 3.6 Cu-Mediated Radiofluorination of 19

Entry	X	[Cu]	[Cu]:Ar ₂ I ⁺	RCC (n = 2) ^b
1	OTs	(CH ₃ CN) ₄ CuOTf	1:2	<1%
2	OTs	(CH ₃ CN) ₄ CuOTf	1:1	<1%
3	OTs	(CH ₃ CN) ₄ CuOTf	5:1	<1%
4	PF ₆	(CH ₃ CN) ₄ CuOTf	1:1	8%
5	PF ₆	(CH ₃ CN) ₄ CuOTf	5:1	7%
6	PF ₆	Cu(OTf) ₂	1:1	20%
7	PF ₆	Cu(OTf) ₂	2:1	28%
8	PF ₆	Cu(OTf) ₂	5:1	44%
9	PF ₆	Cu(OTf) ₂	10:1	22%

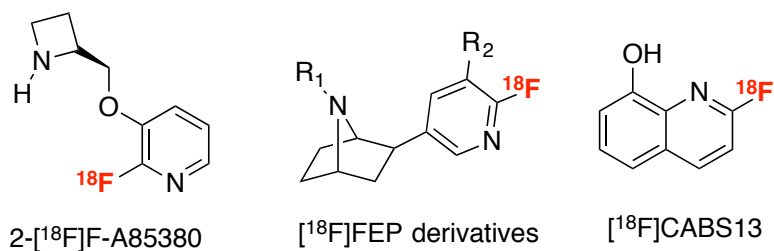
With the reaction conditions for **19-PF₆** (Table 3.6, entry 8) in hand, the automated synthesis of **20** was performed. Unfortunately, the automated synthesis afforded **20** in only 13% RCC. Furthermore, a full automated synthesis of 4- ^{18}F]MHPG was attempted, but only 1.5 mCi of activity (RCY = 0.1%) was isolated in the preliminary investigation (Scheme 3.12). The low overall yield of ^{18}F]MHPG may be due to the presence of a super-stoichiometric amount of Cu in the subsequent deprotection steps. Unfortunately, the automated module does not allow the HPLC purification of intermediates, but removal of Cu was possible by running through a plug of Chelex[®], wherein 95% of Cu was successfully removed. This filtration step can be accomplished between radiofluorination and deprotection steps. We anticipate that this should improve the overall yield of product **16**, and pursuing this strategy is a key future goal for this project.

Scheme 3.12 Automated Synthesis of [¹⁸F]MHPG 16



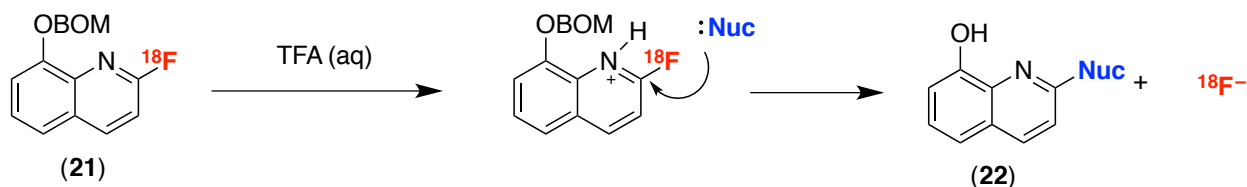
Application to Syntheses of Heterocycles. A number of pharmaceuticals that contain fluoropyridine scaffolds have been used for increasing applications in PET (Figure 3.6).

Figure 3.6 Representative Radiotracers Containing 2-[¹⁸F]fluoropyridine



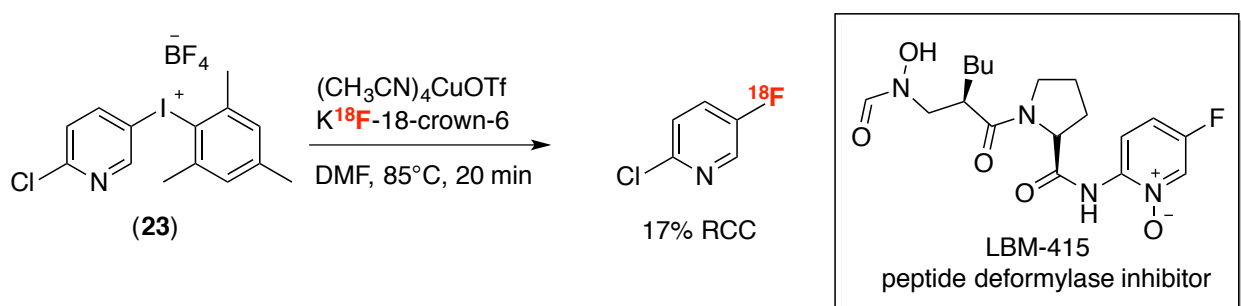
Although 2-fluoropyridine can be prepared from S_NAr methodologies,⁴⁹ the 2-position of pyridine is activated and prone to further S_NAr by other nucleophiles, which can result in the loss of ¹⁸F-fluoride.⁵⁰ The synthesis of [¹⁸F]CABS13 exemplified such concern.^{49a} Treatment of **21** with aqueous trifluoroacetic acid led to acid-catalyzed nucleophilic displacement (Nuc = undefined in the publication) to form **22** and free ¹⁸F-fluoride (Scheme 3.13). Installation of [¹⁸F]fluoride at 3-position may circumvent the undesired side reactions as it is less activated toward nucleophilic functionalization.

Scheme 3.13 Acid-Promoted S_NAr Reaction and Loss of ¹⁸F-label from the CABS13



Efficient methods for synthesizing 3-fluoropyridines are currently rare.⁵¹ The 3-fluoropyridine can be found as a component of LBM-415, a peptide deformylase inhibitor that is used for the treatment of community-acquired respiratory tract disease and serious infections caused by microbial gram-positive bacteria.⁵² Therefore, we attempted to radiofluorinate pyridine substrate **23** under the same reaction conditions as described above. As shown in Scheme 3.13, [¹⁸F]2-chloro-5-fluoropyridine was formed in 17% RCC. Further optimization is required specifically for radiolabeling of heterocycles (Scheme 3.14)

Scheme 3.14 Radiofluorination of (Mesityl)(2-chloro-3-iodopyridine)Iodonium Salt **23**⁵³



3.3 CONCLUSIONS

This chapter describes the development of a general, mild, high-yielding, and user-friendly procedure for the radiofluorination of diverse aromatic substrates through the merger of transition metal catalysis with the fluorination of diaryliodonium salts. Electronically varied diaryl iodonium salts show high reactivity with nucleophilic [¹⁸F]fluoride under our optimal conditions; in particular, high yields with electron-rich arenes are observed, which is complementary to traditional radiofluorination methods. Simply switching from Cu^{II} to a Cu^I catalyst, (CH₃CN)₄CuOTf, allowed us to develop a highly reproducible and robust method that was tolerant of ambient reaction conditions. This reaction has been applied to the radiofluorination of a series of clinically relevant

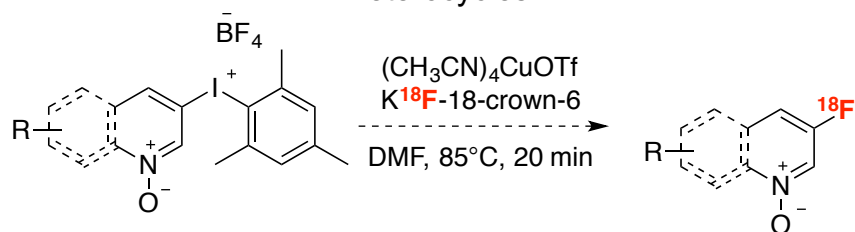
molecules such as amino acids (phenylalanine, tyrosine, and DOPA) and 4- $[^{18}\text{F}]$ -MHPG. Furthermore, initial investigations suggest that this transformation may be further expanded upon for the radiofluorination of medically relevant heterocycles.

3.4 PERSPECTIVE AND OUTLOOK

Merging transition metal catalysis and radiotracer syntheses has enabled the radiofluorination of challenging substrates. The biggest remaining challenge is the validation of the clinical synthesis of radiotracers through automation and establishing adequate product purification. Preliminary results for the automated synthesis of $[^{18}\text{F}]$ MHPG suggest that the removal of excess Cu is necessary for subsequent Boc-group deprotection steps and to ensure acceptable purity of the radiolabeled product.

In addition, new developments are needed such that the scope of the Cu-mediated radiofluorination of (mesityl)(aryl)iodonium salts can be expanded for the synthesis of fluorinated heterocycles. The presence of Lewis basic heterocycles in a substrate may lead to undesired Lewis base/acid interaction with Cu catalysts, and thus result in decreased product yields. For optimization, one approach could be to synthesize N-oxide iodonium salts for two benefits: (a) the N-oxide could potentially prevent undesired oxidation reactions from excess I(III) reagents and (b) the N-oxide would block the N-atom, and limit binding to the Cu catalyst.⁵⁴ Thus, such iodonium salts may enable a good RCY for desired the heterocycles (Scheme 3.15).

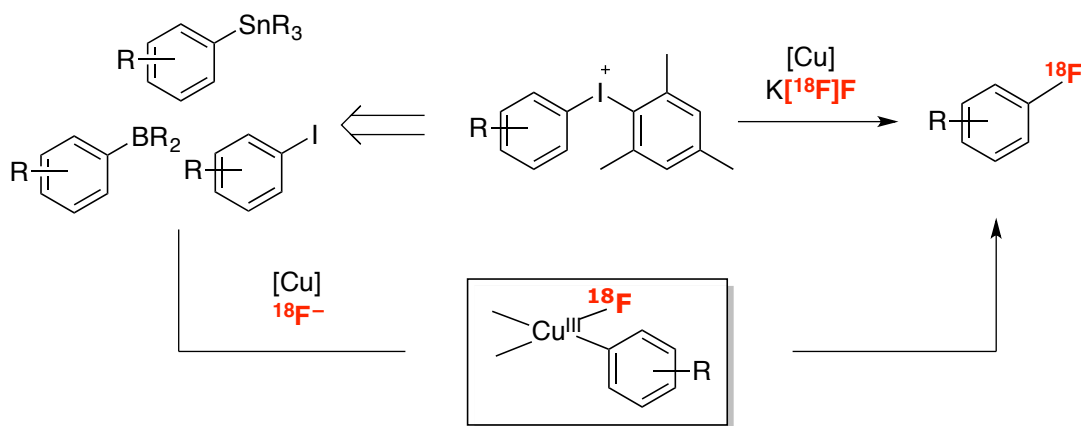
Scheme 3.15 Possible Future Direction for the radiofluorination of pyridyl-containing Heterocycles



Another expansion of this Cu-mediated radiofluorination of I(III) reagents would be to develop Cu-mediated methods for the radiofluorination of aryl boronic acids, aryl stannanes, and aryl iodides. From a practical perspective, these are ideal radiofluorination precursors, as they are easily synthesized and/or commercially available as well as being extremely stable. However, at the time that we started this

work, there were no nucleophilic radiofluorination methods available for electron-rich aryl boronic acids, stannanes, or iodides. Thus, it is of interest to develop processes to fluorinate Ar–X using the combination of a Cu mediator and either $K^{18}F$ (X = B or Sn)⁵⁵ or $Ag^{18}F$ (X = I).⁵⁶ Progress towards these goals is discussed in chapter 4. Subsequently, applying any new methodologies to the synthesis of radiotracers of interest for clinical applications, such as ^{18}F -MHPG, L-DOPA, MPPF, and L-phenylalanine, will be ideal (Scheme 3.16).

Scheme 3.16 Direct Fluorination of Iodonium Salt Precursors by a Cu-Mediated pathway



Furthermore, a significant difference in stoichiometry, air/moisture sensitivity of reaction systems exists between fluorination and radiofluorination, but there is still little mechanistic understanding between these closely related fields. This lack of understanding tends to lead to failure in attempts to translate ^{19}F -fluorination methods to radiofluorination.⁵⁷ Therefore, conducting mechanistically driven experiments for new radiofluorination reactions could help to facilitate the translation of current state-of-art fluorination methods to the analogous ^{18}F -transformations. Utilizing fluorine-18 in mechanistic studies of fluorination reactions could provide a way to not only provide new methods for radiofluorination but give greater insight into the reaction mechanism being studied due to the ease with which fluorine-18 containing molecules can be detected even at low concentrations.

3.5 EXPERIMENTAL

I. General Procedures and Materials and Methods

Instrumental Information. NMR spectra were obtained on a Varian MR400 (400.52 MHz for ^1H ; 100.71 MHz for ^{13}C ; 376.87 MHz for ^{19}F), a Varian vnmrs 500 (500.10 MHz for ^1H), or a Varian vnmrs 700 (699.76 MHz for ^1H ; 175.95 MHz for ^{13}C) spectrometer. ^1H and ^{13}C NMR chemical shifts are reported in parts per million (ppm) relative to TMS, with the residual solvent peak used as an internal reference. ^{19}F NMR spectra are referenced based on an internal standard, 1,3,5-trifluorobenzene (-110.00 ppm). ^1H and ^{19}F multiplicities are reported as follows: singlet (s), doublet (d), triplet (t), quartet (q), and multiplet (m). High performance liquid chromatography (HPLC) was performed using a Shimadzu LC-2010A HT system equipped with a Bioscan B-FC-1000 radiation detector. Radio-TLC analysis was performed using a Bioscan AR 2000 Radio-TLC scanner with EMD Millipore TLC silica gel 60 plates (3.0 cm wide x 6.5 cm long).

Materials and Methods. Diaryliodonium tetrafluoroborate **1**, and the substrates for fluorides **3-5**, **7**, **8**, and **11** were prepared according to a literature procedure.²⁸ The salts [*p*-OMePh-I-Mes]*X* (*X* = Br, OTf, OTs, PF₆) were prepared according to a literature procedure.⁵⁸ MesI(OAc)₂ was obtained from TCI America. BF₃•OEt₂ was obtained from Alfa Aesar or Aldrich. *m*-CPBA was obtained from Sigma Aldrich. Arylboronic acids were obtained from Aldrich, Frontier Scientific, Oakwood Products and Combi Blocks. Anhydrous DMF, (CH₃CN)₄CuOTf, and 18-crown-6 were obtained from Aldrich. 1,3,5-Trifluorobenzene was obtained from Oakwood Products. Authentic ^{19}F samples of compounds **2**, **5**, **7**, **9**, **10**, **11** were purchased from the following vendors: 4-fluoroanisole **2** (Oakwood), 2-fluoroanisole **5** (Aldrich), 4-fluorobiphenyl **7** (Oakwood), 4-fluoroiodobenzene **9** (Oakwood), 3-methyl-fluoroacetate **10** (Acros), and 3-fluorobenzaldehyde **11** (Acros). Standards of ^{19}F -fluorinated compounds **3**, **4**, **6**, **8**, and **13** were prepared according to literature procedure, and all spectroscopic data were in accordance with the literature. All reactions were conducted under a nitrogen atmosphere or using standard Schlenk techniques unless otherwise stated. All reactions conducted at elevated temperatures were heated on a hot plate using an aluminum block. Temperatures were regulated using a thermocouple.

II. Radiochemistry

A. General Methods

Material and Methods. Unless otherwise stated, reagents and solvents were commercially available and used without further purification. Ethanol was purchased from American Regent. HPLC grade acetonitrile was purchased from Fisher Scientific. 18-Crown-6 and anhydrous *N,N*-dimethylformamide were purchased from Sigma-Aldrich. Sterile product vials were purchased from Hollister-Stier. QMA-light Sep-Paks were purchased from Waters Corporation. QMA-light Sep-Paks were flushed with 10 mL of ethanol followed by 10 mL of 0.5 M sodium bicarbonate solution, and finally 10 mL of sterile water prior to use.

B. Radiosynthesis of ^{18}F Labeled Molecules

Synthesis of [^{18}F]KF18-crown-6 Complex. All loading operations were conducted under ambient atmosphere. Argon was used as a pressurizing gas during automated sample transfers. Potassium [^{18}F]fluoride was prepared using a TRACERLab FX_{FN} automated radiochemistry synthesis module (General Electric, GE). [^{18}F]Fluoride was produced via the $^{18}\text{O}(\text{p},\text{n})^{18}\text{F}$ nuclear reaction using a GE PETTrace cyclotron (40 μA beam for 2 min generated ca. 150 mCi of [^{18}F]fluoride). The [^{18}F]fluoride was delivered to the synthesis module in a 1.5 mL bolus of [^{18}O]water and trapped on a QMA-light Sep-Pak to remove [^{18}O]water. [^{18}F]Fluoride was eluted into the reaction vessel using aqueous potassium carbonate (3.5 mg in 0.5 mL of water). A solution of 18-crown-6 (15 mg in 1 mL of acetonitrile) was added to the reaction vessel, and the resulting solution was dried by azeotropic distillation to give dry [^{18}F]KF-18-crown-6. Evaporation was achieved by heating the reaction vessel to 100 °C and drawing vacuum for 4 min. After this time, the reaction vessel was subjected to an argon stream and simultaneous vacuum draw for an additional 4 min. Finally, *N,N*-dimethylformamide (8 mL) was added to the dried reagent, and the resulting solution was transferred to a sterile vial for subsequent use in reactions (approx. 30 mCi of prepared ^{18}F reagent was transferred).

General Procedures for Manual Synthesis of ^{18}F -labeled Compounds (activity of 300-700 μCi per reaction).

On the bench top, solid [Mes-I-Ar]X (6 μmol) was weighed into a 4 mL amber glass vial containing a stir bar and was then dissolved in DMF (350 μL). A stock solution of tetrakis(acetonitrile)copper(I) triflate $(\text{CH}_3\text{CN})_4\text{CuOTf}$ was prepared (14.3 mg in 1 mL of anhydrous DMF, 0.04 M), and aliquots of this solution were used for several reactions. A 150 μL aliquot of CuOTf solution (6 μmol) was added to the vial containing [Mes-I-Ar]X. The reaction vial was sealed under an atmosphere of ambient air with a PTFE/Silicone septum cap, and then the solution was thoroughly mixed (vortex shaker, Barnstead® Thermolyne Type 16700). Via a syringe, a 250 μL aliquot of [^{18}F]KF•18-crown-6 complex (typically 300-700 μCi , prepared as described above) was added to the reaction vial.* The vial was then heated in an aluminum block with stirring at 85 °C for 20 min. After 20 min, the reaction was allowed to cool to room temperature. A 100 μL aliquot was withdrawn from the vial and added to 400 or 900 μL of CH_2Cl_2 in a 4 mL vial (choice of volume of CH_2Cl_2 was dependent on activity). The CH_2Cl_2 mixture was shaken by hand and then used for radio-TLC analysis to obtain radiochemical yields (RCY).† In addition, an 100 μL aliquot of the reaction solution was used for radio-HPLC analysis by diluting the sample into 50/50 MeCN/ H_2O (300 μL total volume).

* On a typical day, several reactions (4-20) were set up together. Due to this, the time of mixing and time of incubation at room temperature prior to heating varied slightly from day to day. However, the results of the radiofluorination appear to be insensitive to this variation.

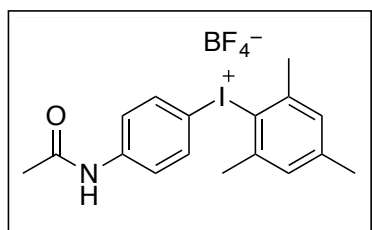
† The reaction mixture was diluted to obtain more reproducible TLC results. Undiluted samples of the reaction showed the same RCY; however, broadening was observed as a result of the DMF, and this made accurate integration more difficult. Radio-TLCs were counted immediately after being developed. This was particularly critical when the fluoroarene was volatile (e.g., 4-fluoroanisole), because the apparent RCY was found to decrease as a function of time due to the product evaporating off of the TLC plate. The RCY was determined by dividing the integrated area under the fluoroarene spot by the total integrated area of the TLC plate.

General Procedures for Automated Synthesis of ^{18}F -labeled Compounds (initial activity of 1.5 Ci).

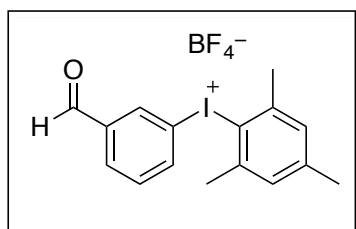
The production-scale synthesis of radiolabeled arenes was conducted using a TRACERLab FX_{FN} automated radiochemistry synthesis module (General Electric, GE). The synthesis module was pre-charged with a solution of the [Mes-I-Ar]X precursor (18 μmol) and tetrakisacetonitrile copper(I) triflate (8.0 mg, 20 μmol) in DMF (0.75 mL) to be added from an automated port prior to ^{18}F delivery. [^{18}F]Fluoride was produced via the $^{18}\text{O}(\text{p},\text{n})^{18}\text{F}$ nuclear reaction using a GE PETTrace cyclotron (40 μA beam for 30 min generated 1,500 mCi of [^{18}F]fluoride). The [^{18}F]fluoride was delivered to the synthesis module (in a 1.5 mL bolus of [^{18}O]water) and trapped on a QMA-light Sep-Pak to remove [^{18}O]water. [^{18}F]Fluoride was eluted into the reaction vessel using aqueous potassium carbonate (3.0 mg in 0.5 mL of water). A solution of 18-crown-6 (5 mg in 1 mL of acetonitrile) was added to the reaction vessel, and the resulting solution was dried by azeotropic distillation to give dry [^{18}F]KF•18-crown-6. Evaporation was achieved by heating the reaction vessel to 100 °C and drawing vacuum for 4 min. After this time, the reaction vessel was subjected to an argon stream and simultaneous vacuum draw for an additional 4 min. The reaction vessel was cooled to 50 °C, DMF (0.75 mL) was added, and the resulting mixture was stirred for 1 min. A preloaded solution of iodonium salt and copper was added to the reaction vessel, and the vessel was sealed, heated to 85 °C, and held at that temperature for 20 min. The reaction vessel was then cooled to 50 °C, and DMF (8.5 mL) was added. The additional DMF was not necessary, but was used to reduce hand exposure during sample manipulations and analysis. The resulting solution (10 mL) was transferred to a sterile vial for analysis (radio-TLC and radio-HPLC).

3.6 CHARACTERIZATION

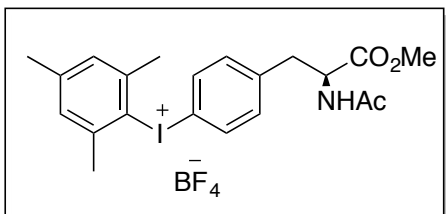
a. Iodonium Salts



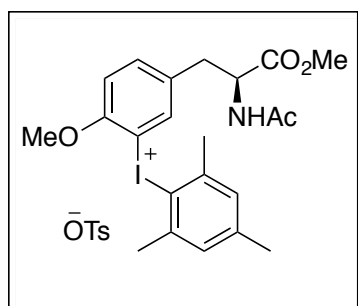
(*Mesityl*)(*para*-acetamidophenyl)iodonium tetrafluoroborate was prepared by the following procedure adapted from the literature.⁵⁹ A brown powder (395 mg, 40% yield). ¹H NMR (700 MHz, DMSO-*d*₆): δ 10.3 (s, 1H), 7.91 (d, *J* = 9.1 Hz, 2H), 7.67 (d, *J* = 9.1 Hz, 2H), 7.20 (s, 2H), 2.60 (s, 6H), 2.29 (3H), 2.05 (s, 3H). ¹³C NMR (176 MHz, DMSO-*d*₆): δ 169.0, 142.9, 142.4, 141.4, 135.8, 129.7, 122.9, 121.5, 105.8, 26.2, 24.1, 20.5. ¹⁹F NMR (376 MHz, DMSO-*d*₆): δ -148.2, -148.3. HRMS (ESI⁺) [M-BF₄]⁺ Calcd for C₁₇H₁₉INO⁺: 380.0506; Found: 380.0518.



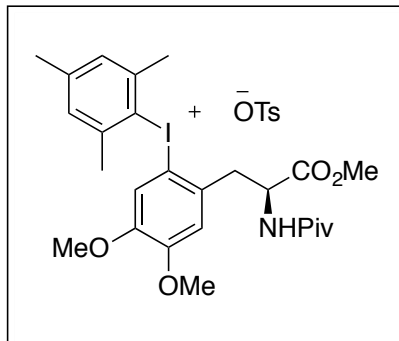
(*Mesityl*)(3-formylphenyl)iodonium tetrafluoroborate was prepared by the following procedure adapted from the literature.⁵⁹ A white powder (276 mg, 63% yield). ¹H NMR (700 MHz, DMSO-*d*₆): δ 9.99 (s, 1H), 8.45 (s, 1H), 8.19 (d, *J* = 7.0 Hz, 1H), 8.14 (d, *J* = 7.0 Hz, 1H), 7.72 (t, *J* = 7.0 Hz, 1H), 7.24 (s, 2H), 2.61 (s, 6H), 2.31 (s, 3H). ¹³C NMR (176 MHz, DMSO-*d*₆): δ 191.6, 143.3, 141.7, 139.4, 138.4, 134.3, 132.7, 132.6, 129.9, 122.6, 115.1, 26.3, 20.5. ¹⁹F NMR (376 MHz, DMSO-*d*₆): δ -148.2, -148.3. HRMS (ESI⁺) [M-BF₄]⁺ Calcd for C₁₆H₁₆IO⁺: 351.0240; Found: 351.0251.



(Mesityl)(*N*-acetyl-4-phenylalanine)iodonium tetrafluoroborate was prepared by the 4 step syntheses whose details are reported in the manuscript.²⁹ A white solid (201 mg, 1.5 mmol, 46% yield). ¹H NMR (500 MHz, CDCl₃) δ 7.64 (d, *J* = 8.4 Hz, 2H), 7.23 (d, *J* = 8.4 Hz, 2H), 7.11 (s, 2H), 6.42 (d, *J* = 7.8 Hz, 1H), 4.77 (m, 1H), 3.67 (s, 3H), 3.16 (dd, *J* = 14.0, 5.5 Hz, 1H), 3.05 (dd, *J* = 14.0, 7.1 Hz, 1H), 2.60 (s, 6H), 2.34 (s, 3H), 1.92 (s, 3H). ¹³C NMR (126 MHz, CDCl₃) δ 171.5, 170.3, 144.7, 142.6, 141.6, 133.4, 133.2, 130.6, 119.7, 110.0, 52.9, 52.6, 37.2, 27.1, 22.8, 21.1. HRMS (ESI⁺) [M–BF₄]⁺ Calcd for C₂₁H₂₅INO₃⁺: 466.0879; Found: 466.0874.

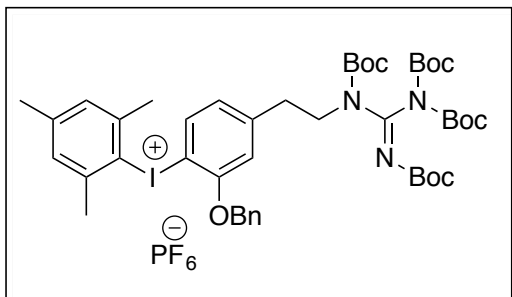


(Mesityl)((*S*)-methyl 2-acetamido-5-(2-methoxyphenyl)iodonium tosylate was prepared by the following 6 step synthesis whose details are reported in the manuscript.²⁹ A white solid (56 mg, 0.084 mmol, 42% yield) ¹H NMR (700 MHz, CD₃OD) δ 7.74 (d, *J* = 2.0 Hz, 1H), 7.65 (d, *J* = 7.9 Hz, 2H), 7.45 (dd, *J* = 8.5, 2.0 Hz, 1H), 7.18 (d, *J* = 7.9 Hz, 2H), 7.15-7.12 (m, 3H), 4.61 (dd, *J* = 9.1, 5.6 Hz, 1H), 3.86 (s, 3H), 3.64 (s, 3H), 3.12 (dd, *J* = 14.1, 5.6 Hz, 1H), 2.90 (dd, *J* = 14.1, 9.1 Hz, 1H), 2.62 (s, 6H), 2.35 (s, 3H), 2.32 (s, 3H), 1.85 (s, 3H). ¹³C NMR (176 MHz, CD₃OD) δ 171.7, 171.5, 156.0, 143.9, 142.4, 142.0, 140.3, 136.3, 135.4, 132.9, 129.7, 128.4, 125.5, 119.6, 112.6, 101.7, 56.7, 53.5, 51.4, 35.6, 25.5, 20.9, 19.9, 19.6. HRMS (ESI⁺) [M–OTs]⁺ Calcd for C₂₂H₂₇INO₄⁺: 496.0985; Found: 496.0982.



(Mesityl)(N-(tert-butylcarbonyl)-3,4-di(methoxy)-L-phenylalanine methyl ester)-2-iodonium tosylate was prepared by the following 6 step synthesis whose details are reported in the manuscript.²⁹ A white solid. ¹H NMR (700 MHz, CD₃OD) δ 8.04 (d, *J* = 7.8 Hz, 1H, exchanges), 7.69 (d, *J* = 7.0 Hz, 2H), 7.21 (d, *J* = 7.0 Hz, 2H), 7.19 (s, 2H), 7.13 (s, 1H), 7.06 (s, 1H), 4.58 (apparent q, *J* = 7.5 Hz, 1H), 3.83 (s, 3H), 3.71 (s, 3H), 3.66 (s, 3H), 3.40 (dd, *J* = 14.5, 7.2 Hz, 1H), 3.22 (dd, *J* = 14.5, 8.1 Hz, 1H), 2.60 (s, 6H), 2.36 (s, 3H), 2.34 (s, 3H), 1.08 (s, 9H).

¹³C NMR (176 MHz, CD₃OD) δ 180.1, 171.7, 152.5, 149.9, 144.3, 142.0, 140.2, 133.8, 130.0, 128.4 (2C), 125.7, 120.7, 117.6, 113.9, 105.0, 55.4, 55.3, 52.6, 51.7, 38.6, 38.1, 26.2, 25.4, 19.8, 19.5. HRMS (ESI⁺) [M-OTs]⁺ Calcd for C₂₆H₃₅INO₅⁺: 568.1554; Found: 568.1554.

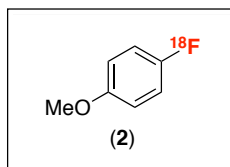


(Mesityl)(MHPG)iodonium hexafluorophosphate was prepared by the following procedure. The corresponding *tetra*Boc protected (MHPG)-SnMe₃ was prepared according the procedure adapted from literature.⁶⁰ In an oven-dried flask, iodomesitylene diacetate (2.0 equiv) was added with CH₃CN (0.2M) and cooled to 5°C using an ice bath. To the color solution, was *p*-TsOH•H₂O (1.1 equiv) added in one portion, and the solution immediately turned color to yellow and let it stir for 10 minutes. The arylstannane dissolved in mesitylene chloride (0.1M) was added dropwise. The

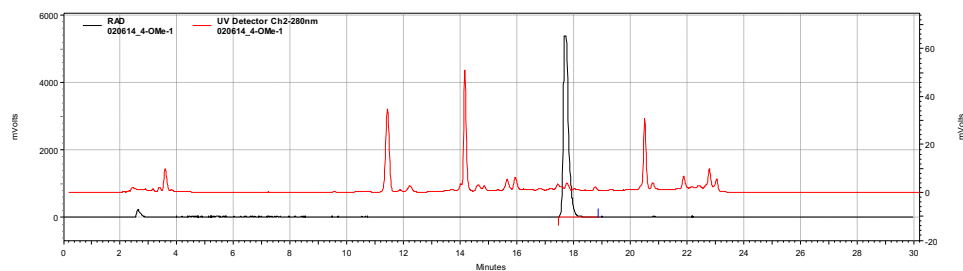
reaction was warmed up to room temperature and stir for 2 days. To the reaction, saturated LiPF_6 (aq) was added and vigorously stirred for 30 minutes. The organic layer was separated, and the aqueous layer was extracted with methylene chloride twice and concentrated. The colorless oil was triturated with hexane to afford a white powder (52% yield). ^1H NMR (700 MHz, CD_3OD) δ 7.43-7.34 (m, 5H), 7.04 (s, 2H), 7.01 (s, 1H), 6.87 (d, $J = 7$ Hz, 1H), 6.78 (d, $J = 7$ Hz, 1H), 3.90 (t, $J = 7$ Hz, 2H), 2.90 (t, $J = 7.0$ Hz, 2H), 2.51 (s, 6H), 2.34 (s, 3H), 1.50-1.44 (m, 36H).

^{13}C NMR (176 MHz, CD_3OD) δ 157.9, 151.4, 147.8, 144.7, 144.0, 143.4, 141.9, 135.1, 131.8, 130.3, 129.3, 129.2, 128.4, 124.9, 124.4, 114.8, 84.2, 82.5, 71.9, 48.6, 33.5, 28.3, 28.3, 28.2, 21.4. HRMS (ESI⁺) $[\text{M}-\text{OTs}]^+$ Calcd for $\text{C}_{45}\text{H}_{61}\text{IN}_3\text{O}_9^+$: 914.3447; Found: 914.3459.

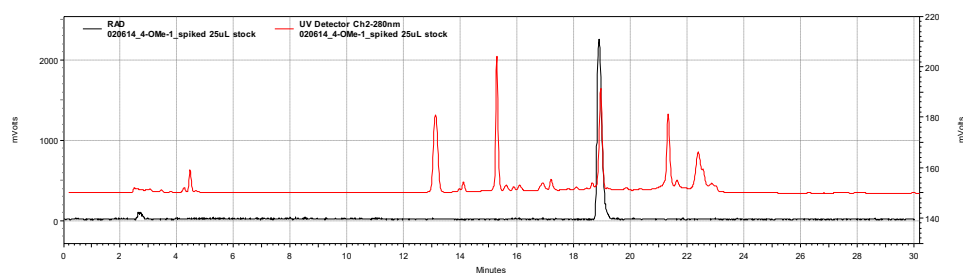
b. Radio-HPLC/Radio-TLC analysis for ^{18}F -labeled Compounds 2-11, 13, 15, and 17



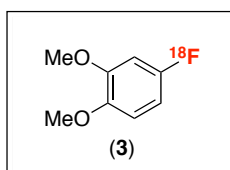
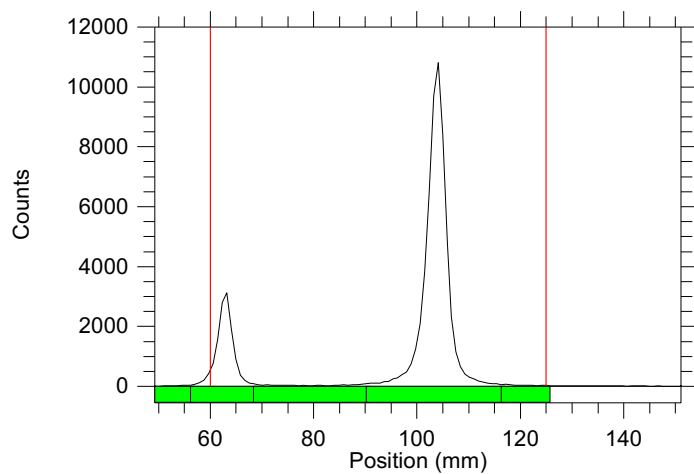
4- ^{18}F]fluoroanisole **2** RAD trace overlaid with UV trace (280 nm)



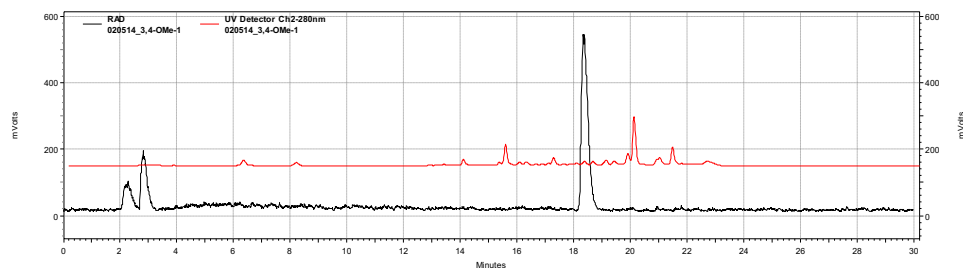
4- ^{18}F]fluoroanisole **2** RAD trace overlaid with UV trace (280 nm) spiked with 4-fluoroanisole



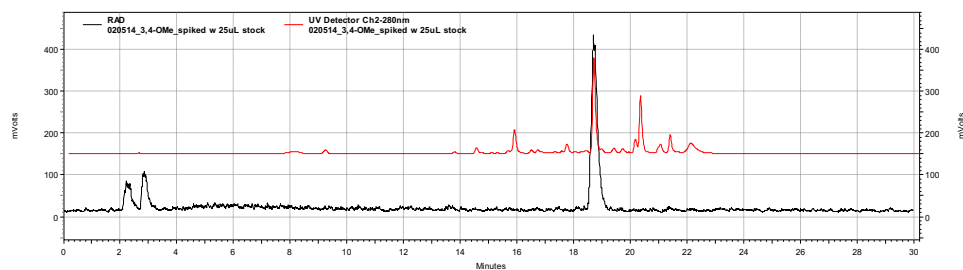
Radio-TLC Conditions: 20% EtOAc/Hexane



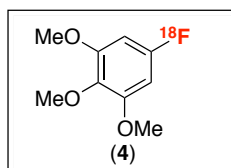
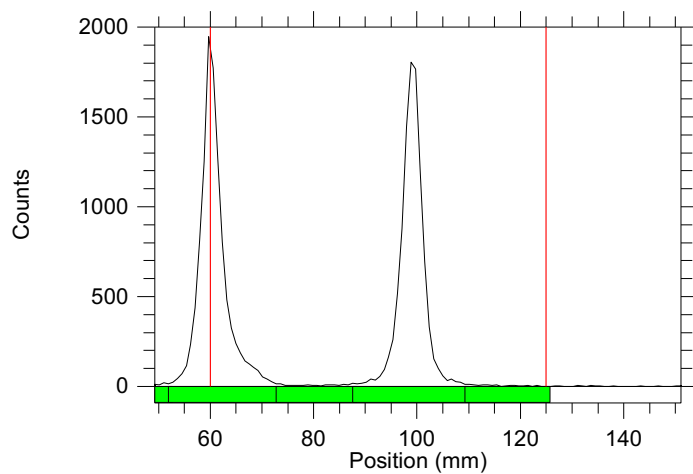
$[^{18}\text{F}]$ 3,4-(dimethoxy)fluorobenzene **3** RAD trace overlaid with UV trace (280 nm)



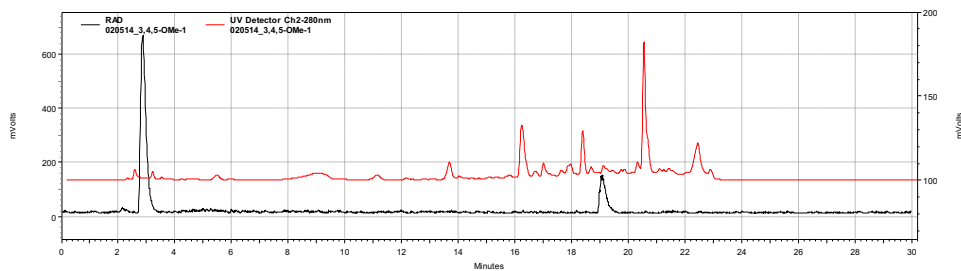
$[^{18}\text{F}]$ 3,4-(dimethoxy)fluorobenzene **3** RAD trace overlaid with UV trace (280 nm) spiked with with 3,4-(dimethoxy)fluorobenzene



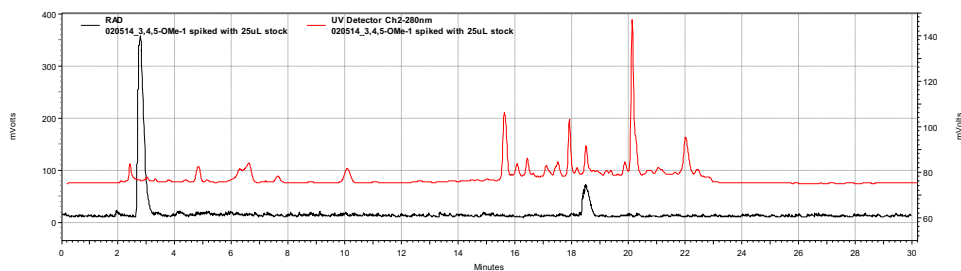
Radio-TLC Conditions: 50% EtOAc/Hexanes



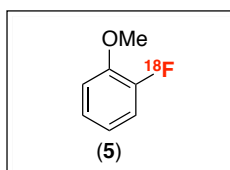
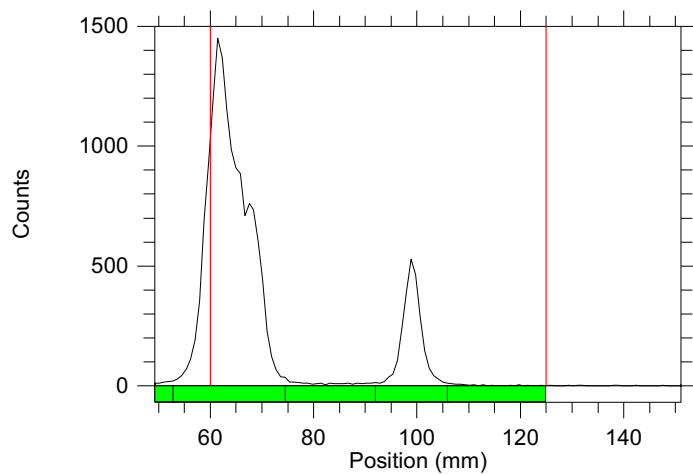
[¹⁸F](3,4,5-trimethoxy)fluorobenzene **4** RAD trace overlaid with UV trace (280 nm)



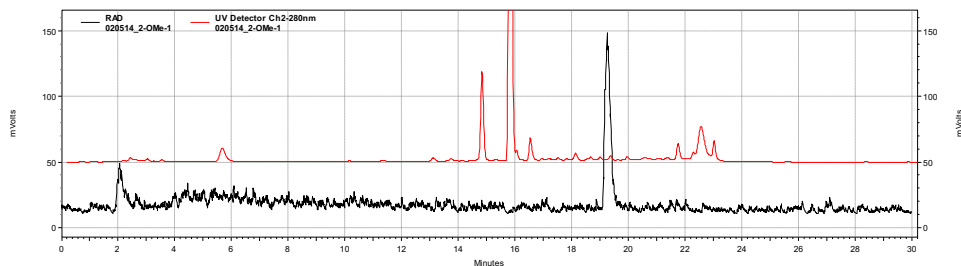
[¹⁸F](3,4,5-trimethoxy)fluorobenzene **4** RAD trace overlaid with UV trace (280 nm) spiked with 3,4,5-trimethoxyfluorobenzene



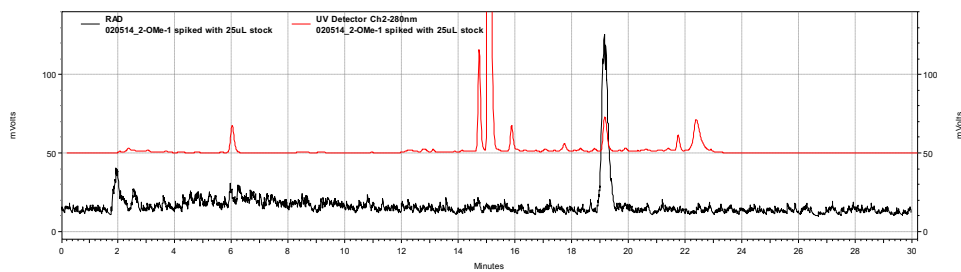
Radio-TLC Conditions: 50% EtOAc/Hexanes



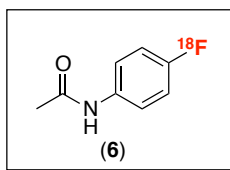
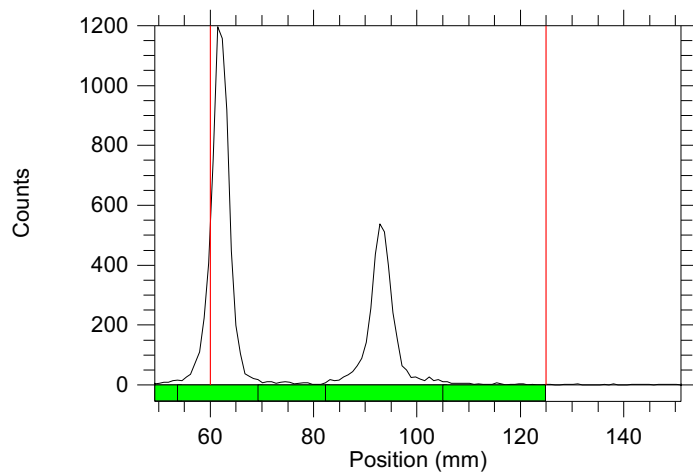
2-[¹⁸F]fluoroanisole **5** RAD trace overlaid with UV trace (280 nm)



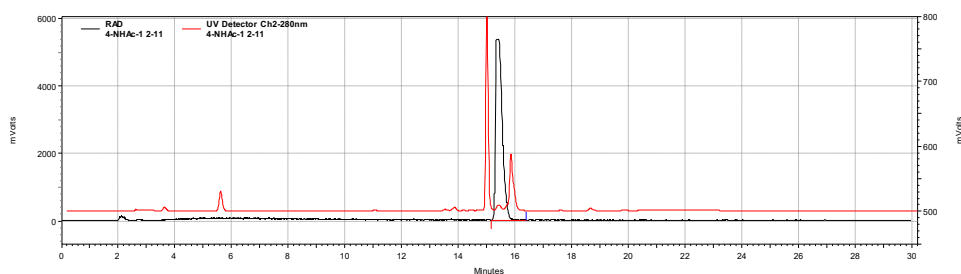
2-[¹⁸F]fluoroanisole **5** RAD trace overlaid with UV trace (280 nm) spiked with 2-fluoroanisole



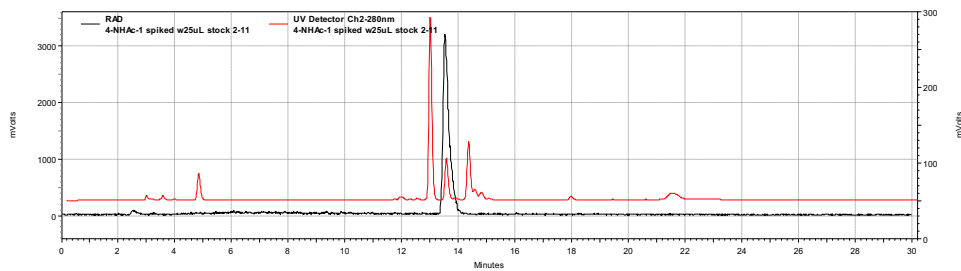
Radio-TLC Conditions: 20% EtOAc/Hexane



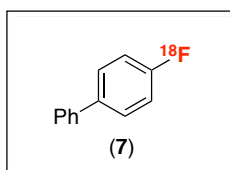
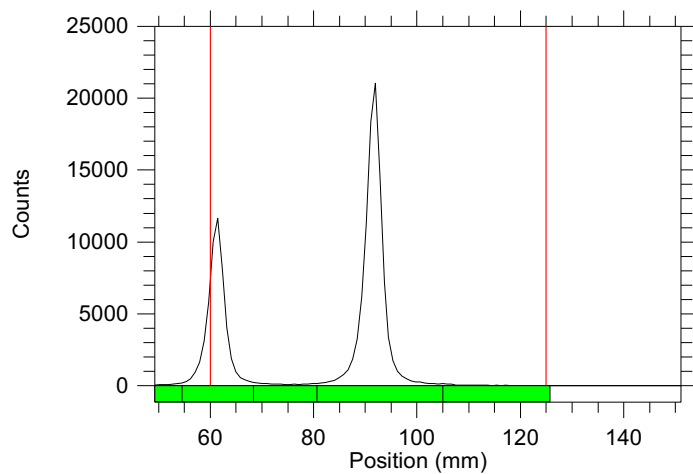
4- ^{18}F fluorophenylacetamide **6** RAD trace overlaid with UV trace (280 nm)



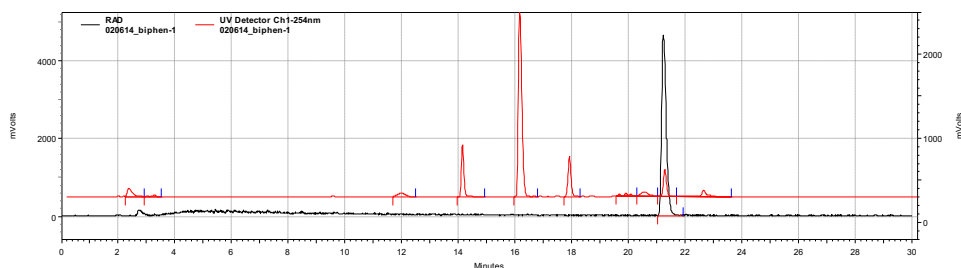
4- ^{18}F fluorophenylacetamide **6** RAD trace overlaid with UV trace (280 nm) spiked with 4-fluorophenylacetamide



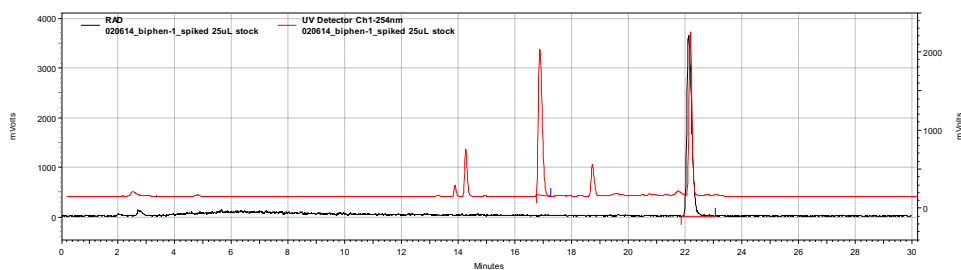
Radio-TLC Conditions: 80% EtOAc/Hexane



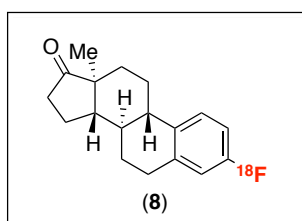
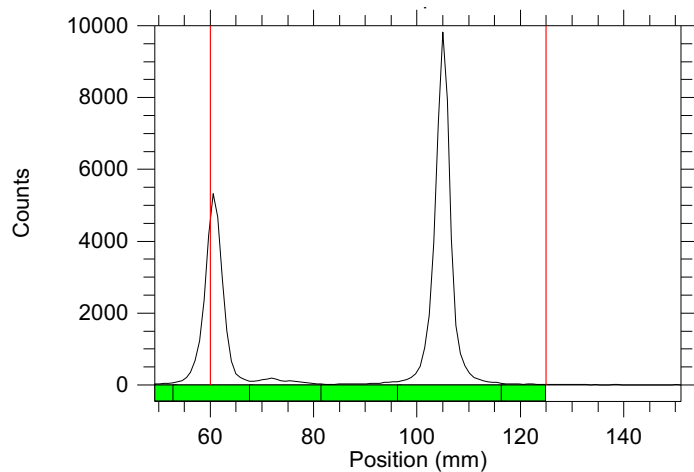
4-[¹⁸F]fluorobiphenyl 7 RAD trace overlaid with UV trace (254 nm)



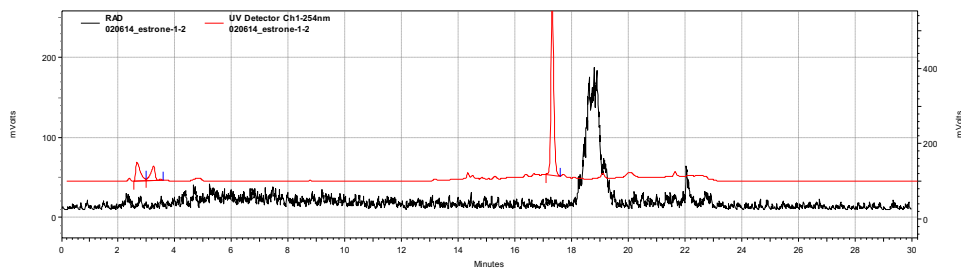
4-[¹⁸F]fluorobiphenyl 7 RAD trace overlaid with UV trace (254 nm) spiked with 4-fluorobiphenyl



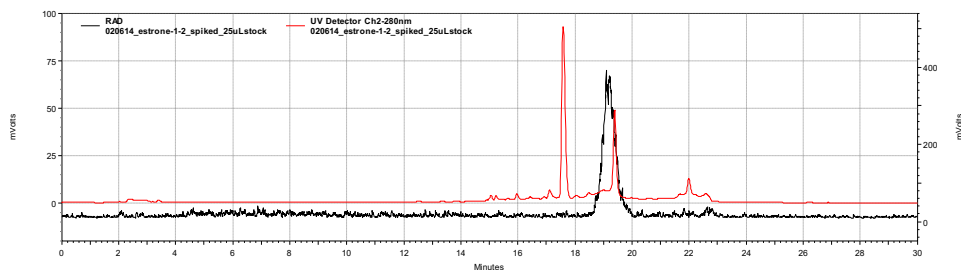
Radio-TLC Conditions: 100% EtOAc



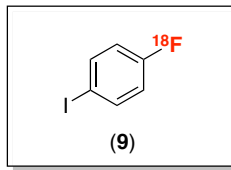
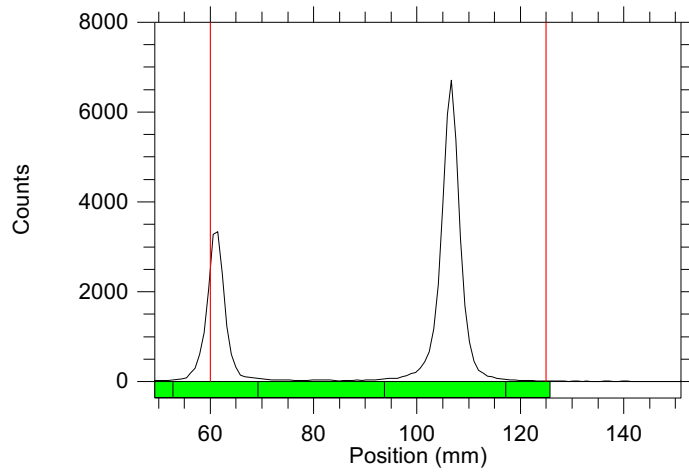
[¹⁸F]fluoro-estrone **8** RAD trace overlaid with UV trace (254 nm)



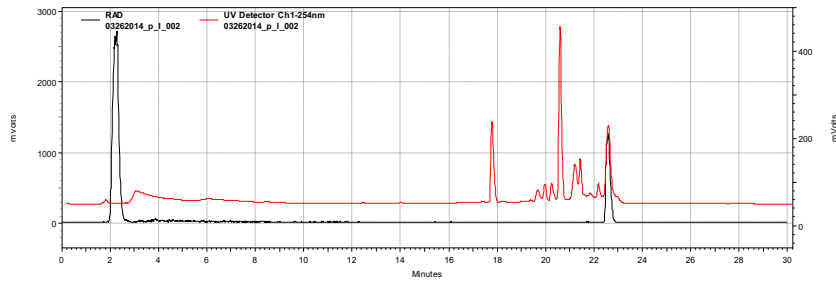
[¹⁸F]fluoro-estrone **8** RAD trace overlaid with UV trace (254 nm) spiked with fluoro-estrone



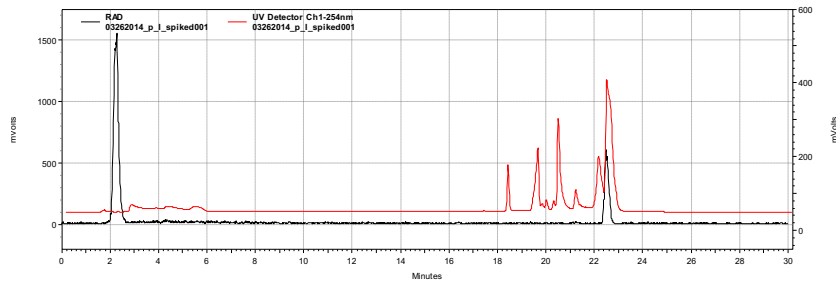
Radio-TLC Conditions: 50% EtOAc/Hexanes



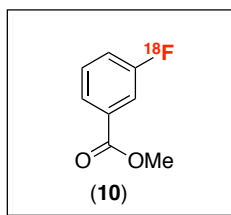
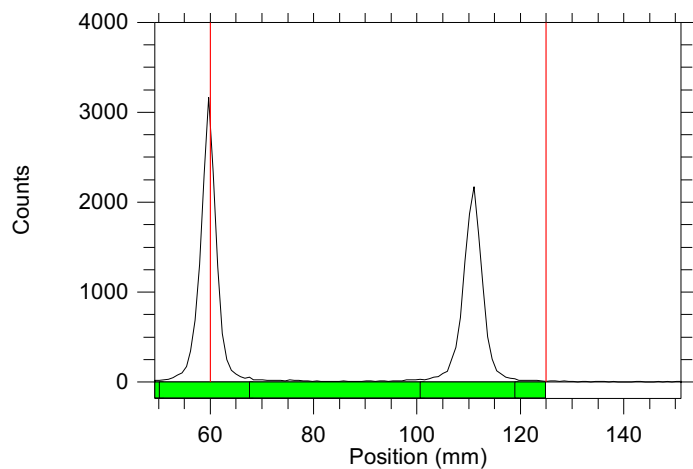
4-[¹⁸F]fluoro-iodobenzene **9 RAD trace overlaid with UV trace (280 nm)**



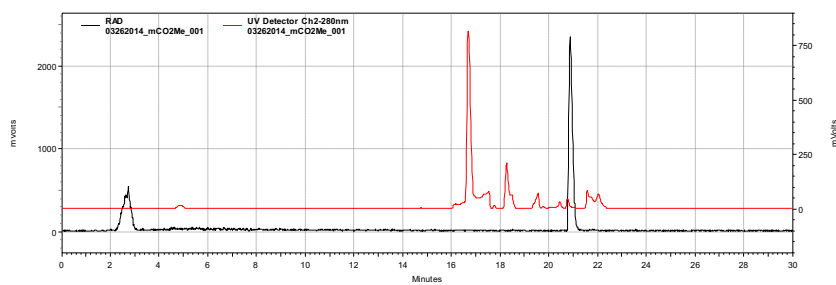
4-[¹⁸F]fluoro-iodobenzene **9 RAD trace overlaid with UV trace (280 nm) spiked with 4-fluoro-iodobenzene**



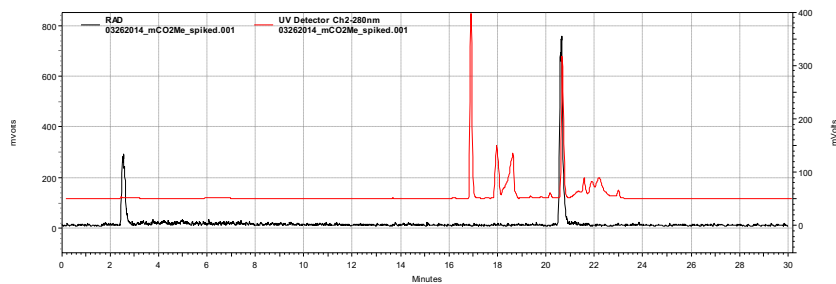
Radio-TLC Conditions: 50% EtOAc/Hexanes



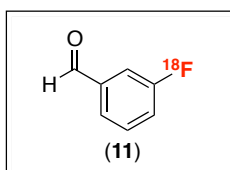
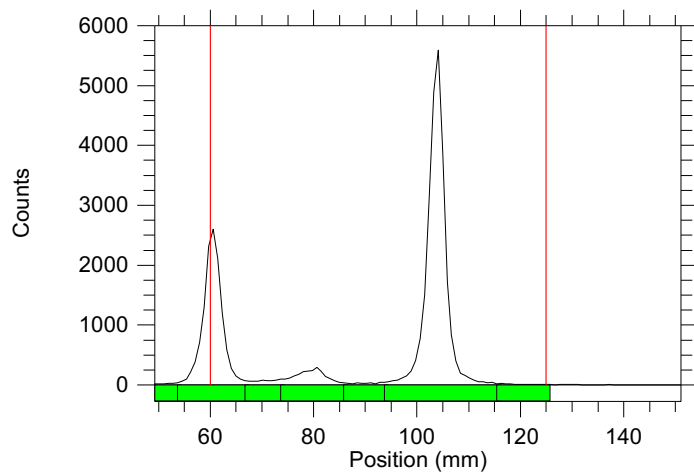
Methyl 3-[¹⁸F]fluorobenzoate **10** RAD trace overlaid with UV trace (280 nm)



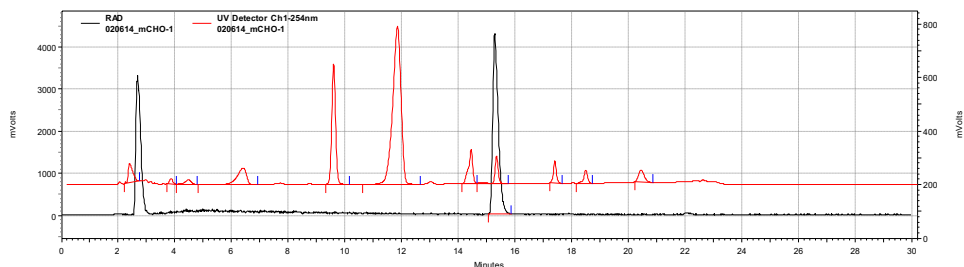
Methyl 3-[¹⁸F]fluorobenzoate **10** RAD trace overlaid with UV trace (280 nm) spiked with methyl-3-fluorobenzoate



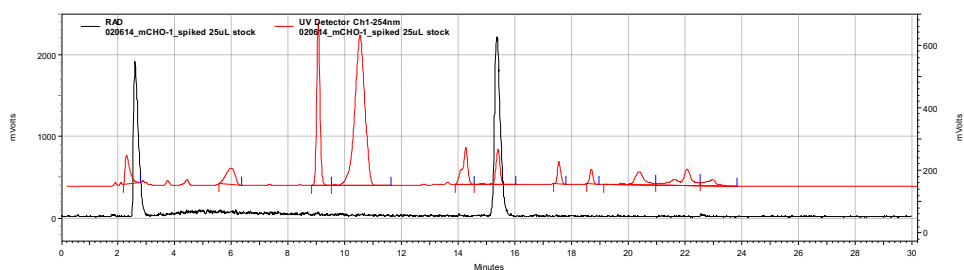
Radio-TLC Conditions: 100% EtOAc



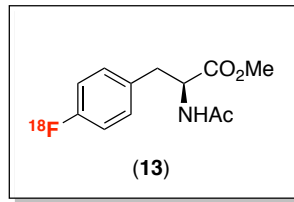
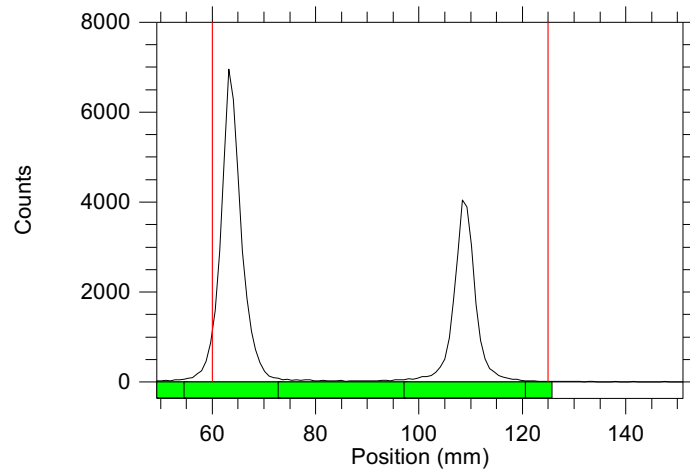
3-[¹⁸F]fluorobenzaldehyde **11** RAD trace overlaid with UV trace (254 nm)



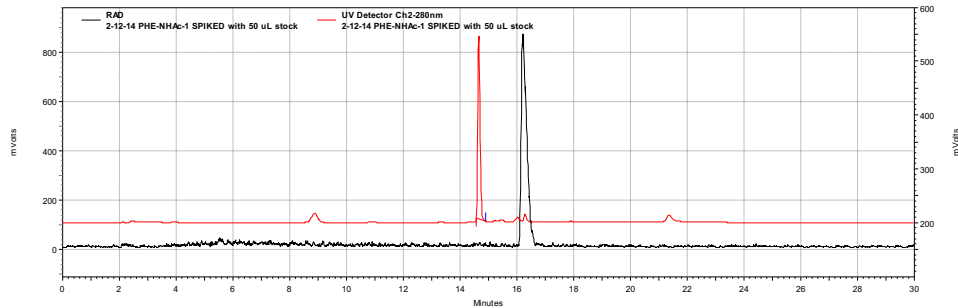
3-[¹⁸F]fluorobenzaldehyde **12** RAD trace overlaid with UV trace (254 nm) spiked with 3-fluorobenzaldehyde



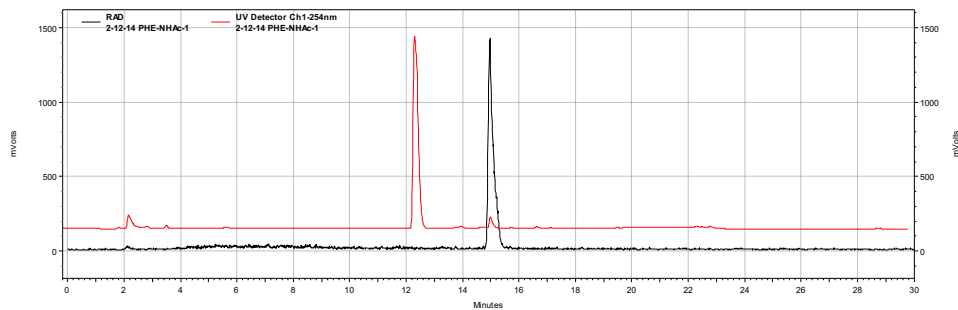
Radio-TLC Conditions: 100% EtOAc/Hexan



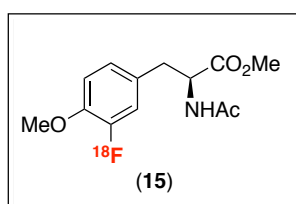
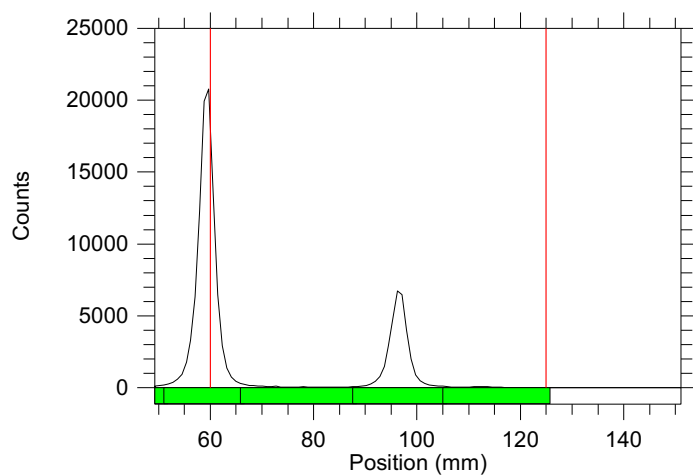
[¹⁸F]fluoro-L-phenylalanine 13 RAD trace overlaid with UV trace (254 nm)



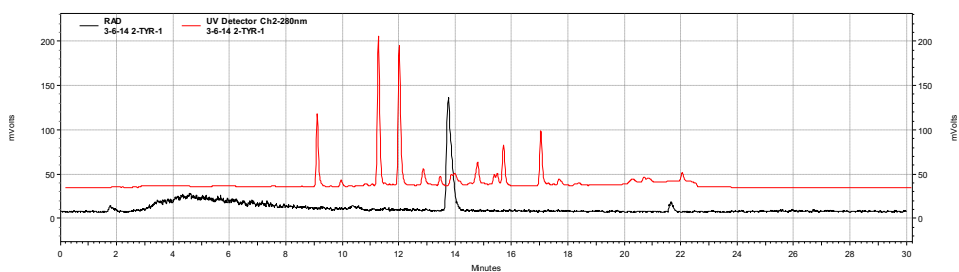
[¹⁸F]fluoro-L-phenylalanine 13 RAD traced overlaid with UV trace (254 nm) spiked with fluoro-L-phenylalanine



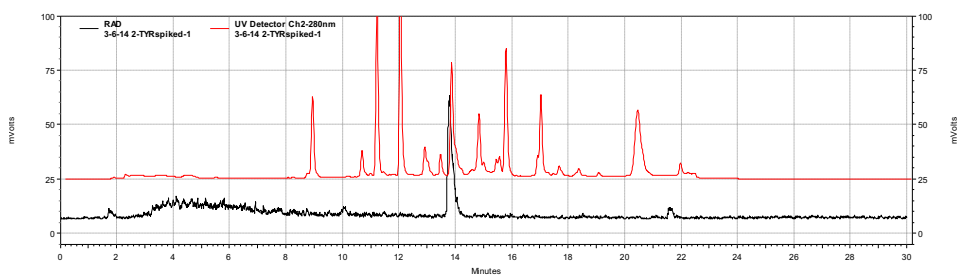
Radio-TLC Conditions: 100% EtOAc



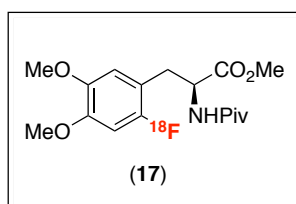
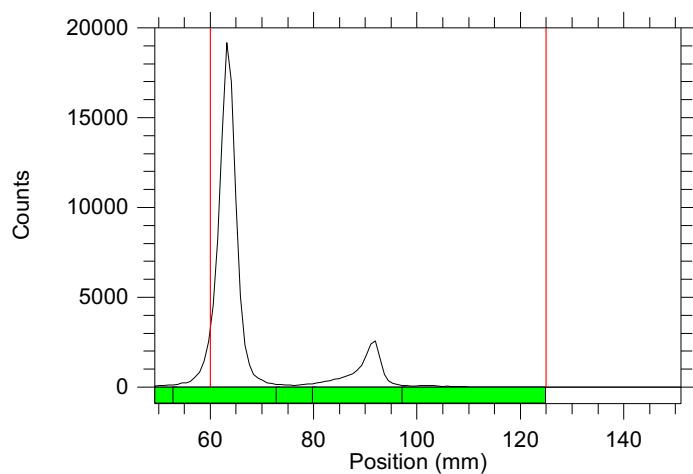
3-[¹⁸F]fluoro-tyrosine **15** RAD trace overlaid with UV trace (280 nm)



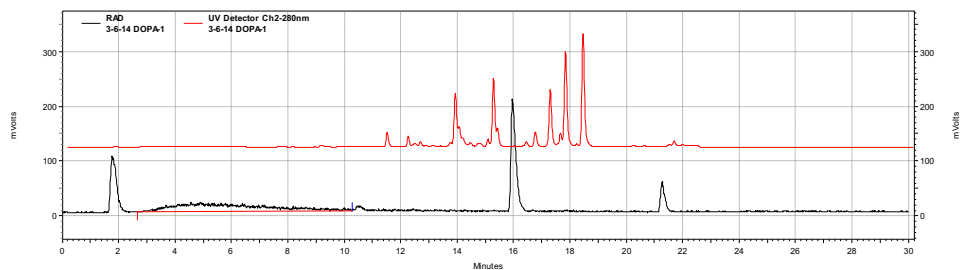
3-[¹⁸F]fluoro-tyrosine **15** RAD trace overlaid with UV trace (280 nm) spiked with 3-fluoro-tyrosine



Radio-TLC Conditions: 80% EtOAc/Hexane

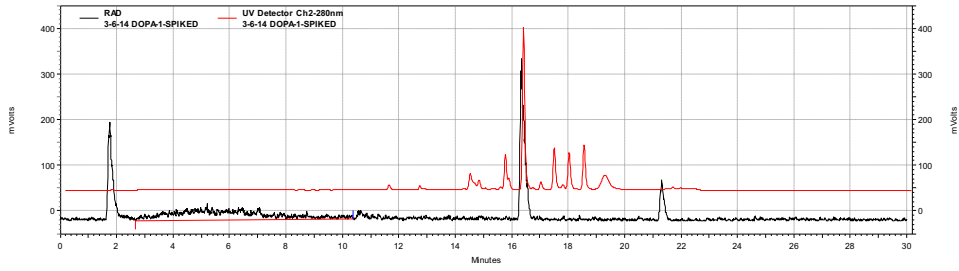


6-[¹⁸F]fluoro-DOPA 17 RAD trace overlaid with UV trace (280 nm)[‡]

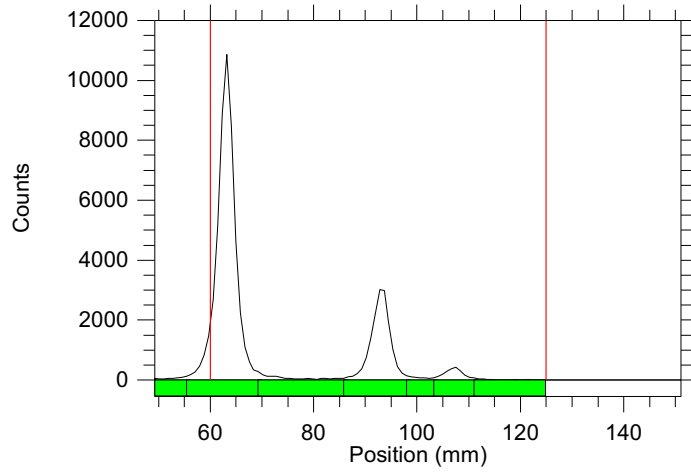


6-[¹⁸F]fluoro-DOPA 17 RAD trace overlaid with UV trace (280 nm) spiked with 6-fluoro-DOPA

[‡] The Rad peak at ca. 21.5 min corresponds to [¹⁸F]fluoromesitylene. The ratio between fluoromesitylene and fluoro-DOPA is 87:13.



Radio-TLC Conditions: 60% EtOAc/Hexane



3.7 REFERENCE

- (1) (a) Cai, L.; Lu, S.; Pike, V. W. *Eur. J. Org. Chem.* **2008**, 2853. (b) Ametamey, S. M.; Honer, M.; Schubiger, P. A. *Chem. Rev.* **2008**, *108*, 1501. (c) Miller, P. W.; Long, N. J.; Vilar, R.; Gee, A. D. *Angew. Chem. Int. Ed. Engl.* **2008**, *47*, 8998. (d) Littich, R.; Scott, P. J. H. *Angew. Chem. Int. Ed.* **2012**, *51*, 1106.
- (2) Tredwell, M.; Gouverneur, V. *Angew. Chem., Int. Ed.* **2012**, *51*, 11426.
- (3) (a) Hickey, J. L.; Lim, S.; Hayne, D. J.; Paterson, B. M.; White, J. M.; Villemagne, V. L.; Roselt, P.; Binns, D.; Cullinane, C.; Jeffery, C. M.; Price, R. I.; Barnham, K. J.; Donnelly, P. S. *J. Am. Chem. Soc.* **2013**, *135*, 16120. (b) Smith, S. Scan may detect signs of NFL players' brain disease. http://www.cnn.com/2013/01/22/health/cte-study/index.html?hpt=hp_c2 (accessed March 17, 2016).
- (4) Shin, J.; Kepe, V.; Barrio, J. R.; Small, G. W. *J. Alzheimers Dis.* **2011**, *26* (s3), 135.
- (5)(a) Shoup, T. M.; Yokell, D. L.; Rice, P. A.; Jackson, R. N.; Livni, E.; Johnson, K. A.; Brady, T. J.; Vasdev, N. *J. Labelled Compds. Radiopharm.* **2013**, *56*, 736. (b) Liang, S. H.; Yokell, D. L.; Normandin, M. D.; Rice, P. A.; Jackson, R. N.; Shoup, T. M.; Brady, T. J.; El Fakhri, G.; Collier, T. L.; Vasdev, N. *Mol. Imaging* **2014**, *13*, 1535.
- (6) Harada, R.; Okamura, N.; Furumoto, S.; Furukawa, K.; Ishiki, A.; Tomita, N.; Hiraoka, K.; Watanuki, S.; Shidahara, M.; Miyake, M.; Ishikawa, Y.; Matsuda, R.; Inami, A.; Yoshikawa, T.; Tago, T.; Funaki, Y.; Iwata, R.; Tashiro, M.; Yanai, K.; Arai, H.; Kudo, Y. *Eur. J. Nucl. Med. Mol. Imaging* **2015**, *42*, 1052.
- (7) [¹¹C]PBB3 is a ¹¹C tau tracer clinically used: Hashimoto, H.; Kawamura, K.; Takei, M.; Igarashi, N.; Fujishiro, T.; Shiomi, S.; Watanabe, R.; Muto, M.; Furutsuka, K.; Ito, T.; Yamasaki, T.; Yui, J.; Nemoto, K.; Kimura, Y.; Higuchi, M.; Zhang, M.-R. *Nucl. Med. Bio.* **2015**, *42*, 905.
- (8) Wolf, L. K. Racing to Detect Brain Trauma. <http://cen.acs.org/articles/92/i29/Racing-Detect-Brain-Trauma.html> (accessed March 17, 2016).
- (9) (a) Kaitin, K.I. and DiMasi, J.A. Pharmaceutical innovation in the 21st century: new drug approvals in the first decade, 2000–2009. In *Clinical Pharmacology and Therapeutics*, **2011**, *89*, 183. (b) DiMasi, J.A., Hansen, R.W., and Grabowski, H.G. The price of innovation: new estimates of drug development costs. In *Journal of Health Economics*, **2003**, *22*, 151. (c) Adams, C.P. and Brantner, V.V. Estimating the cost of new drug development: is it really 802 million dollars? In *Health Affairs*, **2006**, *25*, 420. (d) Adams, C.P. and Brantner, V.V. Spending on new drug development1. In *Health Economics*, **2010**, *19*, 130.
- (10) (a) Brooks, A. F.; Topczewski, J. J.; Ichiishi, N. Sanford, M. S.; Scott, P. J. H. *Chem. Sci.* **2014**, *5*, 4545. (b) Fowler, J. S.; Volkow, N. D.; Wang, G.-J. Ding, Y. -S.; Dewey, S. L. *J. Nuc. Med.* **1999**, *40*, 1154. (c) Miller, P. W.; Long, N. J.; Vilar, R.; Gee, A. D. *Angew. Chem. Int. Ed.* **2008**, *47*, 8998.
- (11) (a) Pither, R. *Expert Rev. Mol. Diagn.* **2003**, *3*, 703. (b) Sanabria-Bohorquez, S. M.; van Brugen, N.; Marik, J. Developing Targeted PET Tracers in the Era of Personalized Medicine. In *Medicinal Chemistry Approaches to Personalized Medicine*. **2014**, Wiley-VCH Verlag GmbH & Co. KGaA, Weinheim, Germany.; p289.
- (12) Van der Veldt, A. A. M.; Lubberink, M.; Mathijssen, R. H. J.; Loos, W. J.; Herder, G. J. M.; Greuter, H. N.; Comans, E. F. I.; Rutten, H. B.; Eriksson, J.; Windhorst, A. D.;

Hendrikse, N. H.; Postmus, P. E.; Smit, E. F.; Lammertsma, A. A. *Clin. Cancer Res.* **2013**, *19*, 4163.

(13) Van den Abbeele, A. D. *The Oncologist* **2008**, *13 Suppl 2* (Supplement 2), 8.

(14) Salat, D.; Noyce, A. J.; Schrag, A.; Tolosa, E. *Lancet Neurol.* **2016**, *9*, 363.

(15) Yu, S. *Biomed. Imaging Interv. J.* **2006**, *2*, e57.

(16) Jacob, M. J.; Pandit, A. G.; Jora, C.; Mudalsha, R.; Sharma, A.; Pathak, H.C. *J. Nuc. Med.* **2011**, *26*, 139.

(17) Rotstein, B. H.; Stephenson, N. A.; Vasdev, N.; Liang, S. H. *Nat. Comms* **2014**, *5*.

(18) Edwards, R.; Wirth, T. *J. Labelled Compds Radiopharm.* **2015**, *58*, 183.

(19) Brooks, A. F.; Topczewski, J. J.; Ichiishi, N.; Sanford, M. S.; Scott, P. J. *Chem. Sci.* **2014**, *5*, 4545.

(20) (a) Grushin, V. V.; Kantor, M. M.; Tolstoya, T. P.; Shcherbina, T. M. *Russ. Chem. Bull.* **1984**, *33*, 2130. (b) Shah, A.; Pike, V. W.; Widdowson, D. A. *J. Chem. Soc., Perkin Trans. 1* **1998**, 2043. (c) (d) Chun, J.; Telu, S.; Lu, S.; Pike, V. W. *Org. Biomol. Chem.* **2013**, *11*, 5094. (e) Chun, J.; Pike, V. W. *Org. Biomol. Chem.* **2013**, *11*, 6300. (f) Yusubov, M. S.; Svitich, D. Y.; Larkina, M. S.; Zhdankin, V. V. *Arkivoc* **2013**, 364.

(21) (a) Martín-Santamaría, S.; Carroll, M. A.; Carroll, C. M.; Carter, C. D.; Rzepa, H. S.; Widdowson, D. A.; Pike, V. W. *Chem. Commun.* **2000**, 649. (b) Ross, T. L.; Ermert, J.; Hocke, C.; Coenen, H. H. *J. Am. Chem. Soc.* **2007**, *129*, 8018. (c) Carroll, M. A.; Jones, C.; Tang, S.-L. *J. Label. Compd. Radiopharm.* **2007**, *50*, 450. (d) Jang, K. S.; Jung, Y.-W.; Gu, G.; Koeppe, R. A.; Sherman, P. S.; Quesada, C. A.; Raffel, D. M. *J. Med. Chem.* **2013**, *56*, 7312.

(22) In our hands, (2-thienyl)(aryl)iodonium derivatives exhibit modest stability; for example, [(4-OMePh)(2-thienyl)I]Br was found to decompose within two weeks under ambient condition.

(23) Only one report in the patent literature has described accessing F-DOPA from diaryliodonium salts: DiMagno, S. Fluorination of Aromatic Ring Systems. WO2010/048170A2, April 29, 2010.

(24) Kuik, W.-J.; Kema, I. P.; Brouwers, A. H.; Zijlma, R.; Neumann, K. D.; Dierckx, R. A. J. O.; DiMagno, S. G.; Elsinga, P. H. *J. Nucl. Med.* **2015**, *56*, 106.

(25) For transition metal-catalyzed aryl radiofluorination see: (a) Lee, E.; Kamlet, A. S.; Powers, D. C.; Neumann, C. N.; Boursalian, G. B.; Furuya, T.; Choi, D. C.; Hooker, J. M.; Ritter, T. *Science* **2011**, *334*, 639. (b) Kamlet, A. S.; Neumann, C. N.; Lee, E.; Carlin, S. M.; Moseley, C. K.; Stephenson, N.; Hooker, J. M.; Ritter, T. *PLoS One* **2013**, *8*, e59187. (c) Lee, E.; Hooker, J. M.; Ritter, T. *J. Am. Chem. Soc.* **2012**, *134*, 17456. (d) Ren, H.; Wey, H.-Y.; Strebl, M.; Neelamegam, R.; Ritter, T.; Hooker, J. M. *ACS Chem. Neurosci.*, **2014**, *5*, 611.

(e) Hoover, A. J.; Lazari, M.; Ren, H.; Narayanam, M. K.; Murphy, J. M.; van Dam, R. M.; Hooker, J. M.; Tobias, R. *Organometallics* **2016**, DOI: 10.1021/acs.organomet.6b00059.

(26) For metal catalyzed sp³ radiofluorination see: (a) Topczewski, J. J.; Tewson, T. J.; Nguyen, H. M. *J. Am. Chem. Soc.* **2011**, *133*, 19318. (b) Benedetto, E.; Tredwell, M.; Hollingworth, C.; Khotavivattana, T.; Brown, J. M.; Gouverneur, V. *Chem. Sci.*, **2013**, *4*, 89. (c) Graham, T. J. A.; Lambert, R. F.; Ploessl, K.; Kung, H. F.; Doyle, A. G. *J. Am. Chem. Soc.* **2014**, *136*, 5291.

-
- (27) After our investigations there were a series of transition metal mediated radiofluorinations disclosed see reference 5 (a) and reviews: (a) Preshlock, S.; Tredwell, M.; Gouverneur, V. *Chem. Rev.* **2016**, *116*, 719. (b) Liang, S. H.; Vasdev, N. *Angew. Chem. Int. Ed.* **2014**, *53* (43), 11416.
- (28) Ichiishi, N.; Canty, A. J.; Yates, B. F.; Sanford, M. S. *Org. Lett.* **2013**, *15*, 5134.
- (29) Ichiishi, N.; Brooks, A. F.; Topczewski, J. J.; Rodnick, M. E.; Sanford, M. S.; Scott, P. J. H. *Org. Lett.* **2014**, *16*, 3224.
- (30) Brooks, A. F.; Topczewski, J. J.; Ichiishi, N.; Sanford, M. S.; Scott, P. J. *Chem. Sci.* **2014**, *5*, 4545.
- (31) Ichiishi, N.; Canty, A. J.; Yates, B. F.; Sanford, M. S. *Org. Lett.* **2013**, *15*, 5134.
- (32) Chun, J.-H.; Telu, S.; Lu, S.; Pike, V. W. *Org. Biomol. Chem.* **2013**, *11*, 5094.
- (33) Dolan, J. "HPLC Solutions #36: End-Capping," <http://www.sepscience.com/Techniques/LC/Articles/321-/HPLC-Solutions-36-Endcapping> (Accessed on April 3, 2016)
- (34) Liang, W.; An, J.; Zhao, X.; Shao, Y. *J. Nucl. Med.* **2015**, *56* (sp 3), 1170.
- (35) (a) Chekhlov, A. N. *Russ J Gen Chem* **2009**, *79*, 744. (b) Mühle, J.; Sheldrick, W. S. *Zeitschrift für anorganische und allgemeine Chemie* **2003**, *629*, 2097.
- (36) Typically, fluorination requires extensive drying of reagents: Watson, D. A.; Su, M.; Teverovskiy, G.; Zhang, Y.; Garcia-Fortanet, J.; Kinzel, T.; Buchwald, S. L. *Science* **2009**, *325*, 1661.
- (37) (a) Goulding, R. W.; Palmer, A. J.; Thakur, M. L. *Radioisotopy* **1971**, *12*, 1045. (b) Cottrall, M. F.; Taylor, D. M.; McElwain, T. J. *Brit. J. Radiol.* **1973**, *46*, 277. (c) Bodsch, W.; Coenen, H. H.; Stöcklin, G.; Takahashi, K.; Hossmann, K. A. *J. Neurochem.* **1988**, *50*, 979.
- (38) Since then, O-(2-[¹⁸F]fluoroethyl)-L-tyrosine has been utilized as a less than ideal but accessible surrogate for phenylalanine. See: (a) Wester, H. J.; Herz, M.; Weber, W.; Heiss, P.; Senekowitsch-Schmidtke, R.; Schwaiger, M.; Stöcklin, G. *J. Nucl. Med.* **1999**, *40*, 205. (b) Langen, K. -J.; Hamacher, K.; Weckesser, M.; Floeth, F.; Stoffels, G.; Bauer, D.; Coenen, H. H.; Pauleit, D. *Nucl. Med. Biol.* **2006**, *33*, 287.
- (39) (a) Garnett, E. S.; Firnau, G.; Chan, P. K. H.; Sood, S.; Belbeck, L. W. *Proc. Natl. Acad. Sci. U.S.A.* **1978**, *75*, 464. (b) Garnett, E. S.; Firnau, G.; Nahmias, C. *Nature* **1983**, *305*, 137. (c) Luxen, A.; Guillaume, M.; Melega, W. P.; Pike, V. W.; Solin, O.; Wagner, R. *Int. J. Nucl. Med. Biol.* **1992**, *19*, 149. (d) Rakshi, J. S.; Uema, T.; Ito, K.; Bailey, D. L.; Morrish, P. K.; Ashburner, J.; Dagher, A.; Jenkins, I. H.; Friston, K. J.; Brooks, D. J. *Brain* **1999**, *122*, 1637.
- (40) For the application of 6-[¹⁸F]F -DOPA to tumor imaging, see: (a) Hoegerle, S.; Althoefer, C.; Ghanem, N.; Koehler, G.; Waller, C. F.; Scheruebl, H.; Moser, E.; Nitzsche, E. *Radiology* **2001**, *220*, 373. (b) Becherer, A.; Szabo, M.; Karanikas, G.; Wunderbaldinger, P.; Angelberger, P.; Raderer, M.; Kurtaran, A.; Dudczak, R.; Kletter, K. *J. Nucl. Med.* **2004**, *45*, 1161. (c) Chen, W.; Silverman, D. H. S.; Delaloye, S.; Czernin, J.; Kamdar, N.; Pope, W.; Satyamurthy, N.; Schiepers, C.; Cloughesy, T. J. *Nucl. Med.* **2006**, *47*, 904.
- (41) Jauregui-Osoro, M. et al. *Eur. J. Nucl. Med. Mol. Imaging.* **2010**, *37*, 2108.
- (42) Berridge, M. S.; Crouzel, C.; Comar, D. J. *Labelled. Compds. Radiopharm.* **1985**, *22*, 687.

-
- (43) Knochel, A. and Zwerner, O. *Appt. Radiat. Isot.* **1991**, 42, 1077.
- (44) Chun, J.-H.; Lu, S.; Pike, V. W. *Eur. J. Org. Chem.* **2011**, 4439.
- (45) If $^{18}\text{F}/^{19}\text{F}$ exchange were rapid, the expected specific activity of 4- ^{18}F fluoroanisole would be <1 Ci/mmol.
- (46) Jang, K. S.; Jung, Y.-W.; Gu, G.; Koeppe, R. A.; Sherman, P. S.; Quesada, C. A.; Raffel, D. M. *J. Med. Chem.* **2013**, 56, 7312.
- (47) (a) Wieland, D. M.; Brown, L. E.; Rogers, Les, W.; Worthington, K. C.; Wu, J.-L.; Clinthorne, N. H.; Otto, C. A.; Swanson, D. P.; Beierwaltes, W. H. *J. Nucl. Med.* **1981**, 22, 22-31. (b) DeGrado, T. R.; Zalutsky, M. R.; Vaidyanathan, G. *Nucl. Med. Biol.* **1995**, 22, 1. (c) Raffel, D. M.; Wieland, D. M. *Nucl. Med. Biol.* **2001**, 28, 541. (d) Flotats, A.; Carrio, I. *J. Nucl. Cardiol.* **2004**, 11, 587.
- (48) Washington University School of Medicine. "Missing link in Parkinson's disease found: Discovery also has implications for heart failure." ScienceDaily. www.sciencedaily.com/releases/2013/04/130425142357.htm (accessed March 24, 2016). <https://www.sciencedaily.com/releases/2013/04/130425142357.htm>
- (49) (a) Liang, S. H.; Holland, J. P.; Stephenson, N. A.; Kassenbrock, A.; Rotstein, B. H.; Daigault, C. P.; Lewis, R.; Collier, L.; Hooker, J. M.; Vasdev, N. *ACS Chem. Neurosci.* **2015**, 6, 535. (b) Malik, N.; Solbach, C.; Voelter, W.; Machulla, H. *J. Radioanal. Nucl. Chem.* **2010**, 283, 757.
- (50) Fier, P. S.; Hartwig, J. F. *J. Am. Chem. Soc.* **2014**, 136, 10139.
- (51) (a) Rotstein, B. H.; Stephenson, N. A.; Vasdev, N.; Liang, S. H. *Nature Commun.* **2014**, 5, 4365. (b) Chun, J. H.; Morse, C. L.; Chin, F. T.; Pike, V. W. *Chem. Comm.* **2013**, 49, 2151. (c) Carroll, M. A.; Naime, J. Woodcraft, J. L. *J. Labelled Comp. Radiopharm.* **2007**, 50, 452. (d) Karamkam, M.; Hinnen, F.; Vaufrey, F.; Dolle, F. *J. Labelled Comp. Radiopharm.* **2003**, 46, 979.
- (52) Fritsche, T. R.; Sader, H. S.; Cleeland, R.; Jones, R. N. *Antimicrob. Agents Chemother.* **2005**, 49, 1468.
- (53) Unpublished Results
- (54) Malik, H. A.; Taylor, B. L. H.; Kerrigan, J. R.; Grob, J. E.; Houk, K. N.; Bois, Du, J.; Hamann, L. G.; Patterson, A. W. *Chem. Sci.* **2014**, 5, 2352.
- (55) Ye, Y.; Schimler, S. D.; Hanley, P. S.; Sanford, M. S. *J. Am. Chem. Soc.* **2013**, 135, 16292.
- (56) Fier, P. S.; Hartwig, J. F. *J. Am. Chem. Soc.* **2012**, 134, 10795.
- (57) Cardinale, J.; Ermert, J.; Kügler, F.; Helfer, A.; Brandt, M. R.; Coenen, H. H. *J. Labelled Comp. Radiopharm.* **2012**, 55, 450.
- (58) Basuli, F.; Wu, H.; Griffiths, G. L. *J. Label. Comp. Radiopharm.* **2011**, 54, 224.
- (59) Phipps, R. J.; Grimster, N. P.; Gaunt, M. J. *J. Am. Chem. Soc.* **2008**, 130, 8172.
- (60) Chun, J.-H.; Pike, V. W. *J. Org. Chem.* **2012**, 77, 1931.

CHAPTER 4. DEVELOPMENT OF CU-MEDIATED $[^{18}\text{F}]$ FLUORINATION OF ARYL BORONATES AND SYNTHESIS OF $\text{Ag}[^{18}\text{F}]\text{F}$ AND ITS APPLICATION

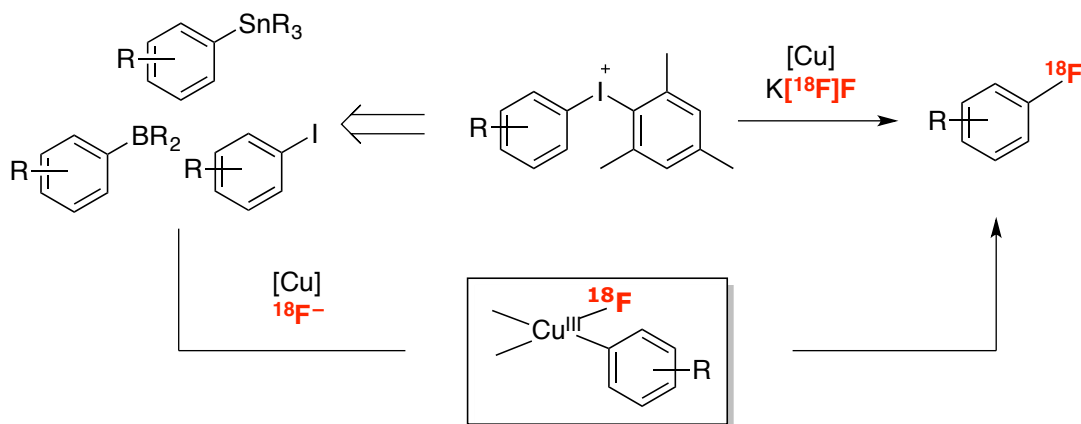
4.1 INTRODUCTION

Positron emission tomography (PET) imaging is a powerful diagnostic imaging technique, and today over 1.5 million PET scans are performed annually just in the U.S.¹ Despite the utility and explosive growth of modern PET technology, the synthetic techniques used to incorporate radionuclides such as ^{11}C and ^{18}F into radiopharmaceuticals have remained relatively unchanged since the inception of the field in the 1950's. Indeed, many of the reactions used towards ^{18}F labeling such as $\text{S}_{\text{N}}2$ and Halex reactions are considered "classical", having been developed as early as 1900.² This trend is attributable to the lack of collaboration between chemists focused on method development and those focused on radiotracer synthesis, as both play a role in the development of suitable synthetic protocols that can be translated to radiofluorination. After almost a decade of renaissance in transition metal-catalyzed aromatic fluorination reactions (see Chapter 1 for more details), there has likewise been an explosion in the development of metal-catalyzed ^{18}F -radiofluorination methodologies over the last 3-4 years. There are multiple active collaborations between radiochemistry experts and synthetic/organometallic chemists, which have spurred various inventions in methodology development for ^{18}F -incorporation.³

This chapter details our exploration into Cu-mediated radiofluorination of aryl boronates and aryl iodides (Scheme 4.1). From a practical perspective, these are ideal radiofluorination precursors, as they are easily synthesized and/or commercially available, and are typically bench-stable. However, at the time that we started this work, there were no nucleophilic radiofluorination methods available for electron-rich aryl boronic acids, stannanes, or iodides. Developing such Cu-catalyzed fluorination

methods would allow synthetic chemists to bypass a step to synthesize iodonium salts to access desired [^{18}F]fluoroarenes, simply by introducing Cu catalysts. Thus, it is of interest to develop processes to fluorinate Ar-X using the combination of a Cu catalyst and either K^{18}F ($\text{X} = \text{B}$ or Sn)⁴ or Ag^{18}F ($\text{X} = \text{I}$).⁵

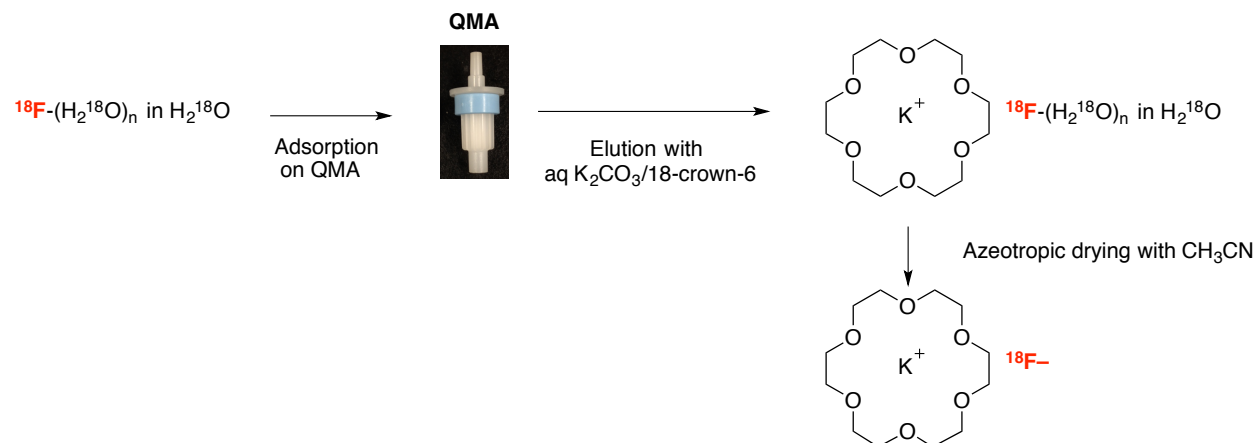
Scheme 4.1 Cu-Mediated Fluorination of Precursors for (Mesityl)(aryl)iodonium salts



In addition to developing a new Cu-mediated method, our PET team was also interested in developing new methods to prepare and isolate organic-soluble metal ^{18}F -fluoride salts. The most commonly used ^{18}F -fluoride source is $\text{K}[^{18}\text{F}]\text{F}$ (Figure 4.1), which is typically prepared and dried in the presence of K_2CO_3 and a phase transfer reagent, typically a cryptand.⁶ The procedure for $\text{K}^{18}\text{F}\cdot\text{cryptand}$ synthesis involves passing aqueous $^{18}\text{F}^-$ through a quaternary methylammonium (QMA) anion exchange cartridge. The QMA resin causes $^{18}\text{F}^-$ to localize on the cartridge via anion exchange. An aqueous solution containing $\text{K}_2\text{CO}_3/\text{cryptand}$ (typically Kryptofix or 18-crown-6) is then passed through the cartridge to desorb (elute) the $^{18}\text{F}^-$ as the $\text{K}^{18}\text{F}\cdot\text{cryptand}$ hydrate complex. Azeotropic drying with CH_3CN affords anhydrous $\text{K}^{18}\text{F}\cdot\text{cryptand}$ complex, which is then re-dissolved in a dry polar aprotic solvent for use in radiolabelling reactions. The current problem with this method is that the isolation of $\text{K}^{18}\text{F}\cdot\text{cryptand}$ requires several azeotropic drying cycles that take approximately 10 min, leading to an $^{18}\text{F}^-$ loss of 5-6% due to radioactive decay. Furthermore, the presence of K_2CO_3 and cryptands can be detrimental to Cu-catalyzed reactions. For instance, K_2CO_3 can promote ring cyclization of iodonium salts in the presence of amine functionality.⁷ Also, carbonate salts are commonly used in Cu-catalyzed aryl-aryl cross coupling reactions, which may lead to the formation of undesirable impurities.⁸ In addition, many current-state-of-art cold

fluorination protocols utilize different nucleophilic fluorides sources, including $\text{Bu}_4\text{NF}(t\text{BuOH})$,⁹ Me_4NF ,¹⁰ CsF ¹¹ and AgF .⁵ Therefore, further exploration of new fluoride elution methods could provide techniques that complement metal-mediated ^{18}F -radiotracer synthesis.

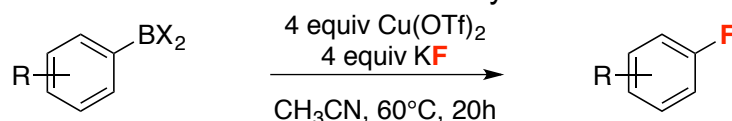
Figure 4.1 Dry-Down Procedure for Synthesis of KF-Cryptand Complex



This chapter describes our investigation into (1) translating Cu-mediated fluorination of aryl boronates and boronic acids to radiofluorination and (2) establishing synthesis of Ag^{18}F salt and its application to radiofluorination of aryl iodides. In both cases, the development of new $^{18}\text{F}^-$ elution procedures was critical for successful reaction development and optimization.

4.2 RESULTS AND DISCUSSION

Cu-mediated Fluorination of Aryl Boron Compounds. In 2013, the Sanford lab disclosed the Cu-mediated fluorination of aryl trifluoroborates, arylboronate esters, and aryl boronic acids with KF (Scheme 4.2).¹² We immediately sought to translate this discovery to a radiofluorination of aryl boron compounds with K^{18}F for the following reasons: (1) aryl boron compounds are readily available, (2) no-carrier-added nucleophilic fluorination with K^{18}F is ideal, (3) there are much lower safety concerns with residual Cu compared to Pd^{13} or Ni^{14} and (4) this is an operationally simple fluorination method with commercially available reagents.

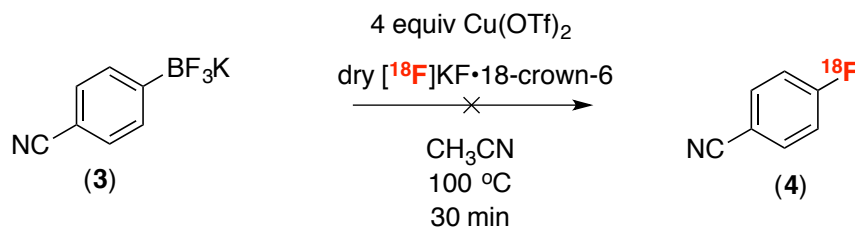
Scheme 4.2 Cu-Mediated Fluorination of Aryl Trifluoroborates with KF^{12} 

In order to examine the feasibility of translating this method to radiofluorination, this protocol was further examined for air and water tolerance. It was found that the reaction can tolerate water and air (entry 1-3) and afford modest to good yields (Table 4.1). This offers the possibility of this Cu-mediated fluorination could work without needing an air-free glovebox set up at the PET facility.

Table 4.1 Examination on Air and Water Tolerance of the Protocol

Entry	Conditions	^{18}F NMR Yield
1	Set up inside of the glovebox	72%
2	Set up outside the glovebox	81%
3	5 equiv of H_2O	41%

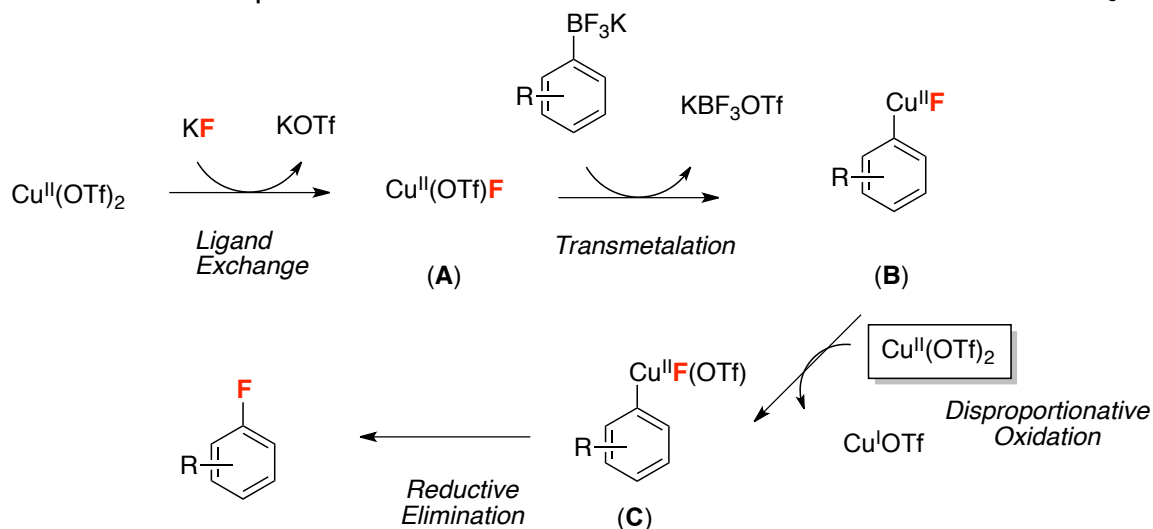
As a first attempt, an electronically activated 4-cyanophenyl trifluoroborate **3** was selected as a model compound. In the presence of $\text{Cu}(\text{OTf})_2$ and $\text{K}^{18}\text{F}\cdot 18\text{-crown-6}$ in acetonitrile for 30 minutes, we did not observe 4- ^{18}F fluorobenzonitrile **4** on radio-TLC (Scheme 4.3).

Scheme 4.3 Initial Attempt on Cu-mediated Fluorination

Given that ^{19}F -fluorination needs a reaction time of 20 h, we next decided to optimize the reaction condition based on the proposed mechanism of the cold reaction (Scheme 4.4). Kinetic studies determined the reaction is first-order in aryl trifluoroborates.¹⁵ Hence, that led us to hypothesize that a possible rate-limiting step of the reaction is

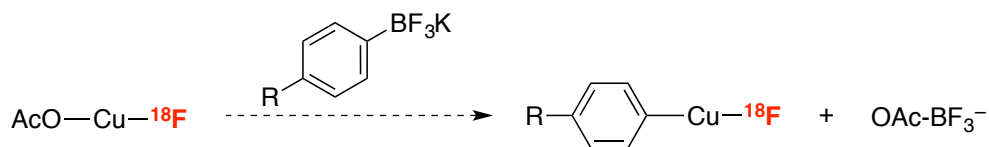
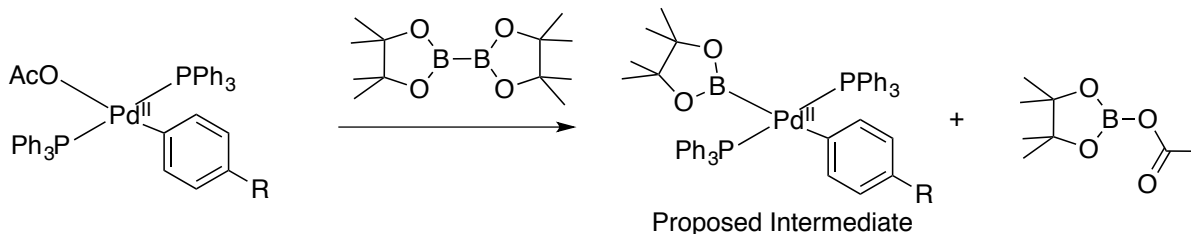
transmetalation, disproportionative oxidation, or reductive elimination. In addition, our computational studies in iodonium chemistry showed that fluoride has a high affinity toward Cu^{I} ,¹⁶ so it was a reasonable starting point to consider how to accelerate the transmetalation step of Cu-mediated fluorination with aryl trifluoroborates.

Scheme 4.4 Proposed Mechanism of the Cu-Mediated Fluorination of $\text{Ar-BF}_3\text{K}$



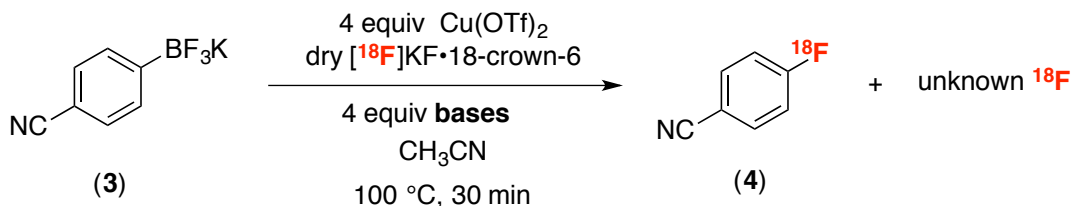
Acceleration of Transmetalation. We first sought to find a set of conditions that would show some reactivity with aryl trifluoroborates. Rationalized by the high affinity of fluoride to Cu catalysts in the iodonium system (detailed in chapter 2), we hypothesized that transmetalation can be a problematic step in the mechanism (Scheme 4.5). Therefore, we surmised that the activation of the $\text{C}_{\text{aryl}}\text{-B}$ bond through Lewis acid-base interaction might accelerate fluorination. Miyaura et. al, reported a detailed mechanistic study on Pd-catalyzed borylation of aryl halides by $\text{B}_2(\text{pin})_2$ in the presence of $\text{PdCl}_2(\text{dppf})$ and excess KOAc as an additive. Their study highlighted the crucial role that acetate plays in the reaction, as an isolated *trans*- $\text{ArPd}(\text{OAc})(\text{PPh}_3)_2$ intermediate rapidly undergoes transmetalation with $\text{B}_2(\text{pin})_2$, a process that is mediated by the acetate ligand. An acceleration effect via bases was also seen in Suzuki coupling.¹⁷ In addition, the high oxophilicity of boron has to be considered as a driving force for the transmetalation step, which involves an acetate ligand. Thus, we hypothesized that addition of excess acetate salt might accelerate the transmetalation at the Cu center via the hypothetical Cu and boron intermediate outlined in Scheme 4.5.

Scheme 4.5 Acceleration of Transmetalation in Miyaura Borylation and Possible Application to Cu-Mediated Fluorination of Aryl Trifluoroborates



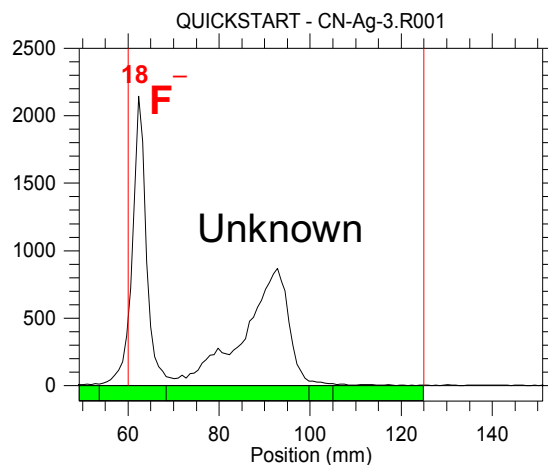
In spite of the observation of a peak on radio TLC, HPLC analysis confirmed the addition of bases did not produce the desired product 4- ^{18}F fluorobenzonitrile **4** (Table 4.2). The identity of the unknown compound in the presence of bases was not confirmed in this study; however, it was speculated that the formation of a tetrahedral activated boron species was generated through isotopic exchange between ^{19}F from potassium trifluoroborate substrate and free ^{18}F -fluoride ($[\text{}^{18}\text{F}]\text{OAcBF}_3^-$). This (likely) outcome inspired us to shift our focus on aryl boron pinacol esters, which cannot undergo isotopic exchange in the presence of suitable bases that activate the boron center towards transmetalation.

Table 4.2 Acetate Salt Additives for Cu-mediated Reactions



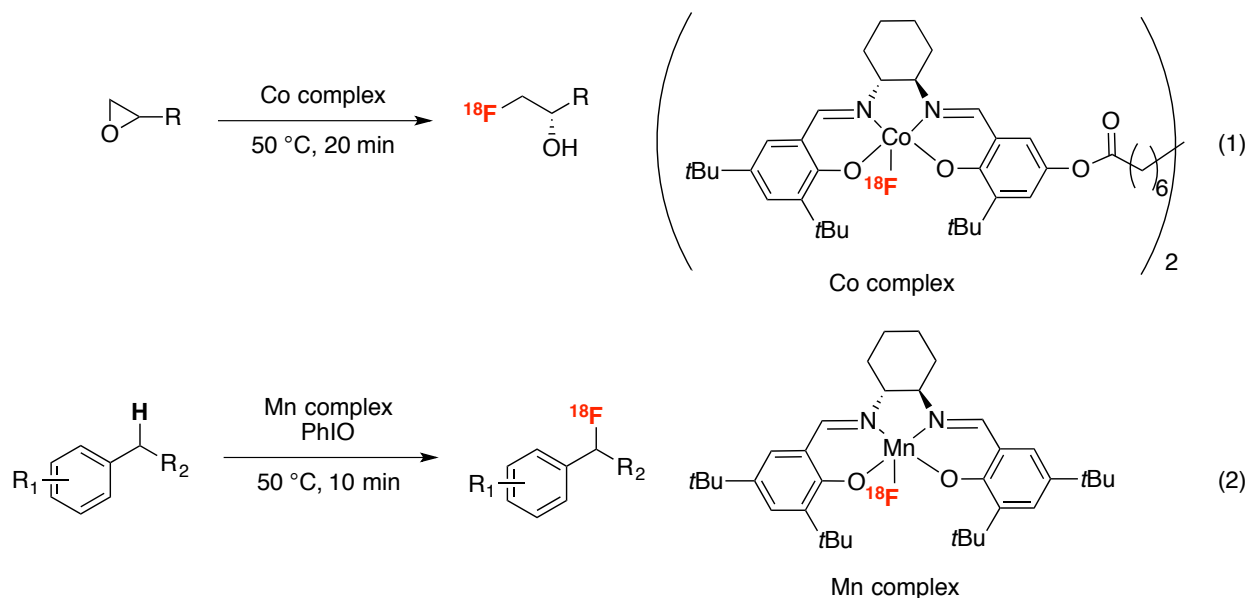
Entry	M-OAc	RCC
1	KOAc	0%
2	TBAOAc	0%
3	AgOAc	0%

Figure 4.2 TLC Scan Image of the Reaction with TBAOAc (Entry 2, Table 4.2)

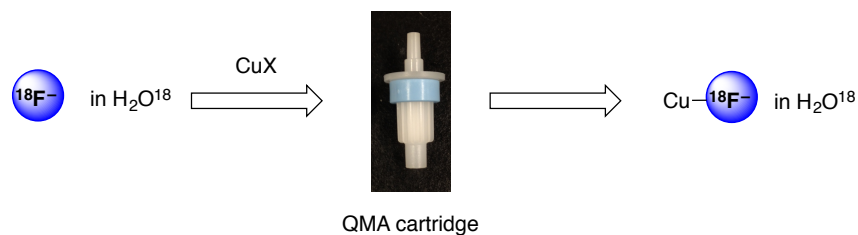


Elution Studies: Cu Salts. Elution studies were commenced in parallel to the aforementioned preliminary studies. Given our hypothesis that our active catalyst was a Cu^{II} fluoride, it was critical to figure out a way to make the material quickly under the given conditions, as only traces of ¹⁸F-fluoride (< nM concentration) are actually available in the solution during radiolabelling. During the course of our investigation, two seminal reports by Doyle¹⁸ and Groves¹⁹ were separately disclosed. They proposed an operationally simple method to form a discrete M-¹⁸F complex by tweaking K[¹⁸F]F processing and purification. In 2014, Doyle reported enantioselective ring opening reactions of epoxides using (*R,R*)-(salen)CoOTs as a precursor. A [¹⁸F](salen)CoF species suitable for the radiofluorination of epoxides was generated by eluting [¹⁸F]fluoride from a QMA ion-exchange cartridge with the salen precursor complex (eq 1, Scheme 4.6). This ion exchange cartridge approach was also taken by Groves and his colleagues to synthesize a [¹⁸F](salen)MnF species by eluting with the corresponding Mn-salen-tosylate complex (eq 2, Scheme 4.6). This ¹⁸F-labeled complex was utilized to radiofluorinate benzylic C-H bonds in a wide variety of substrates. They used the reaction to append ¹⁸F to a number of drug molecules.

Scheme 4.6 Doyle's and Grove's Elution [^{18}F]fluoride with Metal Complexes



We hypothesized that QMA cartridges could also be utilized for the analogous production of $\text{Cu-}^{18}\text{F}$, in order to enhance the efficiency of our Cu-mediated fluorination of boronate esters method. Evaluating the elution of $^{18}\text{F}^-$ from QMA cartridges with different Cu^{2+} salts in various solvents then commenced this part of the study. The percent $^{18}\text{F}^-$ recovery from QMA resin was calculated by dividing the amount of activity that passed through the QMA on elution by the total amount of activity (i.e, total trapped $^{18}\text{F}^-$) originally present on the QMA cartridge. Fluoride recovery was found to be strongly dependent on the solvent used to dissolve the Cu salt. For instance, poor $^{18}\text{F}^-$ recovery was observed with acetone and acetonitrile solutions of $(\text{MeCN})_4\text{CuOTf}$ (entry 1-2, Table 4.3). On the other hand, methanol and DMF solutions afforded a substantial $^{18}\text{F}^-$ fluoride recovery from the QMA (entry 3,4). Switching to 100% MillQ water, fluoride recovery increased to 97%. The efficiency was identical when $\text{CuMeCN}_4\text{OTf}$ was switched to $\text{Cu}(\text{OTf})_2$, resulting in 96% of trapping efficiency using H_2O as eluent (entry 7, Table 4.3).

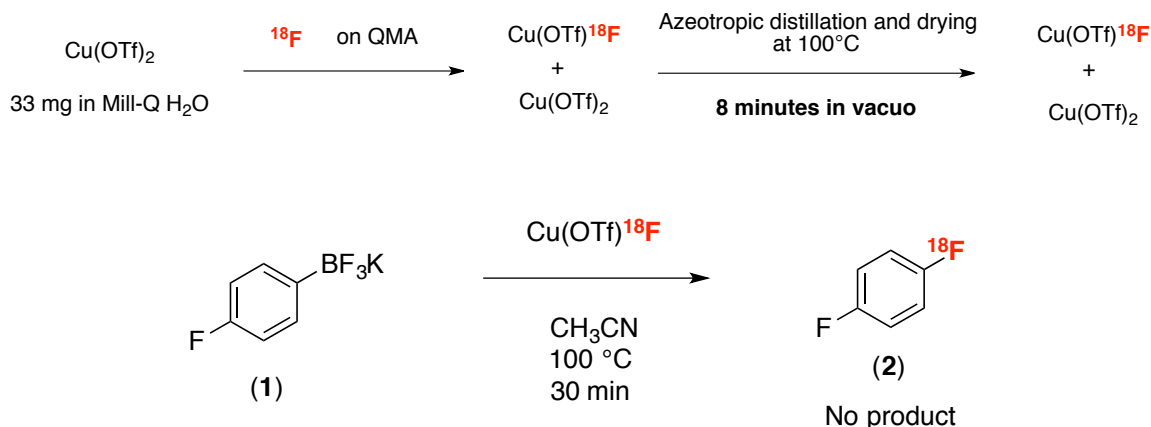
Table 4.3 Elution Studies with Cu Catalysts

Entry	Cu Salt ^a	Solvent	% ¹⁸ F ⁻ Recovery
1 ^b	(CH ₃ CN) ₄ CuOTf	Acetone	0.7
2 ^b	(CH ₃ CN) ₄ CuOTf	CH ₃ CN	2.1
3	(CH ₃ CN) ₄ CuOTf	MeOH	64
4	(CH ₃ CN) ₄ CuOTf	DMF	21
5	(CH ₃ CN) ₄ CuOTf	DMF:H ₂ O	76
5	(CH ₃ CN) ₄ CuOTf	H ₂ O	97
6	Cu(OTf) ₂	DMF	29
7	Cu(OTf) ₂	H ₂ O	96

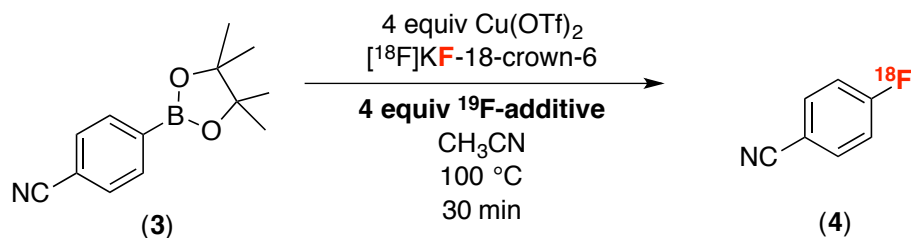
^a 0.1M of Cu solution was used. ^b 0.01 M of Cu solution was used.

Based on this elution study, the procedure outlined in Scheme 4.7 was undertaken: (1) Cu(OTf)₂ was dissolved in Mill-Q water; (2) this Cu solution was passed through a QMA cartridge pre-loaded with ¹⁸F⁻; (3) the filtrate was concentrated and redissolved in acetonitrile to produce a “dry” Cu(OTf)¹⁸F stock solution (along with free Cu(OTf)₂, as it was added in excess). This stock solution was then treated with potassium 4-fluorophenyl trifluoroborate at 100 °C for 30 minutes. Unfortunately, no reactivity was observed under these reaction conditions (Scheme 4.7). We hypothesized that lack of reactivity was due to the presence of copper hydrate complexes, from which water cannot be easily removed in 8 minutes of azeotropic drying.

Scheme 4.7 Cu-¹⁸F Formation Through Elution Method

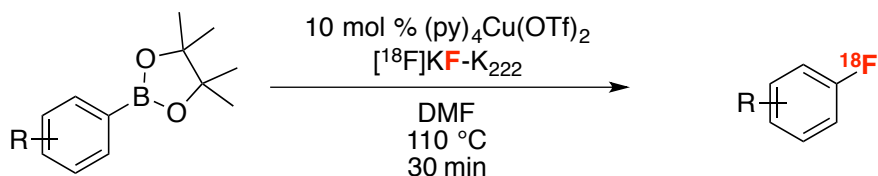


Carrier-Added Fluorination. The stoichiometry between Cu salt and KF was found to be critical in the original Cu-mediated fluorination of aryl trifluoroborates.⁴ The ratio of Cu: KF needs to be 1:1 in order to obtain a maximum yield of the product. One of the challenges in radiofluorination (also discussed in Chapter 3) is that ¹⁸F⁻ is present only in 10⁻⁹–10⁻¹² M scale. Therefore, adjustment of the stoichiometry between copper and fluoride by adding carrier (a ¹⁹F⁻ fluoride source) was considered, though that would result in a significant dilution in the amount of ¹⁸F⁻ in the product and hence lead to lower SA (Table 4.4). Upon the addition of 4 equiv of ¹⁹F KF carrier, we were pleased to see 17% radiochemical conversion (RCC) to 4-[¹⁸F]fluorobenzonitrile, which was confirmed by HPLC analysis (entry 4, Table 4.4). Ichihara and coworkers have found that the combination of potassium fluoride and calcium fluoride is effective and practical for nucleophilic fluorination of aryl halides, so this solid mixture was also tested in our reaction conditions. This carrier-added reaction led to a higher yield of 23% RCC by HPLC (entry 5). This carrier-added study suggests the importance of sufficient formation of active copper fluoride complex to induce the desired reactivity, according to the proposed catalytic cycle (Scheme 4.4).

Table 4.4 Carrier-Added Cu-Mediated Fluorination

Entry	Carrier	HPLC RCC
1	none	0
2	NaF	0
3	LiF	0
4	KF	17
5	KF–CaF ₂	23

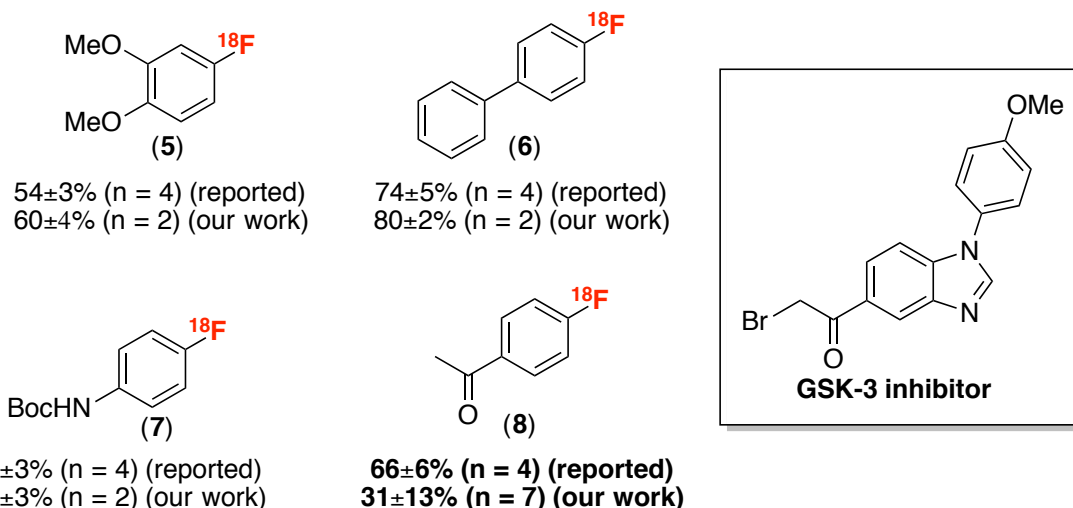
Notably, as our project was underway, the Gouverneur group reported a related Cu-mediated radiofluorination of aryl boronate esters using commercially available $(\text{py})_4\text{Cu}(\text{OTf})_2$ as a precatalyst (py = pyridine; Scheme 4.8).²⁰ Their studies revealed that they require catalytic amounts of $(\text{py})_4\text{Cu}(\text{OTf})_2$ and O_2 in the reaction atmosphere. However, this protocol had several drawbacks including: (1) the requirement for an expensive copper salt $(\text{py})_4\text{Cu}(\text{OTf})_2$; (2) incompatibility with more abundant organoboron precursors such as boronic acids and aryl trifluoroborate salts; and (3) incompatibility with automation because of the requirement for O_2 in the (rendering the reaction incompatible with the inert push gases (argon or N_2) used in modern automated radiochemistry synthesis modules). The third point is particularly important given that all modern radiopharmaceuticals in routine clinical use are prepared according to current good manufacturing practice (cGMP) via automated syntheses.²¹

Scheme 4.8 Gouverneur's Cu-catalyzed Radiofluorination of Boron Pinacol Esters

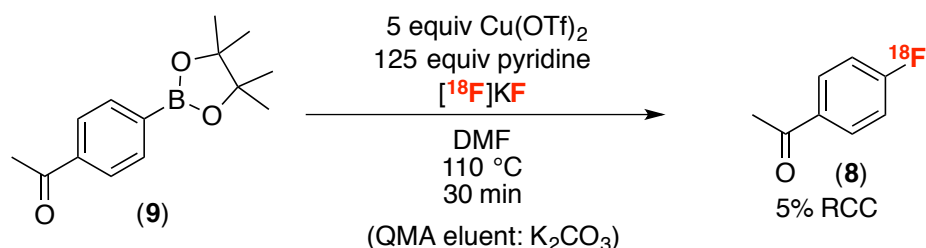
In addition to the aforementioned shortcomings, the irreproducibility of the protocol was recognized as a problem. Boron pinacol esters of 3,4-methoxybenzene **5**,

biphenyl **6**, aniline **7**, and 4-acetophenone **8** were synthesized and subjected to Gouverneur's reaction conditions to check its reproducibility. In our hands, the RCC of these transformations was quite varied depending on the substrate. We were particularly interested in radiolabeling 4-acetylphenyl boron pinacol ester as a model compound in connection with a program developing radiotracers for glycogen synthase kinase-3 (GSK-3). GSK-3 is a therapeutically valuable kinase that is very promising for Alzheimer's disease. GSK-3 inhibitors offer a valuable approach for a future therapy against Alzheimer's disease, and for our purposes, as imaging modalities for prodromal identification of early-stage Alzheimer's with PET.²² When this substrate was exposed to Gouverneur's conditions, we obtained 4-fluoroacetophenone **8** in just 31±1% (n = 7) RCC as opposed to their reported RCC (66±6%) (Scheme 4.9). Hence, our team decided to further pursue investigations focused on optimizing the radiofluorination of arylboronic acid pinacol esters.²³

Scheme 4.9 Radiofluorination of Boron Pinacol Ester



Optimization of Radiofluorination of Boron Pinacol Ester. Dr. Andrew Mossine led this part of the project. We first examined whether Cu(OTf)₂ can mediate the radiofluorination of 4-acetylphenyl boron pinacol ester **9** in the presence of pyridine in analogy to Gouverneur's condition. 4-[¹⁸F]Fluoroacetophenone was observed in 5% RCC in the presence of 125 equivalents of pyridine using cGMP automated condition (Scheme 4.10). We decided to examine if more commercially abundant boronic acids work under similar conditions.

Scheme 4.10 Utilization of Less Expensive Cu(OTf)₂

Elution Studies: Salts. After seeing the report by Gouverneur, our next goal was to further improve the fluorination protocol to address unresolved limitations, most notably to develop an alternative QMA eluent, as we hypothesized that the K₂CO₃ that was used in the Gouverneur method to elute K[¹⁸F]F could be negatively affecting our Cu-mediated reaction, as it can potentially form CuCO₃ and/or promote cross coupling reactions. We also noted that Gouverneur and coworkers diluted their ¹⁸F⁻ stock solutions (thereby diluting the amount of K₂CO₃ and Kryptofix present in each reaction).²⁰ In contrast, the ¹⁸F⁻ concentration we prepared followed cGMP standard methods.^{20,21} In addition to using Cu salts with QMA eluents, we studied a series of weaker ionic acids and bases (Table 4.5), so as to avoid strong bases that could poison the copper catalyst. Each salt required a different concentration to achieve an optimal ¹⁸F⁻ recovery, so the table shows the concentration that yielded optimal results. As with K₂CO₃, other salts such as KOTf, NH₄OTf, NH₄Cl, and TBACl, all resulted in high ¹⁸F⁻ recoveries (entry 2-5, Table 4.5). Interestingly, the acidic organic salt pyridinium *p*-toluenesulfonate (PPTS) also afforded 76% ¹⁸F⁻ recovery (entry 6).

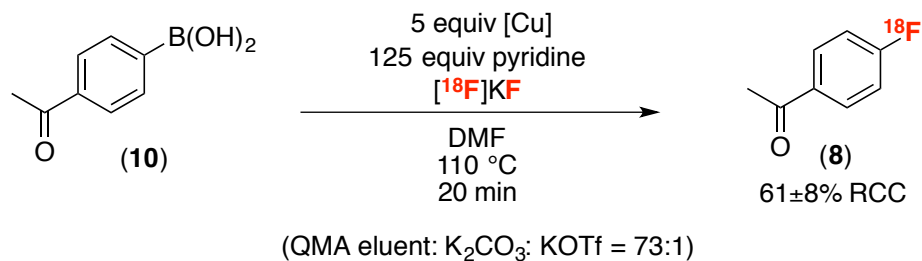
Table 4.5 Evaluation of Weak Ionic bases/acids for ¹⁸F-Fluoride Elution

Entry	QMA Eluent	Concentration (M) ^a	[¹⁸ F]Recovery
1	K ₂ CO ₃	0.025	97%
2	KOTf	0.109	97%
3	NH ₄ OTf	0.170	93%
4	NH ₄ Cl	7.00	>99%
5	TBACl	1.75	96%
6	PPTS ^b	0.111	76%

^aWater was used for solvent. ^bPPTS = Pyridinium *p*-Toluene Sulfonate.

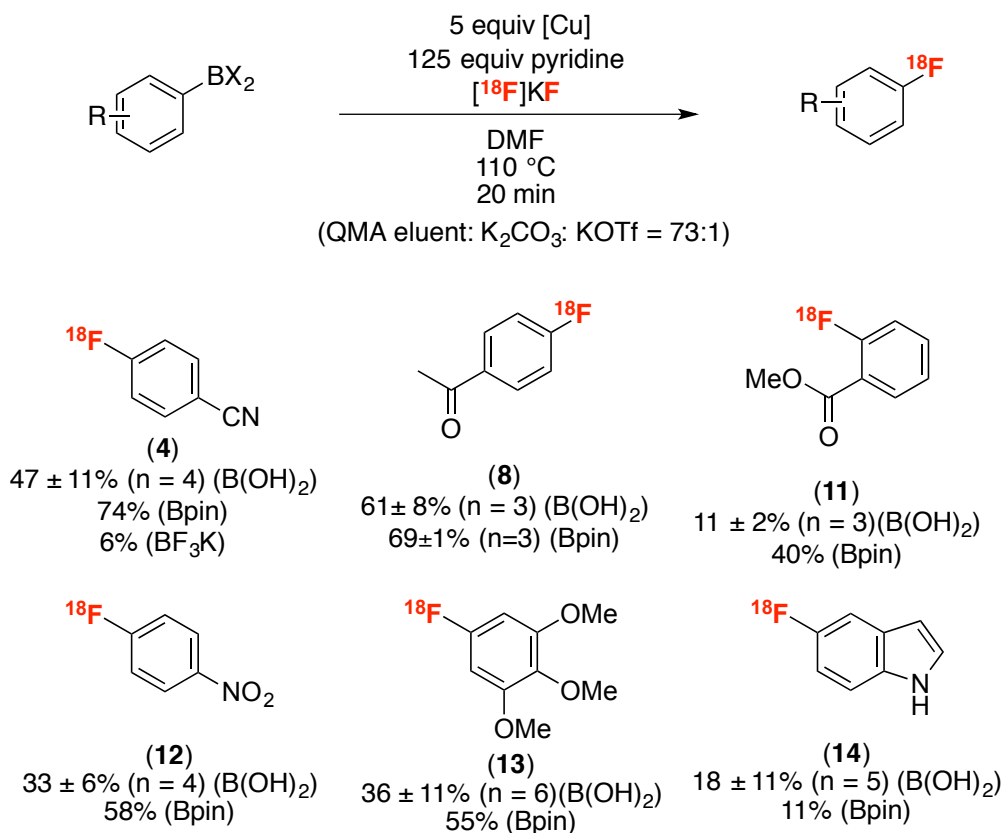
*Application of New Elution Method.*²³ Neumaier has shown that the use of large quantities of strongly basic K_2CO_3 to elute $^{18}F^-$ from quaternary methyl ammonium (QMA) ion cartridges can be problematic for downstream copper-mediated radiofluorination reactions.²⁴ As such, minimization or elimination of K_2CO_3 from the eluent was considered as the optimal method by which to ensure greater yields in this reaction. Given the importance of pyridine in these reactions,²⁰ elution with a solution of pyridinium *p*-toluenesulfonate (PPTS), was examined which gave 76% $^{18}F^-$ -recovery (Table 4.5). The eluted $^{18}F^-$ was then azeotropically dried and combined with $Cu(OTf)_2$, 4-acetophenylboronic acid, and pyridine in DMF. The reaction was heated at 110 °C for 20 minutes, after which time radio-TLC and radio-HPLC confirmed the formation of 4- $[^{18}F]$ fluoroacetophenone in 48±2% RCC (n = 2), which is a significant improvement versus elution with K_2CO_3 (Scheme 4.10). These key findings led into further optimization of the Cu-mediated radiofluorination of aryl boronic acids, which was conducted by Dr. Andy Mossine and Dr. Allen Brooks. It was identified that QMA eluent of $KOTf/K_2CO_3$ gives the optimal condition, affording the 4- $[^{18}F]$ fluoroacetophenone in 61±8% RCC. The combination of $KOTf/K_2CO_3$ (73:1) allowed significant decrease in the amount of K_2CO_3 (which may cause cross coupling reaction to take place) and eliminated the loss of radioactivity during the azeotropic drying procedure, as the absence of acidic proton sources precluded the formation of HF (Scheme 4.11). It was particularly surprising to observe product formation using boronic acids as precursors for nucleophilic radiofluorination, affording the comparable yield (70% RCC starting with **9**). It was initially predicted protons from $B(OH)_2$ might hydrogen bond to fluoride and shut down the nucleophilic radiofluorination reaction^{4,25} although boronic acids are successful substrates for distinctly electrophilic fluorinations such Ritter's Ag-catalyzed method.²⁶ This optimized conditions were successfully applied to synthesize a wide variety of electronically variant $[^{18}F]$ fluoroarenes in modest to good yields (shown 18 examples).²³

Scheme 4.11 Cu-mediated Radiofluorination of Aryl Boronic Acids



Application to Other Boron Reagents. With the optimized condition, we next decided to revisit pinacol boronate esters and potassium trifluoroborates, in order to include the generality of the new Cu method. The corresponding boron pinacol esters of **4**, **8**, **11-14** were prepared, and they were subjected to radiofluorination conditions by Dr. Andy Mossine and Dr. Allen Brooks. Using boronate esters, fluorinated products were formed in comparable yields to the boronic acid reactions (Figure 4.3). For example, the radiofluorination of **9** afforded product **8** in 69 ± 1% RCC (n = 3). Radiofluorination of aryltrifluoroborates also proceeded, albeit in low yields. For example, the radiofluorination of **3** yielded **9** in up to 6% RCC. As identified in the preliminary study, aryltrifluoroborates are less desirable as radiofluorination precursors due to the potential for isotopic exchange (see Table 4.2 for early studies). Notably, the new QMA elution method and addition of stoichiometric pyridine and Cu(OTf)₂ enabled the radiofluorination of boron pinacol esters while the stoichiometric amount of (py)₄Cu(OTf)₂ did not work in the Gouverneur's method.

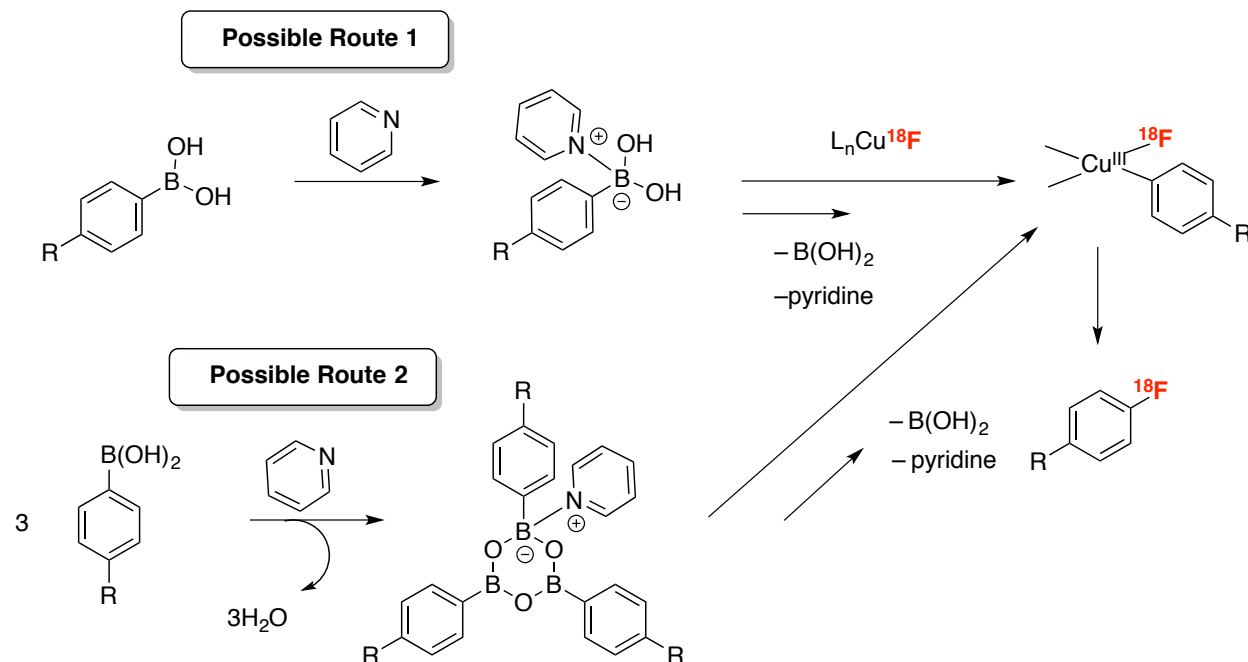
Figure 4.3 Cu-mediated Radiofluorination of Other Boron Reagents



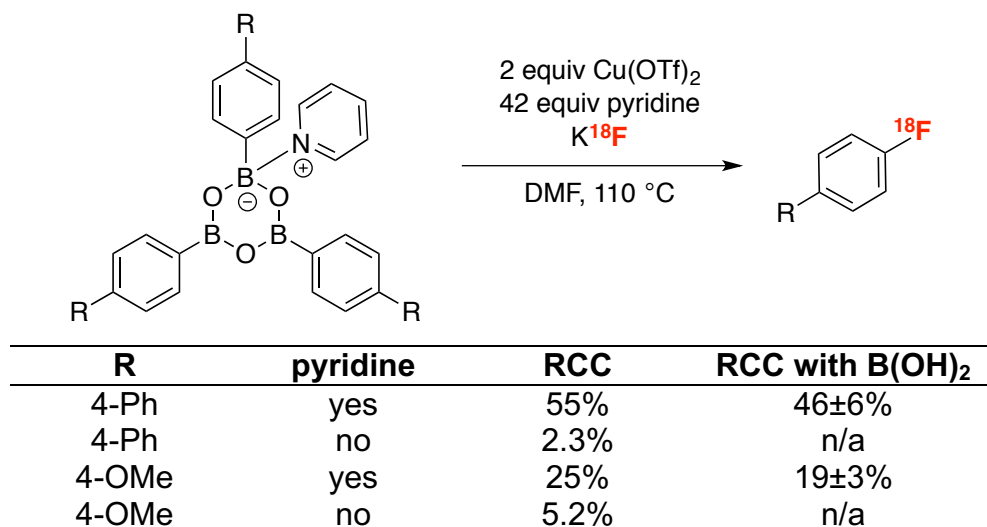
Role of Pyridine. Addition of pyridines to the reaction was found to be critical for this radiofluorination, as we observe that the reaction does not occur in the absence of pyridine. There could be several possible roles of pyridine in the reaction, including as a ligand, solvent, or in the activation of the Csp₂-B bond by coordinating to the boron center to form a tetracoordinate boron species that accelerates the transmetalation step (possible route 1, Scheme 4.12). In 1958, Snyder and colleagues reported the synthesis of a 1:1 complex between triphenylboroxine and pyridine, (PhBO)₃·pyridine, and proposed that the coordination of the pyridine occurs at one boron atom within the B₃O₃ ring.²⁷ Dakternieks and coworkers revisited the synthesis of (PhBO)₃·pyridine and reported full details of its molecular structure with crystallographic data of the compound.²⁸ Furthermore, commercial boronic acid samples come as a mixture of boronic acid and the corresponding boroxines.²⁹ Well-defined (ArBO₃)·pyridine complexes were synthesized and tested under the optimal radiofluorination conditions

to examine if the reaction undergoes boroxine intermediates to generate desired [^{18}F]fluoroarenes (possible route, Scheme 4.12).

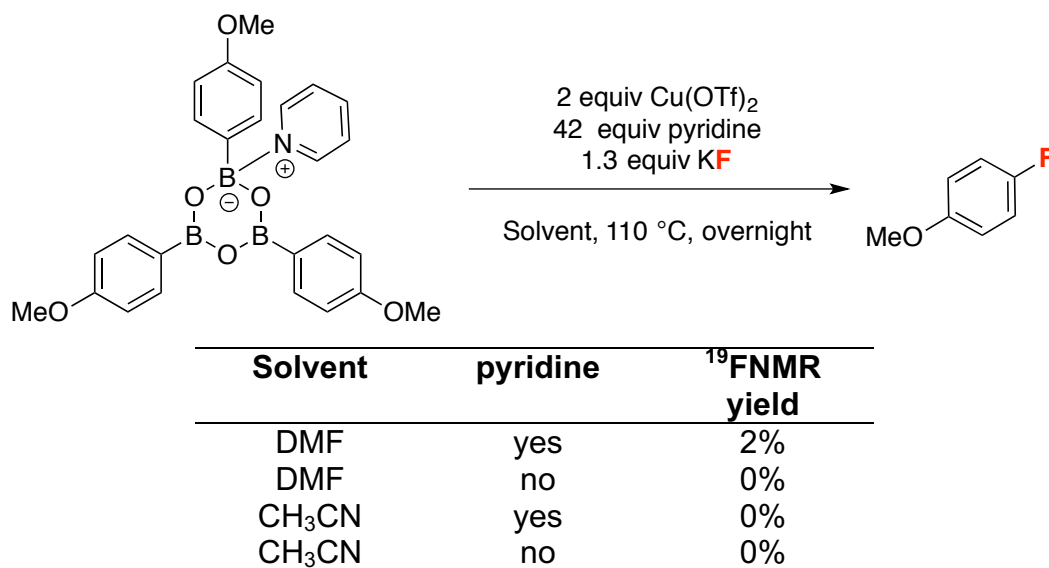
Scheme 4.12 Possible Roles of Pyridine in the Cu-Mediated Radiofluorination



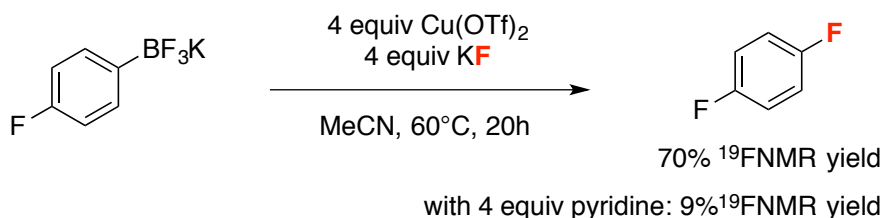
Both the biphenyl and 4-methoxyphenyl boroxines afforded higher yields (55% and 25% respectively) than those with the corresponding boronic acids in the presence of 42 equivalents of pyridine as an additive. However, the exclusion of the pyridine additive resulted in a steep decrease in the yields of the products (2.3% and 5.2%, respectively). The role of pyridine in this protocol is therefore still inconclusive, as it was originally hypothesized that pyridine was only required to form the reactive boroxine complex *in situ*. Further mechanistic studies are required to shed light on the mechanism. For instance, analyzing the reaction mixture after the radiofluorination to understand by-product distributions would provide important information about the roles of each reagent in this reaction.

Table 4.6 Radiofluorination of Aryl Boroxines

In addition, the radiofluorination of (ArBO)₃·pyridine was translated to ¹⁹F-fluorination using (4-OMePhBO₃)·pyridine under an inert atmosphere (Table 4.7). 4-fluoroanisole was generated in 2% yield in the presence of pyridine and Cu(OTf)₂ in DMF. In contrast, the reaction in CH₃CN did not proceed, which agrees well with our previous findings, where the addition of pyridines in the cold fluorination of aryl trifluoroborates in acetonitrile solvent decreased the yield significantly (Scheme 4.13).³⁰

Table 4.7 Cu-Mediated Fluorination of Aryl Boroxines

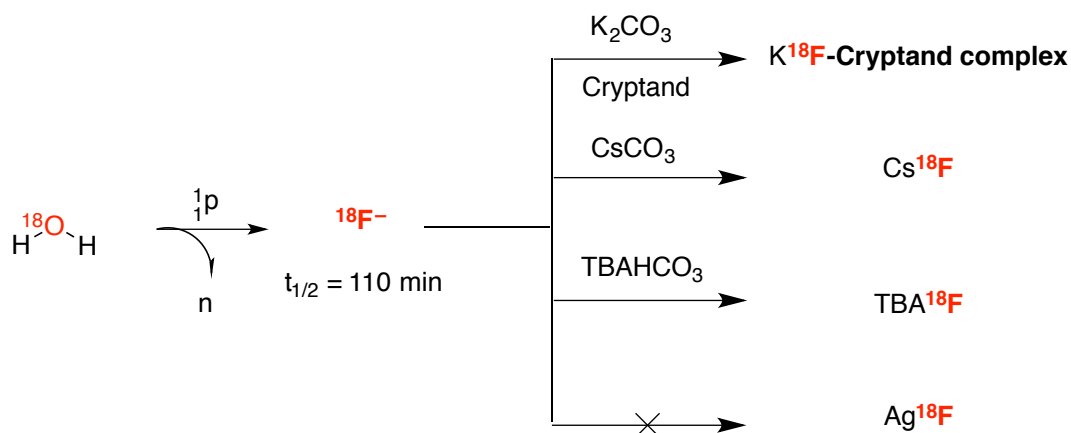
Scheme 4.13 Cu-Mediated Fluorination of Aryl Trifluoroborates



In summary, this part of Chapter 4 has detailed a mild and general Cu-mediated method for the radiofluorination of organoboron compounds with K^{18}F . Alternate QMA eluents ($\text{KOTf}/\text{K}_2\text{CO}_3$) enabled highly reproducible Cu-mediated reactions. This method represents the first high yielding nucleophilic fluorination of boronic acids (using ^{18}F or ^{19}F), is compatible with aryl, heteroaryl and vinyl boronic acids, and thus fills an important gap in the late-stage fluorination space. The method is also suitable for the radiofluorination of boronate esters and potassium trifluoroborates. Finally, this process can be automated on a commercial radiochemistry synthesis module and applied to clinically relevant radiotracers, such as $[\text{}^{18}\text{F}]\text{FPEB}$, synthesized by Katarina Makaravage. Validation of the method for cGMP clinical production of $[\text{}^{18}\text{F}]\text{FPEB}$ and other radiotracers is currently under investigation.

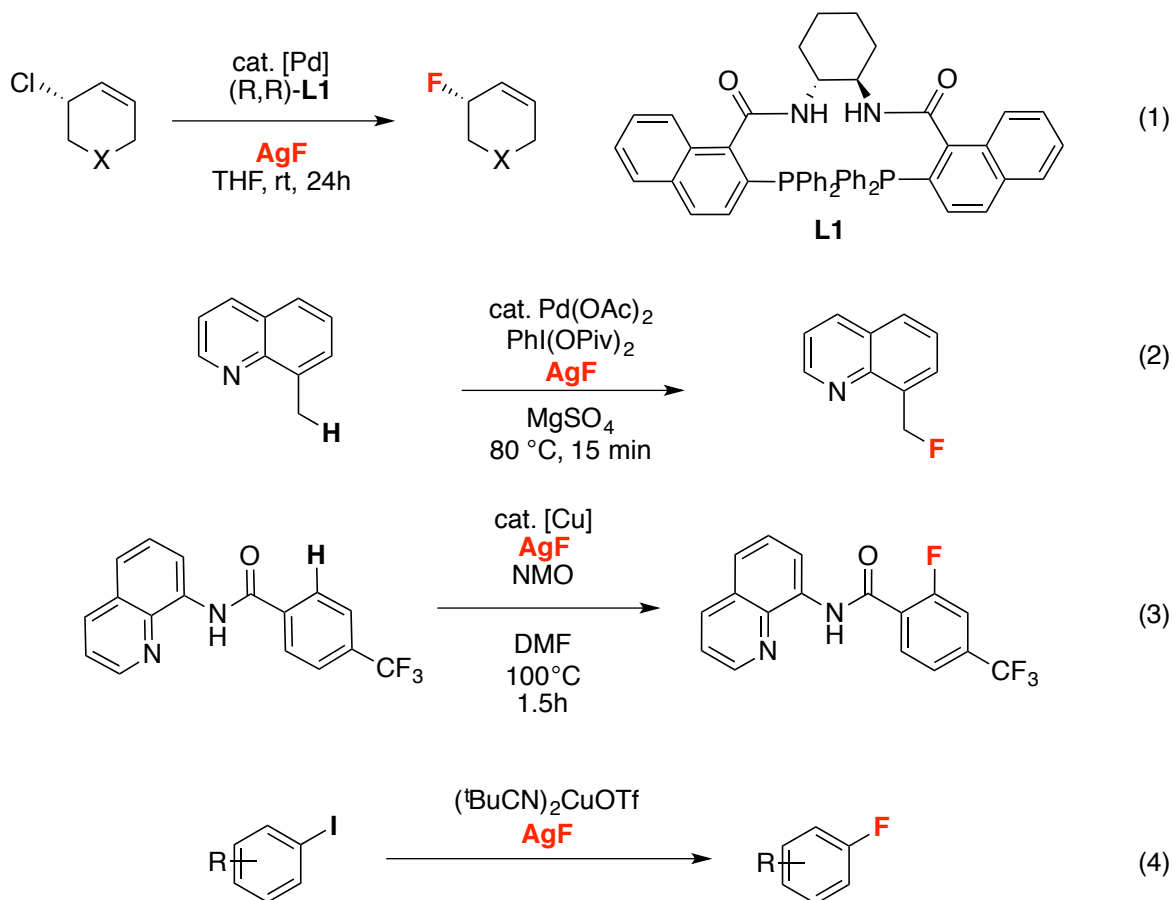
Exploration of Ag^{18}F Chemistry. This part of Chapter 4 describes investigations into the development of an operationally simple preparation of anhydrous Ag^{18}F . Herein, the work detailed was performed in collaboration with Dr. Allen Brooks and Katarina Makaravage. Over the past few decades, there have been sporadic examples where Ag and/or $\text{Ag}[\text{}^{18}\text{F}]$ have been employed to promote the ^{18}F -fluorination of bioactive molecules. The synthesis of Ag^{18}F has been known since 1973, but an operationally simple method to produce Ag^{18}F has still not been realized.³¹ Most of the reported examples use specialized equipment (e.g. platinum reaction vessels,^{31a} custom cyclotron targets) or insoluble silver sources (Ag_2O ,^{31c-e} Ag_2CO_3 ,^{31e} silver wool^{31f}) that are not readily adaptable to automated radiosynthesis modules. A synthetically useful method for preparing $\text{Ag}[\text{}^{18}\text{F}]$ using the ion exchange (QMA) techniques employed in modern radiochemistry has not been reported. We have initiated preliminary efforts to address this gap.

Figure 4.4 Available Automated Nucleophilic [^{18}F]fluoride

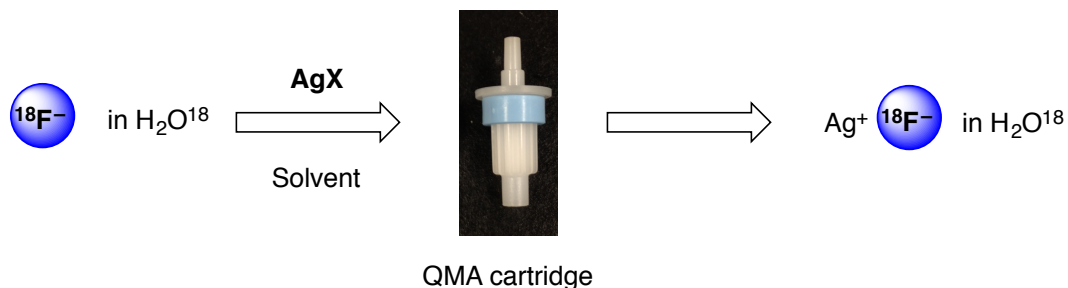


Development of an operationally simple Ag^{18}F synthesis method is expected to allow the translation of a number of recently reported fluorination reactions using Ag^{18}F . There has been a series of seminal reports on transition metal catalyzed fluorinations using Ag^{18}F as a fluorinating reagent (Scheme 4.14). Such robust nucleophilic fluorinating reagents opens up possibility for investigating the corresponding radiofluorinations, including Pd-catalyzed asymmetric allylic fluorination (eq 1),³² Pd-catalyzed benzylic C–H fluorination (eq 2),³³ Cu-catalyzed $\text{C}_{\text{aryl}}\text{–H}$ fluorination (eq 3)³⁴ and Cu-catalyzed fluorination of aryl iodides (eq 4).³⁵

Scheme 4.14 Fluorination Protocols with AgF



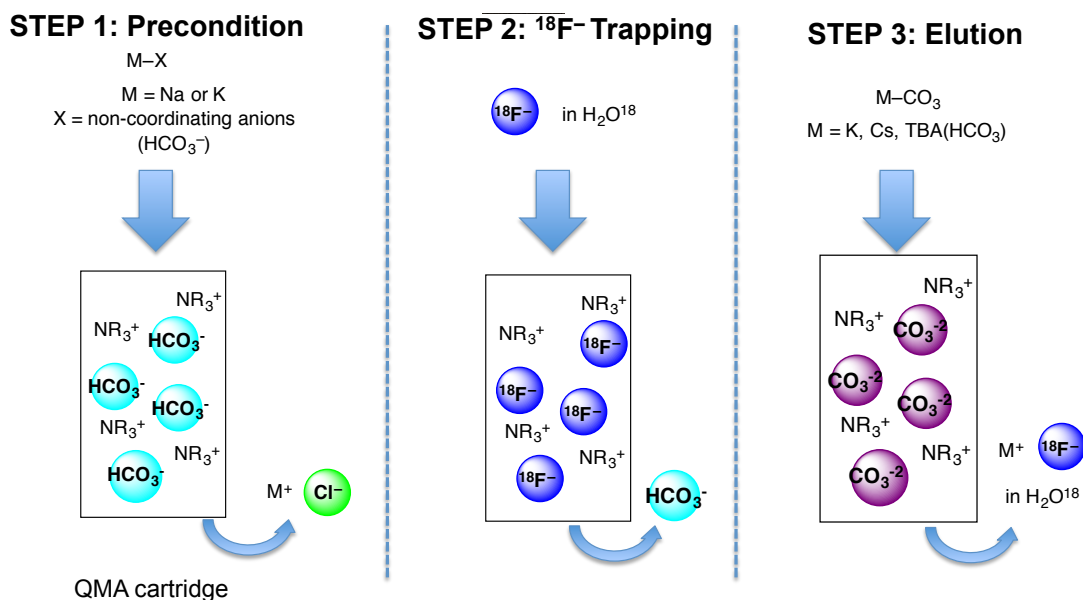
Ag¹⁸F Elution Method. The standard approach to prepare K¹⁸F is to pass a solution of ¹⁸F⁻ in H₂¹⁸O through a quaternary ammonium Sep-Pak cartridge. The ¹⁸F⁻ is trapped on the cartridge, and is subsequently eluted with aqueous K₂CO₃ to generate K¹⁸F (Table 4.8). Although a similar approach with Ag₂CO₃ for Ag¹⁸F preparation was unsuccessful (entry 2), replacing Ag₂CO₃ with water-soluble AgOAc, AgBF₄, AgOTf, AgNO₃ and (CH₃CN)₄AgBF₄ resulted in the formation of Ag¹⁸F in 95-99% of ¹⁸F⁻ recovery (Table 4.8, entry 4-8). A problem that was quickly identified was that once elution is complete, the filtrate is a heterogeneous mixture, which would cause problems for automated synthesis. This was tracked to the bicarbonate counterion associated with the QMA resin, which was leading to the formation of AgHCO₃ particulate during the elution process.

Table 4.8 Synthesis of Ag^{18}F 

Entry	QMA eluent	solvent	[^{18}F]Recovery (%)
1	K_2CO_3	H_2O	97
2	Ag_2CO_3	H_2O	0
3	AgOTf	CH_3CN	0
4	AgOAc	H_2O	97
5	AgBF_4	H_2O	99
6	AgOTf	H_2O	98
7	AgNO_3	H_2O	95
8	$(\text{CH}_3\text{CN})_4\text{AgBF}_4$	H_2O	88

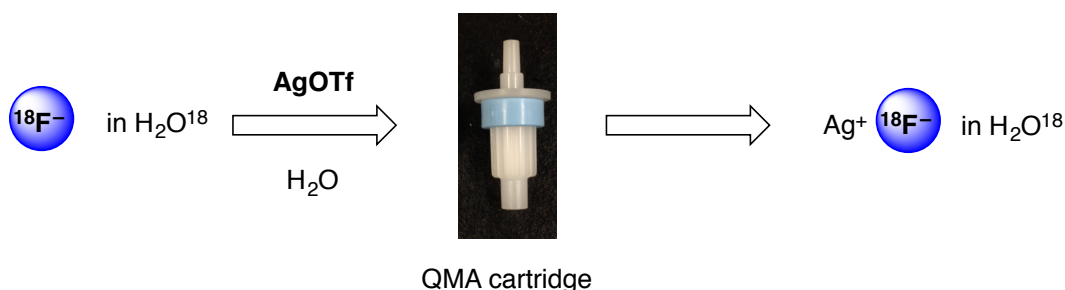
As such, we turned our attention to revising the preconditioning method. QMA cartridges contain chloride as the counterion to the quaternary ammonium resin. This is a problem, as chloride can often behave analogously to fluoride in reactions, which leads to the formation of an impurity that is largely inseparable from the fluorinated radiotracer. As such, chloride needs to be removed/exchanged for another counterion prior to trapping $^{18}\text{F}^-$. To do so, the QMA is typically pre-conditioned with NaHCO_3 solution in order to displace chlorides with bicarbonate ions (STEP 1, in Figure 4.5). Bicarbonate is weakly basic and also in equilibrium with carbonate, so we sought to identify an alternative salt in order to avoid any carbonates/bicarbonates that could cause precipitation of Ag^+ .

Figure 4.5 Diagram of QMA and Standard Operating Procedure



Hence, KNO_3 , KOTf , KOAc and NaBF_4 were evaluated for preconditioning of the QMA cartridge. All showed similar $^{18}\text{F}^-$ recovery 94-98% (entry 1-3, Table 4.9) except for NaBF_4 (40% $^{18}\text{F}^-$ recovery), possibly due to isotopic exchange with the fluoroborate counterion. To directly test Ag^{18}F with the existing Cu method, KOTf was chosen for preconditioning, as copper triflate salts were utilized for its optimized condition.

Table 4.9 Preconditions of QMA Cartridge for Ag^{18}F Synthesis

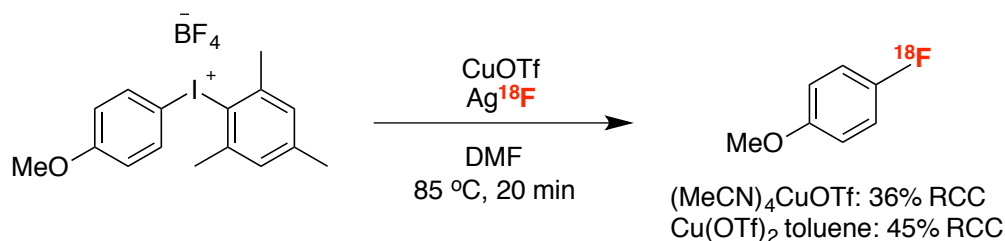


Entry	Salt for Precondition	^{18}F Recovery (%)
1	KNO_3	98
2	KOTf	94
3	KOAc	96
4	NaBF_4	40

To confirm the formation of Ag^{18}F , this fluorinating reagent was subjected to the conditions used for Cu-mediated ^{18}F fluorination of iodonium salts. To our delight, the

reaction provided 36% RCC of 4-[^{18}F]fluoroanisole (Scheme 4.15). This result suggests that we have successfully established a practical Ag^{18}F synthesis.

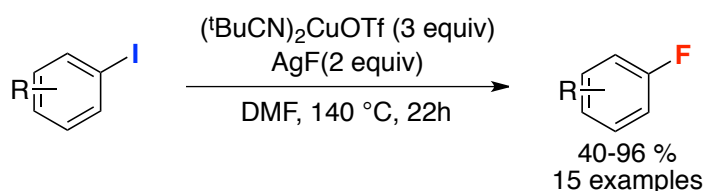
Scheme 4.15 Cu-Mediated [^{18}F]fluorination of (mesityl)(aryl)iodonium Tetrafluoroborates with Ag^{18}F



Cu-mediated Fluorination of Aryl Iodides. Aryl iodides are ideal radiofluorination precursors, because they are indefinitely shelf-stable and can be synthesized using straightforward methods under mild conditions.³⁶ Furthermore, thousands of (hetero)aryl iodides are commercially available. However, despite the great potential utility of the nucleophilic radiofluorination of aryl iodides, this transformation has not, to our knowledge, been reported. The closest known reaction involves nucleophilic aromatic substitution ($\text{S}_{\text{N}}\text{Ar}$). However, the $\text{S}_{\text{N}}\text{Ar}$ fluorination of aryl halides is fundamentally limited to electron deficient precursors. The nucleophilic fluorination of electron rich aryl iodides remains an exceedingly challenging transformation even outside of the realm of radiochemistry.

To date, there is just a single reported example of this transformation. In 2012, Hartwig disclosed Cu-mediated fluorination of aryl iodides. This reaction requires an excess of AgF as the fluorinating reagent and a reaction time of 22 h (Scheme 4.16).³⁵

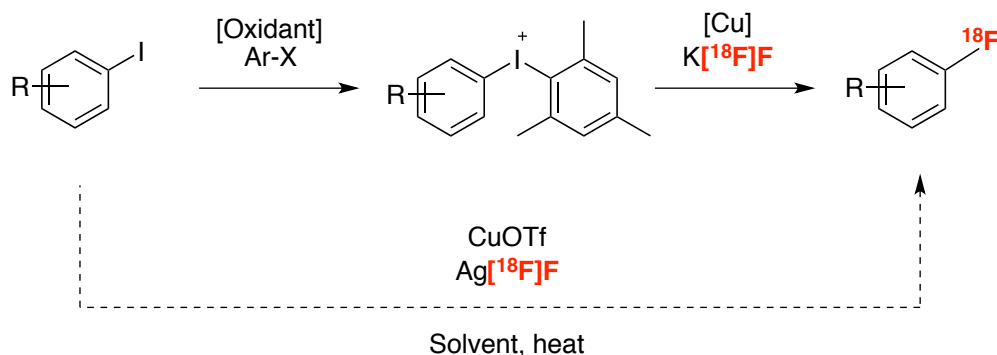
Scheme 4.16 Hartwig's Cu-mediated Fluorination of Aryl Iodides³⁵



Such methods also provide a direct route to ^{18}F fluoroarenes with Cu^{1+} , bypassing oxidation of the iodine center required for the previously disclosed iodonium chemistry (Scheme 4.17).³⁷ Inspired by the work above, our goal was to use Ag^{18}F as a fluoride

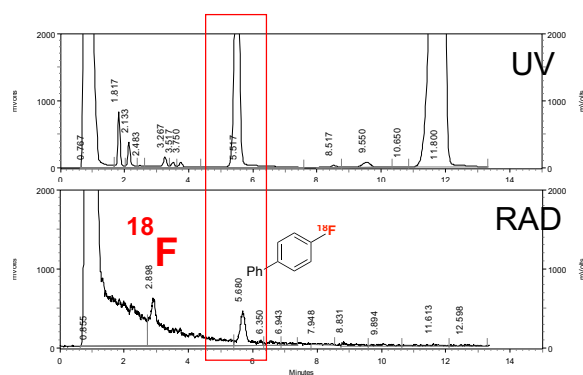
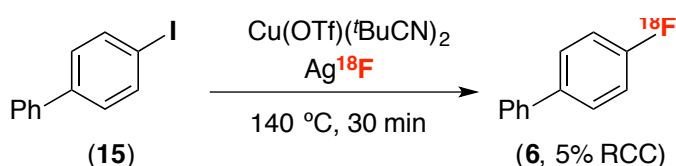
source for the Cu-mediated radiofluorination of aryl iodides. To translate this transformation into a practical radiofluorination, two challenges must be addressed. First, conditions must be developed that employ fluoride as the limiting reagent. Hartwig and his co-workers demonstrated that 1.0 equiv of AgF can be used for conversion of 4-iodobenzaldehyde to afford 75% yield, which suggests that Ag¹⁸F can be a limiting reagent for desired transformation. Second, the original fluorination requires 22 hours of reaction time; therefore we need to find a means to accelerate the reaction rate.

Scheme 4.17 Direct Access by Cu-mediated [¹⁸F]Fluorination with Ag¹⁸F



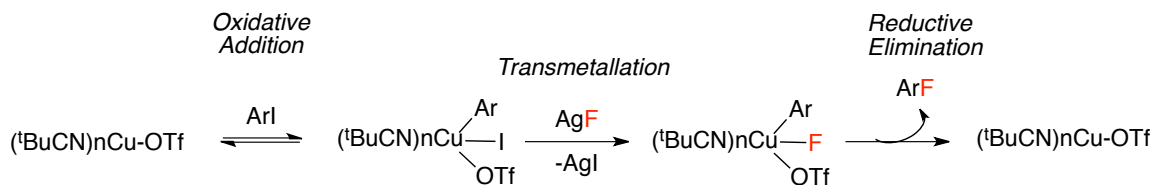
With an optimized synthesis of Ag¹⁸F in hand, we conducted preliminary experiments on the radiofluorination of 4-iodobiphenyl with Ag¹⁸F over a reaction time of 40 minutes. An initial screen of Cu salts revealed that the radiofluorination conducted at 14 mM in DMF, using a 3 :1 ratio of Cu(OTf)(*t*BuCN)₂ : **15** gave 5% RCC of 4-[¹⁸F]fluorobiphenyl **6** (Scheme 4.18). Carrier-added-fluorination (2 equiv AgF) did not improve the yield.

Scheme 4.18 Fluorination of **15** with Ag¹⁸F



Our efforts moving forward focused on further optimizing the radiofluorination of **15** with Ag¹⁸F, with the goal of achieving $\geq 50\%$ RCC. We hypothesize that the main reason for the modest RCCs is that the reaction is too slow to proceed to completion within 40 min. The original report proposed that oxidative addition of aryl iodides is the rate-limiting step (Scheme 4.19). Two strategies were considered in order to accelerate the reaction rate. First, we have evaluated different solvents with high boiling points to raise the reaction temperature. Second, a series of electron-rich ligands were evaluated for the Cu complex, as literature precedent suggests that oxidative addition should be fastest with electron rich Cu^I complexes.³⁸

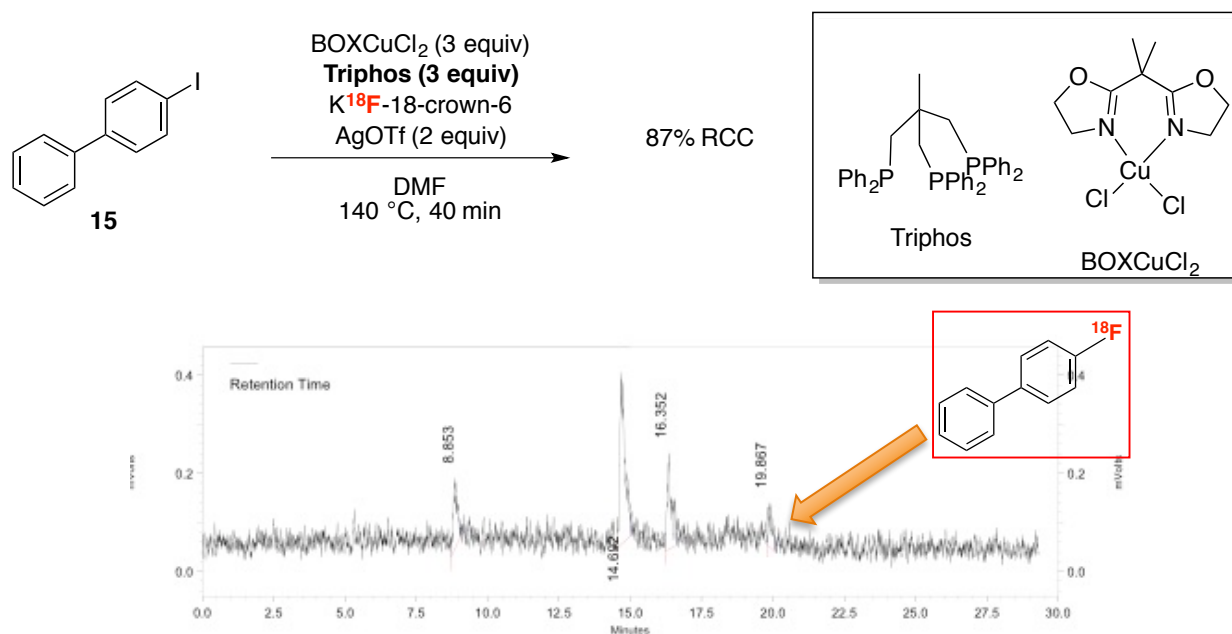
Scheme 4.19 Proposed Mechanism of Cu-mediated fluorination of Aryl Iodide



Unknown Stable M-¹⁸F Complexes. Both solvent screens and ligand screens were conducted and unknown large peaks were identified on radio-TLC in both cases. For instance, 87% of RCC of an unknown product was observed by radio-TLC when triphos was utilized with 3 equiv of BOXCuCl₂ (Figure 4.6). However, radio-HPLC showed multiple product peaks, and spiking with authentic sample confirmed that the 4-[¹⁸F]fluorobiphenyl product was a relatively minor product at 19.7 minutes (Figure 4.6).

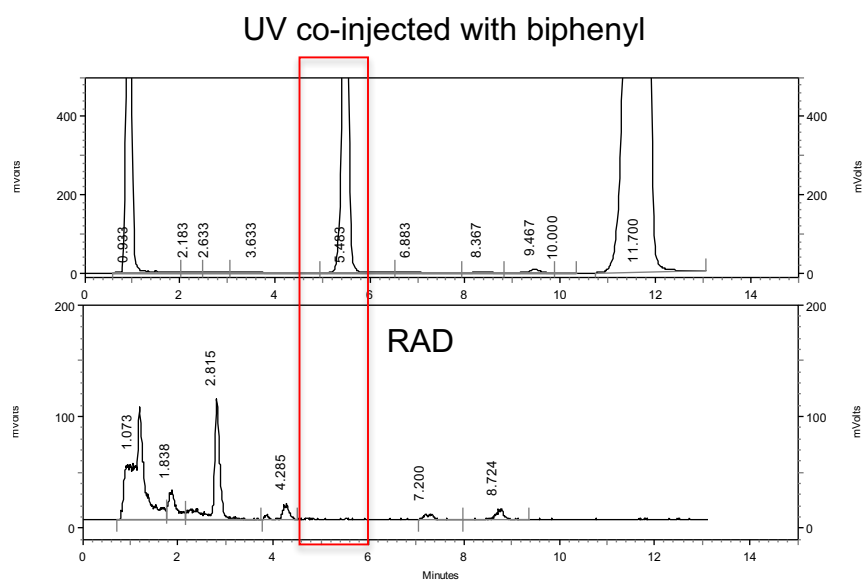
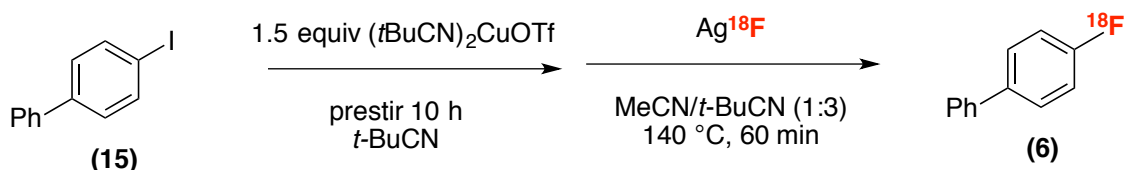
The identity of the major products is still unknown. Other ligands, including bis(oxazoline)s, bipyridines, diimines, NHCs, and phosphines were evaluated, but they led to either no yield or unproductive side product formation. Control studies revealed that those unknown peaks were formed in the absence of **15**. Therefore, it was hypothesized that an unknown stable $M-^{18}\text{F}$ complex was formed under these conditions.

Figure 4.6 Radiofluorination of 4-iodobiphenyl



Solvents were also screened, and several different classes of high-boiling-point solvents were evaluated towards fluorination of aryl iodides. When dioxane or *t*BuCN were utilized, unknown products were formed in greater than 50% RCC, according to radio-TLC. As shown in Figure 4.6, they were again not the desired products, as co-injection on HPLC revealed no product formation (Figure 4.7). Unfortunately, a current lack of diagnostic spectroscopic analysis for radioactive materials hindered our attempt to figure out the identity of the unknowns. However, it seems conclusive that Cu-mediated fluorination of aryl iodides is very slow (low yield <10% RCC) and stable $M-^{18}\text{F}$ complexes were detected within the first 60 minutes of these reactions.

Figure 4.7 Radiofluorination of **15** in *t*BuCN/CH₃CN



In summary, the second part of this chapter has described our attempts at translating Hartwig's Cu-mediated fluorination of aryl iodides. It is the first example that demonstrated that radiofluorination of aryl iodides is possible in the presence of superstoichiometric Cu and Ag¹⁸F. The formation of the desired product was observed in Cu-mediated radiofluorination of iodonium salts, albeit lower yield than that reported previously (Scheme 4.16).³⁷ This may suggest that optimization of the azeotropic drying procedure is required in order to eliminate adventitious water from the reaction, considering Ag¹⁸F may exist as hydrate complexes.

4.3 CONCLUSIONS

In summary, Chapter 4 describes efforts toward developing Cu-mediated radiofluorinations of aryl boronic acids and aryl iodides. New elution methods were developed for each protocol as a means to produce effectively dry metal [^{18}F]fluoride. Aryl boronic acids were successfully radiofluorinated in the presence of $\text{Cu}(\text{OTf})_2$ and pyridine, and this method is highly reproducible and uses all commercially available reagents to conduct the reaction. Importantly, pyridine was not used in the cold chemistry but is essential for this radiofluorination protocol. A practical, rapid synthesis of Ag^{18}F was established, and it was used in Cu-mediated radiofluorination of aryl iodides. However, to date, the yields of this transformation remain low. Application of Ag^{18}F into other protocols is worth considering.

4.4 PERSPECTIVE AND OUTLOOK

The radiofluorination of boronic acids has already proven highly reproducible at other PET facilities, and we will continue to improve the scope of the chemistry as well as elucidate the mechanism of the protocol. Our investigations on the radiofluorination of aryl boronic acids revealed the necessity of pyridine in the reaction. The preliminary results (such as boroxine chemistry) did not give conclusive data to elucidate the role of pyridine in the reaction. Hence, a key focus of future research will be to gain a detailed mechanistic understanding of the role of this additive in order to further optimize the reaction. Boronic acids are widely commercially available and byproducts of the reaction were readily separable by HPLC (even protodeborated products of simple precursors). For Ag^{18}F chemistry, though, translation to the Cu-mediated [^{18}F]fluorination of aryl iodides was shown to be challenging. However, this Ag^{18}F chemistry could potentially be applicable to other fluorination methods in the literature, some examples of which are shown, but not limited to, in Scheme 4.15.

4.5 EXPERIMENTAL

Instrumental Information: NMR spectra were obtained on a Varian MR400 (400.52 MHz for ^1H ; 100.71 MHz for ^{13}C ; 376.87 MHz for ^{19}F), a Varian VNMRS 500 (500.10 MHz for ^1H), or a Varian VNMRS 700 (699.76 MHz for ^1H ; 175.95 MHz for ^{13}C) spectrometer. ^1H and ^{13}C NMR chemical shifts are reported in parts per million (ppm) relative to trimethylsilane (TMS), with the residual solvent peak used as an internal reference. ^{19}F NMR spectra are referenced based on an internal standard, 1,3,5-trifluorobenzene (-110.00 ppm). ^1H and ^{19}F multiplicities are reported as follows: singlet (s), doublet (d), triplet (t), quartet (q), and multiplet (m). High performance liquid chromatography (HPLC) was performed using a Shimadzu LC-2010A HT system equipped with a Bioscan B-FC-1000 radiation detector. Radio-TLC analysis was performed using a Bioscan AR 2000 Radio-TLC scanner with EMD Millipore TLC silica gel 60 plates (3.0 cm wide x 6.5 cm long).

Material and Methods Boronic acid precursors were purchased from Frontier Scientific, Oakwood Products and Sigma Aldrich and used as received. B(pin)-PEB³⁹ and B(OH)₂-PEB were prepared according to the literature procedure. Unless otherwise stated, reagents and solvents were commercially available and used without further purification. Ethanol was purchased from American Regent. HPLC grade acetonitrile was purchased from Fisher Scientific. Anhydrous acetonitrile were purchased from Acros. Trimethylacetone was purchased from Alfa Aesar and dried over mole sieves 4A. Sterile product vials were purchased from Hollister-Stier. QMA-light Sep-Paks were purchased from Waters Corporation. Boroxines were prepared according to the literature procedure.⁴⁰

Elution Studies. QMA-light Sep-Paks were flushed with 10 mL of ethanol followed by 10 mL of 0.5 M potassium triflate solution, and finally 10 mL of ultrapure water prior to use. [^{18}F]fluoride was trapped on a QMA cartridge and washed with dry CH_3CN (2-5 mL). The activity of QMA cartridge was recorded. Then [^{18}F]fluoride was eluted with a freshly prepared QMA eluent (1 mL total volume). After the elution, the remaining activity was recorded to calculate the ^{18}F -recovery.

Synthesis of K¹⁸F.

All loading operations were conducted under an ambient atmosphere. Argon was used as a pressurizing gas during automated sample transfers. Potassium [¹⁸F]fluoride was prepared using a TRACERLab FX_{FN} automated radiochemistry synthesis module (General Electric, GE). [¹⁸F]Fluoride was produced via the ¹⁸O(p,n)¹⁸F nuclear reaction using a GE PETTrace cyclotron (40 μA beam for 2-5 min generated ca. 150-375 mCi of [¹⁸F]fluoride). The [¹⁸F]fluoride was delivered to the synthesis module in a 1.5 mL bolus of [¹⁸O]water and trapped on a QMA-light Sep-Pak to remove [¹⁸O]water and other impurities. [¹⁸F]Fluoride was eluted into the reaction vessel using 550 μL of aqueous solution containing 5 mg potassium trifluoromethanesulfonate and 50 μg of potassium carbonate. One milliliter of acetonitrile was added to the reaction vessel, and the resulting solution was dried by azeotropic distillation to provide anhydrous K¹⁸F. Azeotropic drying/evaporation was achieved by heating the reaction vessel to 100 °C and drawing vacuum for 6 min. The reaction vessel was then subjected to an argon stream and simultaneous vacuum draw for an additional 6 min. Overall, 70% of activity remained after azeotropic drying (68 ± 9%, n=12; calculated from TRACERLab FX_{FN} reactor radiation detector by comparing activity before and after azeotropic drying). *N,N*-dimethylformamide (6 mL) was added to the dried reagent, and heated at 120 °C with stirring for 5 min. The resulting solution was cooled to 40 °C and was transferred to a sterile vial for subsequent use in reactions (% activity recovery into dose vial: 40 ± 10%, n=7; calculated by comparing activity of recovered solution by Capintec with final reading from TRACERLab FX_{FN} reactor radiation detector. As an example, approx. 80 mCi of prepared K¹⁸F in 6 mL DMF is isolated with a 5 min beam.

General Procedures for Manual Synthesis of ¹⁸F-labeled Compounds (activity of 500-1500 μCi per reaction) for Cu-mediated Radiofluorination of Boronic Acids.

Unless otherwise noted, this procedure was used for the synthesis of the [¹⁸F] fluorinated substrates described in Figure 1 of the main text. Stock solutions of boronic acid precursor (40 mM), copper (II) trifluoromethanesulfonate (200 mM), and pyridine (1 M) in DMF were prepared immediately prior to the start of the reaction. Aliquots of these solutions were used to carry out subsequent [¹⁸F]fluorination reactions. In a typical reaction, a 100 μL (20 μmol, 5 equiv) of copper (II) trifluoromethanesulfonate

aliquot was mixed with a 500 μL (500 μmol , 25 equiv) pyridine aliquot in a colorless borosilicate 4 mL scintillation vial. The solution was briefly agitated using a vortex shaker (Barnstead® Thermolyne Type 16700), then a 100 μL (4 μmol , 1 equiv) aliquot of boronic acid precursor was added. The reaction vial was sealed under an atmosphere of ambient air with a PTFE/Silicone septum cap, and a 100-300 μL aliquot of K^{18}F (150-3000 μCi , depending on the time required for HPLC analysis) was added to the reaction vial through the septum via a syringe. Additional anhydrous DMF was also added (as required) to bring the total solution volume to 1000 μL . The vial was then heated in an aluminum block (Chemglass Part# CG-1991-04) without stirring at 110 $^{\circ}\text{C}$ for 20 min. After 20 min, the reaction was allowed to cool to room temperature. Radio-TLC analysis was conducted to determine radiochemical conversion (RCC %). Crude reaction mixture was spotted onto standard silica coated glass plates and developed with 1:1 hexane/ethyl acetate in a glass TLC chamber. The RCC was determined by dividing the integrated area under the fluorinated product spot by the total integrated area of the TLC plate. To prepare samples for HPLC analysis, 50 μL of the reaction mixture was mixed with 50 μL acetonitrile or spiked with 50 μL of 1 mg/mL fluorinated standard solution in acetonitrile. Eluent systems and columns used for HPLC analysis are described below.

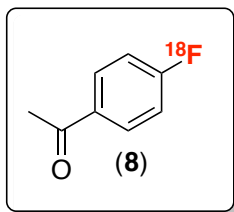
Synthesis of $[\text{}^{18}\text{F}]\text{AgF}$. All loading operations were conducted under ambient atmosphere. Argon was used as a pressurizing gas during automated sample transfers. silver $[\text{}^{18}\text{F}]\text{fluoride}$ was prepared using a TRACERLab FX_{FN} automated radiochemistry synthesis module (General Electric, GE). $[\text{}^{18}\text{F}]\text{fluoride}$ was produced via the $^{18}\text{O}(\text{p},\text{n})^{18}\text{F}$ nuclear reaction using a GE PETTrace cyclotron (40 μA beam for 2 min generated ca. 150 mCi of $[\text{}^{18}\text{F}]\text{fluoride}$). The $[\text{}^{18}\text{F}]\text{fluoride}$ was delivered to the synthesis module in a 1.5 mL bolus of $[\text{}^{18}\text{O}]\text{water}$ and trapped on a QMA-light Sep-Pak to remove $[\text{}^{18}\text{O}]\text{water}$. $[\text{}^{18}\text{F}]\text{fluoride}$ was eluted into the reaction vessel using aqueous silver triflate (10 mg in 1.0 mL of water). Acetonitrile (2 mL) was added to the reaction vessel, and the resulting solution was dried by azeotropic distillation to give dry $[\text{}^{18}\text{F}]\text{AgF}\cdot\text{AgOTf}$. Evaporation was achieved by heating the reaction vessel to 100 $^{\circ}\text{C}$ and drawing vacuum for 6 min. After this time, the reaction vessel was subjected to an argon stream and simultaneous vacuum draw for an additional 4 min. Finally, DMF (or solvent of reaction) (3 mL) was

added to the dried reagent, and the resulting solution was transferred to a sterile vial for subsequent use in reactions (approx. 30 mCi of prepared ^{18}F reagent was transferred).

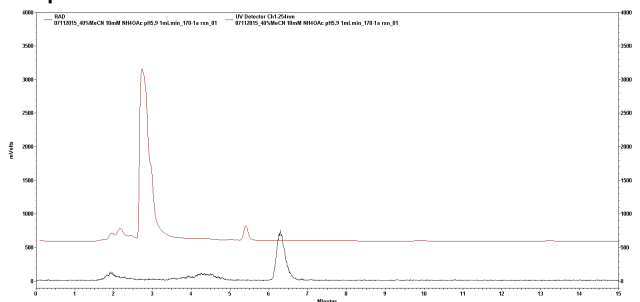
General Procedures for Manual Synthesis of ^{18}F -labeled Compounds (activity of 500-1500 μCi per reaction) of Radiofluorination of Aryl Iodides.

In a dry box, aryl iodide (1 μmol) and Cu salt (1.5 μmol , 1.5 equiv) was weighed into a 4 mL amber glass vial containing a stir bar and was then dissolved in DMF (300 μL). The reaction vial was sealed under an atmosphere of ambient air with a PTFE/Silicone septum cap. Via a syringe, a 100 μL aliquot of ^{18}F AgF (typically 500- 1500 μCi , prepared as described above) was added to the reaction vial. On a typical day, several reactions (4-20) were set up together. Due to this, the time of mixing and time of incubation at room temperature prior to heating varied slightly from day to day. However, the results of the radiofluorination appear to be insensitive to this variation. The vial was then heated in an aluminum block with stirring at 140 $^{\circ}\text{C}$ for 40 min. After 40 min, the reaction was allowed to cool to room temperature. The raw reaction mixture was used for radio-TLC analysis to obtain radiochemical conversions (RCC). In addition, a 100 μL aliquot of the reaction solution was used for radio-HPLC analysis by diluting the sample into MeCN (300 μL total volume). The RCC was determined by dividing the integrated area under the fluoroarene spot by the total integrated area of the TLC plate (see below for representative TLC traces). The RCC reported here do not reflect losses during the preparation of ^{18}F AgF.

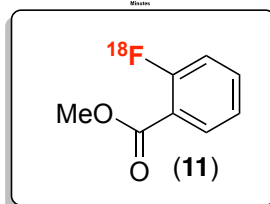
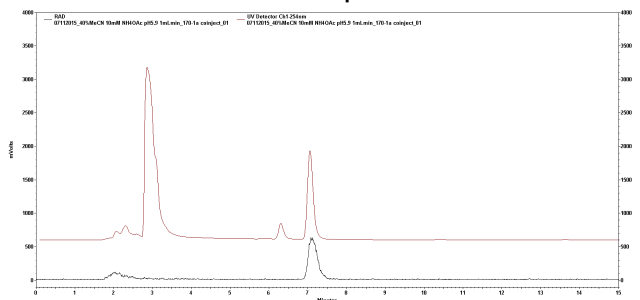
4.6 CHARACTERIZATION



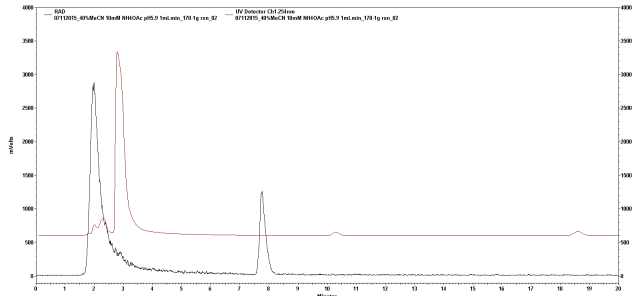
4-[¹⁸F]fluoroacetophenone **8** RAD trace overlaid with UV trace (256 nm)



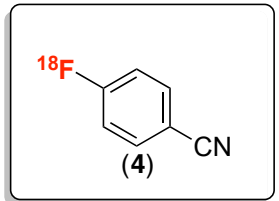
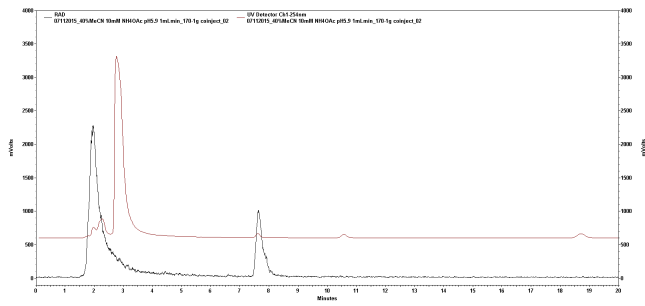
4-[¹⁸F]fluoroacetophenone **8** RAD trace overlaid with UV trace (256 nm) spiked with 4-fluoroacetophenone



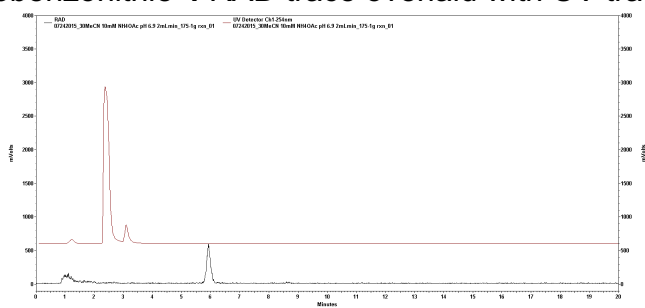
2-[¹⁸F]fluoromethylbenzoate **11** RAD trace overlaid with UV trace (256 nm)



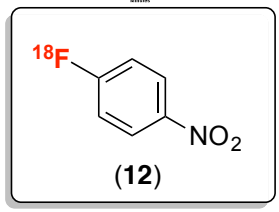
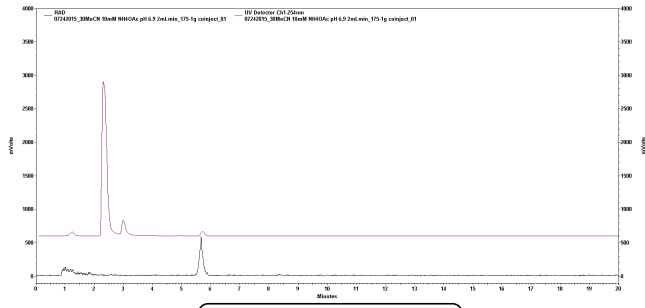
2-[¹⁸F]fluoromethylbenzoate **11** RAD trace overlaid with UV trace (256 nm) spiked with 2-fluoromethylbenzoate



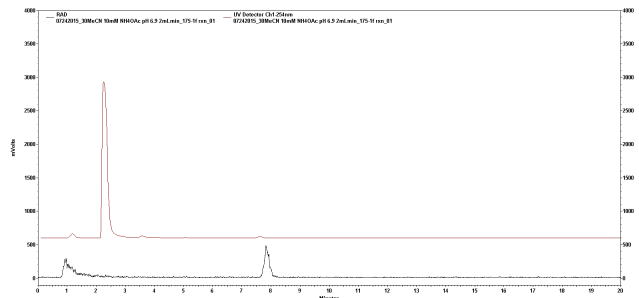
4-[¹⁸F]fluorobenzonitrile **4** RAD trace overlaid with UV trace (256 nm)



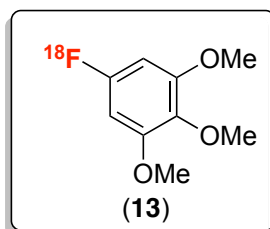
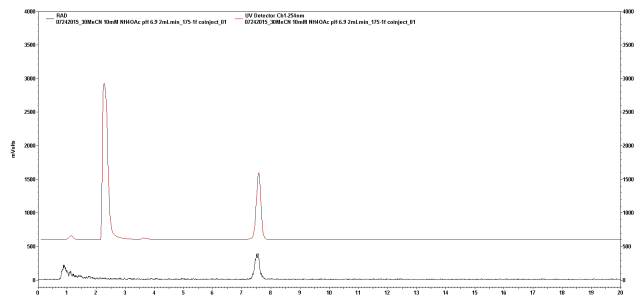
4-[¹⁸F]fluorobenzonitrile **4** RAD trace overlaid with UV trace (256 nm) spiked with 4-fluorobenzonitrile



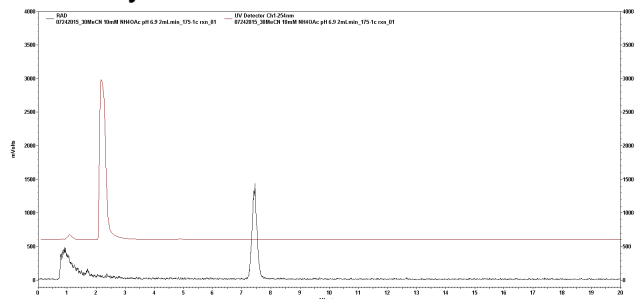
4-[¹⁸F]fluoronitrobenzene **12** RAD trace overlaid with UV trace (256 nm)



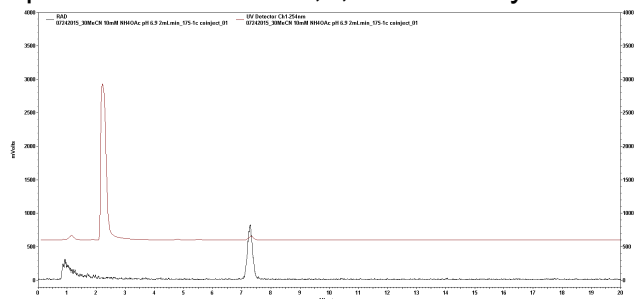
4-[¹⁸F]fluoronitrobenzene **12** RAD trace overlaid with UV trace (256 nm) spiked with 4-fluoronitrobenzene

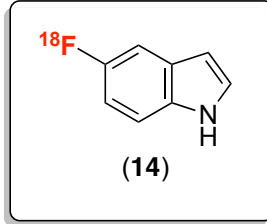


1-[¹⁸F]fluoro-3,4,5-trimethoxybenzene **13** RAD trace overlaid with UV trace (256 nm)

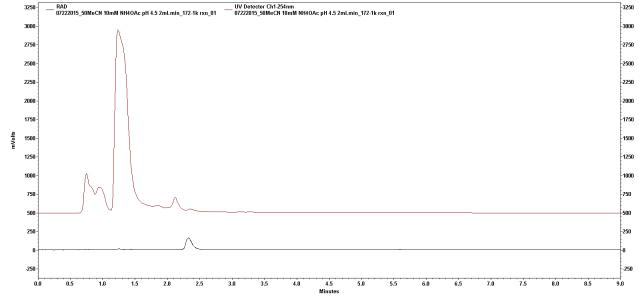


1-[¹⁸F]fluoro-3,4,5-trimethoxybenzene **13** RAD trace overlaid with UV trace (256 nm) spiked with 1-fluoro-3,4,5-trimethoxybenzene

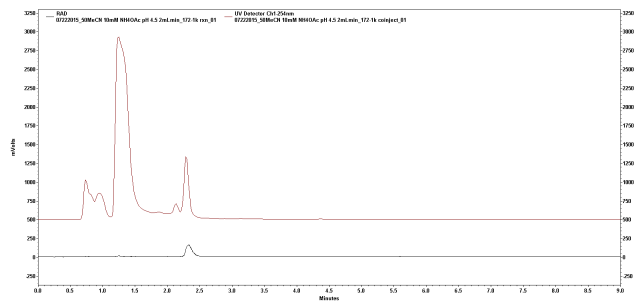




5-[¹⁸F]fluoroindole **14** RAD trace overlaid with UV trace (256 nm)



5-[¹⁸F]fluoroindole **14** RAD trace overlaid with UV trace (256 nm) spiked with 5-fluoroindole



4.7 REFERENCES

- (1) (a) Amatamey, S. M.; Honer, M.; Schubiger, P. A. *Chem. Rev.* **2008**, *108*, 1051. (b) Miller, P. W.; Long, N. J.; Vilar, R.; Gee, A. D. *Angew. Chem. Int. Ed.* **2008**, *47*, 8998.
- (2) (a) Finger, G. C.; Kruse, C. W. *J. Am. Chem. Soc.* **1956**, *78*, 6034. (b) Pleschke, A.; Marhold, A. Schneider, A M.; Kolomeit- sev; Röschenthaler, G.-V. *J. Fluorine Chem.* **2004**, *125*, 1031. (c) Sun, H.; DiMagno, S. G. *Angew. Chem.* **2006**, *118*, 2786; *Angew. Chem. Int. Ed.* **2006**, *45*, 2720.
- (3) Brooks, A. F.; Topczewski, J. J.; Ichiishi, N.; Sanford, M. S.; Scott, P. J. H. *Chem. Sci.* **2014**, *5*, 4545.
- (4) Ye, Y.; Schimler, S. D.; Hanley, P. S.; Sanford, M. S. *J. Am. Chem. Soc.* **2013**, *135*, 16292.
- (5) Fier, P. S.; Hartwig, J. F. *J. Am. Chem. Soc.* **2012**, *134*, 10795.
- (6) Hamacher, K.; Coenen, H. H.; Stocklin, G. *J. Nuc. Med.* **1986**, *27*, 235.
- (7) Feldman, K. S.; Bruendl, M. M.; Schildknecht, K. A.; Bohnstedt, A. C. *J. Org. Chem.* **1996**, *61*, 5440.
- (8) Copper-catalyzed cross coupling reactions: (a) Monnier, F.; Taillefer, M. *Angew. Chem. Int. Ed.* **2009**, *48*, 6954. (b) Evano, G.; Theunissen, C.; Pradal, A. *Nat. Prod. Rep.* **2013**, *30* (12), 1467.
- (9) (a) Kim, D. W.; Jeong, H. –J.; Lim, S. T.; Sohn, M. –H.; Katzenellenbogen, J. A. A.; Chi, D. Y. *J. Org. Chem.* **2008**, *73*, 957. (b) Kim, D. W.; Jeong, H. J.; Lim, S. T.; Sohn, M. H. *Angew. Chem.* **2008**, *120*, 8532.
- (10) Schimler, S. D.; Ryan, S. J.; Bland, D. C.; Anderson, J. E.; Sanford, M. S. *J. Org. Chem.* **2015**, *80*, 12137.
- (11) Watson, D. A.; Su, M.; Teverovskiy, G.; Zhang, Y.; Garcia-Fortanet, J.; Kinzel, T.; Buchwald, S. L. *Science* **2009**, *325*, 1661.
- (12) Ye, Y.; Schimler, S. D.; Hanley, P. S.; Sanford, M. S. *J. Am. Chem. Soc.* **2013**, *135*, 16292.
- (13) Lee, E.; Kamlet, A. S.; Powers, D. C.; Neumann, C. N.; Boursalian, G. B.; Furuya, T.; Choi, D. C.; Hooker, J. M.; Tobias, R. *Science* **2011**, *334*, 639.
- (14) Lee, E.; Hooker, J. M.; Tobias, R. *J. Am. Chem. Soc.* **2012**, *134*, 17456.
- (15) Unpublished Results. Discussion during Dow Meeting in November 2014.
- (16) Ichiishi, N.; Canty, A. J.; Yates, B. F.; Sanford, M. S. *Organometallics* **2014**, *33*, 5525.
- (17) Miyaura, N.; Suzuki, A. *Chem. Rev.* **1995**, *95*, 2457.
- (18) Graham, T. J. A.; Lambert, R. F.; Ploessl, K.; Kung, H. F.; Doyle, A. G. *J. Am. Chem. Soc.* **2014**, *136*, 5291.
- (19) Huang, X.; Liu, W.; Ren, H.; Neelamegam, R.; Hooker, J. M.; Groves, J. T. *J. Am. Chem. Soc.* **2014**, *136*, 6842.
- (20) Tredwell, M.; Preshlock, S. M.; Taylor, N. J.; Gruber, S.; Huiban, M.; Passchier, J.; Mercier, J.; Génicot, C.; Gouverneur, V. *Angew. Chem. Int. Ed.* **2014**, *53*, 7751.
- (21) U.S. Department of Health and Human Services Food and Drug Administration Center for Drug Evaluation and Research (CDER) “PET Drugs — Current Good Manufacturing Practice,” 2011.

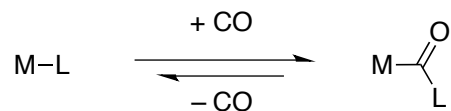
- <http://www.fda.gov/downloads/Dmgs/GuidanceComplianceRegulatoryInformation/Guidances/UCM266640.pdf> (accessed April 1, 2016)
- (22) Perez, D. I.; Palomo, V.; Pérez, C.; Gil, C.; Dans, P. D.; Luque, F. J.; Conde, S.; Martínez, A. *J. Med. Chem.* **2011**, *54*, 4042.
- (23) Mossine, A. V.; Brooks, A. F.; Makaravage, K. J.; Miller, J. M.; Ichiishi, N.; Sanford, M. S.; Scott, P. J. H. *Org. Lett.* **2015**, *17*, 5780.
- (24) Zlatopolskiy, B. D.; Zischler, J.; Krapf, P.; Zarrad, F.; Urusova, E. A.; Kordys, E.; Endepols, H.; Neumaier, B. *Chem. –Eur. J.* **2015**, *21*, 5972.
- (25) Ye, Y.; Sanford, M. S. *J. Am. Chem. Soc.* **2013**, *135*, 4648.
- (26) Furuya, T.; Tobias, R. *Org. Lett.* **2009**, *11*, 2860.
- (27) Snyder, H.R. Konecky, M.S. Lennarz, W. J. *J. Am. Chem. Soc.* **1958**, *80*, 3611.
- (28) Beckmann, J.; Dakternieks, D.; Duthie, A.; Lim, A. E. K.; Tiekink, E. R. T. *J. Organometallic Chem.* **2001**, *633*, 149.
- (29) Lennox, A. J. J.; Lloyd-Jones, G. C. *Chem. Soc. Rev.* **2013**, *43*, 412.
- (30) Unpublished Results
- (31) (a) Clark, J. C.; Goulding, R. W.; Palmer, A. J. *Radiopharm. Label. Compounds, Proc. Symp.* **1973**, *1*, 411. (b) Gatley, S. J.; Hichwa, R. D.; Shaughnessy, W. J.; Nickles, R. J. *Int. J. Appl. Radiat. Isot.* **1981**, *32*, 211. (c) Caires, C. C.; Guccione, S. US Patent 2010/0152502 A1. (f) Yagi, M.; Izsawa, G.; Murano, M. *Kakuriken Kenkyu Ho Koku (Research Report of Laboratory of Nuclear Science)*, **1981**, *14*, 62. (d) Gatley, S. J. *Int. J. Appl. Radiat. Isot.* **1982**, *33*, 255. (e) Shalom, E.; Takroui, K.; Metsuyanin, N.; Grufi, A.; Katzhendler, J.; Srebnik, M. *Appl. Radiat. Isot.* **2007**, *65*, 204.
- (32) Katcher, M. H.; Doyle, A. G. *J. Am. Chem. Soc.* **2010**, *132*, 17402.
- (33) McMurtrey, K. B.; Racowski, J. M.; Sanford, M. S. *Org. Lett.* **2012**, *14*, 4094.
- (34) Wu, T.; Yin, G.; Liu, G. *J. Am. Chem. Soc.* **2009**, *131*, 16354.
- (35) Fier, P. S.; Hartwig, J. F. *J. Am. Chem. Soc.* **2012**, *134*, 10795.
- (36) (a) Waldvogel, S. R.; Wehming, K. M.; “Product Subclass 2: Iodoarenes,” *Science of Synthesis*, Volume 31b Ramsden, C. (Ed.), Thieme, 2007, 235-273; (b) Waldvogel, S. R. “Iodoarenes,” *Science of Synthesis, Knowledge Updates*, Thieme, 2010 (Issue 1), 487-498.
- (37) Ichiishi, N.; Brooks, A. F.; Topczewski, J. J.; Rodnick, M. E.; Sanford, M. S.; Scott, P. J. H. *Org. Lett.* **2014**, *16*, 3224.
- (38) Hartwig, J. *Organotransition Metal Chemistry: From Bonding to Catalysis*. University Science Books: Sausalito, CA, 2010, p. 261-312.
- (39) (a) Telu, S. *et al.*, *Org. Biomol. Chem.*, **2011**, *9*, 6629. (b) Kil, K-E. *et al.*, *ACS Med. Chem. Lett.*, **2014**, *5*, 652. (c) Perttu, E. K. *et al.*, *Tetrahedron Lett.*, **2005**, *46*, 8753. (d) Tzschucke, C. C. *et al.*, *Org. Lett.*, **2007**, *9*, 761.
- (40) Beckmann, J.; Dakternieks, D.; Duthie, A.; Lim, A. E. K.; Tiekink, E. R. T. *J. Organometallic Chem.* **2001**, *633*, 149.

CHAPTER 5. PD-CATALYZED DECARBONYLATIVE CARBON-HETEROATOM BOND FORMATION

5.1 INTRODUCTION

Catalytic reactions involving carbon monoxide (CO) transfer via transition metals are important transformations in the field of organometallic chemistry. Migratory CO insertion is a key fundamental step that occurs at a number of transition metal centers in which CO inserts into a metal-ligand (M–L) bond to form a metal–acyl intermediate (Scheme 5.1).¹ This is a well-established process and widely utilized in a number of industrial-scale transformations such as hydroformylation,² the Fisher-Tropsch process,³ and the Monsanto process (Cativa process).⁴ In marked contrast, CO-deinsertion, the microscopic reverse of CO insertion, is much less utilized, in part, because the dissociation of CO from the metal center is generally slow⁵ due to strong π -backbonding from CO⁶ (Scheme 5.1).

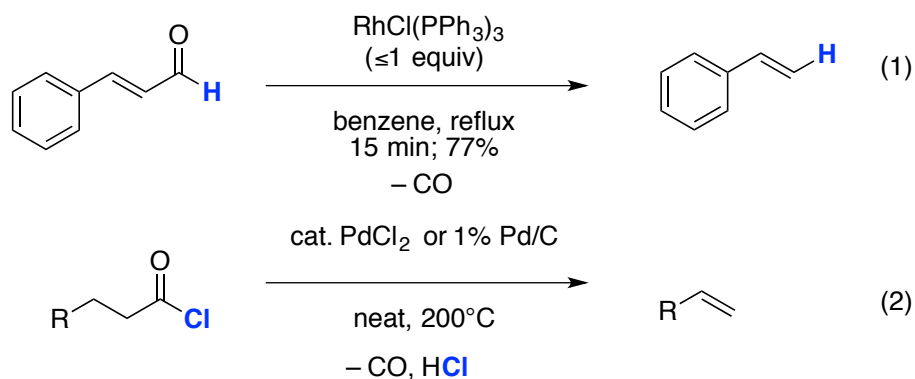
Scheme 5.1 CO-insertion vs. CO-deinsertion



Transition metal-catalyzed (mediated) decarbonylation reaction was first discovered by Tsuji and Ohno in 1965. The use of catalytic PdCl₂ or Pd/C⁷ and stoichiometric (PPh₃)₃RhCl (Wilkinson's catalyst) afforded the decarbonylation of aldehydes and acid chlorides (Scheme 5.2).⁸ Further studies found that numerous aliphatic, aromatic, and α,β -unsaturated aldehydes can be decarbonylated in good yields at or above room temperature in the substoichiometric amount of Wilkinson's catalyst.^{9,10} Further studies found that catalytic amounts of (PPh₃)₂(CO)RhCl could be used at elevated temperature

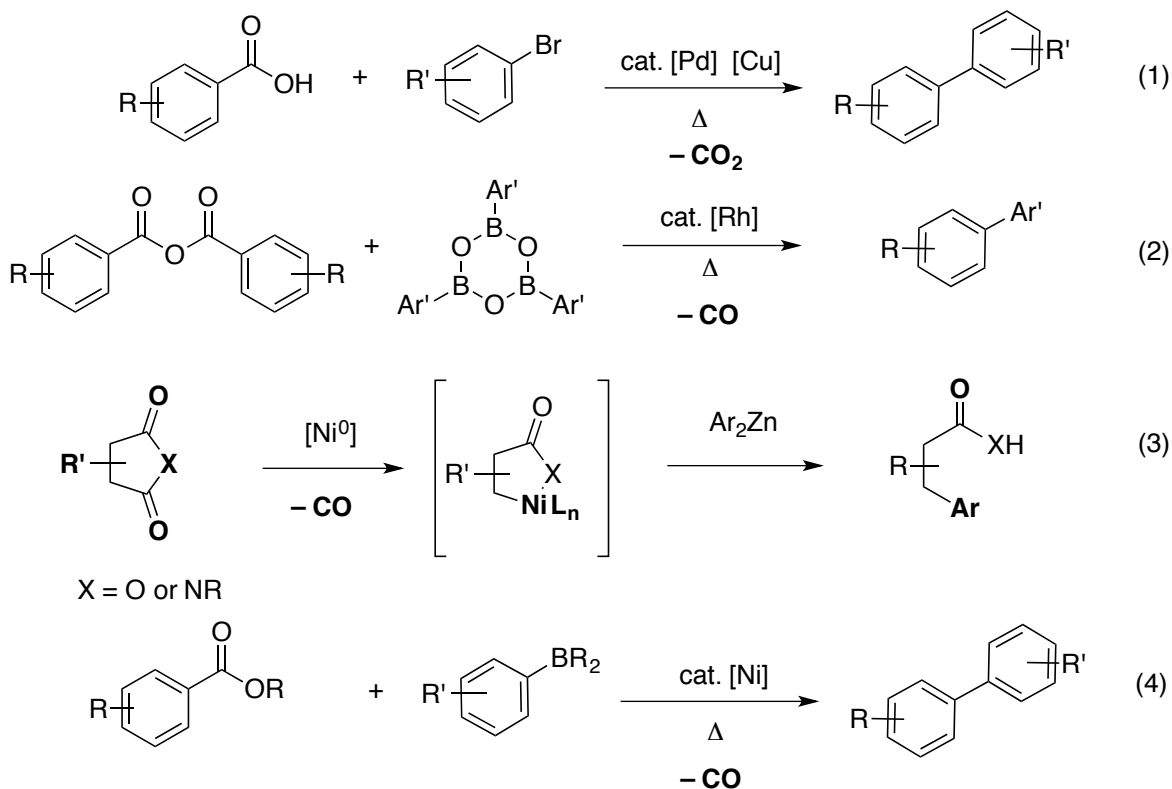
because carbon monoxide is released from the coordination sphere of the rhodium and the catalyst is regenerated.¹¹

Scheme 5.2 Decarbonylation of Aldehydes (eq. 1) and Acid Chlorides (eq.2)



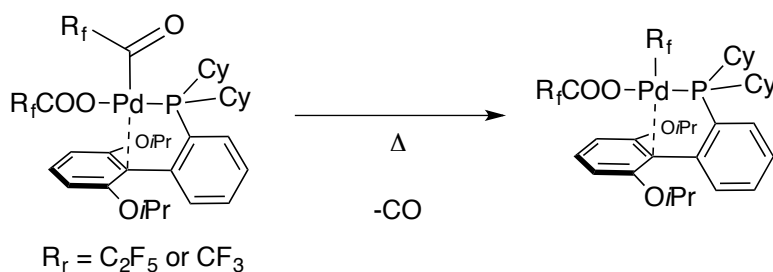
In recent years, there is a growing interest in the use of aroyl compounds in metal-catalyzed decarboxylative or decarbonylative coupling. For example, Gooßen employed a palladium-copper bimetallic catalytic system to achieve decarboxylative cross coupling of carboxylic acids and haloarenes (eq 1, Scheme 5.3).¹² Carboxylic acids are the most abundant functionality present in organic molecules and the use of such chemical feedstocks in transition metal catalysis is highly desired. Since then a number of decarboxylative and decarbonylative cross coupling reactions with aroyl compounds have been disclosed.¹³ Gooßen and Paetzoid reported the Rh-catalyzed decarboxylative cross coupling of arylcarboxylic anhydrides and aryl boroxines (eq 2).¹⁴ The stoichiometric studies were conducted on the decarbonylative coupling of diphenyl zinc and cyclic anhydrides or phthalimides to provide the corresponding decarbonylative arylation product (eq 3).^{15,16} More recently, Itami and coworkers have succeeded in Ni-catalyzed decarbonylative Suzuki-Miyaura coupling of esters and aryl boronic acids (eq 4).¹⁷ As such, modern examples of transition metal-catalyzed decarbonylation mainly focuses on the intermolecular reaction between aroyl compounds and nucleophiles/transmetalating reagents. In contrast, intramolecular examples of decarbonylative coupling remains still scarce.

Scheme 5.3 Decarboxylative and Decarbonylative Cross Coupling Reactions



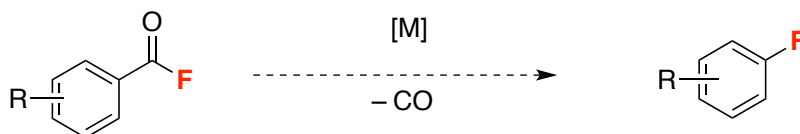
Based on the recent development in catalysis, we reasoned that careful tuning of a transition metal catalyst might further facilitate this challenging decarbonylation step thereby allowing Tsuji-Wilkinson type direct decarbonylative coupling under milder conditions. Notably, our lab demonstrated in 2014 that stoichiometric decarbonylation is feasible at a Pd^{II}(Ruphos) complex at 80 °C (Scheme 5.4).¹⁸

Scheme 5.4 Sanford's Decarbonylation at Pd^{II}(Ruphos)(R_fCOO)



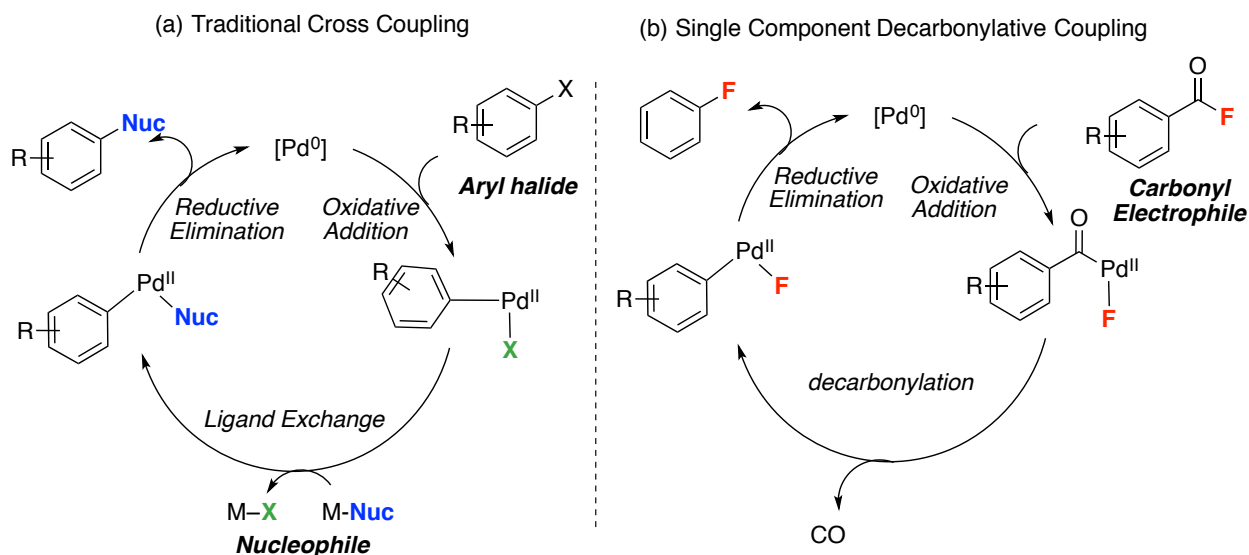
The premise of this project is to develop a transition metal catalyzed decarbonylative coupling method. Our preliminary studies targeted the development of a mild decarbonylative fluorination as a means to access aryl fluorides (Scheme 5.5). Notably, literature examples utilizing benzoyl fluoride as a fluorinating reagent are scarce,¹⁹ and there are currently no examples in which an aryl fluoride is converted to fluoroarene via CO-deinsertion.²⁰

Scheme 5.5 Our Ultimate Aim: Decarbonylative Fluorination



This strategy would utilize a single reagent that serves as both oxidant and coupling partner in the presence of a catalyst. This would circumvent several challenges often associated with aromatic fluorination including: (1) it would obviate the poor solubility of alkali metal fluorides and (2) it could be more sustainable and atom-economical than traditional cross-coupling methods that require multiple components (nucleophiles/transmetalating reagents and bases) (Figure 5.1a). Ultimately, the fundamental understanding of the CO-insertion process would help further improve the design of competent catalysts and reaction conditions for this transformation. We envision that this reaction could occur through the catalytic cycle shown in Scheme 5.1b.

Figure 5.1 Comparison of (a) Cross-Coupling Reactions and (b) Proposed Mechanism of Decarbonylative Fluorination

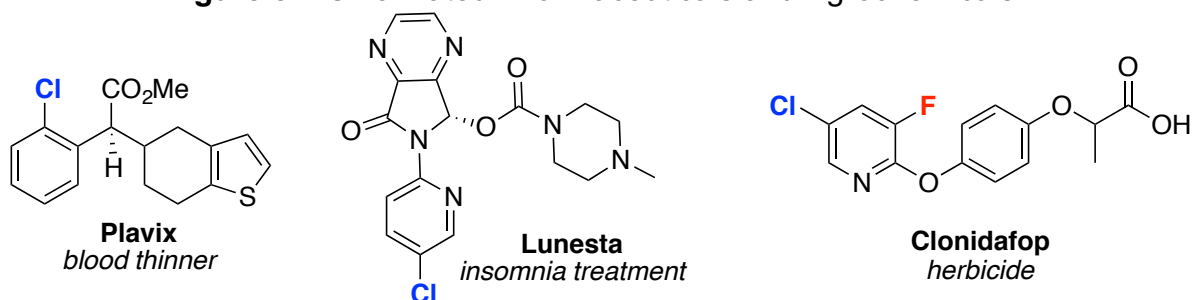


This chapter describes our investigations into Pd-catalyzed decarbonylative functionalizations. The initial focus of the project was to first develop transition-metal catalyzed decarbonylative chlorination reactions using aryl chlorides since the oxidative addition of aryl chlorides to Pd⁰ was previously reported. Next, this initial strategy was further broadened to probe decarbonylative C–S, C–N, C–O, and C–C coupling. Finally, efforts aimed at the initial target reaction – decarbonylative fluorination – were pursued. This project, specifically initial investigations of decarbonylative thioetherification reactions, was in collaboration with Łukasz Woźniak, an exchange graduate student from ICIQ in Spain.

5.2 RESULTS AND DISCUSSION

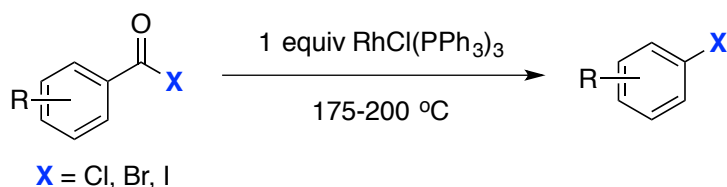
C-Cl Bond Formation. The first part of this chapter describes our preliminary explorations of Pd-catalyzed decarbonylative chlorination reactions so as to apply this preliminary study on decarbonylative carbon-heteroatom bond formation. Carbon–chlorine (C–Cl) bonds are abundant in natural products,²¹ pharmaceuticals²² and agrochemicals (Fig. 5.2).²³ They are widely utilized in cross coupling reactions (Figure 5.1) and in nucleophilic aromatic substitution (S_NAr) reactions.

Figure 5.2 Chlorinated Pharmaceuticals and Agrochemicals



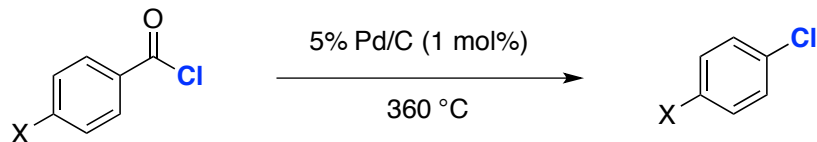
There are a few literature examples of transition metal-catalyzed decarbonylative chlorination reactions. In the 1960s, Blum was the first to investigate stoichiometric Rh-mediated decarbonylative halogenations, demonstrating successful decarbonylation of aryl chlorides,²⁴ aryl bromides,²⁵ and aryl iodides using Wilkinson's complex (Scheme 5.6).²⁶

Scheme 5.6 Rh-mediated Decarbonylative Halogenation²³⁻²⁶



In 1982, Verbickey and coworkers reported the most recent decarbonylative chlorination.²⁷ In this protocol, aryl chlorides were decarbonylated at 360 °C in the gas phase in the presence of 1 mol% of Pd/C (Scheme 5.7). The reaction required forcing conditions, thus resulting in narrow substrate scope. During the past two decades, there has been significant progress in catalyst and ligand developments that may allow more general decarbonylative chlorination reactions.²⁸

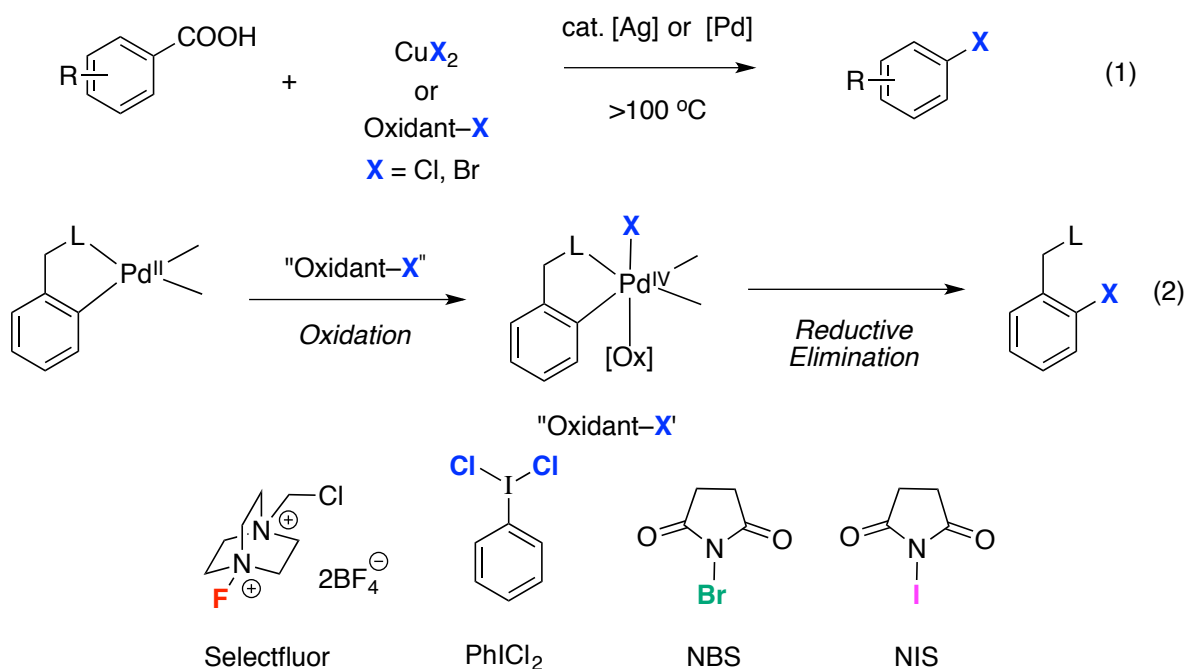
Scheme 5.7 Pd-catalyzed Decarbonylative Chlorination²⁷



Two relevant transition metal-catalyzed electrophilic halogenation approaches have been disclosed. One approach is Hunsdiecker type decarboxylative halogenations (Scheme 5.8, eq 1).²⁹ In this approach, either stoichiometric copper halides or electrophilic halogenating reagents undergo Ag or Pd-catalyzed reaction with benzoate derivatives to afford aryl halide products. Alternatively, our lab has developed Pd^{II/IV} catalyzed halogenations, utilizing a halogenating oxidant to access a high-valent Pd^{IV}

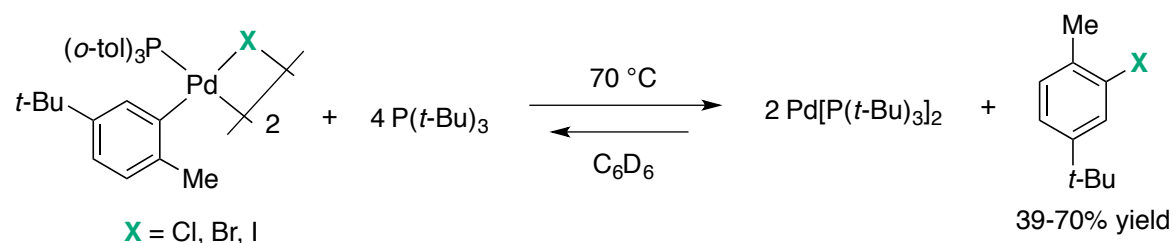
halide intermediate, followed by relatively facile reductive elimination to generate aryl halides (Scheme 5.8, eq 2).^{30,31} A common drawback in these two approaches is the control in regioselectivity and the use of stoichiometric expensive halogenating reagents.

Scheme 5.8 Hunsdiecker Type Halogenation (eq 1) and Halogenation via a High-Valent Pd^{IV} (eq 2) and Representative "Oxidant-X" for the Oxidation of Pd^{II}



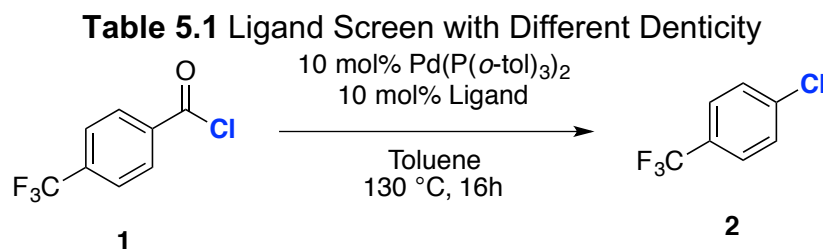
Ligand Screen. Our initial studies began with a survey of ligands for this transformation. A solution of 4-trifluoromethyl benzoyl chloride **1** in toluene was refluxed in the presence of 10 mol % of Pd(P(*o*-tol)₃)₂ (Table 5.1, entry 1). This Pd⁰ precatalyst was predicted to be a good catalyst for two reasons: (1) oxidative addition of acid chlorides is well-known to occur at electron-rich Pd⁰ centers and (2) reductive elimination of aryl halides from Pd^{II} have been reported by Hartwig and coworkers with Pd(P(*o*-tol)₃)₂ and P(*t*-Bu)₃ (Scheme 5.9).³²

Scheme 5.9 C_{sp2}-Halogen Bond Formation



Using this precatalyst in the initial studies, we were pleased to see 4-chlorobenzotrifluoride **2** in 4% yield. Observing 89% of starting material remained at the

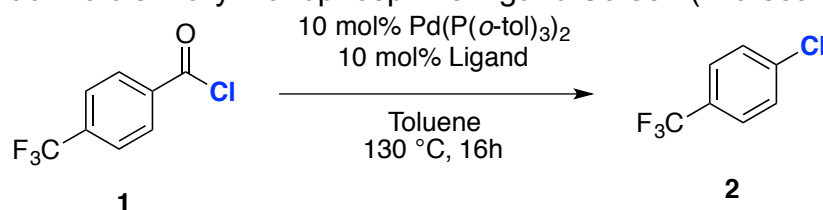
end of reaction, we hypothesized that the addition of electron rich phosphine ligands might lead to enhancement in catalytic activity by facilitating oxidative addition. Hence, a variety of phosphine ligands were evaluated under the reaction conditions. However, neither mono-dentate phosphine ligands (entries 2-3) nor bidentate ligands (entries 4-6) led to an improvement in the desired reactivity. Presumably, these ligands may block an open coordination site at Pd^{II}, thus hindering the decarbonylation step as seen that starting material left over at the end of reaction time.⁹



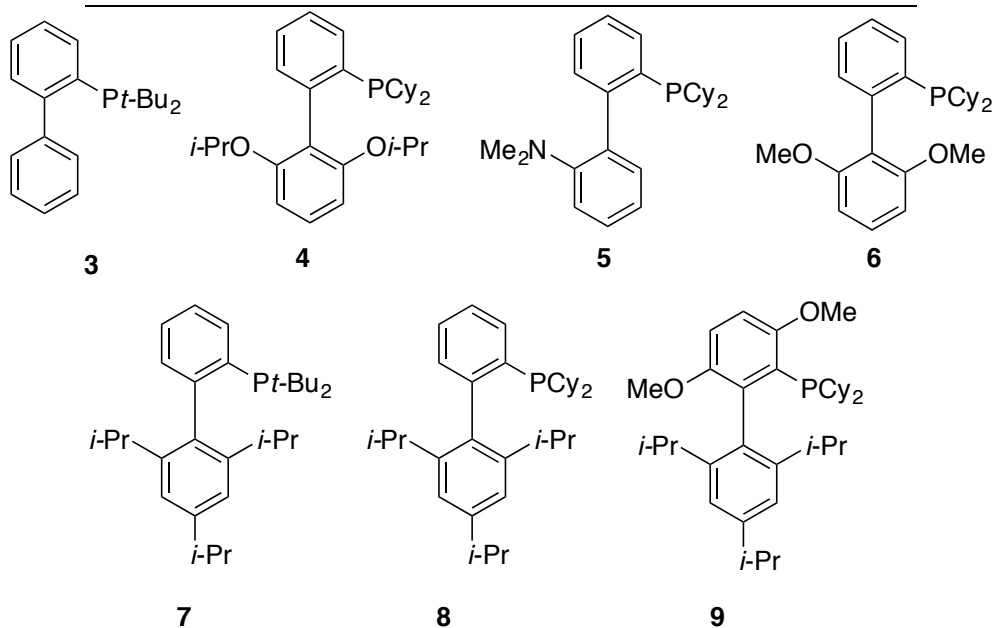
Entry	Ligand	Denticity	GC % Yield (2)	GC % Recovery (1)
1	none	1	4	89
2	P(<i>o</i> -tol) ₃	1	5	81
3	P(Ad) ₂ <i>n</i> -Bu	1	4	75
4	Xantphos	2	9	28
5	dppb	2	0	74
6	<i>rac</i> -BINAP	2	0	85

It is known that CO deinsertion from a coordinatively unsaturated three-coordinate Pd^{II} species is expected to be significantly more facile than from a square-planar tetracoordinate Pd^{II} center.³³ Maleckis and Sanford have demonstrated that Ruphos, Buchwald's biarylmonophosphine ligand, allows for the stabilization of the three-coordinated Pd^{II} intermediate via a C_{ipso}-Pd^{II} interaction that is indicated by the dash line in Scheme 5.2.^{18a}

Therefore, inspired by the previous study with Ruphos **4**, a variety of commercially available Buchwald biarylmonophosphine ligands were evaluated (Table 5.2). The use of Ruphos **4** provided 8% of **2** (entry 2, Table 5.2). Gratifyingly, an increase in the yield of **2** to 23% was observed by GC analysis when the ligand was switched to the bulky *t*BuXPhos ligand **7** (entry 5). The use of the related XPhos ligand **8** afforded a comparable yield for **2** (entry 6). The best yield of **2** was obtained with BrettPhos (29%, entry 7) and 44% of starting material **1** remained at the end of reaction.

Table 5.2 Buchwald's Biarylmonophosphine Ligand Screen (in a sealed 4 mL vial)

Entry	Ligand (L)	(L)	GC % Yield (2)
1	JohnPhos	3	5
2	RuPhos	4	8
3	DavePhos	5	8
4	SPhos	6	9
5	<i>t</i> BuXPhos	7	23
6	XPhos	8	22
7	BrettPhos	9	29



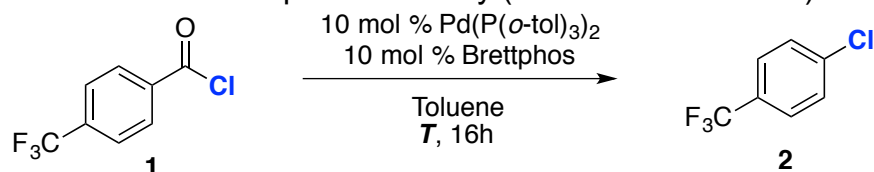
Palladium Screen. As the Pd (P(*o*-tol)₃)₂ only displayed moderate reactivity under catalytic conditions, a series of Pd^{II/0} precatalysts were examined. Previous studies have suggested that the Pd center needs to be sufficiently electron-rich for the oxidative addition of acid chlorides to occur.³⁴ Both Pd⁰ and Pd^{II} catalysts were screened and the results are shown in Table 5.3. As predicted, using the Pd^{II} pre-catalysts (entries 1-7, Table 5.3), very poor reactivity of acid chloride **1** was observed, producing <10% of the desired product **2**. In contrast, the Pd⁰ catalyst, Pd₂(dba)₃, showed a slightly better performance (entry 8), although the initially identified Pd(P(*o*-tol)₃)₂ gave the best reactivity among all precatalysts examined (entry 10).

Table 5.3 Palladium Precatalyst Screening (in a sealed 4 mL vial)

Reaction scheme showing the conversion of 4-(trifluoromethyl)benzoyl chloride (**1**) to 4-(trifluoromethyl)chlorobenzene (**2**) using 10 mol% Pd catalyst and 10 mol% Brettphos in Toluene at 130 °C for 16h.

Entry	Pd Catalyst	GC % Yield (2)
1	[cinnamylPdCl] ₂	9
2	(COD)Pd(CH ₂ TMS) ₂	0
3	(PPh ₃) ₂ PdCl ₂	0
4	(Cp)Pd(allyl)	5
5	(Allyl)PdCl ₂	5
6	Pd(TFA) ₂	0
7	Pd(OAc) ₂	0
8	Pd ₂ (dba) ₃	10
9	Pd(PPh ₃) ₄	6
10	Pd(P(o-tol)₃)₂	29

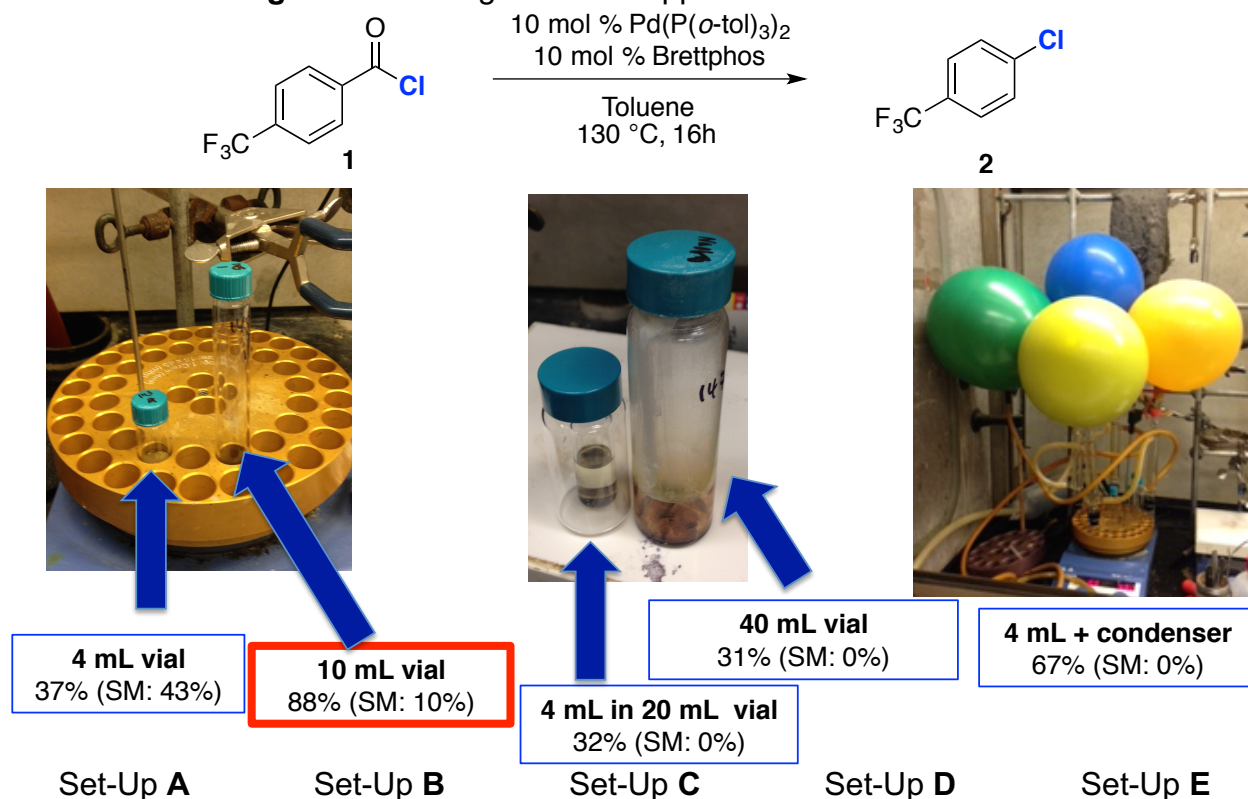
Temperature Studies. Considering that CO deinsertion is a challenging step at a Pd^{II} center, it is possible that oxidative addition is reversible, leading to recovered starting material at the end of reaction. However, quantifying the starting material **1** by GC clearly showed consumption of **1** over time, regardless of the examined temperature (rt to 130 °C). Furthermore, the consumption of **1** was observed even in the presence of the acid chloride. It is also possible Pd^{II} acyl complex had formed and might have slowly decomposed into dicationic Pd^I dimer through disproportionation at low temperatures.^{18a} Importantly, the reactions significantly slowed down below the boiling point of toluene (b.p. = 110 °C), or a decreased yield of product **2** is observed (entry 2) in a sealed 4 mL vial. This result led us to hypothesize that modifying the reaction apparatus to promote carbon monoxide dissociation from Pd^{II} could have a favorable effect on product formation. Another way to shift the equilibrium in a reversible oxidative addition is by having an open system that can remove CO from the solution.

Table 5.4 Temperature Study (in a sealed 4 mL vial)

Entry	Temperature °C	GC % Yield (2)	GC % Recovery (1)
1	130	29	44
2	100	10	52
3	80	8	58
4	60	9	74
5	22	9	59

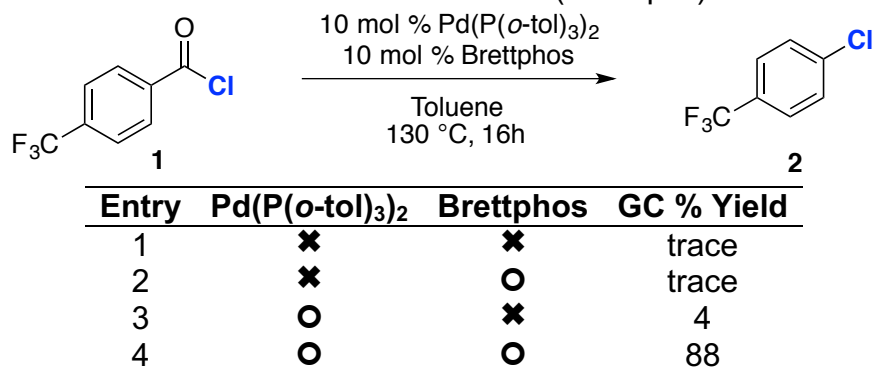
Tuning Reaction Set-Up. We next sought to develop a system that could shift the equilibrium that favors toward the decarbonylative coupling reaction. We hypothesized that having a larger headspace in the reaction vessel could facilitate carbon monoxide to vaporize out of the solution. Indeed, instead of using a sealed 4 mL vial (set-up **A**), running the reaction in a sealed 10 mL tall vial greatly improved the yield, generating 88% of **2** under the reaction conditions in Figure 5.3 (set up **B**). Other apparatuses were tested to further improve the system. Simply increasing the reaction volume using setup **C**, Figure 5.3 did not lead to a better yield, as this resulted in evaporation of the solvent from the reaction mixture. Finally, increasing the headspace further to a 40 mL vials (Set-up **D**) led to evaporation of toluene at 130 °C. Based on these results, we decided to equip the 4 mL vial with a reflux condenser and an argon balloon (Set-up **E**) with the prediction that carbon monoxide should be displaced by the dense argon ($d_{\text{Ar}} = 1.661 \text{ kg/m}^3$; $d_{\text{CO}} = d_{\text{N}_2} = 1.165 \text{ kg/m}^3$). Set-up **E** showed an improved the yield compared to set-ups **A**, **C** and **D**, but still resulted in lower yield (67%) than set-up **B**. Since the system does not seem to build a lot of CO pressure when we vented a system, for the remained chlorination study, set-up **B** was utilized. Imperfect mass balance (0% SM was observed) seems to suggest that some Pd may remain as a Pd-acyl complex or that the desired product oxidatively adds to the Pd center under the reaction conditions.

Figure 5.3 Tuning Reaction Apparatus for CO Extrusion



Control Studies. Control studies were performed and confirmed that both Pd and ligand are necessary to facilitate this transformation (Table 5.5).

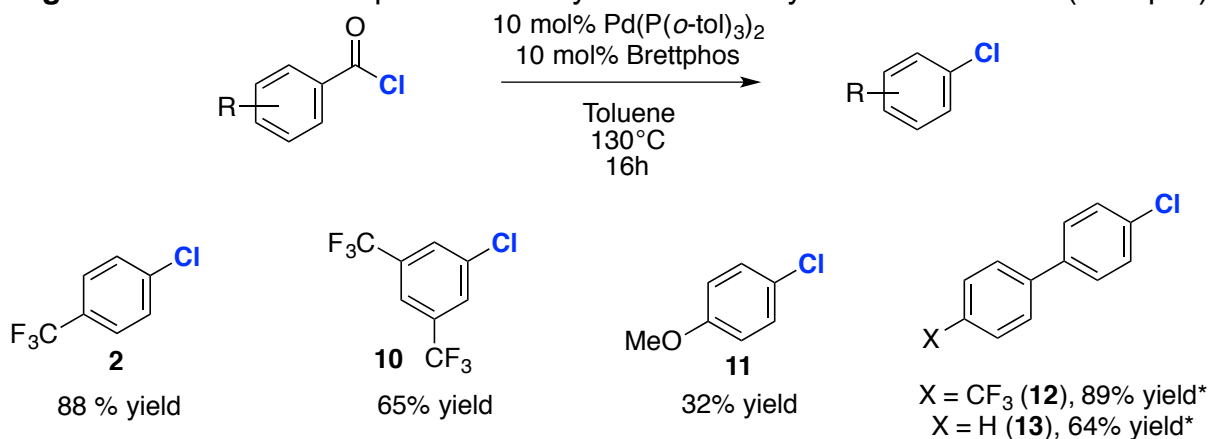
Table 5.5 Control Studies (Set-Up B)



Substrate Scope. With the optimal conditions in hand, preliminary evaluation of the substrate scope was conducted. The reaction worked well with substrates bearing electron-withdrawing (**2**, **10**, **12**) and electron-neutral (**13**) substituents on the aromatic ring. However, substrates bearing electron-donating substituents, such as 4-methoxybenzoyl chloride **11** did not show good reactivity under the conditions, which

may be due to slow oxidative addition. Further investigation of substrate scope is currently underway.

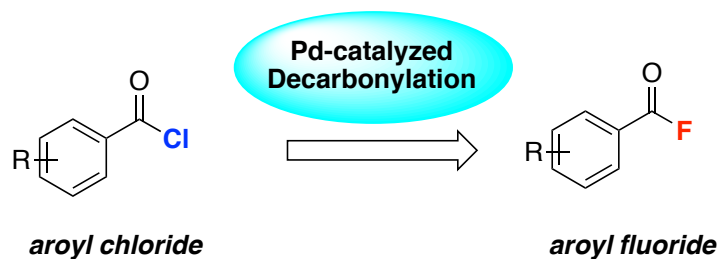
Figure 5.4 Substrate Scope of Pd-catalyzed Decarbonylative Chlorination (set-up B)



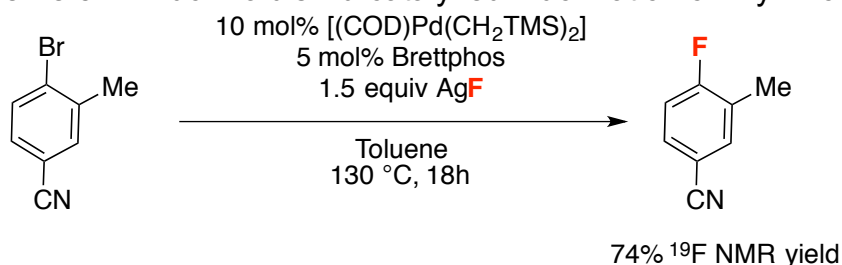
*isolated yield

In summary, a mild Pd-catalyzed decarbonylative chlorination was demonstrated utilizing a Pd⁰ catalyst, a commercially available monophosphine ligand, and a strategically designed reaction set-up. Our next aim is to translate our preliminary chlorination studies to Pd-catalyzed decarbonylative fluorination (Scheme 5.10).

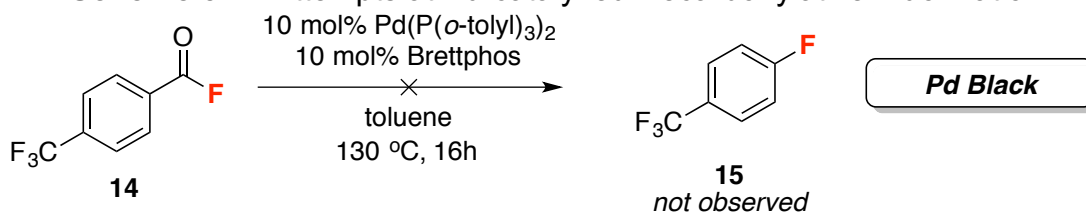
Scheme 5.10 Translating Pd-Catalyzed Decarbonylative Chlorination to Fluorination



C–F Bond Formation. Aromatic fluorination is a very challenging transformation,³⁵ leading us to initially target the corresponding decarbonylative chlorination reaction. These preliminary investigations showed that decarbonylative chlorination is feasible. Moreover, the Buchwald lab demonstrated fluorination of aryl bromides utilizing [(COD)Pd(CH₂TMS)₂] and BrettPhos, the same optimal ligand for our decarbonylative conditions, which indicates that our decarbonylative pathway may potentially be translatable (Scheme 5.11).

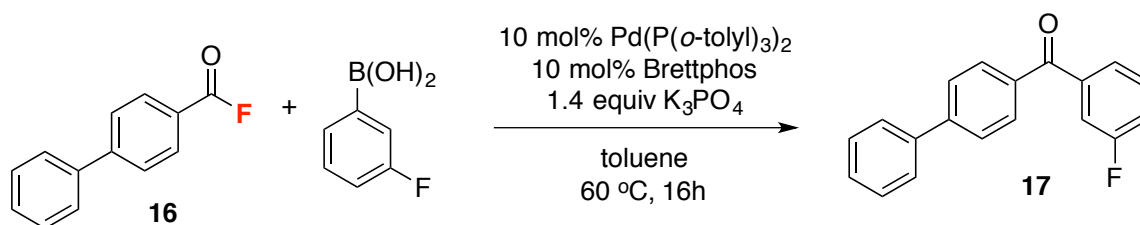
Scheme 5.11 Buchwald's Pd-catalyzed Fluorination of Aryl Bromide

Decarbonylative C–F Coupling. The optimal chlorination conditions were applied to the model substrate 4-trifluoromethyl benzoyl fluoride **14**. This electronically activated substrate was predicted to exhibit a good reactivity in the optimized reaction condition. Upon heating in refluxing toluene, an immediate color change from yellow to dark orange was observed, suggesting that a possible change in the oxidation state of Pd as such color change did not occur in the absence of the Pd catalyst. However, 100% starting material was recovered along with detection of Pd black, and none of the desired fluorinated product **15** was observed (Scheme 5.12).

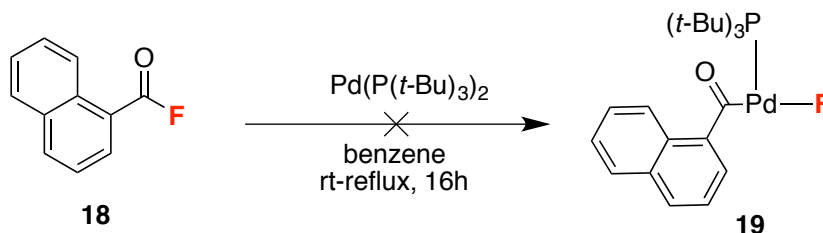
Scheme 5.12 Attempts at Pd-catalyzed Decarbonylative Fluorination

It is possible that oxidative addition of benzoyl fluoride may have occurred but the reversibility of this process led back to the starting benzoyl fluoride back under the reaction conditions (Scheme 5.12)^{36,37} Notably, when 3-fluorophenylboronic acid was reacted with aryl fluoride **16** in the presence of the Pd, Brettphos and K₃PO₄, benzophenone **17** was observed as a cross-coupled product (16% of **16** remained at the end of reaction) (Scheme 5.13). The identity of **17** was confirmed by GC-MS.³⁸ This seemed to suggest oxidative addition of benzoyl fluoride is occurring in the condition. Stoichiometric reaction of **18** was also conducted but no oxidative addition product **19** was detected but free P(*t*-Bu)₃ and Pd(P(*t*-Bu)₃) (Scheme 5.14). Hence, there was no direct evidence of Pd-acyl(F) complex through oxidative addition. After initial attempts, a series of Pd precatalysts, ligands, and solvents were evaluated but no decarbonylative fluorination was observed.

Scheme 5.13 Formation of Cross-Coupled Product

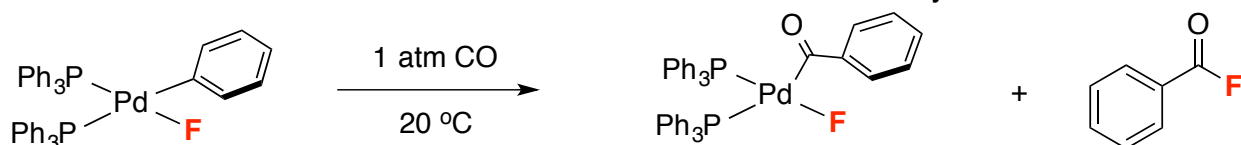


Scheme 5.14 Stoichiometric Reaction of Benzoyl Fluoride **18** to Pd(P(*t*-Bu)₃)₂



The hypothesis that reductive elimination of the acyl fluoride may be facile is supported by Grushin's stoichiometric study with (PPh₃)₂Pd^{II}PhF.³⁹ In this report, subjecting (PPh₃)₂Pd^{II}PhF to 1 atm of CO resulted in reductive elimination of benzoyl fluoride along with an observed (PPh₃)₂Pd^{II}(COPh)F intermediate at room temperature (Scheme 5.9). In contrast, reductive elimination of other benzoyl halides from analogous (PPh₃)₂Pd^{II}(COPh)X (X = Cl, Br I) was not observed, due to the high stability of Pd(acyl)halide complex (Scheme 5.15).⁴⁰

Scheme 5.15 Grushin's Stoichiometric Study

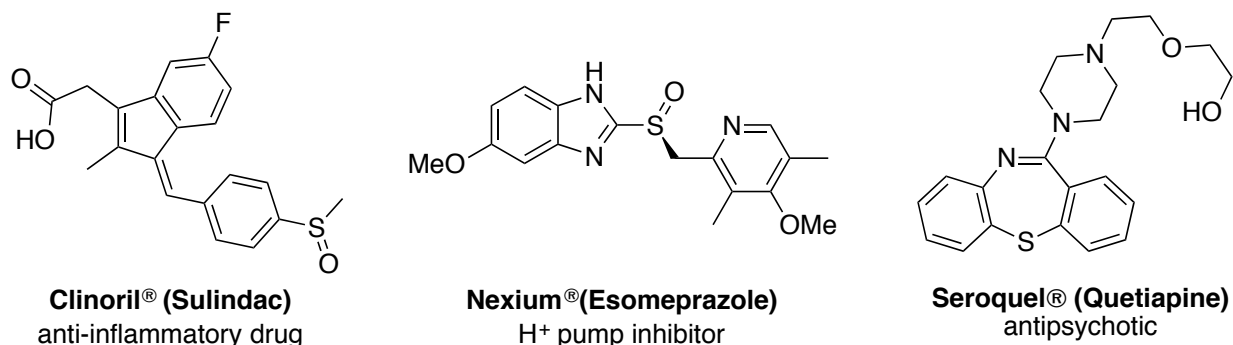


Another factor could be due to the thermodynamic stability of the benzoyl fluorides. Acyl fluorides have the strongest C–X bond and thus are the least electrophilic acyl halides amongst other acyl halides.⁴¹ Therefore, the reductive elimination of stable benzoyl fluoride readily occurs upon 1 atm of carbon monoxide, whereas the less stable benzoyl halides are thermodynamically unfavorable to form through reductive elimination from Pd^{II}(COPh)X complex.

C–S Bond Formation. As part of our ongoing efforts toward the development of decarbonylative coupling methods, we sought to apply these optimized decarbonylative chlorination conditions for the formation of other aryl-heteroatom bonds. Our initial

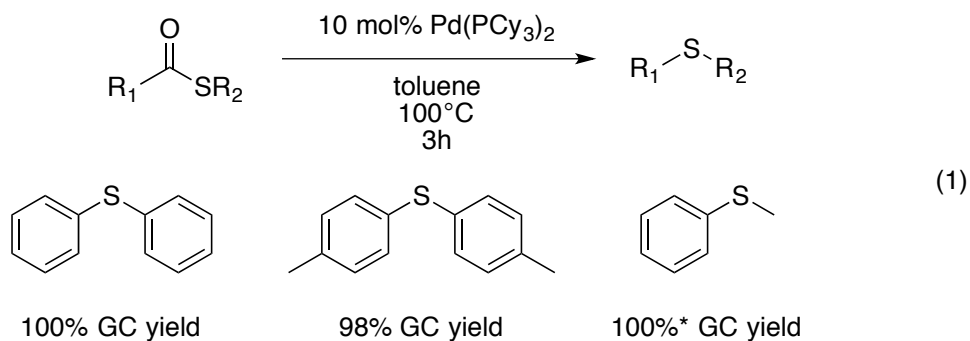
studies targeted diaryl sulfides because they are important scaffolds that are prevalent in natural products,⁴² materials,⁴³ and pharmaceuticals⁴⁴ (Figure 5.5). Such scaffolds are also widely utilized as useful intermediates in organic synthesis⁴⁵ and as ligands in transition metal catalysis.⁴⁶ Thus, the development of mild methods for their synthesis has attracted significant interest.

Figure 5.5 Representative Organic Molecules Containing Diaryl Sulfides

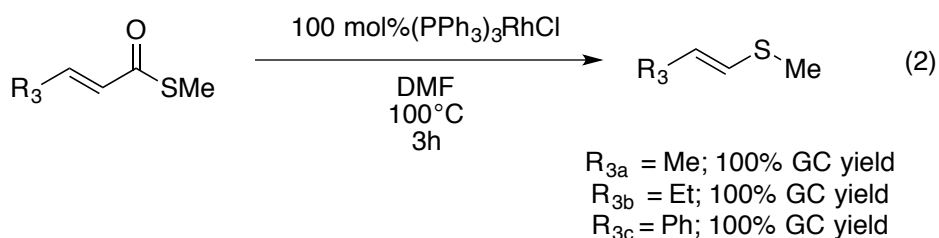


According to the Swain-Scott nucleophilicity parameters, n_x the nucleophilicity of thiophenolate is 9.92, while Cl is 4.3. It suggests that our optimized conditions could be even more favorable for C-S coupling.⁴⁷ In 1987, Yamamoto demonstrated the decarbonylation of thioesters to form S-phenyl phenyl thioate with 5 mol % of Pd(PCy₃)₂ (eq 1, Scheme 5.16) or with an equimolar amount of Wilkinson's catalyst (eq 2) under negative pressure. In all cases, quantitative conversion of diaryl sulfides and vinyl(alkyl) sulfides were observed under the corresponding conditions by GC analysis.⁴⁸ However, limitations of this system include a narrow substrate scope (3 examples for Pd) and reaction conditions (evacuation of the system). Weinert has subsequently demonstrated decarbonylative C-S bond formation using stoichiometric amounts of NiCl₂•6H₂O (2 equiv). However, there has been no follow-up study of catalytic decarbonylative coupling for diaryl sulfide formation.⁴⁹ Therefore, we decided to apply the optimized catalytic conditions for decarbonylative C-Cl coupling to the development of C-S cross coupling reactions. This part of project was in collaboration with Łukasz Woźniak.

Scheme 5.16 Yamamoto's Decarbonylative Thioetherification

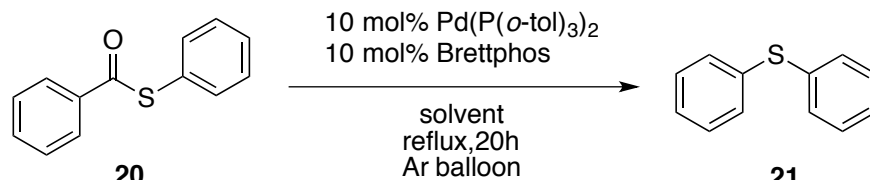


*Reaction was performed at 140°C



Expansion of Decarbonylative Chlorination to Thioetherification. Our investigation into C–S bond formation started with *S*-phenyl benzene thiolate as the model substrate. Gratifyingly, 32% yield of phenyl sulfide was observed by GC analysis under the reaction conditions for decarbonylative chlorination (entry 1, Table 5.6). Using refluxing *p*-xylene (b.p. 138 °C) resulted in improved yield (up to 58% as determined by GC analysis). It is important to note that the original chlorination was conducted at 0.05 M concentration in aroyl chloride with set-up **B**. For the analogous C–S coupling reaction set-up **E** was found effective (yield differ by 1-2% lower) when the reaction concentration was increased to 0.2 M. Thus, for safety reasons, the rest of the investigations utilize set-up **E**.

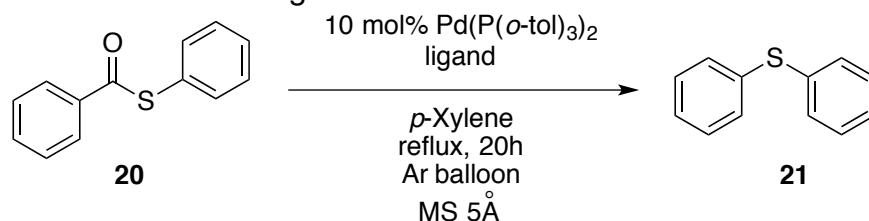
Table 5.6 Preliminary Investigation of Decarbonylative C–S Cross-Coupling Reactions for the Synthesis of Diaryl Sulfide (Set-Up **B** or **E**)



Entry	Solvent	Temperature (°C)	GC Yield (%)
1	Toluene	130	32
2	<i>p</i> -Xylene	130	46
3	<i>p</i> -Xylene	150	58

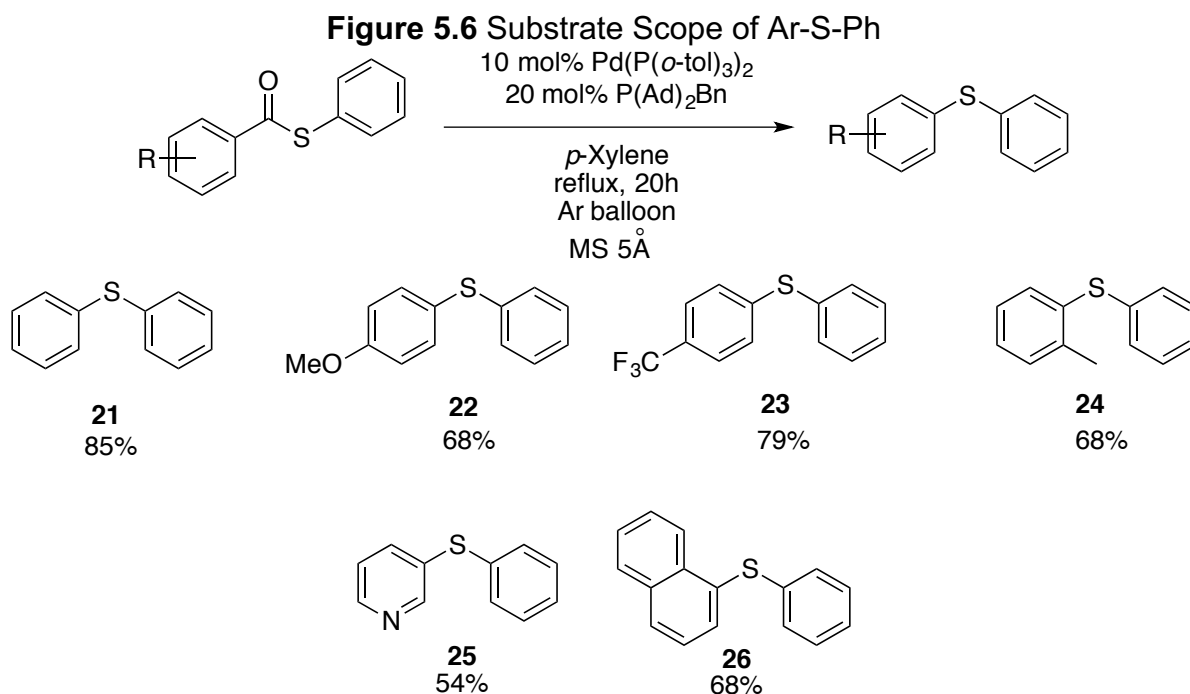
Ligand Screen. Ligands were reevaluated to find optimal conditions for the thioetherification reactions. The use of JohnPhos (entry 1, Table 5.7) or XantPhos (entry 2) gave appreciable yields of 20% and 52% yield of **21**, respectively. The use of 20 mol % of bidentate ligands such as XantPhos (entry 3), *rac*-BINAP (entry 5), dppf (entry 6) and dppb (entry 7) increased the yields of phenyl sulfide **21**. We hypothesized that bulky monodentate phosphine ligands would further promote this reaction. Indeed, P(Ad)₂*n*-Bu further improved the yield of the product (entry 9). Finally, the use of 20 mol % P(Ad)₂Bn gave the best yield (78%, entry 10) of phenyl sulfide **21** under the reaction conditions. Therefore, we chose to use P(Ad)₂Bn as a ligand for studying the scope of the decarbonylative thioetherification reactions.

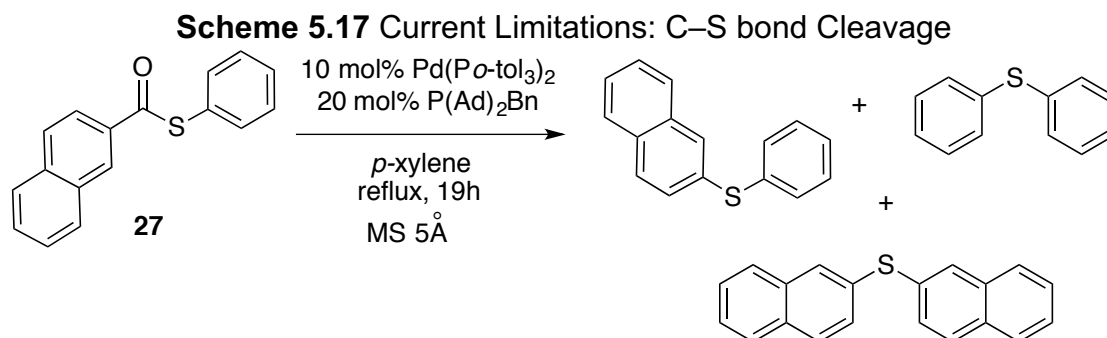
Table 5.7 Ligand Screen for Thioetherification



Entry	Ligand (L)	L mol%	GC Yield (%)
1	JohnPhos	10	22
2	Xantphos	10	52
3	Xantphos	20	61
4	<i>t</i> Bu-Xantphos	20	15
5	<i>rac</i> -BINAP	20	59
6	dppf	20	61
7	dppb	20	64
8	dppe	20	19
9	P(Ad) ₂ <i>n</i> -Bu	20	67
10	P(Ad)₂Bn	20	78

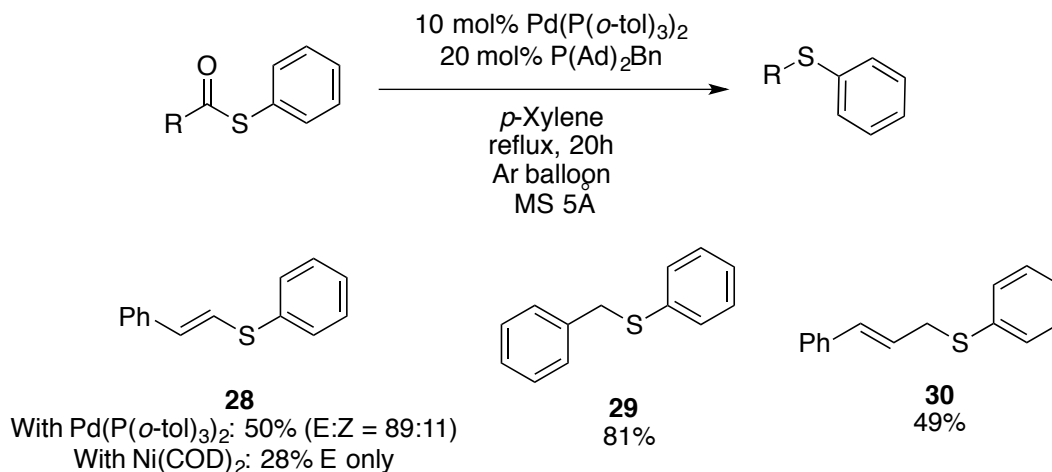
Substrate Scope. With the optimized conditions in hand, the substrate scope of the decarbonylative thioetherification was next examined. Phenyl (**21**), *p*-OMe (**22**), *p*-CF₃ (**23**), *o*-Me (**24**) and 1-naphthoyl (**26**) substituents were tolerated and afforded moderate to good yields (Figure 5.6). Notably, the substrate containing the electron-rich 4-methoxyl substituent led to poor yields, due to the formation of diphenyl sulfide as a by-product. Pyridine substrate tolerated the reaction condition affording 54% of product **25**. One limitation of this protocol is the persistent formation of phenyl sulfides as byproducts, which might occur via carbonyl C–S bond cleavage by the palladium catalyst.⁵⁰ For instance, when *S*-phenyl 2-naphthoyl thiolate (**27**) was subjected to the reaction conditions, the formation of biaryl sulfide mixtures was observed (Scheme 5.17). This product distribution is attributed to C–S activation by Pd.⁵¹ Further mechanistic studies, including kinetics and more detailed studies on electronic and steric effects will be required to improve the reaction conditions.





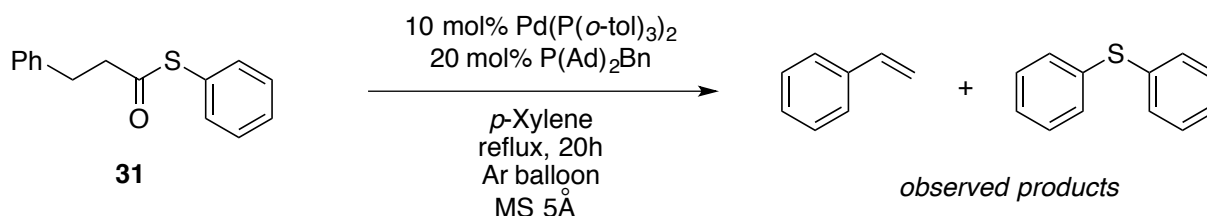
Vinyl and Aliphatic Substrates. This work was further extended to non-aromatic substrates. For example, this protocol works with cinnamyl thioesters, affording phenyl(styryl)sulfane **24** (E:Z = 89:11) in 50% yield. However, isomerization occurs during this reaction, resulting in a mixture of alkene stereoisomers. Interestingly, changing the catalyst from Pd(P(*o*-tol)₃)₂ to Ni(COD)₂ led to the single *E* isomer **28** in 28% yield, suggesting that isomerization is readily at the Ni^{II} center. Moreover, a benzylic substrate also underwent the desired decarbonylation reaction to form **29** in high yield (81%) (Scheme 5.18). Notably, we found that if the allylic substrate is also substantially activated, affording the desired product **30** in 49% yield. It is known that the decarbonylation of aliphatic aldehyde is stereospecific: the configuration of the stereocenter to which the formyl group is attached to is retained using Wilkinson's catalyst.⁵² Such finding has been used in the total syntheses of several natural products including 7-(±)-deoxypancratistatin.⁵³ Therefore, we envision that extension of scope to aliphatic substrates will find great synthetic applications because of the abundances of C–S bonds in important organic molecules.

Scheme 5.18 Decarbonylation of Vinyl and Benzylic Substrates



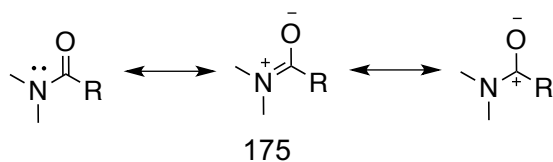
Competitive β -H Elimination Pathway. These preliminary results led us to further investigate the reactivity of aliphatic substrates. However, products attributed to β -H elimination were observed when *S*-phenyl 3-phenylpropanethioate was used as the substrate, resulting in no desired product (Scheme 5.19). The current substrate structure has a β -hydride that can be easily abstracted by a reactive Pd^{II} center leading to styrene formation. We propose that changing the sterics and electronics on the alkyl chain may slow down the rate of β -H elimination. For example, installing electron-poor arenes on the β -carbon has been shown to slow down β -H elimination.⁵⁴ Chirik and Bercaw have performed systematic studies on the effect of β -carbon substituents on the rate of β -H elimination with zirconocene β -arylethyl complexes. They found that electron-withdrawing substituents slowed down the rate of β -H elimination ($\rho = -1.8$).⁵⁵ We envision that electron-withdrawing groups should have the same effect in our system, slowing down the β -H elimination pathway and thus favoring the desired decarbonylative coupling. In addition, the rate of β -H elimination should also decrease with electron-withdrawing substituents at the α -carbon. Studies on the electronic effects toward decarbonylative thioetherification are a possible future direction.⁵⁶

Scheme 5.19 Outcome of Decarbonylative C–S Coupling with *S*-phenyl 3-Phenylpropane Thiolate



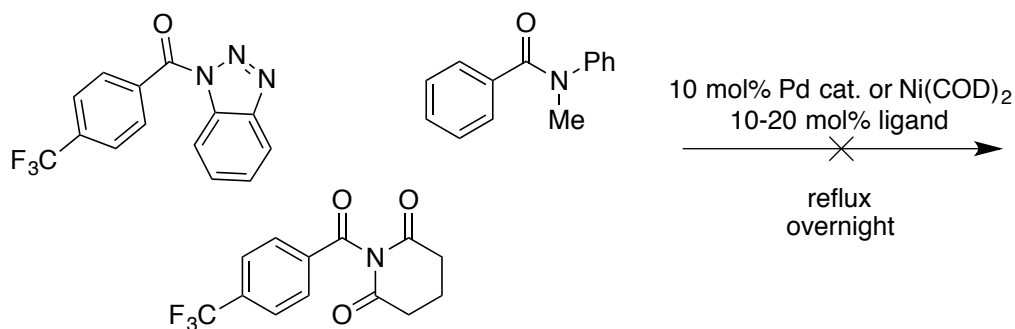
C–N and/or C–O Bond Formation. Having demonstrated the feasibility of C–S bond formation, decarbonylative amination and etherification to form C–N and C–O bonds would be a logical extension of this project. In particular, esters and amides are common functional groups in organic molecules. Despite the abundance of esters and amides functionalities, C_{acyl}–N and C_{acyl}–O bond cleavage is challenging due to resonance stabilization of the amide functionality (Scheme 5.20).

Scheme 5.20 Resonance Stabilization of Amide Functionality



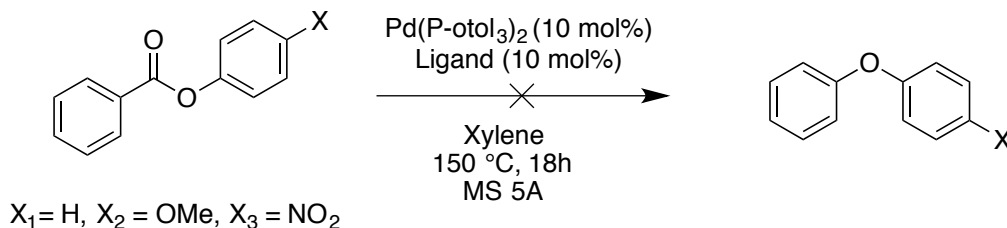
Examples of decarbonylation via metal insertion into $C_{acyl}-N^{57}$ or $C_{acyl}-O^{58}$ bonds are scarce. Such transformations could be highly useful, as amides and esters could serve as protecting groups in complex organic molecule syntheses followed by removal of these protecting groups via late-stage decarbonylative coupling. Our first goal is to identify a good amide for systematically studying its reactivity toward Pd^0 . Three key factors for increasing the reactivity of amides towards oxidative addition/decarbonylative coupling are: (1) ground state destabilization of amide bonds, (2) high reaction temperatures, and (3) the use of labile ligands that promote decarbonylation.⁵⁹ Three different amides were prepared as *N*-methyl-*N*-phenylbenzamide⁶⁰ and *N*-(4-trifluoromethylbenzoyl)glutarimide⁵⁷ have literature precedents for metal insertion into carbonyl-amide bonds. Unfortunately, the desired decarbonylative coupling reactions were not observed after our preliminary studies (Scheme 5.21).

Scheme 5.21 Attempted Decarbonylative Amination Reactions



Similarly, a series of esters were prepared and subjected to various reaction conditions for decarbonylative coupling. Unfortunately, no desired reactivity was observed under our initial conditions (Scheme 5.22). Future efforts will investigate various ligands, solvents, and transition metals to accomplish the transformation.

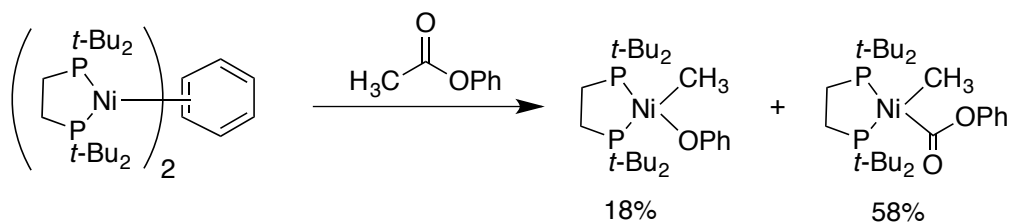
Scheme 5.22 Attempted Decarbonylative C–O Coupling Reactions



One alternative to the current attempts at Pd-catalyzed amination and etherification could be to investigate the corresponding Ni-catalyzed transformations. Recently, Love

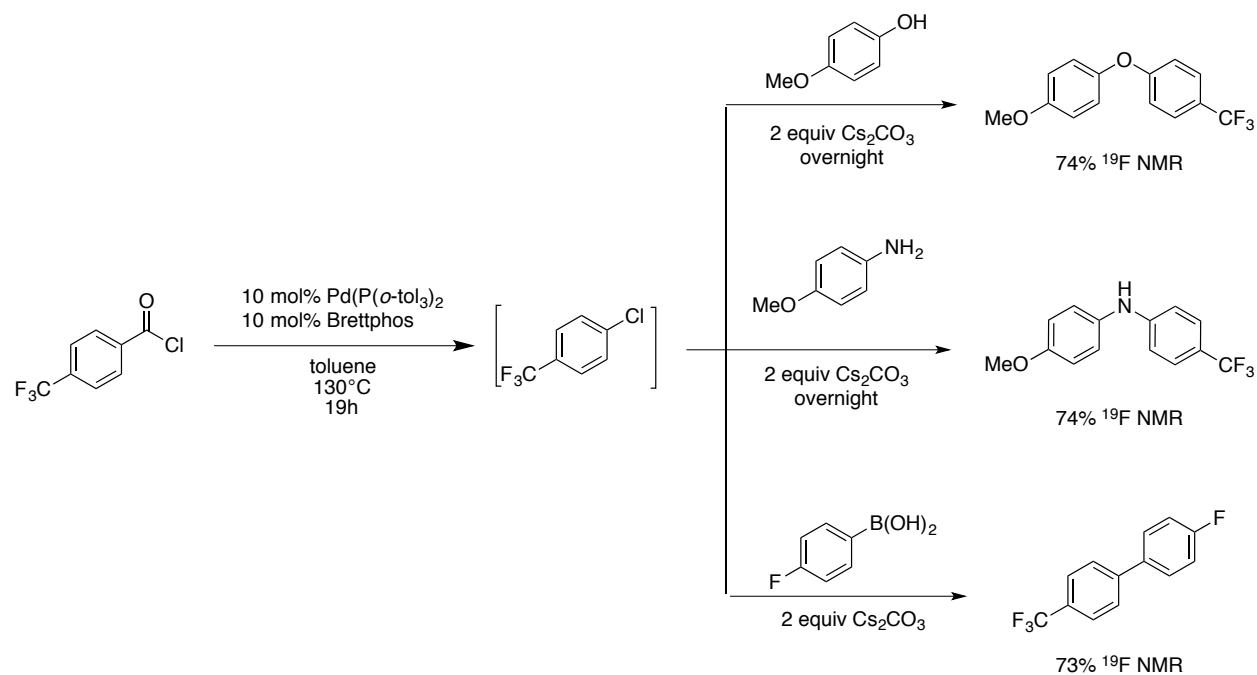
and coworkers have shown that Ni can oxidatively add to a C_{acyl}-O bond followed by decarbonylation to form a Ni^{II}-alkoxy complex albeit in low yield (Scheme 5.23).⁵⁸ In order to facilitate the decarbonylation process at Ni, an appropriate hemilabile ligand will need to be identified that simultaneously leaves a coordination site open at Ni^{II} and provides steric bulk to promote reductive elimination.

Scheme 5.23 Ni Insertion into C_{acyl}-O Bond Cleavage and Decarbonylation⁵⁸



One Pot CN, C-O, and C-C Bond Formation from C-Cl Decarbonylative Cross Coupling. As a side project to these decarbonylation studies, we sought to find a one pot method to convert acid chlorides to ethers and amines using the catalyst and ligand from our optimized decarbonylation conditions. In our first attempt, we were pleased to find that the original chlorination conditions could be used to form C-N, C-O and C-C bonds in high yields (Scheme 5.24). It is noted that the system was vented before nucleophiles were added to the reaction in order to release CO from the system, but the same catalyst could be further used to facilitate the next step. To the best of my knowledge, this is the first example of utilizing an acid chloride to form aryl-N, aryl-O, and aryl-C bonds. The scope of suitable substrates for this transformation will be examined in future studies.

Scheme 5.24 Amination, Etherification and Suzuki Coupling from Acid Chlorides



5.3 CONCLUSIONS

In summary, this chapter describes the development of transition metal catalyzed decarbonylative functionalizations to form a variety of carbon-heteroatom bonds. Using Pd(P(*o*-tol)₃)₂ as a precatalyst, decarbonylative chlorination and thioetherification were achieved under much milder conditions than previous reports. Attempts at developing decarbonylative coupling of aryl fluorides, esters and amides were not successful after extensive studies. However, as a preliminary result, starting from the aroyl halide, one pot decarbonylative C–N, C–O, and C–C cross coupling reactions with corresponding nucleophiles or aryl boronic acids were demonstrated feasible.

5.4 PERSPECTIVE AND OUTLOOK

As part of our continuous effort toward the development of more sustainable chemical transformations, carbonyl groups would be a highly desirable synthon for carbon-heteroatom coupling reactions. For future studies, a fundamental investigation of the mechanism of the decarbonylative chlorination and thioesterification reactions would be useful. In particular, kinetic studies (ex. Hammett studies) under the catalytic conditions would provide insight into the electronic effects of this system. In addition, stoichiometric studies aimed at synthesizing relevant intermediates could provide important insights for catalyst design. Furthermore, computational studies could help clarify or rationalize any ambiguity that could arise from our experimental results. Only a few literature reports on detailed mechanistic studies of catalytic decarbonylative coupling reactions have been disclosed.⁵ Thus, the work from this chapter and its preliminary results opens up the possibility for a number of new applications and enables the design of new synthesis routes.

5.5 EXPERIMENTAL

Instrumental Information. NMR spectra were obtained on a Varian MR400 (400.52 MHz for ^1H ; 100.71 MHz for ^{13}C ; 376.87 MHz for ^{19}F), a Varian vnmrs 500 (500.10 MHz for ^1H), or a Varian vnmrs 700 (699.76 MHz for ^1H ; 175.95 MHz for ^{13}C) spectrometer. ^1H and ^{13}C NMR chemical shifts are reported in parts per million (ppm) relative to TMS, with the residual solvent peak used as an internal reference. ^1H and ^{19}F multiplicities are reported as follows: singlet (s), doublet (d), triplet (t), quartet (q), and multiplet (m).

Materials and Methods. S-phenyl arene thiolates were prepared according to a literature procedure.⁶¹ Anhydrous DMF and $\text{P}(\text{Ad})_2\text{Bn}$ were obtained from Aldrich. $\text{Pd}[(\text{P}(o\text{-tol}_3)_2)]$ was obtained from Alfa Aesar. 4-trifluoromethyl benzoyl chloride **1**, 3,5-bis(trifluoromethyl)benzoyl chloride, 4-anisoyl chloride, biphenyl-4-carbonyl chloride, phenylacetyl chloride were purchased from Acros. BrettPhos was purchased from Strem. All reactions were conducted under a nitrogen atmosphere or using standard Schlenk techniques unless otherwise stated. All reactions conducted at elevated temperatures were heated on a hot plate using an aluminum block. Temperatures were regulated using a thermocouple.

Synthesis of Benzoyl Chloride

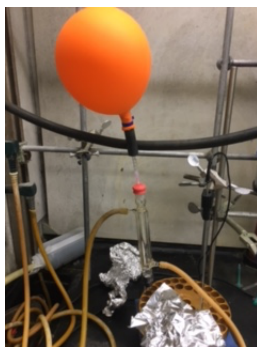
General Procedure A: $\text{Ar}(\text{CO})\text{Cl}$ substrates were prepared by the following procedure adapted from the literature:⁶² the indicated carboxylic acid was suspended to anhydrous toluene (0.25M) and thionyl chloride (2.0 equiv) was added. The reaction was then refluxed overnight. Reaction was cooled and the crude mixture was distilled under reduced pressure to afford acid chlorides.

General Procedure B: $\text{Ar}(\text{CO})\text{Cl}$ substrates were prepared by the following procedure adapted from the literature:⁶³ Oxalyl Chloride (1.1 equiv) was added dropwise to a mixture of the carboxylic acid (1.0 equiv) and DMF (cat.) in dry CH_2Cl_2 under a N_2 atmosphere at 0 °C. The mixture was stirred at the same temperature for 5 h upon which it was allowed to warm up to ambient temperature. The reaction was concentrated in *vacuo* and the crude mixture was used for the next reaction.

General Procedure for Synthesis of S-phenyl Arene Thioate. S-Phenyl thioate was prepared by the following procedure adapted from the literature:⁶¹ A 25 mL two-neck flask was equipped with a Teflon-lined magnetic stir bar and a rubber septum. The flask was evacuated and back-filled with N₂ and this cycle was repeated for three times. Thiophenol (1.0 equiv) and pyridine (1.0 equiv) was added with methylene chloride (0.1M) and cooled to 5°C. To the cooled mixture, was an acyl chloride (1.0 equiv) added by syringe over 5 minutes. The resulting suspension was stirred at 5°C for an additional 5 minutes, and stirred at room temperature for 30 min to overnight (reaction was monitored by TLC). The reaction was then quenched by pouring over water (twice the volume of the solvent). The aqueous phase was separated and extracted with methylene chloride (x2), and the combined organic phases were dried over Na₂SO₄, filtered and concentrated. The crude mixture was purified by flash column chromatography to afford the desired thio ester.

General Procedure for the Decarbonylative Chlorination/Thioetherification

General Procedure (a): Pd-Catalyzed Reaction on Small Scale. In a glovebox, substrate (0.05 mmol, 1 equiv), Pd(P(*o*-tol)₃)₂ (2.9 mg, 0.005 mmol, 0.1 equiv), P(Ad)₂Bn(3.6 mg, 0.2 equiv) , and MS 5A (thioetherification only) were combined with *p*-xylene (0.3 mL) in a 4 ml vial. The vial was connected with a reflux condenser and capped with a rubber septum and the reaction mixture was taken out from the glovebox. Argon balloon was placed on the top of condenser (see picture below) and the reaction was refluxed for 20h at indicated temperature. After cooling to room temperature, the reaction mixture was diluted with CH₂Cl₂ (2 mL), and it was passed through a pad of silica gel before being analyzed by GC and GC-MS. Neopentylbenzene was used for internal standard.

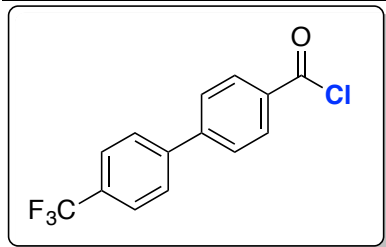


General Procedure (b): Pd-Catalyzed Reaction on Larger Scale for Isolation.

Reactions were conducted analogously to **General Procedure a**, but on a 0.3–0.5 mmol scale as indicated. The reaction mixture was diluted with Et₂O and absorbed into silica and concentrated by rotovap. The resulting crude residue was purified by flash column chromatography. The isolated product was re-dissolved in methylene chloride and CuCl (0.4 equiv) was added and stirred for 20 minutes at room temperature to trap P(*o*-tol₃)₂.⁶⁴ The resultant precipitate was removed by passing through a plug of silica gel using 4:1 Hexanes/EtOAc eluent. The filtrate was concentrated to afford a desired product.

5.6 CHARACTERIZATION

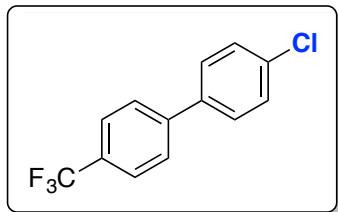
A. Characterizations of Acid Chlorides and Chlorinated Products



Aroyl Chloride 5. The aroyl chloride is prepared according to the following procedure. *Methyl 4'-(trifluoromethyl)-[1,1'-biphenyl]-4-carboxylate*: To a round bottom flask charged with a stir bar, 4-bromobenzotrifluoride (1.74g, 7.75 mmol), 4-methyl carbonyl boronic acid (1.46g, 8.1 mmol, 1.1 equiv), PPh₃ (0.12 g, 0.47 mmol, 0.06 equiv), Pd(OAc)₂ (0.035g, 0.16 mmol, 0.02 equiv) were added and dissolved in acetone/water (1:1). The reaction was refluxed for 5 hours. The reaction was then concentrated and re-dissolved in DCM:hexane (1:1) mixture. The solution was then passed through silica gel to remove Pd black. The filtrate was concentrated to afford methyl 4'-(trifluoromethyl)-[1,1'-biphenyl]-4-carboxylate a white crystalline (0.85g, 40% yield). The product was taken onto a next transformation without further purification.

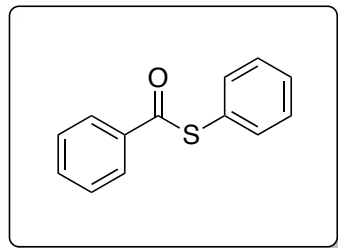
4'-(trifluoromethyl)-[1,1'-biphenyl]-4-carboxylic acid:⁶⁵ To a solution of the ester (0.85g, 3.1 mmol) in THF: H₂O (3:1, 0.2 M), LiOH (0.15g, 6.1 mmol, 2.0 equiv) was added as powder. Then reaction was stirred at 0°C for 3 hours. To the reaction mixture, 1 N HCl was added to acidify the aqueous layer. The aqueous layer was extracted with EtOAc. The combined organic layer was washed with brine and dried over Na₂SO₄. It was concentrated to receive a title compound in quantitative yield.

4'-(trifluoromethyl)-[1,1'-biphenyl]-4-carbonyl chloride:⁶⁶ General Procedure A was followed to receive a title compound as a yellow powder (683mg, 2.4 mmol, 92%). ¹H NMR (700 MHz, CDCl₃): δ 8.23 (d, *J* = 7.0 Hz, 2H), 7.76-7.73 (m, 6H), ¹³C NMR (176 MHz, CDCl₃): δ 167.7, 145.9, 142.5, 132.7, 132.1, 130.8 (q, *J* = 33 Hz), 127.8, 127.7, 126.1, 126.0. ¹⁹F NMR (376 MHz, CDCl₃): δ -62.7. HRMS EI [M+H]⁺ Calcd for C₁₄H₈ClF₃O: 284.0216; Found: 284.0214.

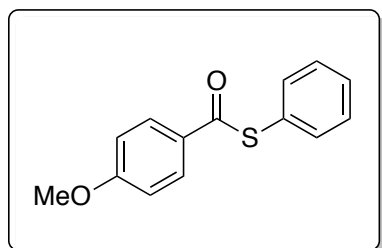


Chlorinated Product 5. General Procedure b was followed using aroyl chloride 5 (0.5 mmol) to receive a title compound in 89% yield. The ^1H , ^{13}C , and ^{19}F NMR spectroscopic data were identical to that reported previously in the literature.⁶⁷ ^{19}F NMR (376 MHz, CDCl_3): δ -62.5. HRMS EI $[\text{M}]^+$ Calcd for $\text{C}_{13}\text{H}_8\text{ClF}_3$: 256.0267; Found 256.0262

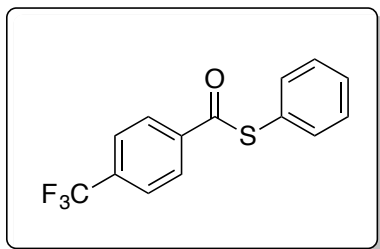
B. Characterization of S-Phenyl Arene Thioate



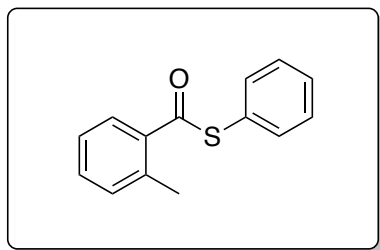
S-Phenyl Phenyl Thioate **1**. General procedure is followed using benzoyl chloride (0.87 mL, 7.5 mmol) and afforded a title compound as off-white crystalline (1.45g, 91% yd). The ^1H , ^{13}C , and ^{19}F NMR spectroscopic data were identical to that reported previously in the literature.⁶⁸ HRMS EI $[\text{M}+\text{H}]^+$ Calcd for $\text{C}_{13}\text{H}_{10}\text{OS}$: 215.0452; Found: 215.0550.



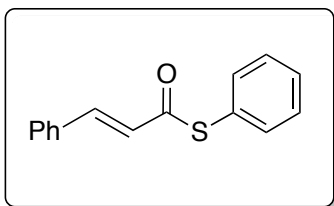
S-phenyl 4-Methoxyphenyl Thioate **2**. General procedure is followed using 4-anisoyl chloride (853 mg, 5.0 mmol) and afforded a title compound as colorless crystalline needles (810 mg, 69% yd). The ^1H , ^{13}C , and ^{19}F NMR spectroscopic data were identical to that reported previously in the literature.⁶⁷ HRMS EI $[\text{M}+\text{H}]^+$ Calcd for $\text{C}_{14}\text{H}_{12}\text{O}_2\text{S}$: 245.0558; Found: 245.0631.



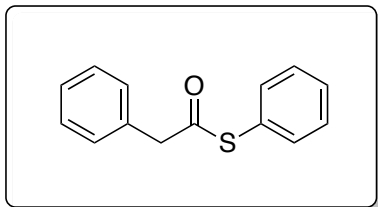
S-phenyl 4-(trifluoromethyl)phenyl Thiolate **3**. General procedure is followed using 4-(trifluoromethyl)benzoyl chloride (1.40g, 5.0 mmol) and afforded a title compound as colorless crystalline needles (510 mg, 38% yd). The ^1H , ^{13}C , and ^{19}F NMR spectroscopic data were identical to that reported previously in the literature.⁶⁹ HRMS EI $[\text{M}+\text{H}]^+$ Calcd for $\text{C}_{14}\text{H}_9\text{F}_3\text{OS}$: 283.0326; Found: 283.0399.



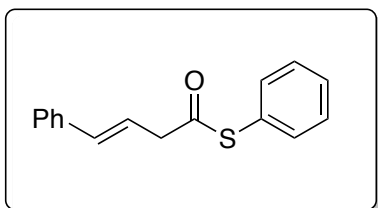
S-phenyl 2-tolyl Thioate **4**. General procedure is followed using 4-toluoyl chloride (773 mg, 5.0 mmol) and afforded a title compound as colorless oil (960 mg, 84% yd). The ^1H and ^{13}C NMR spectroscopic data were identical to that reported previously in the literature.⁶⁷ HRMS EI $[\text{M}+\text{H}]^+$ Calcd for $\text{C}_{14}\text{H}_{12}\text{OS}$: 229.0609 ; Found: 229.0682.



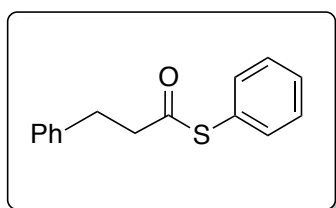
S-phenyl (*E*)-3-phenyl-2-propene Thioate **5**. General procedure is followed using (*E*)-3-phenyl-2-propenoyl chloride (500mg, 3.4 mmol) and afforded a title compound as white crystalline (606mg, 74% yd). The ^1H and ^{13}C NMR spectroscopic data were identical to that reported previously in the literature.⁷⁰ HRMS EI $[\text{M}+\text{H}]^+$ Calcd for $\text{C}_{15}\text{H}_{12}\text{OS}$: 240.0609; Found: 240.0617



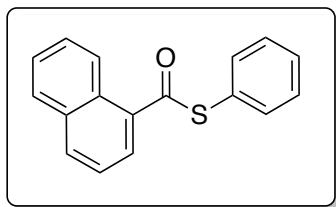
S-Phenyl Phenylthiol acetate **6**. General procedure is followed using phenylacetyl chloride (1.54 g, 10 mmol) and afforded a title compound as yellow oil (959 mg, 78% yd). The ^1H and ^{13}C NMR spectroscopic data were identical to that reported previously in the literature.⁷¹ HRMS EI $[\text{M}+\text{H}]^+$ Calcd for $\text{C}_{14}\text{H}_{12}\text{OS}$: 229.0609; Found: 229.0682.



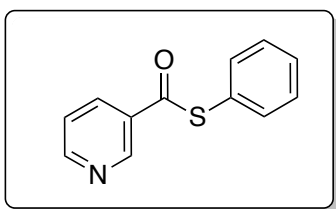
S-phenyl (*E*)-4-phenyl-3-butenethioate **7**. General procedure is followed using (*E*)-4-phenyl-3-butenoyl chloride (900 mg, 5 mmol). Aroyl chloride was prepared according to the general procedure B, afforded a title compound as yellow oil (260 mg, 25% yd). ^1H NMR (700 MHz, CDCl_3): δ 7.44-7.40 (m, 7H), 7.33 (t, $J = 7$ Hz, 2H), 7.26 (s, 1H), 6.60(d, $J = 7$ Hz, 1H), 6.33 (dt, $J = 18, 7$ Hz, 1H), 3.55 (d $J = 7$ Hz, 2H). ^{13}C NMR (176 MHz, CDCl_3): δ 195.48, 136.6, 135.1, 134.5, 129.4, 129.2, 128.6, 127.8, 127.7, 126.4, 120.7, 47.5. HRMS EI $[\text{M}+\text{H}]^+$ Calcd for $\text{C}_{14}\text{H}_{14}\text{OS}$: 255.0838; Found: 255.0835.



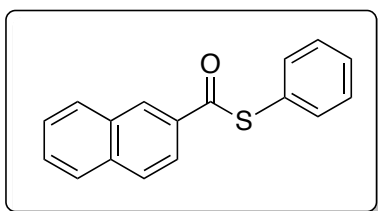
S-phenyl 3-phenylpropanethioate **8**. General procedure is followed using 3-phenylpropanoyl chloride (1.68g, 10 mmol) and afforded a title compound as white crystalline (2.07g, 85% yd). The ^1H and ^{13}C NMR spectroscopic data were identical to that reported previously in the literature.⁷² HRMS EI $[\text{M}+\text{H}]^+$ Calcd for $\text{C}_{15}\text{H}_{14}\text{OS}$: 243.0765; Found: 243.0833.



S-phenyl 1-naphthalyl Thioate **9**. General procedure is followed using 1-naphthoyl chloride (500 mg, 3.0 mmol) and afforded a title compound as off-white powder (204 mg, 77% yd). The ^1H and ^{13}C NMR spectroscopic data were identical to that reported previously in the literature.⁶⁹ HRMS EI $[\text{M}]^+$ Calcd for $\text{C}_{17}\text{H}_{12}\text{OS}$: 264.0609; Found: 264.0609.

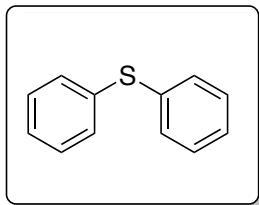


S-phenyl 3-pyridyl Thioate **10**. The title compound is prepared according the literature procedure⁷³ using 3-picolinic acid (370 mg, 3 mmol) and afforded a title compound as off-white powder (610 mg, 46% yd). The ^1H and ^{13}C NMR spectroscopic data were identical to that reported previously in the literature.⁷⁴ HRMS EI $[\text{M}+\text{H}]^+$ Calcd for $\text{C}_{12}\text{H}_9\text{NOS}$: 216.0477; Found: 216.0478.

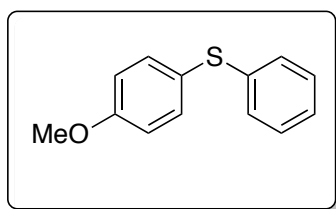


S-phenyl 2-naphthalyl Thioate **11**. General procedure is followed using 2-naphthoyl chloride (953 mg, 5 mmol) and afforded a title compound as off-white powder (610 mg, 46% yd). The ^1H and ^{13}C NMR spectroscopic data were identical to that reported previously in the literature.⁶⁸ HRMS EI $[\text{M}+\text{H}]^+$ Calcd for $\text{C}_{17}\text{H}_{12}\text{OS}$: 265.0609; Found: 265.0682.

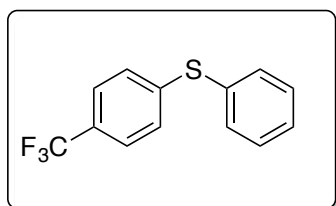
C. Characterization of Diaryl Sulfide Compounds



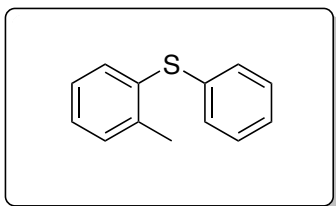
C-S coupled Product 1 General procedure b is followed using substrate **1** (64.2 mg, 0.3 mmol) and afforded a title compound as colorless oil (47.7 mg, 85% yd). ^1H NMR (700 MHz, CDCl_3) δ 7.35–7.30 (m, 5H), 7.28–7.19 (m, 5H). ^{13}C NMR (176 MHz, CDCl_3) δ 135.8, 131.0, 129.2, 127.0. HRMS EI $[\text{M}]^+$ Calcd for $\text{C}_{12}\text{H}_{10}\text{S}$ 186.0503, Found 186.0502.



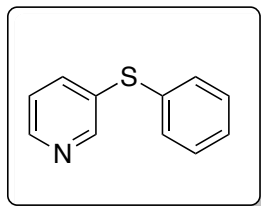
C-S coupled Product 2 General procedure b is followed using substrate **2** (73.2 mg, 0.3 mmol) and afforded a title compound as colorless oil (17.5 mg, 27% yd). The ^1H and ^{13}C NMR spectroscopic data were identical to that reported previously in the literature.⁷⁵ HRMS EI $[\text{M}]^+$ Calcd for $\text{C}_{13}\text{H}_{12}\text{OS}$ 216.0609, Found 216.0612.



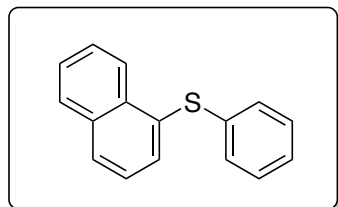
C-S coupled Product 3 General procedure b is followed using substrate **3** (84.7 mg, 0.3 mmol) and afforded a title compound as colorless oil (60.1 mg, 79% yd). The ^1H and ^{13}C NMR spectroscopic data were identical to that reported previously in the literature.⁷⁵ HRMS EI $[\text{M}]^+$ Calcd for $\text{C}_{13}\text{H}_9\text{F}_3\text{S}$ 254.0377, Found 254.0369.



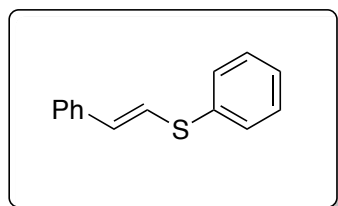
C-S coupled Product 4 General procedure b is followed using substrate **4** (68.4 mg, 0.3 mmol) and afforded a title compound as colorless oil (60.1 mg, 79% yd). The ^1H and ^{13}C NMR spectroscopic data were identical to that reported previously in the literature.⁷⁵ HRMS EI $[\text{M}]^+$ Calcd for $\text{C}_{13}\text{H}_{12}\text{S}$ 200.0660, Found 200.0664.



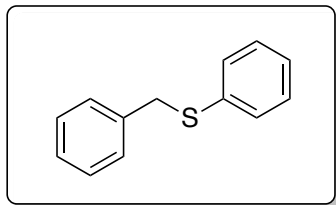
C-S coupled Product 5 General procedure b is followed using substrate **5** (64.5 mg, 0.3 mmol) and afforded a title compound as a colorless oil (30.2 mg, 54% yd). The ^1H and ^{13}C NMR spectroscopic data were identical to that reported previously in the literature.⁷⁵ HRMS EI $[\text{M}]^+$ Calcd for $\text{C}_{11}\text{H}_9\text{NS}$ 188.0528, Found 188.0527.



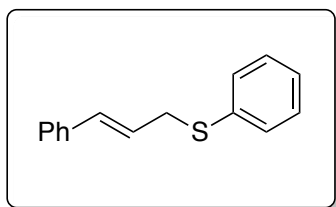
C-S coupled Product 6 General procedure b is followed using substrate **6** (79.3 mg, 0.3 mmol) and afforded a title compound as white powder (47.9 mg, 68% yd). The ^1H and ^{13}C NMR spectroscopic data were identical to that reported previously in the literature.⁷⁵ HRMS EI $[\text{M}]^+$ Calcd for $\text{C}_{16}\text{H}_{12}\text{S}$ 236.0660 Found.236.0653



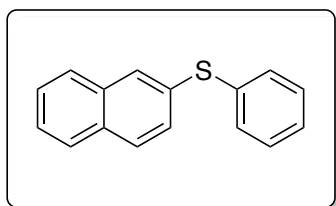
C-S coupled Product 7 General procedure b is followed using substrate **7** (72.1 mg, 0.3 mmol) and afforded a title compound as colorless oil (31.5 mg, 50% yd, E:Z = 89:11). The ^1H and ^{13}C NMR spectroscopic data were identical to that reported previously in the literature.⁷⁶ HRMS EI $[\text{M}]^+$ Calcd for $\text{C}_{14}\text{H}_{12}\text{S}$ 212.0660, Found 212.0659.



C-S coupled Product 8 General procedure b is followed using substrate **8** (68.4 mg, 0.3 mmol) and afforded a title compound as white crystalline (48.6 mg, 81% yd). ^1H NMR (700 MHz, CDCl_3): δ 4.01 (s, 2H), 7.18-7.22 (m, 10H). ^{13}C NMR (176MHz, CDCl_3): δ 39.1, 126.5, 127.3, 127.5, 128.5, 128.9, 129.4, 129.8, 136.9, 137.7. HRMS EI $[\text{M}]^+$ Calcd for $\text{C}_{13}\text{H}_{12}\text{S}$ 200.0660, Found 200.0665.



C-S coupled Product 9 General procedure b is followed using substrate **9** (76.3 mg, 0.3 mmol) and afforded a title compound as white powder (32.9 mg, 49% yd). The ^1H and ^{13}C NMR spectroscopic data were identical to that reported previously in the literature.⁷⁷ HRMS EI $[\text{M}]^+$ Calcd for $\text{C}_{15}\text{H}_{14}\text{S}$ 226.0816, Found 226.0818.



C-S coupled Product 10 General procedure b is followed using substrate **10** (79.3 mg, 0.3 mmol) and afforded a title compound as white powder as inseparable mixture.

5.7 REFERENCES

- (1) Reviews on transition metal-catalyzed carbonylation reactions (a) Brennführer, A.; Neumann, H.; Beller, M. *Angew. Chem. Int. Ed.* **2009**, *48*, 4114. (b) Wu, L.; Liu, Q.; Jackstell, R.; Beller, M. *Angew. Chem. Int. Ed.* **2014**, *53*, 6310.
- (2) Hydroformylation: (a) Franke, R.; Selent, D.; Börner, A. *Chem. Rev.* **2012**, *112*, 5675. (b) Sparta, M.; Børve, K. J.; Jensen, V. R. *J. Am. Chem. Soc.* **2007**, *129*, 8487. (c) Gleich, D.; Hutter, J. *Chem – Eur. J.* **2004**, *10*, 2435. (d) Landis, C. R.; Uddin, J. *J. Chem. Soc., Dalton Trans.* **2002**, 729. (e) Carbó, J. J.; Maseras, F.; Bo, C.; van Leeuwen, P. W. N. M. *J. Am. Chem. Soc.* **2001**, *123*, 7630. (f) Alagona, G.; Ghio, C.; Lazzaroni, R.; Settambolo, R. *Organometallics*, **2001**, *20*, 1161.
- (3) Khodakov, A. Y.; Chu, W.; Fongarland, P. *Chem. Rev.* **2007**, *107*, 1692.
- (4) (a) Hartwig, J. *Organotransition Metal Chemistry: from bonding to catalysis*: University Science Book: Boston, 2010. p 746-748. (b) Hosea Cheung, Robin S. Tanke, G. Paul Torrence "Acetic Acid" in *Ullmann's Encyclopedia of Industrial Chemistry*, 2002, Wiley-VCH, Weinheim. doi: 10.1002/14356007.a01_045.pub3
- (5) Frstrup, P.; Kreis, M.; Palmelund, A.; Norrby, P. -O.; Madsen, R. *J. Am. Chem. Soc.* **2008**, *130*, 5206.
- (6) Hartwig, J. *Organotransition Metal Chemistry: from bonding to catalysis*: University Science Book: Boston, 2010. p 220-223.
- (7) Tsuji, J.; Ohno, K.; Kajimoto, T. *Tetrahedron Lett.* **1965**, *6*, 4565.
- (8) Tsuji, J.; Ohno, K. *Tetrahedron Lett.* **1965**, 3969.
- (9) Ohno, K.; Tsuji, J. *J. Am. Chem. Soc.* **1968**, *90*, 99.
- (10) Reviews on Tsuji-Wilkinson Decarbonylation Reaction: (a) Tsuji, J.; Ohno, K. *Adv. Chem. Series* **1968**, *90*, 94. (b) Tsuji, J.; Ohno, K. *Synthesis* **1969**, 157. (c) Kozikowski, A. P.; Wetter, H. F. *Synthesis* **1976**, 561. (d) Tsuji, J. *Org. Synth. Met. Carbonyls* **1977**, *2*, 595. (e) Murakami, M. Ito, Y. *Top. Organomet. Chem.* **1999**, *3*, 97.
- (11) Beck, C. M.; Rathmill, S. E.; Park, Y. J.; Chen, J.; Crabtree, R. H.; Liable-Sands, L. M.; Rheingold, A. L. *Organometallics* **1999**, *18*, 5311.
- (12) Gooßen, L. J.; Deng, G.; Levy, L. M. *Science* **2006**, *313*, 662.
- (13) (a) Gooßen, L. J.; Rodríguez, N.; Gooßen, K. *Angew. Chem. Int. Ed.* **2008**, *47*, 3100. (b) Dzik, W. I.; Lange, P. P.; Gooßen, L. J. *Chem. Sci.* **2012**, *3*, 2671.
- (14) Gooßen, L. J.; Paetzold, J. *Adv. Synth. Catal.* **2004**, *346* (13-15), 1665.
- (15) O'Brien, E. M.; Bercot, E. A.; Rovis, T. *J. Am. Chem. Soc.* **2003**, *125*, 10498.
- (16) Havlik, S. E.; Simmons, J. M.; Winton, V. J.; Johnson, J. B. *J. Org. Chem.* **2011**, *76*, 3588.
- (17) Muto, K.; Yamaguchi, J.; Musaev, D. G.; Itami, K. *Nat. Comms.* **2015**, *6*, 7508.
- (18) (a) Maleckis, A.; Sanford, M. S. *Organometallics* **2014**, *33*, 2653. (b) Maleckis, A.; Sanford, M. S. *Organometallics* **2014**, *33*, 3831.
- (19) (a) Kalow, J. A.; Schmitt, D. E.; Doyle, A. G. *J. Org. Chem.* **2012**, *77*, 4177. (b) Ryan, S. J.; Schimler, S. D.; Bland, D. C.; Sanford, M. S. *Org. Lett.* **2015**, *17*, 1866. (c) with pyfluor: Nielsen, M. K.; Ugaz, C. R.; Li, W.; Doyle, A. G. *J. Am. Chem. Soc.* **2015**, *137*, 9571.
- (20) Olah and colleagues had published the Rh-catalyzed decarbonylative fluorination (ref a) which later was probed wrong by Ehrenkauffer and coworkers (ref b) (a) Olah, G.;

- Kreienbuhl, P. *J. Org. Chem.* **1967**, *32*, 1614. (b) Ehrenkaufner, R. E.; MacGregor, R. R.; Wolf, A. P. *J. Org. Chem.* **1982**, *47*, 2489.
- (21) Gribble, G. W. *Acc. Chem. Res.* **1998**, *31*, 141.
- (22) (a) Quinn, M. J.; Fitzgerald, D. J. *Circulation* **1999**, *100*, 1667. (b) DeLeon, A.; Patel, N. C.; Crismon, M. L. *Clin. Ther.* **2004**, *26*, 649. (c) Hair, P. I.; McCormack, P. L.; Curran, M. P. *Drugs* **2008**, *68*, 1415.
- (23) Krieger, R. *Hayes' Handbook of Pesticide Toxicology*, Vol. 1; Elsevier: London, 1991.
- (24) Blum, J. *Tetrahedron Lett.* **1966**, 1605.
- (25) Blum, J.; Oppenheimer, E.; Bergmann, E. D. *J. Am. Chem. Soc.* **1967**, *189*, 2238.
- (26) Blum, J.; Rosenman, H.; Bergmann, E. *J. Org. Chem.* **1968**, *33*, 1928.
- (27) Verbicky, J. W.; Dellacoleta, B. A.; Williams, L. *Tetrahedron Lett.* **1982**, *23*, 371.
- (28) Martin, R.; Buchwald, S. L. *Acc. Chem. Res.* **2008**, *41*, 1461.
- (29) (a) Luo, Y.; Pan, X.; Wu, J. *Tetrahedron Lett.* **2010**, *51*, 6646. (b) Peng, X.; Shao, X.-F.; Liu, Z.-Q. *Tetrahedron Lett.* **2013**, *54*, 3079.
- (30) (a) Hull, K. L.; Anani, W. Q.; Sanford, M. S. *J. Am. Chem. Soc.* **2006**, *128*, 7134. (b) Sanford, M. S. *Org. Lett.* **2009**, *11*, 4584. (c) Whitfield, S. R.; Sanford, M. S. *J. Am. Chem. Soc.* **2007**, *129*, 15142.
- (31) A number of other publications has demonstrated halogenation of arenes through high valent PdIV: see Engle, K. M.; Mei, T.-S.; Wasa, M.; Yu, J.-Q. *Acc. Chem. Res.* **2011**, *45*, 788.
- (32) (a) Roy, A. H.; Hartwig, J. F. *J. Am. Chem. Soc.* **2001**, *123*, 1232. (b) Roy, A. H.; Hartwig, J. F. *J. Am. Chem. Soc.* **2004**, *23*, 1533.
- (33) Otsuka, S.; Nakamura, A.; Yoshida, T.; Naruto, M.; Ataka, K. *J. Am. Chem. Soc.* **1973**, *95*, 3180.
- (34) Quesnel, J. S.; Arndtsen, B. A. *J. Am. Chem. Soc.* **2013**, *135*, 16841.
- (35) (a) Grushin, V. V. *Acc. Chem. Res.* **2010**, *43*, 160. (b) Campbell, M. G.; Tobias, R. *Chem. Rev.* **2014**, *115*, 612.
- (36) Ueda, T.; Konishi, H.; Manabe, K. *Org. Lett.* **2013**, *15* (20), 5370.
- (37) Garrou, P. E.; Heck, R. F. *J. Am. Chem. Soc.* **1976**, *98*, 4115.
- (38) There is a peak at -114.6 ppm that is likely product **17** in 38% yield. But the authentic sample was not available to confirm the peak identity.
- (39) (a) Fraser, S. L.; Antipin, M. Y.; Khroustalyov, V. N. A.; Grushin, V.V. *J. Am. Chem. Soc.* **1997**, *119*, 4769. (b) Grushin, V. V. *Chem. Eur. J.* **2002**, *8*, 1006.
- (40) Pd-catalyzed carbonylative fluorination was previously reported: Ueda, T.; Konishi, H.; Manabe, K. *Org. Lett.* **2013**, *15*, 5370.
- (41) Ansell, M. F. *The Chemistry of Acyl Halides*, Patai, S., Ed.; Wiley-Interscience: Chichester, UK, (1972); p 35.
- (42) (a) Nakazawa, T.; Xu, J.; Nishikawa, T.; Oda, T.; Fujita, A.; Ukai, K.; Mangindaan, R. E. P.; Rotinsulu, H.; Kobayashi, H.; Namikoshi, M. *J. Nat. Prod.* **2007**, *70*, 439. (b) Liu, H.; Fujiwara, T.; Nishikawa, T.; Mishima, Y.; Nagai, H.; Shida, T.; Tachibana, K.; Kobayashi, H.; Mangindaan, R. E. P.; Namikoshi, M. *Tetrahedron* **2005**, *61*, 8611.
- (43) (a) Okamoto, T.; Mitsui, C.; Yamagishi, M.; Nakahara, K.; Soeda, J.; Hirose, Y.; Miwa, K.; Sato, H.; Yamano, A.; Matsushita, T.; Uemura, T.; Takeya, J. *Adv. Mater.* **2013**, *25*, 6392. (b) Mori, T.; Nishimura, T.; Yamamoto, T.; Doi, I.; Miyazaki, E.; Osaka,

- I.; Takimiya, K. *J. Am. Chem. Soc.* **2013**, *135*, 13900. (c) Takimiya, K.; Shinamura, S.; Osaka, I.; Miyazaki, E. *Adv. Mater.* **2011**, *23*, 4347.
- (44) (a) Krapcho, J.; Spitzmiller, E. R.; Turk, C. F. *J. Med. Chem.* **1963**, *6*, 544. (b) Krapcho, J.; Turk, C. F. *J. Med. Chem.* **1966**, *9*, 191.
- (45) (a) Bahrami, K.; Khodaei, M. M.; Sohrabnezhad, S. *Tetrahedron Lett.* **2011**, *52*, 6420. (b) Boruah, J. J.; Das, S. P.; Ankireddy, S. R.; Gogoi, S. R.; Islam, N. S. *Green Chem.* **2013**, *15*, 2944. (c) Kamata, K.; Hirano, T.; Mizuno, N. *Chem. Commun.* **2009**, 3958. (d) Rostami, A.; Akradi, J. *Tetrahedron Lett.* **2010**, *51*, 3501. (e) Ruano, J. L. G.; Aleman, J.; Fajardo, C.; Parra, A. *Org. Lett.* **2005**, *7*, 5493.
- (46) Mellah, M.; Voituriez, A.; Schulz, E. *Chem. Rev.* **2007**, *107*, 5133.
- (47) Pearson, R. G.; Sobel, H.; Songstad, J. *J. Am. Chem. Soc.* **1968**, *90*, 319.
- (48) Osakada, K.; Yamamoto, T.; Yamamoto, A. *Tetrahedron Lett.* **1987**, *28*, 6321.
- (49) In the presence of 5 mol % Pd(PPh₃)₄ in toluene at reflux, 40% of Ph₂S was observed from S-phenyl benzene thiolate in the system of Pd-catalyzed carbothiolation of alkynes: see Sugoh, K.; Kuniyasu, H.; Sugae, T.; Ohtaka, A.; Takai, Y.; Tanaka, A.; Machino, C.; Kambe, N.; Kurosawa, H. *J. Am. Chem. Soc.* **2001**, *123*, 5108.
- (50) (a) Iwasaki, M.; Topolovčan, N.; Hu, H.; Nishimura, Y.; Gagnot, G.; Nakorn, R. N.; Yuvacharaskul, R.; Nakajima, K.; Nishihara, Y. *Org. Lett.* **2016**, *18*, 1642. (b) Shimizu, D.; Takeda, N.; Tokitoh, N. *Chem. Commun.* **2006**, 177.
- (51) Munjanja, L.; Brennessel, W. W.; Jones, W. D. *Organometallics* **2015**, *34*, 4574.
- (52) (a) Walborsky, H. M.; Allen, L. E. *J. Am. Chem. Soc.* **1971**, *93*, 5465. (b) Stille, J. K. Huang, F. Regan, M. T. *J. Am. Chem. Soc.* **1974**, *96*, 1514.
- (53) Zhang, H.; Padwa, A. *Tetrahedron Lett.* **2006**, *47*, 3905.
- (54) Hartwig, J. *Organotransition Metal Chemistry: from bonding to catalysis*: University Science Book: Boston, 2010. p 398-402.
- (55) Chirik, P. J.; Bercaw, J. E. *Organometallics* **2005**, *24*, 5407.
- (56) Tanaka, D.; Romeril, S. P.; Myers, A. G. *J. Am. Chem. Soc.* **2005**, *127*, 10323.
- (57) Meng, G.; Szostak, M. *Angew. Chem. Int. Ed.* **2015**, *54*, 14518.
- (58) Desnoyer, A. N.; Friese, F. W.; Chiu, W.; Drover, M. W.; Patrick, B. O.; Love, J. A. *Chem. Eur. J.* **2016**, *22*, 4070.
- (59) Meng, G.; Szostak, M. *Org. Lett.* **2015**, *17*, 4364.
- (60) Hie, L.; Nathel, N. F. F.; Shah, T. K.; Baker, E. L.; Hong, X.; Yang, Y.-F.; Liu, P.; Houk, K. N.; Garg, N. K. *Nature* **2015**, *524*, 79.
- (61) Compton, C. L.; Schmitz, K. R.; Sauer, R. T.; Sello, J. K. *ACS Chem. Biol.* **2013**, *8*, 2669.
- (62) Crabb, T.; Soilleux, S. L. *J. Chem. Soc., Perkin Trans. 1* **1985**, 1381.
- (63) Cera, G.; Haven, T.; Ackermann, L. *Angew. Chem. Int. Ed.* **2016**, *55*, 1484.
- (64) Lipshutz, B. H.; Frieman, B. A.; Birkedal, H. *Org. Lett.* **2004**, *6*, 2305.
- (65) PCT Int. Appl 2005097740, 20 Oct 2005
- (66) Kudelko, A.; Wróblowska, M. *Tetrahedron Letters* **2014**, *55*, 3252.
- (67) Leifang Liu; Yuhong Zhang, A.; Bingwei Xin. *J. Org. Chem.* **2006**, *71*, 3994.
- (68) Rong, G.; Mao, J.; Liu, D.; Yan, H.; Zheng, Y.; Chen, J. *RSC Adv.* **2015**, *5*, 26461.
- (69) Cao, H.; McNamee, L.; Alper, H. *J. Org. Chem.* **2008**, *73*, 3530.
- (70) Xia, Z.; Lv, X.; Wang, W.; Wang, X. *Tetrahedron Lett.* **2011**, *52*, 4906.
- (71) Braga, A. L.; Martins, T. L. C.; Silveira, C. C.; Rodrigues, O. E. D. *Tetrahedron*

2001, 57, 3297.

(72) Métro, T. X.; Bonnamour, J.; Reidon, T.; Duprez, A.; Sarpoulet, J.; Martinez, J.; Lamaty, F. *Chem. Eur. J.* **2015**, 21, 12787.

(73) Korczynska, M.; Le, D. D.; Younger, N.; Gregori-Puigjané, E.; Tumber, A.; Krojer, T.; Velupillai, S.; Gileadi, C.; Nowak, R. P.; Iwasa, E.; Pollock, S. B.; Torres, I. O.; Oppermann, U.; Shoichet, B. K.; Fujimori, D. G. *J. Med. Chem.* **2015**, 59, 1580.

(74) El-Azab, A. S.; Abdel-Aziz, A. A. M. *Phosphorus, Sulfur, and Silicon and the Related Elements* **2012**, 187, 1046.

(75) Xu, H.-J.; Zhao, Y.-Q.; Feng, T.; Feng, Y.-S. *J. Org. Chem.* **2012**, 77, 2878.

(76) Tidei, C.; Sancineto, L.; Bagnoli, L.; Battistelli, B.; Marini, F.; Santi, C. *Eur. J. Org. Chem.* **2014**, 5968.

(77) Ravikumar, P. C.; Yao, L.; Fleming, F. F. *J. Org. Chem.* **2009**, 74, 7294.